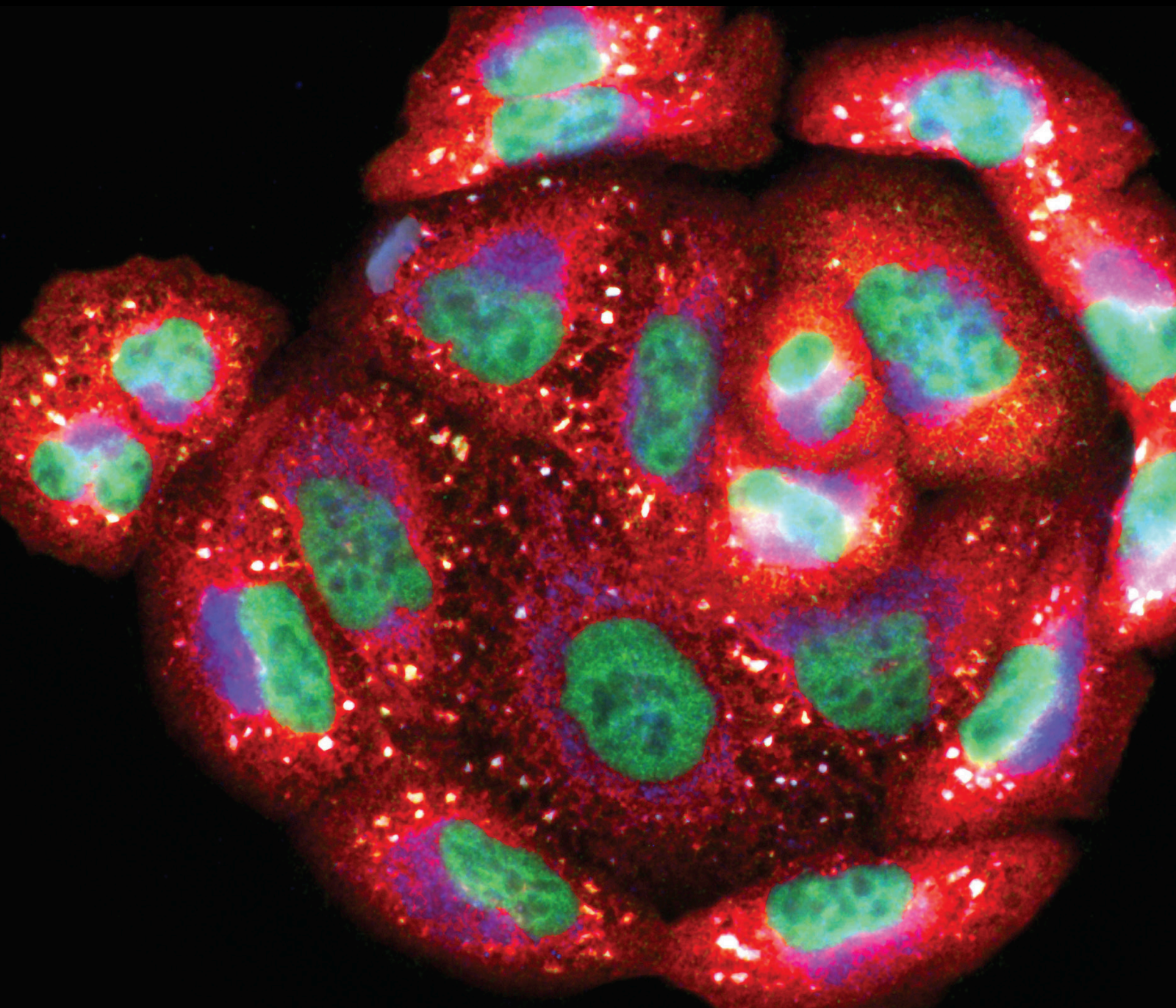


Cellular and Molecular Mechanisms of Oxidative Stress in Wound Healing

Lead Guest Editor: Reggiani Vilela Gonçalves

Guest Editors: Debora Esposito and Mariella Bontempo Freitas





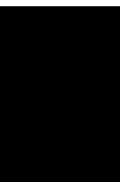
Cellular and Molecular Mechanisms of Oxidative Stress in Wound Healing

Oxidative Medicine and Cellular Longevity

Cellular and Molecular Mechanisms of Oxidative Stress in Wound Healing

Lead Guest Editor: Reggiani Vilela Gonçalves

Guest Editors: Debora Esposito and Mariella
Bontempo Freitas



Copyright © 2022 Hindawi Limited. All rights reserved.

This is a special issue published in "Oxidative Medicine and Cellular Longevity" All articles are open access articles distributed under the Creative Commons Attribution License, which permits unrestricted use, distribution, and reproduction in any medium, provided the original work is properly cited.

Chief Editor

Jeannette Vasquez-Vivar, USA

Editorial Board

Mohd Adnan, Saudi Arabia
Ivanov Alexander, Russia
Fabio Altieri, Italy
Silvia Alvarez, Argentina
Fernanda Amicarelli, Italy
José P. Andrade, Portugal
Cristina Angeloni, Italy
Dr. Amjad Islam Aqib, Pakistan
Daniel Arcanjo, Brazil
Sandro Argüelles, Spain
Antonio Ayala, Spain
Elena Azzini, Italy
Peter Backx, Canada
Amira Badr, Egypt
Damian Bailey, United Kingdom
Jiaolin Bao, China
George E. Barreto, Colombia
Sander Bekeschus, Germany
Ji C. Bihl, USA
Consuelo Borrás, Spain
Nady Braidy, Australia
Ralf Braun, Austria
Laura Bravo, Spain
Matt Brody, USA
Amadou Camara, USA
Gianluca Carnevale, Italy
Roberto Carnevale, Italy
Marcio Carochi, Portugal
Angel Catalá, Argentina
Peter Celec, Slovakia
Giulio Ceolotto, Italy
Giselle Cerchiaro, Brazil
Shao-Yu Chen, USA
Yujie Chen, China
Deepak Chhangani, USA
Ferdinando Chiaradonna, Italy
Zhao Zhong Chong, USA
Xinxin Ci, China
Fabio Ciccarone, Italy
Alin Ciobica, Romania
Ana Cipak Gasparovic, Croatia
Giuseppe Cirillo, Italy
Maria R. Ciriolo, Italy
Massimo Collino, Italy

Graziamaria Corbi, Italy
Manuela Corte-Real, Portugal
Mark Crabtree, United Kingdom
Manuela Curcio, Italy
Andreas Daiber, Germany
Felipe Dal Pizzol, Brazil
Francesca Danesi, Italy
Domenico D'Arca, Italy
Sergio Davinelli, Italy
Claudio de Lucia, Italy
Damião de Sousa, Brazil
Enrico Desideri, Italy
Francesca Diomedea, Italy
Cinzia Domenicotti, Italy
Raul Dominguez-Perles, Spain
Dimitrios Draganidis, Greece
Joël R. Drevet, France
Grégory Durand, France
Alessandra Durazzo, Italy
Anne Eckert, Switzerland
Javier Egea, Spain
Fatma El-Demerdash, Egypt
Pablo A. Evelson, Argentina
Stefano Falone, Italy
Ioannis G. Fatouros, Greece
Qingping Feng, Canada
Gianna Ferretti, Italy
Giuseppe Filomeni, Italy
Pasquale Fino, Italy
Omidreza Firuzi, Iran
Swaran J. S. Flora, India
Teresa I. Fortoul, Mexico
Anna Fracassi, USA
Rodrigo Franco, USA
Joaquin Gadea, Spain
Juan Gambini, Spain
José Luís García-Giménez, Spain
Gerardo García-Rivas, Mexico
Janusz Gebicki, Australia
Alexandros Georgakilas, Greece
Husam Ghanim, USA
Jayeeta Ghose, USA
Rajeshwary Ghosh, USA
Lucia Gimeno-Mallench, Spain

Eloisa Gitto, Italy
Anna M. Giudetti, Italy
Daniela Giustarini, Italy
José Rodrigo Godoy, USA
Saeid Golbidi, Canada
Aldrin V. Gomes, USA
Arantxa González, Spain
Tilman Grune, Germany
Chi Gu, China, China
Nicoletta Guaragnella, Italy
Solomon Habtemariam, United Kingdom
Ying Han, China
Eva-Maria Hanschmann, Germany
Md Saquib Hasnain, India
Md Hassan, India
Tim Hofer, Norway
John D. Horowitz, Australia
Silvana Hrelia, Italy
Dragan Hrcic, Serbia
Juan Huang, China
Zebo Huang, China
Tarique Hussain, Pakistan
Stephan Immenschuh, Germany
Maria Isagulians, Latvia
Luigi Iuliano, Italy
FRANCO J. L, Brazil
Vladimir Jakovljevic, Serbia
sedat kacar, USA
Jason Karch, USA
Peeter Karihtala, Finland
Andleeb Khan, Saudi Arabia
Kum Kum Khanna, Australia
Neelam Khaper, Canada
Thomas Kietzmann, Finland
Ramoji Kosuru, USA
Demetrios Kouretas, Greece
Andrey V. Kozlov, Austria
Chan-Yen Kuo, Taiwan
Esra Küpeli Akkol, Turkey
Daniele La Russa, Italy
Jean-Claude Lavoie, Canada
Wing-Kee Lee, Germany
Simon Lees, Canada
Xin-Feng Li, China
Qiangqiang Li, China
Gaocai Li, China
Jialiang Liang, China




Christopher Horst Lillig, Germany
Paloma B. Liton, USA
Ana Lloret, Spain
Lorenzo Loffredo, Italy
Camilo López-Alarcón, Chile
Daniel Lopez-Malo, Spain
Antonello Lorenzini, Italy
Massimo Lucarini, Italy
Hai-Chun Ma, China
Mateusz Maciejczyk, Poland
Nageswara Madamanchi, USA
Kenneth Maiese, USA
Marco Malaguti, Italy
Tullia Maraldi, Italy
Reiko Matsui, USA
Juan C. Mayo, Spain
Steven McAnulty, USA
Antonio Desmond McCarthy, Argentina
Sonia Medina-Escudero, Spain
Pedro Mena, Italy
Victor M. Mendoza-Núñez, Mexico
Lidija Milkovic, Croatia
Alexandra Miller, USA
Sanjay Misra, USA
Sara Missaglia, Italy
Premysl Mladenka, Czech Republic
Raffaella Molteni, Italy
Maria U. Moreno, Spain
Sandra Moreno, Italy
Trevor A. Mori, Australia
Ryuichi Morishita, Japan
Fabiana Morroni, Italy
Ange Mouithys-Mickalad, Belgium
Iordanis Mourouzis, Greece
Danina Muntean, Romania
Colin Murdoch, United Kingdom
Ryoji Nagai, Japan
Amit Kumar Nayak, India
David Nieman, USA
Cristina Nocella, Italy
Susana Novella, Spain
Hassan Obied, Australia
Julio J. Ochoa, Spain
Pál Pacher, USA
Pasquale Pagliaro, Italy
DR DILIPKUMAR PAL, India
Valentina Pallottini, Italy

Swapnil Pandey, USA
Rosalba Parenti, Italy
Mayur Parmar, USA
Vassilis Paschalis, Greece
Visweswara Rao Pasupuleti, Malaysia
Keshav Raj Paudel, Australia
Ilaria Peluso, Italy
Claudia Penna, Italy
Serafina Perrone, Italy
Tiziana Persichini, Italy
Shazib Pervaiz, Singapore
Vincent Pialoux, France
Alessandro Poggi, Italy
Ada Popolo, Italy
Aijuan Qu, China
José L. Quiles, Spain
Walid Rachidi, France
Zsolt Radak, Hungary
Sachchida Nand Rai, India
Namakkal Soorappan Rajasekaran, USA
Dario C. Ramirez, Argentina
Erika Ramos-Tovar, Mexico
Abdur Rauf Rauf, Pakistan
Sid D. Ray, USA
Muneeb Rehman, Saudi Arabia
Hamid Reza Rezvani, France
Alessandra Ricelli, Italy
Francisco J. Romero, Spain
Mariana G. Rosca, USA
Joan Roselló-Catafau, Spain
Esther Roselló-Lletí, Spain
Subhadeep Roy, India
Josep V. Rubert, The Netherlands
H. P. Vasantha Rupasinghe, Canada
Sumbal Saba, Brazil
Kunihiro Sakuma, Japan
Gabriele Saretzki, United Kingdom
Ajinkya S. Sase, USA
Luciano Saso, Italy
Nadja Schroder, Brazil
Sebastiano Sciarretta, Italy
Ratanesh K. Seth, USA
Anwen Shao, China
Xiaolei Shi, China
Cinzia Signorini, Italy
Mithun Sinha, USA
Giulia Sita, Italy

Eduardo Sobarzo-Sánchez, Chile
Adrian Sturza, Romania
Yi-Rui Sun, China
Eisa Tahmasbpour Marzouni, Iran
Carla Tatone, Italy
Shane Thomas, Australia
Carlo Gabriele Tocchetti, Italy
Angela Trovato Salinaro, Italy
Paolo Tucci, Italy
Rosa Tundis, Italy
Giuseppe Valacchi, Italy
Daniele Vergara, Italy
Victor M. Victor, Spain
László Virág, Hungary
Min-qi Wang, China
Kai Wang, China
Natalie Ward, Australia
Grzegorz Wegrzyn, Poland
Philip Wenzel, Germany
guangzhen wu, China
Jianbo Xiao, China
Qiongmeng Xu, China
Sho-ichi Yamagishi, Japan
Liang-Jun Yan, USA
Guillermo Zalba, Spain
Junmin Zhang, China
Ziwei Zhang, China
Jia Zhang, First Affiliated Hospital of Xi'an
Jiaotong University, Xi'an, Shaanxi Province,
China, China
Junli Zhao, USA
Yong Zhou, China
Chen-he Zhou, China
Mario Zoratti, Italy





Contents





Cellular and Molecular Mechanisms of Oxidative Stress in Wound Healing

Reggiani Vilela Gonçalves , Mariella Bontempo Freitas , and Debora Esposito 

Editorial (2 pages), Article ID 9785094, Volume 2022 (2022)


Doxycycline Hyclate Modulates Antioxidant Defenses, Matrix Metalloproteinases, and COX-2 Activity Accelerating Skin Wound Healing by Secondary Intention in Rats


Luciana S. Altoé , Raul S. Alves , Lyvia L. Miranda , Mariáurea M. Sarandy , Daniel S. S.

Bastos , Elda Gonçalves-Santos , Rômulo D. Novaes , and Reggiani V. Gonçalves 

Research Article (16 pages), Article ID 4681041, Volume 2021 (2021)


Apelin/APJ-Manipulated CaMKK/AMPK/GSK3 β Signaling Works as an Endogenous Counterinjury Mechanism in Promoting the Vitality of Random-Pattern Skin Flaps

Zhi-Ling Lou , Chen-Xi Zhang, Jia-Feng Li, Rui-Heng Chen, Wei-Jia Wu, Xiao-Fen Hu, Hao-Chun Shi,

Wei-Yang Gao, and Qi-Feng Zhao 






Research Article (29 pages), Article ID 8836058, Volume 2021 (2021)



The Effects of Hypoxia-Reoxygenation in Mouse Digital Flexor Tendon-Derived Cells

Chen Chen , Wei Feng Mao , and Ya Fang Wu 

Research Article (13 pages), Article ID 7305392, Volume 2020 (2020)


Effects of Strong Acidic Electrolyzed Water in Wound Healing via Inflammatory and Oxidative Stress Response





Ailyn Fadriquela , Ma Easter Joy Sajo , Johny Bajgai , Dong-Heui Kim , Cheol-Su Kim , Soo-Ki

Kim , and Kyu-Jae Lee 

Research Article (10 pages), Article ID 2459826, Volume 2020 (2020)






What Is the Impact of Depletion of Immunoregulatory Genes on Wound Healing? A Systematic Review of Preclinical Evidence

Bárbara Cristina Félix Nogueira , Artur Kanadani Campos , Raul Santos Alves , Mariáurea Matias

Sarandy , Rômulo Dias Novaes , Debora Esposito , and Reggiani Vilela Gonçalves 

Research Article (19 pages), Article ID 8862953, Volume 2020 (2020)

Were our Ancestors Right in Using Flax Dressings? Research on the Properties of Flax Fibre and Its Usefulness in Wound Healing

Tomasz Gębarowski , Benita Wiatrak , Maciej Janeczek , Magdalena Żuk , Patrycja Pistor , and

Kazimierz Gąsiorowski 

Research Article (10 pages), Article ID 1682317, Volume 2020 (2020)


The Regenerative Potential of Donkey and Human Milk on the Redox-Sensitive and Proliferative Signaling Pathways of Skin Fibroblasts

H. Kocic , T. Langerholc, M. Kostic, S. Stojanovic, S. Najman, M. Krstic, I. Nestic, A. Godic, and U.


Wollina

Research Article (8 pages), Article ID 5618127, Volume 2020 (2020)

Antioxidant and Antimicrobial Potentials of Seed Oil from *Carthamus tinctorius* L. in the Management of Skin Injuries

Ikram Khémiri , Badiia Essghaier, Najla Sadfi-Zouaoui, and Lotfi Bitri
Research Article (12 pages), Article ID 4103418, Volume 2020 (2020)

Peptides from Animal Origin: A Systematic Review on Biological Sources and Effects on Skin Wounds

Raul Santos Alves, Levy Bueno Alves, Luciana Schulthais Altoé, Mariáurea Matias Sarandy, Mariella Bontempo Freitas, Nelson José Freitas Silveira, Rômulo Dias Novaes, and Reggiani Vilela Gonçalves 
Review Article (12 pages), Article ID 4352761, Volume 2020 (2020)

Editorial

Cellular and Molecular Mechanisms of Oxidative Stress in Wound Healing

Reggiani Vilela Gonçalves ¹, Mariella Bontempo Freitas ¹ and Debora Esposito ²

¹Animal Biology Department, Federal University of Viçosa, Viçosa, 36570-000 Minas Gerais, Brazil

²Animal Science Department, Regenerative Medicine, North Carolina State University, 28081 North Carolina, USA

Correspondence should be addressed to Reggiani Vilela Gonçalves; reggysvilela@yahoo.com.br

Received 14 May 2022; Accepted 14 May 2022; Published 17 June 2022

Copyright © 2022 Reggiani Vilela Gonçalves et al. This is an open access article distributed under the Creative Commons Attribution License, which permits unrestricted use, distribution, and reproduction in any medium, provided the original work is properly cited.

Wound healing is a complex biological process characterized by cell activation and by the release of many growth factors responsible to restore tissue integrity after injury [1]. This process can be divided into three stages: inflammation, proliferation, and remodeling [2]. At the beginning of the process, the collagen exposed initiates the coagulation cascade forming the platelet cap, and as the process progresses occur, the release of many cytokines and growth factors promotes cell and vascular proliferation [3]. The next stage is the proliferative phase, characterized by the synthesis of the granulation tissue rich in vessels, cells, and type III collagen. This tissue serves as a framework for type I collagen deposition responsible for the force and resistance to the tissue characterizing the third stage known as remodeling [4].

In skin lesions, the synthesis of free radicals and reactive oxidative species (ROS) by inflammatory cells contributes to the defense against pathogens and mediates important intracellular pathways for the resolution of the inflammatory phase [5]. However, excessive amounts of free radicals and ROS promote tissue oxidative stress, causing deleterious effects on cell membranes, proteins, and nucleic acids [5]. Generally, the higher production of oxidative compounds occurs in the wound healing process associated with diseases such as metabolic (i.e., diabetes mellitus and vasculopathy) and microbial diseases (i.e., bacterial, fungal, and parasitic infections) [6]. So, we believed that understanding the relationship between the interaction of these different mechanisms and the oxidative process is important to provide a guideline for decision-makers in the choice of better treatments and consequently accelerate skin wound closure.

Thinking in the relationship among different phases of the wound healing process, different treatments, and redox metabolism, this special issue gathered 9 studies using *in vivo* and *in vitro* analyses to understand the cellular, immunological, and morphological bases associated with the recovery process of the injured tissue. Concerning new therapies, some studies have shown that external agents such as peptides obtained from animals, plant extract, and acidic electrolyzed water and antibiotics were considered as a rich source of active molecules with potential relevance and applicability indirect or complementary strategies focused on tissue repair. These results showed us that several compounds with proliferation and migration cell potential, antimicrobial properties, and inflammatory modulation have been used with a success in regenerative medicine. However, there is still a gap in knowledge about the main pathways involved in the healing process, and interestingly, some papers published in this edition analyzed the relationship between cell pathway signaling and immunoregulatory genes and wound healing trying to fill the gaps that still exist in this area.

In another study from this issue, the authors showed that mouse tendon-derived cells were highly tolerant to hypoxic environments. During hypoxia/reoxygenation (HR), the authors observed a concentration-dependent increase in cell viability. Under H/R conditions, the expression of vascular endothelial growth factor-A (VEGF-A) and hypoxia-inducible factor HIF-1 α was opposite, whereas type I and type III collagen was downregulated. Considering that although oxidative stress was induced after a period of ischemia, stress responses did not affect cell morphology and growth.

In this issue, in vitro studies have contributed to the field of cellular and molecular mechanisms of oxidative stress in wound healing. One study has shown that medicine dressings made from genetically modified flax fibers had a stronger impact on fibroblasts' proliferative activity, keratinocytes, and microvascular endothelium than traditional flax fiber in several cell lines, such as fibroblasts, epidermal keratinocytes, endothelial, and carcinoma cells. Free oxygen radical levels were reduced in both traditional and genetically modified fibers, corroborating the classical use of this plant as a dressing. Reduced reactive oxygen species production is associated with the protection of DNA damage and favors wound healing. However, especially in difficult-to-heal wounds, other mechanisms such as those which were higher in genetically modified flax fibers wound will be critical to a successful treatment.

We sincerely hope that this special issue's readers will find these findings interesting, advancing knowledge on molecular mechanisms associated with oxidative stress and wound healing.

Conflicts of Interest

The authors declare that there is no conflict of interest regarding the publication of this special issue.

Acknowledgments

The editorial teams are very grateful to the different groups who submitted their scientific findings to this special issue and to the reviewers who kindly provided their time and experience to improve the quality of each study.

*Reggiani Vilela Gonçalves
Mariella Bontempo Freitas
Debora Esposito*

References

- [1] M. G. Roubelakis, O. Trohatou, A. Roubelakis et al., "Platelet-rich plasma (PRP) promotes fetal mesenchymal stem/stromal cell migration and wound healing process," *Stem Cell Rev Reports*, vol. 10, no. 3, pp. 417–428, 2014.
- [2] S. Ellis, E. J. Lin, and D. Tartar, "Immunology of wound healing," *Curr Dermatol Rep.*, vol. 7, no. 4, pp. 350–358, 2018.
- [3] B. Behm, P. Babilas, M. Landthaler, and S. Schreml, "Cytokines, chemokines and growth factors in wound healing," *Journal of the European Academy of Dermatology and Venereology*, vol. 26, no. 7, pp. 812–820, 2012.
- [4] C. Qing, "The molecular biology in wound healing & non-healing wound," *Chinese Journal of Traumatology*, vol. 20, no. 4, pp. 189–193, 2017.
- [5] S. Newbern, "Identifying pain and effects on quality of life from chronic wounds secondary to lower-extremity vascular disease: an integrative review," *Advances in Skin & Wound Care.*, vol. 31, no. 3, pp. 102–108, 2018.
- [6] P. Rousselle, F. Braye, and G. Dayan, "Re-epithelialization of adult skin wounds: cellular mechanisms and therapeutic strategies," *Advanced Drug Delivery Reviews.*, vol. 146, pp. 344–365, 2019.

Research Article

Doxycycline Hyclate Modulates Antioxidant Defenses, Matrix Metalloproteinases, and COX-2 Activity Accelerating Skin Wound Healing by Secondary Intention in Rats

Luciana S. Altoé ¹, Raul S. Alves ¹, Lyvia L. Miranda ¹, Mariáurea M. Sarandy ¹,
Daniel S. S. Bastos ¹, Elda Gonçalves-Santos ², Rômulo D. Novaes ²,
and Reggiani V. Gonçalves ³

¹Department of General Biology, Federal University of Viçosa, Viçosa, Minas Gerais 36570-900, Brazil

²Department of Structural Biology, Federal University of Alfenas, Alfenas, Minas Gerais 37130-001, Brazil

³Department of Animal Biology, Federal University of Viçosa, Viçosa, Minas Gerais 36570-900, Brazil

Correspondence should be addressed to Reggiani V. Gonçalves; reggysvilela@yahoo.com.br

Received 3 August 2020; Revised 16 November 2020; Accepted 31 March 2021; Published 19 April 2021

Academic Editor: Alexandros Georgakilas

Copyright © 2021 Luciana S. Altoé et al. This is an open access article distributed under the Creative Commons Attribution License, which permits unrestricted use, distribution, and reproduction in any medium, provided the original work is properly cited.

The main objective of this study was to investigate the action of doxycycline hyclate (Dx) in the skin wound healing process in Wistar rats. We investigated the effect of Dx on inflammatory cell recruitment and production of inflammatory mediators via *in vitro* and *in vivo* analysis. In addition, we analyzed neovascularization, extracellular matrix deposition, and antioxidant potential of Dx on cutaneous repair in Wistar rats. Male animals ($n = 15$) were divided into three groups with five animals each (protocol: 72/2017), and three skin wounds (12 mm diameter) were created on the back of the animals. The groups were as follows: C, received distilled water (control); Dx1, doxycycline hyclate (10 mg/kg/day); and Dx2, doxycycline hyclate (30 mg/kg/day). The applications were carried out daily for up to 21 days, and tissues from different wounds were removed every 7 days. Our *in vitro* analysis demonstrated that Dx led to macrophage proliferation and increased N-acetyl- β -D-glucosaminidase (NAG) production, besides decreased cyclooxygenase-2 (COX-2), prostaglandin E2 (PGE2), and metalloproteinases (MMP), which indicates that macrophage activation and COX-2 inhibition are possibly regulated by independent mechanisms. *In vivo*, our findings presented increased cellularity, blood vessels, and the number of mast cells. However, downregulation was observed in the COX-2 and PGE2 expression, which was limited to epidermal cells. Our results also showed that the downregulation of this pathway benefits the oxidative balance by reducing protein carbonyls, malondialdehyde, nitric oxide, and hydrogen peroxide (H₂O₂). In addition, there was an increase in the antioxidant enzymes (catalase and superoxide dismutase) after Dx exposure, which demonstrates its antioxidant potential. Finally, Dx increased the number of types I collagen and elastic fibers and reduced the levels of MMP, thus accelerating the closure of skin wounds. Our findings indicated that both doses of Dx can modulate the skin repair process, but the best effects were observed after exposure to the highest dose.

1. Introduction

The skin is a complex organ that serves as a barrier to protect the body from the external environment [1]. However, different aggressive agents, such as trauma and microorganisms, can affect the structure and functions of this organ. In the case of a lesion, there is an exposure of subcutaneous tissue,

which provides a humid and nutritious environment for microbial proliferation and colonization [2]. An infected cutaneous wound increases the risks of chronification, reduces the quality of life, and causes a high mortality rate of patients [3]. Skin wounds represent a serious health problem worldwide and are frequently associated with high costs and inefficient treatments with limited efficiency [4]. The

therapies available today are aimed at improving the healing of wounds by promoting their rapid closure. However, the control of infections is generally neglected [5]. As a result, it is desirable to develop therapeutic interventions that control the infection and increase cutaneous repair.

The repairing of cutaneous wounds is a process that involves a complex interaction between cells, extracellular matrix, blood vessels, and tissue growth factors. Furthermore, the process is separated into the phases of inflammation, proliferation (granulation), and tissue remodeling [6]. During the inflammation phase, there is a migration of leukocytes to the injured site, with the release of cell mediators. During the proliferative phase, there is a multiplication of keratinocytes, fibroblasts, and endothelial cells, resulting in the formation of granulation tissue, which is also rich in vessels and collagen type III [7]. The next phase is characterized by tissue remodeling and maturation, in which collagen III is replaced by collagen I, thus making the scar stronger and more resistant to mechanical forces [8, 9].

The skin healing process is known as acute or chronic, according to its duration and nature [7]. During a chronification process, there is persistent activation of COX way and neutrophils and macrophages release cytokines and chemokines, which attract more cells to the location of the inflammation and promote oxidative stress in the repairing tissue [10, 11]. The excess of proinflammatory mediators increases the peroxide of hydrogen (H_2O_2) and oxide nitric content, which accelerate the peroxidation of lipids and proteins [12]. The prooxidant mediators cause damage to the cutaneous tissue and delay the wound healing process. Therefore, a controlled inflammation process is necessary to avoid persistent tissue damage through the continued action of free radicals and reactive oxygen species (ROS) [13]. Associated with this, we can highlight that the skin healing environment is usually prooxidant and generally presents decreased synthesis and expression of the antioxidant enzymes, such as superoxide, glutathione, and catalase, which impair the healing environment [14].

In general, a desirable repair process results from a balanced process of synthesis and degradation of inflammatory mediators and pro- and antioxidant compounds consequently in the extracellular matrix components, especially collagen [15]. Matrix metalloproteinases (MMP) play an essential role in the turnover of the extracellular matrix (ECM) remodeling, by degrading collagen and noncollagenous elements, such as glycosaminoglycans, proteoglycans, cytokines, growth factors, and their receptors [16]. However, the overexpression of MMP may lead to uncontrolled degradation of ECM and delayed the wound healing process [17–19]. Thus, MMP modulatory drugs may cause an important impact on cutaneous tissue repair, with a particular effect on tissue inflammation and maturation. In this context, doxycycline (Dx) has already been described as an inhibitor of MMP activity [20], and its usage has already been proven in the modulation of tissue levels of collagen in cutaneous repair [21], which stimulates collagen deposition. In addition, Dx proved to be an important tool to inhibit the release of proinflammatory cytokines, such as tumor necrosis factor- α (TNF- α), IL-6, and IL-8 [22]. Thus, we believed that Dx

may affect the cutaneous healing process. Although Dx is effective in treating various disorders [23–25], little is known about the role of Dx in skin tissue repair. Therefore, this study evaluated the effect of Dx on the viability of macrophages, monitored the inflammatory changes *in vitro*, and used an experimental model to understand the effect of Dx on inflammation, oxidative status, angiogenesis, and fibrogenic responses during wound healing in rats.

2. Materials and Methods

2.1. *In Vitro* Assays

2.1.1. Cell Viability. Cell viability for RAW264.7 macrophages was evaluated by 3-[4,5-dimethylthiazol-2-yl]-2,5-diphenyl tetrazolium bromide (MTT) assay as previously described [26, 27]. Cells were cultured in DMEM supplemented with 10% fetal bovine serum and 100 U/mL of penicillin/streptomycin in a humidified 5% CO_2 37°C incubator. To evaluate the effect of Dx on cell viability, RAW264.7 macrophages were seeded into 96-well plates at a density of 1×10^5 cells/well in 200 μ L medium. After 24 h, the various concentrations of Dx (10, 30, 100, and 300 μ g/mL) were added to media, and the incubation continued for the next 24 h at 37°C and 5% CO_2 . The control (100% of growth) was carried out with cells cultured in medium only. The MTT solution was added to each well, and the cells were further incubated for 2 h, at 37°C. The MTT formazan generated during incubation was dissolved in DMSO, and the absorbance was measured at 570 nm. For each sample, the result was expressed as the percentage absorbance in relation to the control group.

2.1.2. Macrophage Challenge with LPS. RAW264.7 macrophages cultured under the same conditions were seeded in 24-well polystyrene plates, at 2.5×10^5 cells, and 1 mL of culture medium per well. After 24 h, the culture medium was replaced, and the RAW264.7 cells were incubated for 24 h with a fresh medium containing 10% FBS, without or with 100 ng/mL LPS (Sigma-Aldrich, St. Louis, Missouri, USA) and different Dx concentrations (10, 30, 100, and 300 μ g/mL). The control cells were treated with a fresh culture medium. After 24 h of incubation, the macrophages were harvested; the cell number was quantified and adjusted by cell counting in a Neubauer chamber. The cells were lysed with 100 mM NaCl/50 mM Tris-HCl buffer and centrifuged (1000g for 15 min at 4°C). The culture supernatant was collected to measure the prostaglandin production enzymatic analysis of MMP, cyclooxygenase-2, and N-acetylglucosaminidase.

(1) Metalloprotease Activity. The enzymatic activity of matrix metalloproteases in macrophage homogenate was measured using a fluorometric enzymatic kit, according to the manufacturer's instructions (ABCAM, Cambridge, MA, USA). The MMP activity was measured at 490 nm/525 nm (excitation/emission), as previously reported [28].

(2) Cyclooxygenase-2 Activity. An aliquot (100 μ L) of the macrophage homogenate was applied to measure the cyclooxygenase-2 (COX-2) activity, which was analyzed

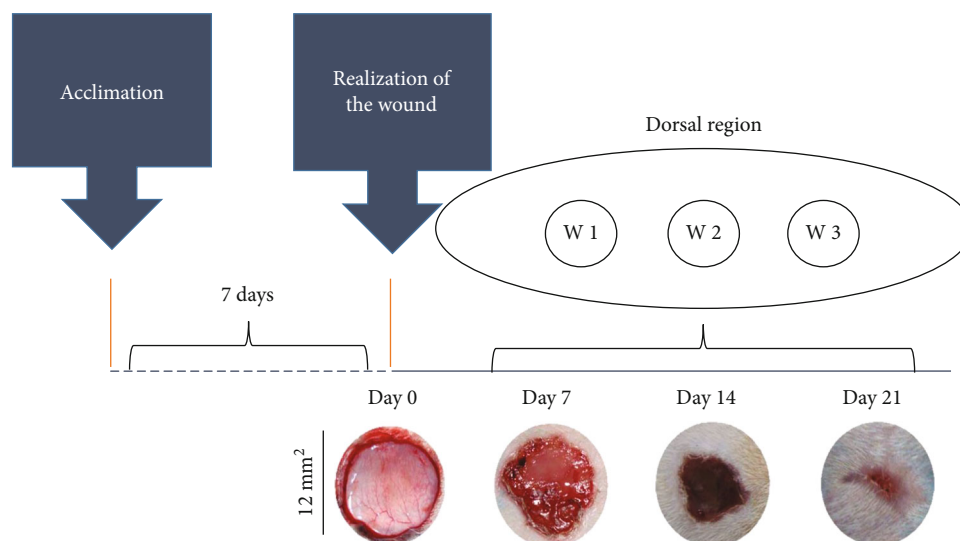


FIGURE 1: Representation of the experimental model of wound healing by secondary intention and time-dependent evolution of wound closure. The top image shows the distribution of the three excisional wounds in the back of the animal. The general appearance of wound closure from the initial wound (day 0) is represented by photographs. W1 (day 7), W2 (day 14), and W3 (day 21); macroscopic aspect of the wounds observed every 7 days. The wound areas were calculated on days 0, 7, 14, and 21 (mean \pm SD), based on the digitized images.

using a biochemical colorimetric kit, following the manufacturer's instructions (Cayman Chemical, Ann Arbor, MI, USA). The enzymatic assay was based on the peroxidase component of cyclooxygenases, in which the peroxidase activity was spectrophotometrically measured by monitoring the production of oxidized N,N,N',N'-tetramethyl-p-phenylenediamine, at 590 nm.

(3) *Prostaglandin Production.* The prostaglandin E2 (PGE2) levels in the macrophage homogenate were quantified by the specific enzyme-linked immunosorbent assay (ELISA) kit, according to the manufacturer's instructions (Cayman Chemical, Ann Arbor, MI, USA). Briefly, 10 μ L homogenates were added to 96-well microplates previously sensitized with specific antibodies against PGE2. Prostaglandin levels were determined by spectrophotometry at 412 nm [29].

(4) *N-Acetylglucosaminidase Activity.* The activation of the RAW264.7 cells was measured based on the quantification of N-acetyl- β -D-glucosaminidase (NAG) activity, which is a lysosomal enzyme intensely produced by activated monocytes/macrophages [30]. The N-acetyl- β -D-glucosaminidase activity was measured in skin homogenate by using a commercial biochemical colorimetric kit, according to the manufacturer's instructions (Abcam, Cambridge, UK). This assay uses a synthetic p-nitrophenol derivative (R-pNP) as a NAG substrate and releases pNP, which is measured by spectrophotometry, at 400 nm.

2.2. In Vivo Assays

2.2.1. *Animals and Ethics.* Fifteen healthy three-month-old male Wistar rats (*Rattus norvegicus*) (339.16 ± 16.25 g) were obtained from the Central House of the health and Biological Sciences Center, Federal University of Viçosa. These animals

were randomly allocated in individual cages, which were cleaned daily and maintained under controlled environmental conditions (temperature: $22 \pm 2^\circ\text{C}$, humidity: 60–70%, and light/dark cycle: 12/12 h). Commercial food and water were provided *ad libitum*. All the experiments were approved by the Animal Ethics Committee of the Federal University of Viçosa (registration no. 72/2017).

2.2.2. *The Procedure of Surgical Wounds.* The rats were anesthetized with an intraperitoneal injection of sodium pentobarbital (70 mg/kg). After anesthesia, the dorsolateral shaving of the animals was performed, and the area was cleaned with 70% alcohol. Three circular skin wounds of 12 mm diameter were created in the dorsolateral region of each rat by secondary intention, with surgical excision of the skin and subcutaneous cellular tissue using surgical scissors. The area of the wound was marked with violet crystal and measured with an analog caliper (Mitutoyo Sul Americana Ltda®, São Paulo, Brazil) [31]. No analgesia was administered after the surgical procedure since the application of drugs can alter cell migration and proliferation and compromise the skin repairing process. Tissue samples were obtained from different wounds at 7, 14, and 21 days, for histological and biochemical analyses, as presented in Figure 1.

2.2.3. *Experimental Design.* The animals were randomized into three groups, with five animals in each group: C (distilled water, control); Dx1 (doxycycline 10 mg/kg/day), and Dx2 (doxycycline 30 mg/kg/day). The treatments were administered by gavage for 21 days. After this period, the animals were euthanized by cardiac puncture and exsanguination, after an anesthetic procedure. The doses were provided according to studies that used oral Dx for corneal reepithelialization in the rabbit model [32], and Dx was given by gavage to inhibit MMP-mediated vascular changes in

hypertension in rats [33]. They found that many animals died after 100 mg/kg daily, thus suggesting that the therapeutic window for doxycycline may be rather narrow. Therefore, we decided to study the effects associated with the 10 and 30 mg/kg dose, because studies have not reported harmful effects on animals.

2.2.4. Calculation of the Area and the Rate of Wound Contraction. The area and rate of contraction of the third wound were evaluated every 7 days, using images scanned with 320×240 pixels (24 bits/pixel) obtained by an Asus Zenfone 2 ZE551ML smartphone (ASUS, Taipei, Taiwan). The wound area was calculated by the formula $A = \pi \times (r)^2$, where r is the radius. The wound contraction index (WCI) was calculated by the ratio: initial wound area (A_0) – the area on a given day (A_i)/initial wound area (A_0) $\times 100$ [34, 35].

2.3. Histological and Stereological Analysis. The samples collected from the wounds, with tissue from the center of the lesion, were immersed in histological fixative for 24 h, dehydrated in ethanol, diaphanized in xylene, and immersed in paraffin. Histological sections ($4 \mu\text{m}$ thick) were obtained on a rotary microtome (Leica Multicut 2045, Reichert-Jung Products, Germany). We used 1 of every 20 sections to avoid repeating the analysis of the same histological area. The sections were stained with hematoxylin and eosin (HE) for the analysis of the fibroblasts and blood vessels [31]. Furthermore, the samples were stained with Sirius red for the analysis of collagen fiber types I and III [36]. Toluidine blue was used to identify mast cells [37], and Verhoeff was used to differentiate elastic fibers [14]. The slides were visualized and captured in a BX601 light microscope (Olympus, São Paulo, Brazil) coupled with a QColor-31 digital camera (Olympus, São Paulo, Brazil). Five images were selected at random using a 20x objective lens. For this analysis, a grid containing 256 points within a standard test area (AT) of $73 \times 10^3 \mu\text{m}^2$ was superimposed over each image. The stereological parameters of volumetric density (V_v) were calculated by counting the points that occurred over cells, blood vessels, types I and III collagen, and elastic fibers, using the ratio: $V_v = \text{PP}/\text{PT}$, where PP is the number of points occurring over the structures of interest and PT is the total number of points on the test system [31, 38]. Collagen fibers were analyzed according to the different properties of birefringence, as thick collagen fibers (type I) appear in shades of bright colors ranging from red to yellow, whereas thin reticular fibers (collagen type III) appear bright green under polarization [31, 39]. The mast cells were analyzed using a 40x objective lens. Ten microscopical fields were randomly analyzed in each histological section to obtain a total area (TA) of 1.96 mm^2 . The number of mast cells per unit of histological area was calculated according to the relation $\text{QA} = \Sigma \text{ mast cells}/\text{TA}$ [40].

2.4. COX-2 Immunohistochemistry. The histological sections ($4 \mu\text{m}$ thick) were dewaxed with xylene and hydrated in distilled water. Antigen recovery was performed with citrate buffer (pH 6) in a pressure cooker for 4 min. The sections were incubated for 10 min in 3% hydrogen peroxide to block endogenous peroxidase, followed by 15 min in 5% nonfat

milk prepared at pH 7.6 TBST (1X Tris-buffered saline with 0.05% Tween 20). Then, the sections were incubated for 12 h, at 4°C , with a primary rabbit anti-COX-2 antibody (ab15191, Abcam, Cambridge, UK), at 1 : 1000 dilution. The slides were washed with TBST and incubated for 2 h at room temperature, with a ready-to-use secondary goat anti-rabbit IgG antibody conjugated with horseradish peroxidase (Dako EnVision™+ Dual Link System-HRP, Agilent, Santa Clara, CA, USA). The slides were washed with TBST, and the COX-2 marking was revealed with 0.5% 3,3'-diaminobenzidine for 5 min. Finally, the slides were released in ethanol, treated with xylene, and mounted with coverslips.

2.5. Biochemical Assays. Tissue fragments were collected from each wound, immediately frozen in liquid nitrogen (-196°C), and stored in a freezer at -80°C . The samples (200 mg) were homogenized in 2 mL phosphate-buffered saline (PBS) and centrifuged for 5 minutes at $10,000g$, under refrigeration, at 5°C [14]. The supernatant and tissue pellets were separately collected and used in all biochemical analyses described below.

2.5.1. Cyclooxygenase-2, N-Acetylglucosaminidase Activity, and Prostaglandin Production. Cyclooxygenase-2, N-acetylglucosaminidase activity, and prostaglandin E2 production in the scar tissue were measured with the aid of the same commercial kits used to quantify these parameters in the *in vitro* model. All measures were performed from intact skin (day 0) and scar tissue collected at days 7, 14, and 21 of wound healing. The enzymatic activity and prostaglandin levels were measured in tissue homogenate supernatant.

2.5.2. Hydrogen Peroxide and Nitric Oxide Production. The hydrogen peroxide (H_2O_2) production was measured in supernatants of tissue homogenates. $50 \mu\text{L}$ of supernatants were incubated with $50 \mu\text{L}$ of α -Phenylenediamine dihydrochloride (OPD) and an equal volume of peroxidase type II 15 mmol/L. The conversion of absorbance into micromolar concentrations of H_2O_2 was calculated based on a standard curve, using a known concentration of H_2O_2 . The results were expressed as $\mu\text{mol}/\text{L}$ [41].

Nitric oxide (NO) was indirectly quantified through the detection of nitrite/nitrate ($\text{NO}_2^-/\text{NO}_3^-$) levels by the standard Griess reaction [42]. $50 \mu\text{L}$ of supernatants were incubated with an equal volume of Griess reagent (1% sulfanilamide, 0.1% N-(1-Naftil) ethylenediamine, and 2.5% H_3PO_4) and kept at room temperature for 10 minutes. The conversion of absorbance into micromolar concentrations of NO was obtained from a sodium nitrite standard curve (0 – $125 \mu\text{M}$) and expressed as NO concentrations ($\mu\text{mol} \times \text{L}^{-1}$).

2.5.3. Determination of Lipid and Protein Oxidation. Lipid peroxidation (LPO) was estimated according to the total malondialdehyde levels (MDA) [43]. The MDA concentration was determined by using the standard curve of known concentrations of 1, 1, 3, 3-tetramethoxypropane (TMPO). The results were expressed as $\mu\text{mol} \times \text{L}^{-1}$ per mg of protein.

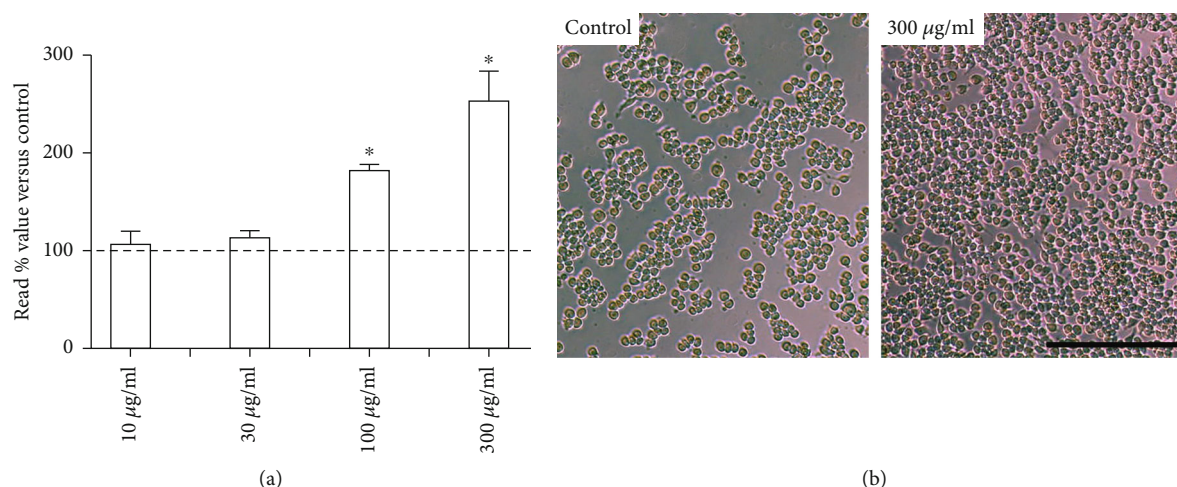


FIGURE 2: Effects of doxycycline hyclate (Dx) on cell viability. (a) RAW264.7 macrophages were treated with various doses of Dx (10, 30, 100, and 300 µg/mL) for 24 h. (b) Representative photomicrographs showing cells in cultured medium (control group) and 300 µg/mL Dx added to the medium (phase-contrast microscopy, bar = 200 µm). The results are presented as the percentage absorbance of the control group. The data are expressed in the graphics as a mean and standard deviation. *Statistical difference compared to control cells (Student-Newman-Keuls test, $p < 0.05$).

Protein oxidation was estimated from protein carbonyl content, which was measured using 2,4-dinitrophenylhydrazine (DNPH) [44], based on the carbonyl group reaction with DNPH. The pellets resulting from the tissue homogenates from previous extractions were used for quantification. The results were expressed as nmol per mL of protein.

2.5.4. Superoxide Dismutase Activity. The activity of superoxide dismutase (SOD) was determined by the superoxide (O_2^-) and hydrogen peroxide reduction method, thereby decreasing the autooxidation of pyrogallol [45]. SOD activity was calculated as units per milligram of protein, with one unit (U) of SOD defined as the amount that inhibited the rate of pyrogallol autooxidation by 50%.

2.5.5. Catalase Activity. The catalase (CAT) activity was evaluated according to the method described by Aebi [46], by measuring the rate of decomposition of hydrogen peroxide. One unit of CAT activity was calculated using the number of enzymes that decompose 1 mmol H_2O_2 for 1 min. The results were expressed as units of catalase/milligram of protein.

2.5.6. Glutathione S-Transferase Activity. The glutathione S-transferase (GST) activity was measured using the method of Habig et al. [47]. Glutathione S-transferase activity was analyzed according to the formation of glutathione-conjugated 2,4-dinitrochlorobenzene (CDNB). One unit of GST activity was defined as the amount of enzyme that catalyzed the formation of one µmol of product/min/mL. GST activity was expressed as U per milligram of protein.

2.5.7. Evaluation of MMP-10 Cutaneous Activity. For the evaluation of MMP-10 activity, 200 mg samples of the skin were homogenized in 1 mL of 5 mM Tris-HCl (pH 7.4) buffer containing 0.15 M NaCl, 10 mM $CaCl_2$, and 0.02% NaN_3 . After centrifugation at 10,000g for 30 min, the supernatant was collected for analysis of MMP activity. For such, an

ELISA commercial immunoenzymatic kit was used according to the manufacturer's instructions (Sigma-Aldrich; Merck KGaA, Darmstadt, Germany).

2.6. Statistical Analysis. The statistical analysis was carried out using the GraphPad Prism 7 software system (GraphPad Software Inc., San Diego, Calif., USA). The results were expressed as mean and standard deviation (mean ± SD). The parametric data were compared using one-way ANOVA variance analysis, followed by the Student-Newman-Keuls *post hoc* test. The nonparametric data were compared using the Kruskal-Wallis test. Statistical significance was established at $p \leq 0.05$.

3. Results

3.1. Impact of Dx on Macrophage Viability, Prostaglandin Production, and COX-2, MMP, and NAG Activity. The effect of Dx on macrophage viability is presented in Figure 2. No cytotoxicity was observed after exposing the macrophages to Dx. Furthermore, the highest cell proliferation was observed after macrophage incubation with 100 µg/mL (182.03 ± 6.57) and 300 µg/mL (253.05 ± 30.92) of Dx, which indicates a clear dose-dependent effect (Figures 2(a) and 2(b)).

In the *in vitro* analysis, Dx also reduced glycoprotein cyclooxygenase-2 (COX-2) in the Dx100 group when compared to CM, Dx10, and Dx30. The Dx300 group presented reduced COX2, in relation to NC, CM, Dx10, Dx30, and Dx100. The prostaglandin E2 levels were higher in CM and Dx (10, 30, and 100), when compared to the NC group. Dx100 presented a decrease in relation to CM, Dx10, and Dx30. Dx300 presented a decrease when compared to NC, CM, and Dx (10, 30, and 100). Metalloproteinases (MMP) presented a decrease in the CM, Dx10, Dx30, and Dx100 groups when compared to the NC group. The Dx100 group values were lower, compared to the CM, Dx10, and Dx30

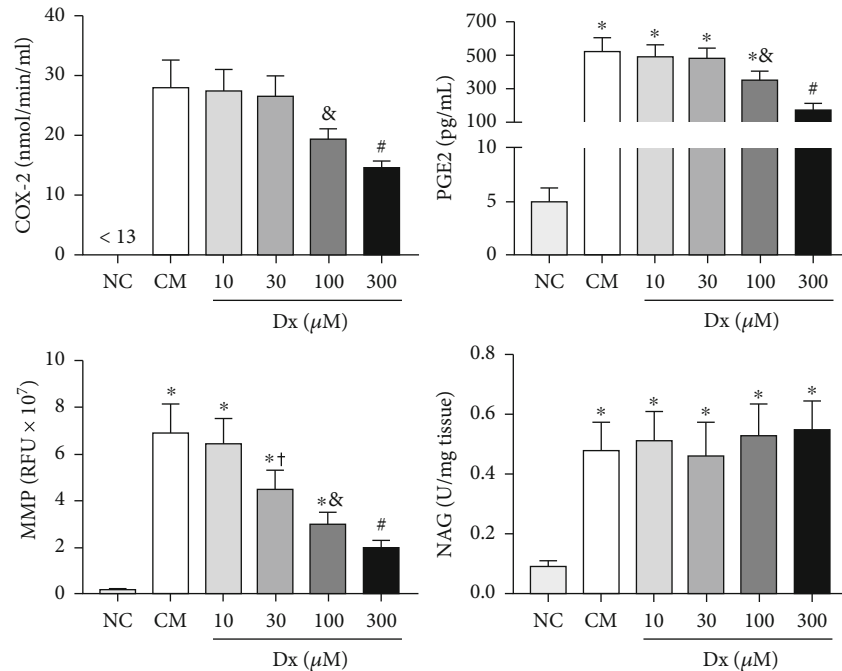


FIGURE 3: Effects of doxycycline hyclate (Dx) on cyclooxygenase-2 (COX-2), prostaglandin E2 production, and metalloproteinases (MMP) and N-acetyl- β -D-glucosaminidase (NAG) activity in LPS-stimulated RAW264.7 macrophages treated with various doses of Dx for 24 h. NC: not stimulated cells (not treated with LPS or Dx), CM: cells treated with culture medium containing LPS, and Dx: cells treated with culture medium containing LPS and Dx at 10, 30, 100, and 300 μM . The data are expressed as mean and standard deviation. Statistical difference (Student-Newman-Keuls test, $p < 0.05$), compared to *NC, &CM, Dx10, and Dx30, #NC, CM, and Dx (10, 30, and 100), and + CM and Dx10.

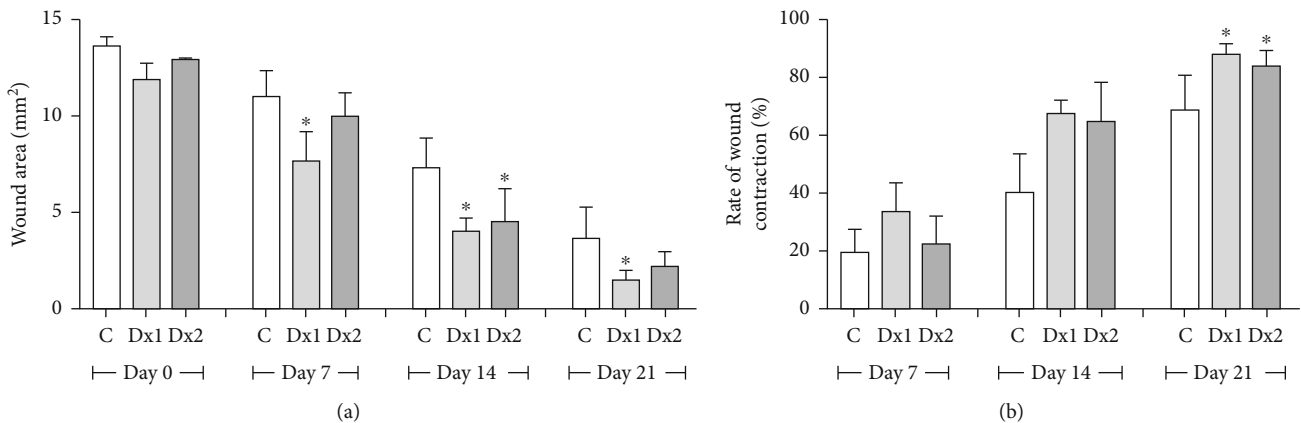


FIGURE 4: (a) Area (mm^2) and (b) rate of wound contraction (%) in rats treated with doxycycline hyclate (Dx) after 7, 14, and 21 days of treatment. Dx1: doxycycline hyclate (10 mg/kg), Dx2: doxycycline hyclate (30 mg/kg). The data are expressed as mean and standard deviation. Statistical difference (Kruskal-Wallis test, $p < 0.05$) compared to the *control group.

groups. The Dx300 group presented lower values when compared to NC, CM, and Dx (10, 30, and 100). The NAG values were increased in all groups (CM, Dx10, Dx30, Dx100, and Dx300) when compared to the NC group (Figure 3).

3.2. Wound Area and Contraction Index. The wound area was smaller on days 7, 14, and 21 in the Dx1 group, compared to the control animals, as well as on day 14, in the Dx2 group, in relation to the control group. The rate of wound contraction was higher in the Dx1 and Dx2 groups, compared to the control group, on day 21 (Figure 4).

3.3. Histopathological Results. On day 7, the proportion of total cells in the tissue was higher in the Dx2 group, compared to other groups. On the same day, Dx1 showed a higher proportion of cells, compared to the control group. On day 14, Dx2 presented a higher proportion of cells in relation to the control group (Figure 5(a)). In relation to blood vessels, Dx1 and Dx2 groups showed an increased proportion of vessels when compared to the control group, on day 7. However, on day 14, the proportion of vessels was reduced in the Dx1 group, compared to the control animals. On day 21, Dx1 presented reduced blood vessels compared to the

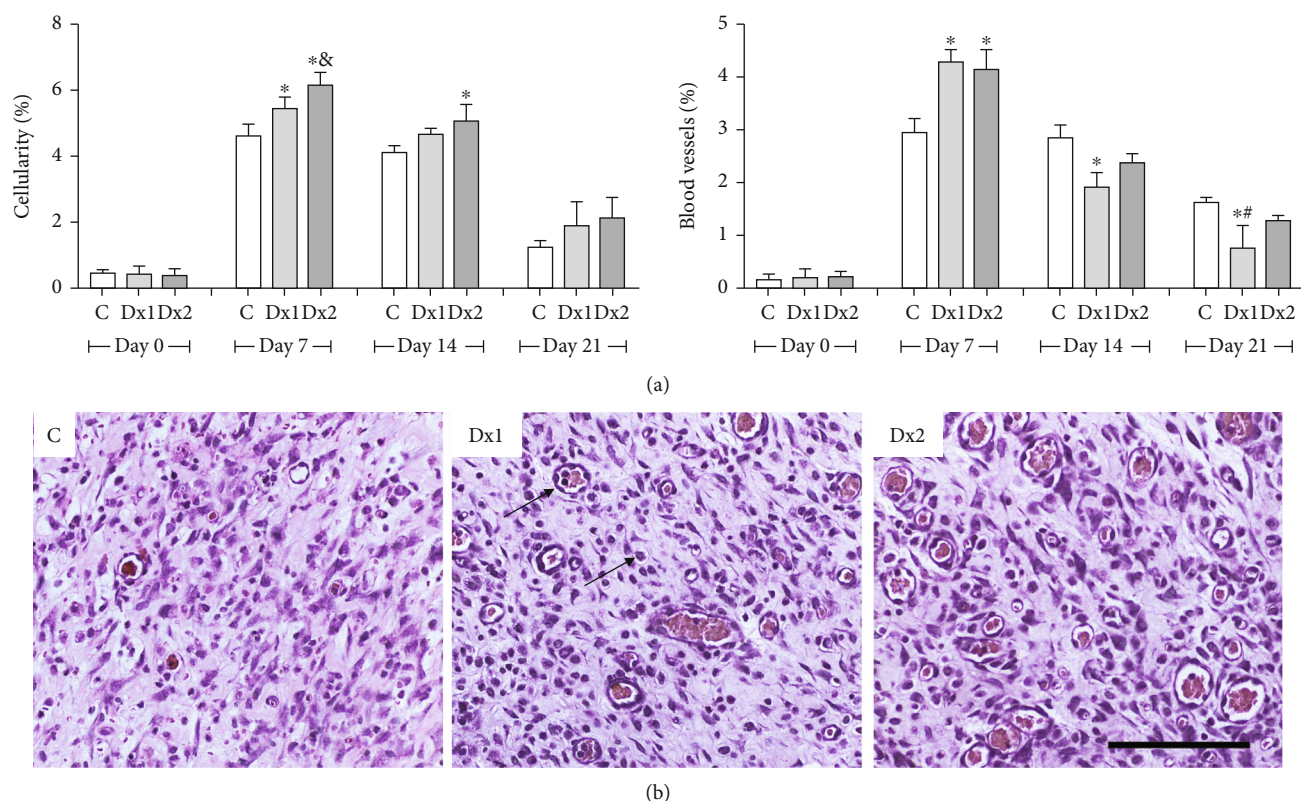


FIGURE 5: The proportion of cell nucleus and blood vessels (a) and representative photomicrographs showing cells and blood vessel distribution (b) in the scar tissue of rats untreated and treated with doxycycline hyclate (Dx), on day 7 (H&E staining, bar = 100 μ m). C: control, Dx1 = 10 mg/kg Dx, and Dx2 = 30 mg/kg Dx. In the graphics, the data are represented as mean and standard deviation. The statistical difference compared to the groups *C, &Dx1, and #Dx2 (Student-Newman-Keuls test, $p < 0.05$).

control and Dx2 groups (Figure 5(a)). The distribution of cells and blood vessels in the scar tissue of the different groups is shown in Figure 5(b).

The number of mast cells, on day 7, was higher in the Dx2 group, compared to the other groups. In addition, the Dx1 group presented a higher number of cells compared to the control group (Figure 6(a)). The distribution of mast cells in the scar tissue in the Dx2 group, on day 7, is shown in Figure 6(b).

A higher proportion of type I collagen fibers were observed in the groups treated with Dx1 and Dx2, on day 21, when compared to the control group. The type III collagen fibers were reduced in Dx1 and Dx2, on day 21, in comparison to the control group (Figure 7(a)). The distribution of type I and type III fibers in the scar tissue of the different groups and the predominance of type I collagen fibers after treatment with Dx are shown in Figure 7(b). On days 14 and 21, the number of elastic fibers was higher in the Dx2 group, compared to the other groups (Figure 7(c)). The representative distribution of elastic fibers in the scar tissue in the Dx2 group, on day 21, is shown in Figure 7(d).

3.4. Biochemical Results

3.4.1. Immunohistochemistry and COX-2, PGE2, and NAG Activity. Figures 8(a) and 8(b) show the results of the COX-2 analysis, which presented lower values in the Dx2 group

when compared to control and Dx1, on day 7. These results were confirmed by the analysis of the photomicrographs, showing decreased COX-2 expression in Dx2, mainly in epithelial cells. In relation to PGE2, the Dx2 group showed lower values compared to the other groups, on day 7 (Figure 8(c)). The macrophage accumulation/activation was proven by increased NAG values in the Dx1 and Dx2 groups when compared to the control (Figure 8(d)).

3.4.2. Oxidative Stress Markers. On day 7, H_2O_2 levels were higher in the Dx1 and Dx2 groups in relation to the control group. On day 14, Dx2 showed lower H_2O_2 levels in relation to the control and Dx1 groups. On day 21, Dx2 showed lower levels of H_2O_2 , when compared to the control group (Figure 9(a)). Nitrite and nitrate levels were lower in the Dx1 and Dx2 groups, compared to the control group, on day 14 (Figure 9(b)). Concerning malondialdehyde, the levels were lower in the Dx1 and Dx2 groups, on day 7, when compared to the control (Figure 9(c)). On the other hand, reduced carbonyl protein levels were identified in the group Dx1, compared to the control group, on day 21 (Figure 9(d)).

3.4.3. Antioxidant Enzymes and Metalloproteinase-10. Superoxide dismutase activity was higher in the Dx1 group, on day 21, when compared to the Dx2 group (Figure 10(a)). Catalase activity was higher on days 7 and 14, in the Dx1 and Dx2 groups when compared to the control. On day 21, CAT

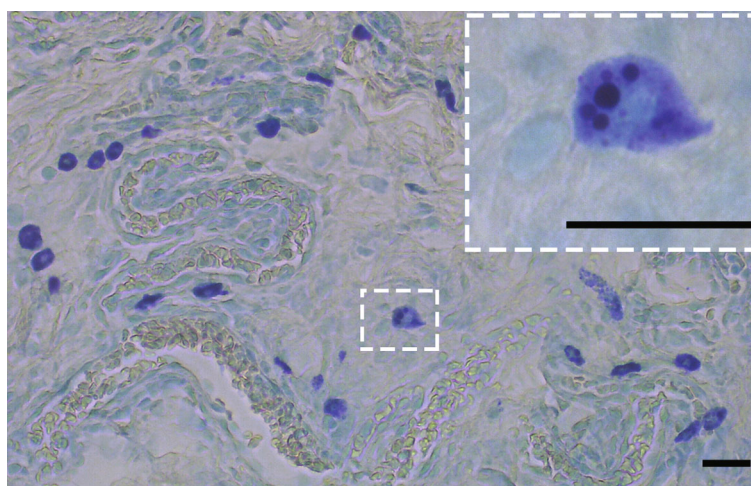
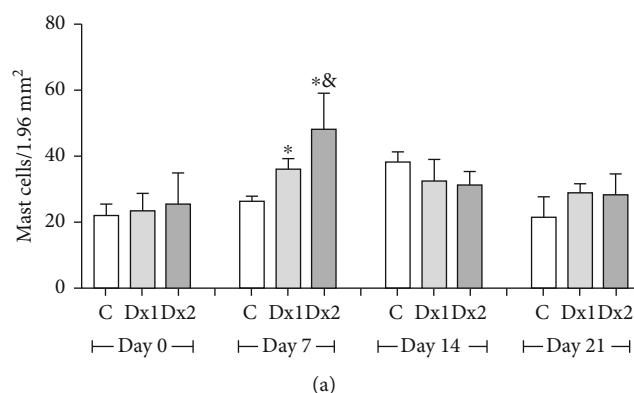


FIGURE 6: The number of mast cells (a) and representative photomicrograph showing mast cell distribution (b) in the scar tissue from a rat treated with doxycycline hyclate (Dx, group 2) on day seven of wound healing (Toluidine blue staining, bar = 50 μm). C: control, Dx1 = 10 mg/kg Dx, and Dx2 = 30 mg/kg Dx. Data represented as mean and standard deviation. In the graphics, the data are represented as mean and standard deviation. The statistical difference compared to the groups *C and &Dx1 (Student-Newman-Keuls test, $p < 0.05$).

activity was lower in Dx2, concerning the Dx1 group (Figure 10(b)). The glutathione S-transferase values were not significantly different over the trial period (Figure 10(c)). On day 14, MMP-10 levels were lower in the group Dx2 compared to Dx1. On day 21, both groups treated with Dx presented lower levels of MMP-10 when compared to the control group (Figure 10(d)).

4. Discussion

Doxycycline constitutes a large group of broad-spectrum antibiotics derived from tetracycline [48]. Studies have suggested that Dx presents therapeutic activities unrelated to its antimicrobial activity [49, 50]. The present study used an integrated cellular and tissue analysis to evaluate the effect Dx when administrated orally in Wistar rats, to repair their skin. Therefore, we observed that Dx was effective for complete wound closure and increased the rate of wound contraction. This effect is possibly associated with Dx antimicrobial and anti-inflammatory capacity [49, 51]. These results showed that Dx has beneficial action for the treatment of skin lesions. However, studies investigating the action of this drug on cutaneous repair are still scarce and limited,

mainly when related to its antioxidant capacity. In a recent systematic review, we found positive results of antibiotic therapy for the treatment of cutaneous wounds. However, there is limited evidence that Dx can exert beneficial effects on the treatment of skin lesions *in vivo* [52]. In this review, sulfonamides were the antibiotic most commonly used, and doxycycline was tested in only one study [52]. As the main mechanisms involved in the cutaneous repair after Dx exposure remain unknown, studies using immunological, biochemical, and oxidative markers are required.

Due to its potent bacteriostatic properties, Dx is an effective antibiotic to treat diseases, such as syphilis [23], periodontal diseases [24], pneumonia [53], and cholera [54]. Although the effect of Dx on cutaneous repair is still poorly explored, this drug increases collagen deposition [55], stimulates tissue reepithelization [20] and favors the elimination of reactive oxygen species, thereby preventing or reducing pathological tissue destruction [56]. In addition, Dx changes the proliferation of inflammatory cells [57]. In this sense, we observed that Dx increased macrophages proliferation *in vitro*, exerting a potential dose-dependent immunoregulatory activity. This effect was aligned with increased macrophage activation, which was indicated by the upregulation

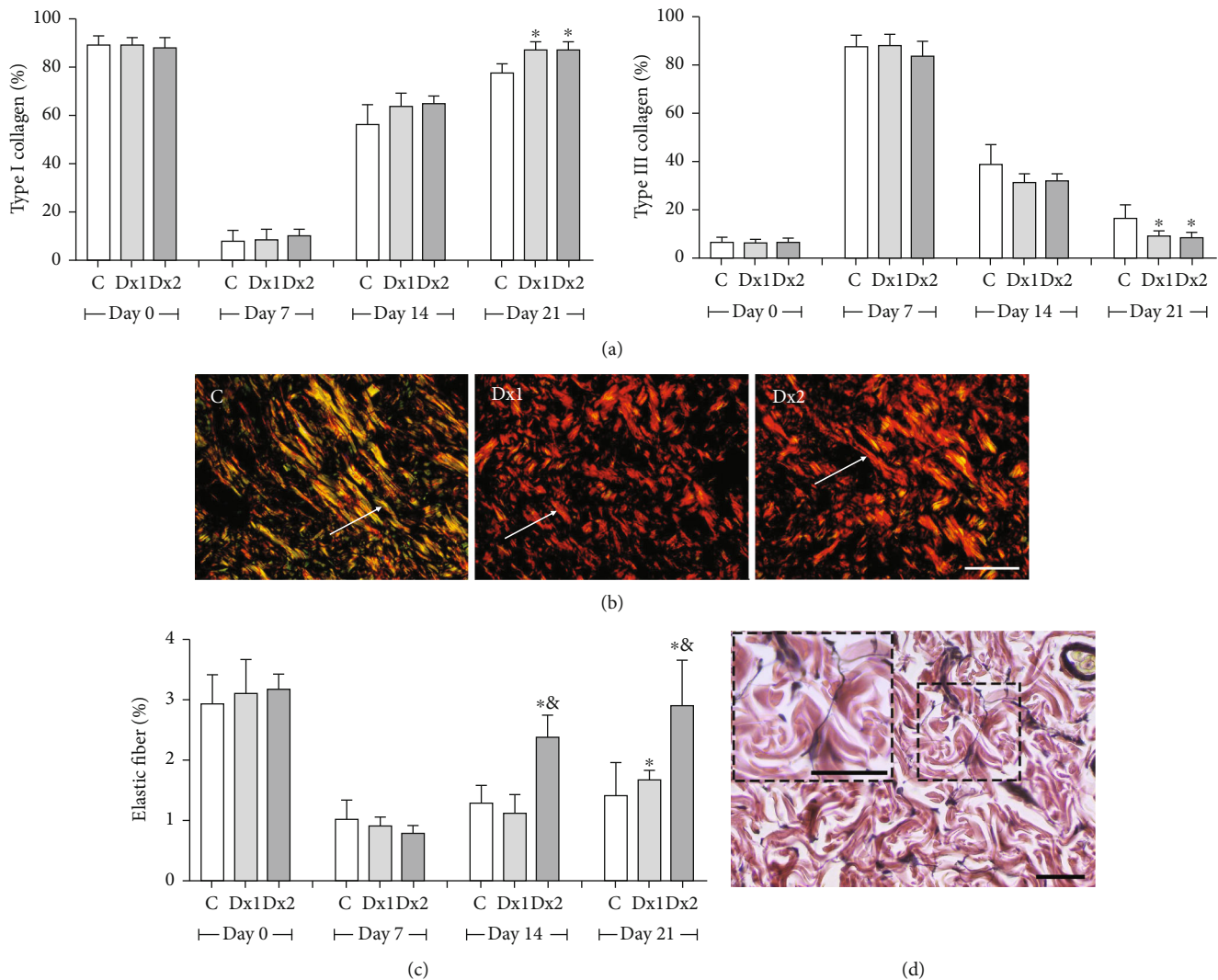


FIGURE 7: The proportion of type I and III collagen fibers (a), representative photomicrographs showing collagen fiber distribution, on day 21 (b) Sirius red staining under polarized light, bar = 100 μ m), the proportion of elastic fibers (c), and representative photomicrograph showing elastic fiber distribution in group Dx2, on day 21 (d) Verhoeff's elastic stain, bar = 50 μ m) in the scar tissue of rats untreated and treated with doxycycline hyclate (Dx). C: control, Dx = 10 mg/kg Dx, and Dx2 = 30 mg/kg Dx. In the graphics, the data are represented as mean and standard deviation. The statistical difference compared to the groups *C and &Dx1 (Student-Newman-Keuls test, $p < 0.05$).

of NAG activity induced by all doses of Dx. Conversely, Dx-treated macrophages exhibited a dose-dependent decrease in COX-2 and PGE2 levels, which indicates that macrophage activation and COX-2 inhibition are regulated by Dx through potentially independent mechanisms, which requires further investigation. However, there is evidence that different drugs with antimicrobial and anti-inflammatory properties such as nimesulide, ibuprofen, and amoxicillin can differentially regulate macrophages activity (i.e., endocytosis and nitric oxide production) and cytokine and prostaglandin secretion [58–60], which corroborates relative independence of these metabolic processes. Thus, this specific effect of Dx on COX-2 and macrophage activity is potentially relevant in wound healing, since it can modulate the intensity of the inflammatory response without inhibiting cell activation in response to antigenic stimulation, which exerts an essential protective role against infections.

In addition, our results also revealed an increased overall amount of scar tissue cells, highlighted by a high amount of mast cells. This was mainly observed when we used higher doses of Dx and in the early stages of the healing process. Mast cells are important for the inflammation phase of the repair process, as they promote the activation of macrophages and the formation of granulation tissue, cell migration, and maturation of collagen fibers [61]. Therefore, we believe that Dx can stimulate the process of cell migration and speed up the closure of the wound and consequently decrease the risk of infection. On the other hand, we observed that Dx stimulates an increase in the proportion of type I collagen, associated with a low proportion of type III collagen, after 21 days of treatment. These characteristics are very important since a high proportion of type I collagen fibers increases tissue resistance and force [62]. These collagen fibers exhibit covalent bonds and are more common in intact

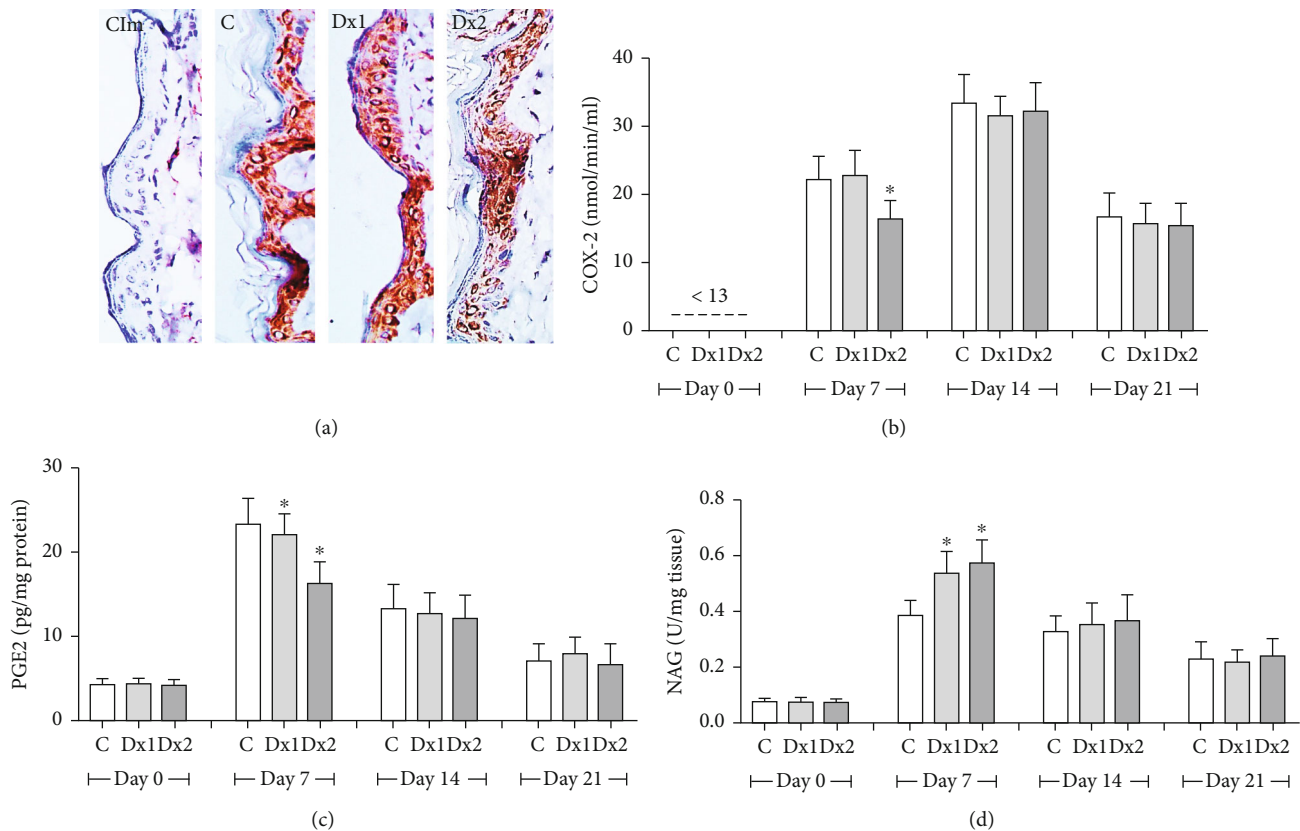


FIGURE 8: Immunohistochemical detection of cyclooxygenase-2 (COX-2) in the epithelial cells (a), COX-2 activity (b), prostaglandin E2 (PGE2) levels (c), and N-acetyl- β -D-glucosaminidase (NAG) activity (d) in the scar tissue from rats untreated and treated with doxycycline hyclate (Dx). Cim: control of the immunohistochemical method (the primary antibody was omitted in the technique), C: control, Dx = 10 mg/kg Dx, and Dx2 = 30 mg/kg Dx. In the graphics, data are represented as mean and standard deviation. *Statistical difference compared to group C (Student-Newman-Keuls test, $p < 0.05$).

skin [63]. In general, at the start of the wound healing process, it is observed high deposition of type III collagen, but as the process progresses, the type III collagen fibers are replaced by type I collagen fibers [14], which makes the tissue more resistant to traction. About elastic fibers, after treatment with Dx, there was an increase in this fiber in the extracellular matrix in the scar tissue, especially in the final phase of tissue remodeling. Similarly, the role of Dx on elastic fibers was analyzed by Chung et al. [64], in the Marfan syndrome, in which Dx preserved the elastic fibers in the thoracic aorta, probably by inhibiting the action of metalloproteinases. Thus, our findings show the induction of the proliferative capacity of cells and, consequently, the synthesis of the extracellular matrix after the application of Dx.

Cellularity and neovascularization are essential to the process of wound healing, especially in the inflammatory phase [6]. A good vascularization can provide oxygen and nutrients for the cells, which are important for the recovery of injured tissue [65]. Besides, the formation of new vessels is directly linked to the formation of a new matrix, called granulation tissue, rich in vessels and cells. When the process advances, the number of vessels and cells decreases, but the number of fibers increases, which characterizes mature scar tissue [66]. Therefore, new effective treatments should promote intense neovascularization at the start of the repair pro-

cess and reduce the levels of vessels at the end of the process. For Altoé et al. [52], the tetracycline class represented by doxycycline increases collagen organization and, consequently, the rupture force of the wound. Corroborating the current evidence, our findings indicate that Dx stimulated the increase of new vessels at the start of the wound process (day 7) and the number of cells, possibly due to the intense migration and activation of the inflammatory cells proven by the increased NAG, at the same time. On the other hand, reduced vessels and cells were observed, while fibers increased in more advanced phases of the wound repair. These changes are very important for the evolution of wound healing and provide resistance and force for the new tissue.

Interestingly, Dx was also effective in attenuating COX-2 activity and PGE2 only in the initial stage of wound healing (day 7). As this inhibition occurred simultaneously to increased cellularity and NAG activity in the scar tissue, the main source of COX-2 activity and PGE2 seems to be unrelated to the increased recruitment of immune cells, including macrophages. Corroborating this proposition, we identified that animals treated with the higher dose of Dx presented a reduced COX-2 expression in the scar tissue, which was limited to epidermal cells. Thus, our findings indicated that keratinocytes are the primary targets of Dx-induced COX-2 downregulation, which represents an effect potentially

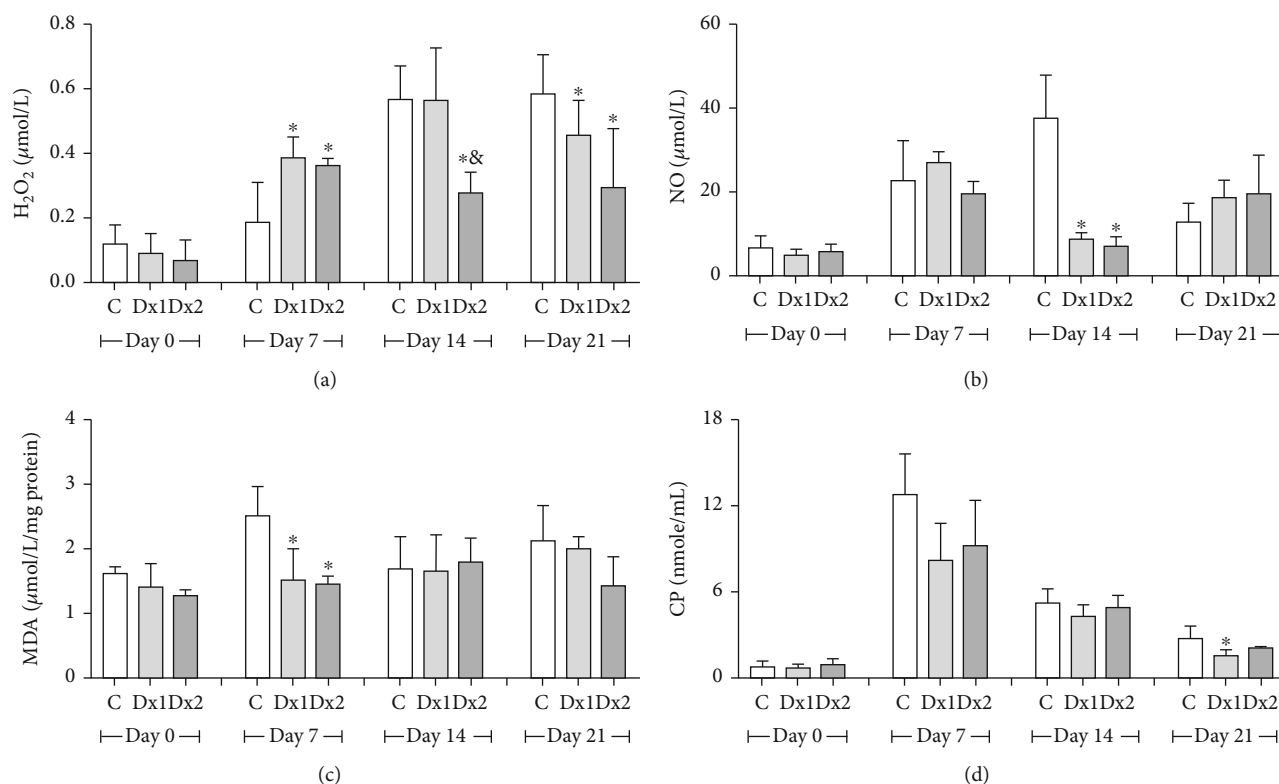


FIGURE 9: Levels of oxidative stress markers in the tissue: (a) hydrogen peroxide (H_2O_2), (b) nitrite and nitrate ($\text{NO}_2^-/\text{NO}_3^-$), (c) malondialdehyde (MDA), and (d) carbonyl proteins (CP) in the scar tissue of rats untreated and treated with doxycycline hyclate (Dx). C: control, Dx1 = 10 mg/kg Dx, and Dx2 = 30 mg/kg Dx. Data are represented as mean and standard deviation. The statistical difference compared to the group *C and &Dx1 (Student-Newman-Keuls test, $p < 0.05$).

limited to the initial stages of wound healing. From COX-2 activity, intense PG levels are detected after skin injuries, which are potent proinflammatory effectors that attract immune cells, stimulate fibroblast, and endothelial cell proliferation and metabolism in the wound area [11]. COX-2 played a central and regulatory role in the arachidonic acid pathway, by regulating hemostasis and inflammation [67] and directly impacting the development of the subsequent phases of wound healing [68]. Thus, controlling the inflammation from COX-2 downregulation may be a relevant strategy by which Dx accelerates the onset of the proliferative and remodeling phases, stimulating the resolution of the healing process. Since PG release mediated by COX-2 activation triggers prooxidant mechanisms, Dx potentially attenuates the oxidative stress as well, which can prolong the inflammatory phase due to secondary reactive molecular damage [49].

The production of intense free radicals is usually observed in the initial stages of the healing process. In skin lesions, phagocytic immune cells produce free radicals in a process known as respiratory burst [69]. Free radicals, reactive species of oxygen (ROS), and reactive species of nitrogen (RNS) promote cellular oxidative stress, damaging membranes, proteins, and genetic material [70, 71]. In respect to ROS, it is important to consider the presence of peroxide hydrogen (H_2O_2), known as an important marker of redox metabolism and more commonly found during the inflammatory phase of the healing process [72]. In our

study, as expected, the levels of H_2O_2 increased on the 7th day in the groups treated with Dx, corresponding to the inflammatory phase, but decreased in the later phases, on days 14 and 21, in the Dx₂ group. In this case, the excess of H_2O_2 probably occurred in the inflammatory phase, due to cell migration, of neutrophils and macrophages, which release mediators and reactive oxygen species during phagocytosis [73]. Also, we believe that, in this phase, the activation of nicotinamide adenine dinucleotide phosphate (NADPH) takes place, which generates H_2O_2 and activates cell proliferation and apoptosis. In our study, we believed that an increased number of macrophages, proven by *in vitro* and *in vivo* analysis of NAG, could justify the increased level of H_2O_2 in the early repair process. On the other hand, H_2O_2 and nitric oxide (NO) showed decreased levels during day 14, which indicates that Dx was efficient to inhibit lipid peroxidation and protein oxidation in the later phase of the process. However, the excess of NO may cause irreversible damage in the cells, impaired homeostasis, and the activation of various signaling cascades, such as mitogen-activated protein (MAP) or c-Jun N terminal kinase (JNK), thus causing cell degeneration and death [74]. In general, it is difficult to measure NO due to the short half-life in tissues. NO, nitrite (NO_2^-), and nitrate (NO_3^-) are the markers usually employed [75, 76]. As a result of this, in our study, we measured the content of nitrite and nitrate in the scar tissue of Wistar rats.

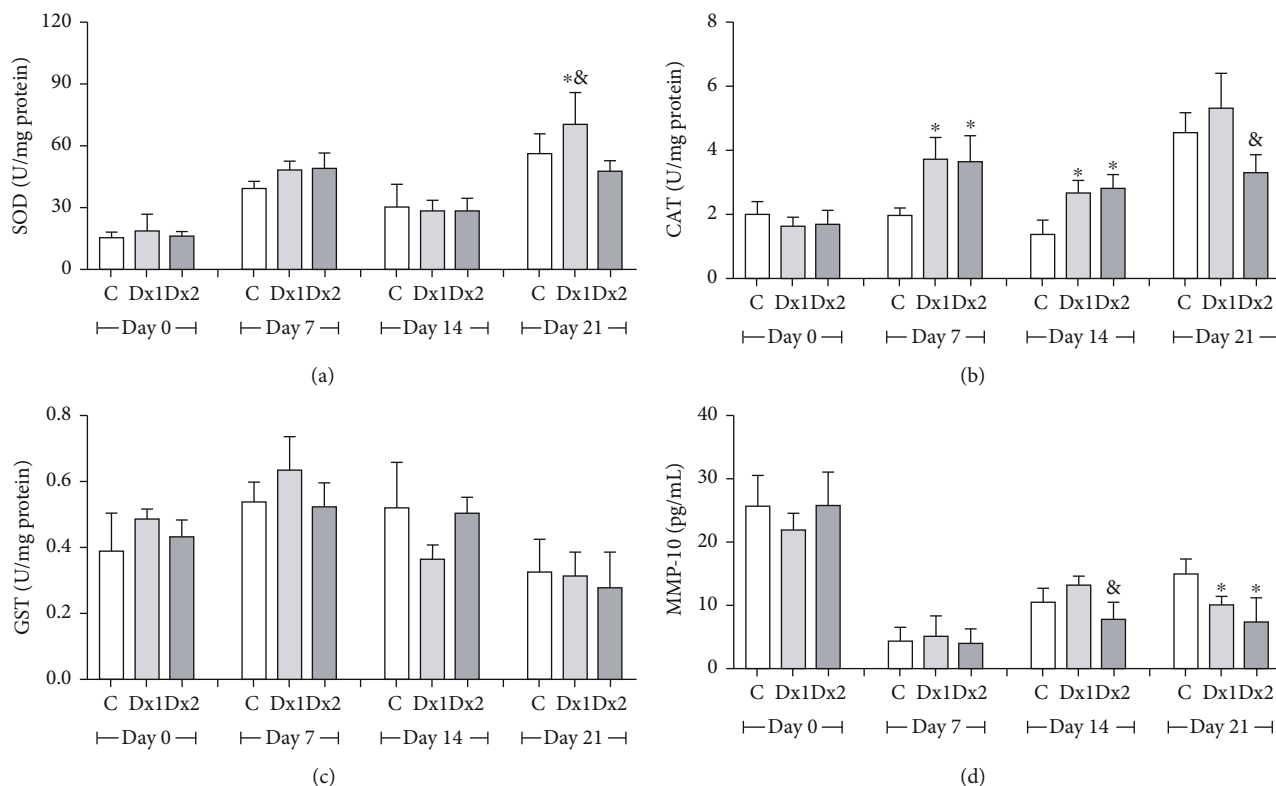


FIGURE 10: Levels of (a) superoxide dismutase (SOD), (b) catalase (CAT), (c) glutathione S-transferase (GST), and (d) metalloproteinase-10 (MMP-10) in the scar tissue of rats untreated and treated with doxycycline hyclate (Dx). C: control, Dx1 = 10 mg/kg Dx, and Dx2 = 30 mg/kg Dx. The data are represented as mean and standard deviation. The statistical difference compared to the group *C, &Dx1, and Dx2 (Student-Newman-Keuls test, $p < 0.05$).

Markers of oxidative stress are important tools to evaluate the redox balance of the healthy and damaged tissues [77]. MDA is a compound of three carbons synthesized from the peroxidation of polyunsaturated fatty acids, generally formed during the oxidation of the cell membrane lipids [78]. During cutaneous repair, MDA usually increases, mainly in the inflammatory phase, which indicates damaged tissue and slow wound closure [79]. In our study, we observed reduced levels of MDA on day 7, after treatment with Dx1 and Dx2, which indicates that doxycycline can help to positively modulate the redox status of tissue in recovery. Similar results were found by Nogueira et al. [80], after the induction of convulsive lesions, following the application of pilocarpine, a parasymphomimetic alkaloid extracted from jaborandi leaves. These authors showed that Dx reduced lipid peroxidation in the brain, thus protecting the tissue from the action of free radicals. Another important marker of the action of ROS and RNS in the tissue is the high content of carbonylated protein, which indicates protein oxidation [66, 81]. In the present study, after treatment with Dx, only using the lower dose, reduced levels of protein carbonylation were observed, suggesting the antioxidant secondary action of this drug. Serra et al. [82] evaluated the antioxidant action of doxycycline and demonstrated that this drug, as well as other tetracyclines, is similar to vitamin E, mainly due to the presence of a phenolic ring with multiple substitutions. This phenolic ring reacts with the free radical and generates a phenolic radical, which is relatively stable and not reactive

to cellular components [83]. In this sense, in addition to acting as an antimicrobial, Dx also presents antioxidant secondary action, which protects the recovering tissue.

To maintain redox homeostasis in an injured tissue the action of the antioxidant defense system is necessary, which exhibits components, such as superoxide dismutase (SOD), catalase (CAT), and glutathione S-transferase (GST) [84, 85]. SOD removes superoxide radical, which is highly dangerous and destructive for the cells [86]. CAT enzyme accelerates the passage of electron and reduces the residence of H_2O_2 inside the cells, consequently avoiding the harmful effect of this compound on the tissues [87]. This means that, for a drug to be considered effective to treat lesions caused by free radicals, it is highly desirable that it stimulates the transcription and translation of these antioxidant enzymes. Our findings demonstrated that Dx increases SOD and CAT activity in the tissue. Increased CAT was mainly found in the inflammatory phase, which corroborates our findings in relation to the levels of H_2O_2 . We believed that increased SOD and CAT reduced superoxide ion (O_2^-) and H_2O_2 , thus protecting the tissue.

The imbalance between collagen synthesis and degradation is a common feature in cutaneous lesions, mainly in infected wounds [88]. A common consequence of this imbalance is the formation of hypertrophic scars and keloid, which results in fibrosis and loss of tissue function [8]. MMPs are enzymes found in acute or chronic skin wounds, which regulate the deposition of collagen and degrade the extracellular

matrix, which is essential for wound reepithelization [19]. The excess of these enzymes may cause disorganization in the epithelium, cell-cell contact changes, and increased apoptosis of fibroblasts and keratinocytes [89]. In our study, we observed decreased levels of MMP in *in vivo* analysis, after treatment with Dx1 and Dx2, which corroborates our findings for decreased wound area and increased rate of wound contraction in these groups. For the healing process to occur smoothly and efficiently, a balance between the synthesis and degradation of collagen is required. If there is a predominance of MMP in the tissue, an exacerbated degradation of the extracellular matrix may occur, which compromises wound closure [19]. Other studies demonstrate that the administration of Dx speeds up the closure of cutaneous wounds by inhibiting MMP-9 [82] and accelerates the recovery of gastric wounds by inhibiting MMP-2 and H₂O₂ [90]. The balance in the synthesis of this enzyme is required for efficient cutaneous repair and can facilitate cellular migration and accelerate the recovery of the tissue.

5. Conclusions

Taken together, our findings indicate that both doses of Dx can modulate the repair of skin wounds in rats. However, in general, the best results in cellularity, mast cells, elastic fibers, hydrogen peroxide levels, and metalloproteinase-10 were observed after exposure to the highest dose of doxycycline hyclate (30 mg/kg). *In vitro*, our findings showed that Dx increased macrophage proliferation but decreased the COX-2 and PGE-2 levels. This indicates that macrophage activation and COX-2 inhibition are possibly regulated by independent mechanisms. Our findings showed that, *in vitro*, despite the increased in the number of cells in the initial phase of wound healing, there was a reduction in the expression of COX-2, which was limited to epidermal cells. Therefore, our results indicated that keratinocytes are the primary targets of Dx-induced COX-2 downregulation, and this capacity of modulating the intensity of the inflammatory response without inhibiting cell activation can play an important role in the favorable evolution of the healing process. In addition, since the COX-2 is involved in prooxidant mechanisms, the regulation of this pathway by Dx also favored the oxidative balance into the cell and protected the molecules against the action of free radicals, showing an antioxidant potential in cutaneous wound repair. This information may be relevant for the selection of the treatment, mainly in the acute phase of cutaneous wound healing.

Data Availability

The data used to support the findings of this study are available from the corresponding author upon request.

Conflicts of Interest

The authors declare that there are no conflicts of interest regarding the publication of this manuscript.

Acknowledgments

The authors are grateful to the support provided by the Fundação do Amparo à Pesquisa do Estado de Minas Gerais (FAPEMIG, processes APQ-01895-16, PPM-00687-17, and PPM-00077-18), Conselho Nacional de Desenvolvimento Científico e Tecnológico (CNPq, processes 303972/2017-3, 423594/2018-4, 305093/2017-7, and MCTIC 408503/2018-1), and Coordenação de Aperfeiçoamento de Pessoal de Nível Superior, Brazil (CAPES, finance code 001).

References

- [1] L. Marrot, "Pollution and sun exposure: a deleterious synergy. mechanisms and opportunities for skin protection," *Current Medicinal Chemistry*, vol. 25, no. 40, pp. 5469–5486, 2019.
- [2] T. Dai, Y. Huang, S. K. Sharma, J. T. Hashmi, D. B. Kurup, and M. R. Hamblin, "Topical antimicrobials for burn wound infections," *Recent Patents on Anti-Infective Drug Discovery*, vol. 5, no. 2, pp. 124–151, 2010.
- [3] J. M. Badia, A. L. Casey, N. Petrosillo, P. M. Hudson, S. A. Mitchell, and C. Crosby, "Impact of surgical site infection on healthcare costs and patient outcomes: a systematic review in six European countries," *Journal of Hospital Infection*, vol. 96, no. 1, pp. 1–15, 2017.
- [4] C. K. Sen, "Human wounds and its burden: an updated compendium of estimates," *Advances in Wound Care*, vol. 8, no. 2, pp. 39–48, 2019.
- [5] S. Sarabahi, "Recent advances in topical wound care," *Indian Journal of Plastic Surgery*, vol. 45, no. 2, pp. 379–387, 2012.
- [6] J. Larouche, S. Sheoran, K. Maruyama, and M. M. Martino, "Immune regulation of skin wound healing: mechanisms and novel therapeutic targets," *Advances in Wound Care*, vol. 7, no. 7, pp. 209–231, 2018.
- [7] R. G. Frykberg and J. Banks, "Challenges in the treatment of chronic wounds," *Advances in Wound Care*, vol. 4, no. 9, pp. 560–582, 2015.
- [8] M. Xue and C. J. Jackson, "Extracellular matrix reorganization during wound healing and its impact on abnormal scarring," *Advances in Wound Care*, vol. 4, no. 3, pp. 119–136, 2015.
- [9] R. V. Gonçalves, R. D. Novaes, M. M. Sarandy et al., "5 α -Dihydrotestosterone enhances wound healing in diabetic rats," *Life Sciences*, vol. 152, pp. 67–75, 2016.
- [10] S. A. Eming, P. Martin, and M. Tomic-Canic, "Wound repair and regeneration: mechanisms, signaling, and translation," *Science Translational Medicine*, vol. 6, no. 265, p. 265sr6, 2014.
- [11] S. A. Abd el-Aleem, S. Abdelwahab, H. AM-Sherief, and A. Sayed, "Cellular and physiological upregulation of inducible nitric oxide synthase, arginase, and inducible cyclooxygenase in wound healing," *Journal of Cellular Physiology*, vol. 234, no. 12, pp. 23618–23632, 2019.
- [12] I. Dalle-Donne, A. Scaloni, D. Giustarini et al., "Proteins as biomarkers of oxidative/nitrosative stress in diseases: the contribution of redox proteomics," *Mass Spectrometry Reviews*, vol. 24, no. 1, pp. 55–99, 2005.
- [13] M. Mittal, M. R. Siddiqui, K. Tran, S. P. Reddy, and A. B. Malik, "Reactive oxygen species in inflammation and tissue injury," *Antioxidants & Redox Signaling*, vol. 20, no. 7, pp. 1126–1167, 2014.
- [14] M. M. Sarandy, L. L. Miranda, L. S. Altoé et al., "Strychnos pseudoquina modulates the morphological reorganization of

- the scar tissue of second intention cutaneous wounds in rats," *PLoS One*, vol. 13, no. 4, article e0195786, 2018.
- [15] C. Bonnans, J. Chou, and Z. Werb, "Remodelling the extracellular matrix in development and disease," *Nature Reviews Molecular Cell Biology*, vol. 15, no. 12, pp. 786–801, 2014.
- [16] B. Yue, "Biology of the extracellular matrix," *Journal of Glaucoma*, vol. 23, 8 Suppl 1, pp. S20–S23, 2014.
- [17] P. Lu, K. Takai, V. M. Weaver, and Z. Werb, "Extracellular matrix degradation and remodeling in development and disease," *Cold Spring Harbor Perspectives in Biology*, vol. 3, no. 12, pp. 1–24, 2011.
- [18] P. Rousselle, F. Braye, and G. Dayan, "Re-epithelialization of adult skin wounds: Cellular mechanisms and therapeutic strategies," *Advanced Drug Delivery Reviews*, vol. 146, pp. 344–365, 2019.
- [19] M. P. Caley, V. L. C. Martins, and E. A. O'Toole, "Metalloproteinases and wound healing," *Advances in Wound Care*, vol. 4, no. 4, pp. 225–234, 2015.
- [20] G. Simona, B. Buchanan, A. Kundu et al., "Stability, activity, and application of topical doxycycline formulations in a diabetic wound case study," *Wounds : a compendium of clinical research and practice*, vol. 31, pp. 49–54, 2019.
- [21] J. Stechmiller, L. Cowan, and G. Schultz, "The role of doxycycline as a matrix metalloproteinase inhibitor for the treatment of chronic wounds," *Biological Research For Nursing*, vol. 11, no. 4, pp. 336–344, 2010.
- [22] R. Di Caprio, S. Lembo, L. Di Costanzo, A. Balato, and G. Monfrecola, "Anti-inflammatory properties of low and high doxycycline doses: an in vitro study," *Mediators of Inflammation*, vol. 2015, 10 pages, 2015.
- [23] T. Dai, R. Qu, J. Liu, P. Zhou, and Q. Wang, "Efficacy of doxycycline in the treatment of syphilis," *Antimicrobial Agents and Chemotherapy*, vol. 61, no. 1, 2017.
- [24] S. Spasovski, Z. Belazelkoska, M. Popovska et al., "Clinical therapeutic effects of the application of doxycycline in the treatment of periodontal disease," *Open Access Macedonian Journal of Medical Sciences*, vol. 4, no. 1, pp. 152–157, 2016.
- [25] D. A. Barbie and B. K. Kennedy, "Doxycycline: new tricks for an old drug," *Oncotarget*, vol. 6, no. 23, pp. 19336–19337, 2015.
- [26] Y. Liu, W. Su, S. Wang, and P. Li, "Naringin inhibits chemokine production in an LPS-induced RAW 264.7 macrophage cell line," *Molecular Medicine Reports*, vol. 6, no. 6, pp. 1343–1350, 2012.
- [27] M. Tyszka-Czochara, P. Paško, W. Reczyński, M. Szłószarczyk, B. Bystrowska, and W. Opoka, "Zinc and propolis reduces cytotoxicity and proliferation in skin fibroblast cell culture: total polyphenol content and antioxidant capacity of propolis," *Biological Trace Element Research*, vol. 160, no. 1, pp. 123–131, 2014.
- [28] M. V. Dias, A. P. Castro, C. C. Campos et al., "Doxycycline hyclate: A schistosomicidal agent *in vitro* with immunomodulatory potential on granulomatous inflammation *in vivo*," *International Immunopharmacology*, vol. 70, pp. 324–337, 2019.
- [29] E. C. Santos, R. D. Novaes, D. S. S. Bastos et al., "Modulation of oxidative and inflammatory cardiac response by nonselective 1- and 2-cyclooxygenase inhibitor and benzimidazole in mice," *The Journal of Pharmacy and Pharmacology*, vol. 67, no. 11, pp. 1556–1566, 2015.
- [30] F. H. Guedes-da-Silva, D. Shrestha, B. C. Salles et al., "Trypanosoma cruzi antigens induce inflammatory angiogenesis in a mouse subcutaneous sponge model," *Microvascular Research*, vol. 97, pp. 130–136, 2015.
- [31] R. V. Gonçalves, R. D. Novaes, S. L. P. Matta, G. P. Benevides, F. R. Faria, and M. V. M. Pinto, "Comparative study of the effects of gallium-aluminum-arsenide laser photobiomodulation and healing oil on skin wounds in Wistar rats: a histomorphometric study," *Photomedicine and Laser Surgery*, vol. 28, no. 5, pp. 597–602, 2010.
- [32] H. D. Perry, L. W. Hodes, J. A. Seedor, E. D. Donnenfeld, T. F. McNamara, and L. M. Golub, "Effect of doxycycline hyclate on corneal epithelial wound healing in the rabbit alkali-burn model," *Cornea*, vol. 12, no. 5, pp. 379–382, 1993.
- [33] D. A. Guimaraes, E. Rizzi, C. S. Ceron et al., "Doxycycline dose-dependently inhibits MMP-2-mediated vascular changes in 2K1C hypertension," *Basic & Clinical Pharmacology & Toxicology*, vol. 108, no. 5, pp. 318–325, 2011.
- [34] M. S. Ågren, P. M. Mertz, and L. Franzén, "A comparative study of three occlusive dressings in the treatment of full-thickness wounds in pigs," *Journal of the American Academy of Dermatology*, vol. 36, no. 1, pp. 53–58, 1997.
- [35] N. Lemo, G. Marignac, E. Reyes-Gomez, T. Lilin, O. Crosaz, and D. M. D. Ehrenfest, "Cutaneous reepithelialization and wound contraction after skin biopsies in rabbits: a mathematical model for healing and remodelling index," *Veterinarski Arhiv*, vol. 80, pp. 637–652, 2010.
- [36] P. C. Dolber and M. S. Spach, "Conventional and confocal fluorescence microscopy of collagen fibers in the heart," *Journal of Histochemistry and Cytochemistry*, vol. 41, no. 3, pp. 465–469, 1993.
- [37] C. J. Churukian and E. A. Schenk, "A toluidine blue method for demonstrating mast cells," *Journal of Histotechnology*, vol. 4, no. 2, pp. 85–86, 1981.
- [38] R. D. Novaes, R. V. Gonçalves, M. C. Cupertino et al., "The energy density of laser light differentially modulates the skin morphological reorganization in a murine model of healing by secondary intention," *International Journal of Experimental Pathology*, vol. 95, no. 2, pp. 138–146, 2014.
- [39] M. C. Cupertino, K. L. C. Costa, D. C. M. Santos et al., "Long-lasting morphofunctional remodelling of liver parenchyma and stroma after a single exposure to low and moderate doses of cadmium in rats," *International Journal of Experimental Pathology*, vol. 94, no. 5, pp. 343–351, 2013.
- [40] C. A. Mandarim-de-Lacerda, "Stereological tools in biomedical research," *Anais da Academia Brasileira de Ciencias*, vol. 75, no. 4, pp. 469–486, 2003.
- [41] J. M. Oliveira, N. F. Losano, S. S. Condessa et al., "Exposure to deltamethrin induces oxidative stress and decreases of energy reserve in tissues of the Neotropical fruit-eating bat *Artibeus lituratus*," *Ecotoxicology and Environmental Safety*, vol. 148, pp. 684–692, 2018.
- [42] D. Tsikas, "Analysis of nitrite and nitrate in biological fluids by assays based on the Griess reaction: appraisal of the Griess reaction in the l-arginine/nitric oxide area of research," *Journal of Chromatography B*, vol. 851, no. 1–2, pp. 51–70, 2007.
- [43] J. A. Buege and S. D. Aust, "[30] Microsomal lipid peroxidation," *Methods in Enzymology*, vol. 52, pp. 302–310, 1978.
- [44] R. L. Levine, J. A. Williams, E. R. Stadtman, and E. Shacter, "[37] Carbonyl assays for determination of oxidatively modified proteins," *Methods in Enzymology*, vol. 233, pp. 346–357, 1994.

- [45] S. Dieterich, U. Bielgk, K. Beulich, G. Hasenfuss, and J. Prestle, "Gene expression of antioxidative enzymes in the human heart - increased expression of catalase in the end-stage failing heart," *Circulation*, vol. 101, no. 1, pp. 33–39, 2000.
- [46] H. Aebi, "[13] Catalase *in vitro*," *Methods in Enzymology*, vol. 105, pp. 121–126, 1984.
- [47] W. H. Habig, M. J. Pabst, and W. B. Jakoby, "Glutathione S-Transferases: the First Enzymatic Step in mercapturic acid formation," *The Journal of Biological Chemistry*, vol. 249, no. 22, pp. 7130–7139, 1974.
- [48] C. U. Chukwudi, "rRNA binding sites and the molecular mechanism of action of the tetracyclines," *Antimicrobial Agents and Chemotherapy*, vol. 60, no. 8, pp. 4433–4441, 2016.
- [49] D. Clemens, M. Duryee, C. Sarmiento et al., "Novel antioxidant properties of doxycycline," *International Journal of Molecular Sciences*, vol. 19, no. 12, p. 4078, 2018.
- [50] H. E. desJardins-Park, A. L. Moore, M. P. Murphy et al., "Abstract 45," *Plastic and Reconstructive Surgery-Global Open*, vol. 6, pp. 35–36, 2018.
- [51] A. Riba, L. Deres, K. Eros et al., "Doxycycline protects against ROS-induced mitochondrial fragmentation and ISO-induced heart failure," *PLoS One*, vol. 12, no. 4, article e0175195, 2017.
- [52] L. S. Altoé, R. S. Alves, M. M. Sarandy, M. Morais-Santos, R. D. Novaes, and R. V. Gonçalves, "Does antibiotic use accelerate or retard cutaneous repair? A systematic review in animal models," *PloS One*, vol. 14, no. 10, article e0223511, 2019.
- [53] R. Mokabberi, A. Haftbaradaran, and K. Ravakhah, "Doxycycline vs. levofloxacin in the treatment of community-acquired pneumonia," *Journal of Clinical Pharmacy and Therapeutics*, vol. 35, no. 2, pp. 195–200, 2010.
- [54] Y. Leibovici-Weissman, A. Neuberger, R. Bitterman et al., "Antimicrobial drugs for treating cholera," *The Cochrane Database of Systematic Reviews*, vol. 6, article CD008625, 2014.
- [55] J. C. Tharappel, S. K. Ramineni, D. Reynolds, D. A. Puleo, and J. S. Roth, "Doxycycline impacts hernia repair outcomes," *Journal of Surgical Research*, vol. 184, no. 1, pp. 699–704, 2013.
- [56] F. Bahrami, D. L. Morris, and M. H. Pourgholami, "Tetracyclines: drugs with huge therapeutic potential," *Mini Reviews in Medicinal Chemistry*, vol. 12, no. 1, pp. 44–52, 2012.
- [57] N. Nanda, D. K. Dhawan, A. Bhatia, A. Mahmood, and S. Mahmood, "Doxycycline Promotes Carcinogenesis & Metastasis via Chronic Inflammatory Pathway: An In Vivo Approach," *PloS One*, vol. 11, no. 3, article e0151539, 2016.
- [58] T. A. Sato, J. A. Keelan, M. Blumenstein, and M. D. Mitchell, "Efficacy and specificity of non-steroidal anti-inflammatory drugs for the inhibition of cytokine-stimulated prostaglandin E₂ secretion by amnion-derived WISH cells," *Prostaglandins, Leukotrienes and Essential Fatty Acids*, vol. 66, no. 5–6, pp. 525–527, 2002.
- [59] C. Gunaydin and S. S. Bilge, "Effects of nonsteroidal anti-inflammatory drugs at the molecular level," *The Eurasian Journal of Medicine*, vol. 50, no. 2, pp. 116–121, 2018.
- [60] E. N. Silva, T. V. F. Martins, T. M. Miyauchi-Tavares et al., "Amoxicillin-induced gut dysbiosis influences estrous cycle in mice and cytokine expression in the ovary and the caecum," *American Journal of Reproductive Immunology*, vol. 84, no. 1, article e13247, 2020.
- [61] M. Krystel-Whittemore, K. N. Dileepan, and J. G. Wood, "Mast cell: A multi-functional master cell," *Frontiers in Immunology*, vol. 6, p. 620, 2016.
- [62] A. Sorushanova, L. M. Delgado, Z. Wu et al., "The collagen suprafamily: from biosynthesis to advanced biomaterial development," *Advanced Materials*, vol. 31, no. 1, article 1801651, 2019.
- [63] L. Arseni, A. Lombardi, and D. Orioli, "From structure to phenotype: impact of collagen alterations on human health," *International Journal of Molecular Sciences*, vol. 19, no. 5, p. 1407, 2018.
- [64] A. W. Y. Chung, H. H. C. Yang, M. W. Radomski, and C. van Breemen, "Long-term doxycycline is more effective than atenolol to prevent thoracic aortic aneurysm in Marfan syndrome through the inhibition of matrix metalloproteinase-2 and -9," *Circulation Research*, vol. 102, no. 8, pp. e73–e85, 2008.
- [65] R. J. Bodnar, "Chemokine regulation of angiogenesis during wound healing," *Advances in Wound Care*, vol. 4, no. 11, pp. 641–650, 2015.
- [66] D. F. Rosa, M. M. Sarandy, R. D. Novaes, M. B. Freitas, M. do Carmo Gouveia Pelúzio, and R. V. Gonçalves, "High-fat diet and alcohol intake promotes inflammation and impairs skin wound healing in Wistar rats," *Mediators of Inflammation*, vol. 2018, Article ID 4658583, 12 pages, 2018.
- [67] K. I. Strauss, "Antiinflammatory and neuroprotective actions of COX2 inhibitors in the injured brain," *Brain, Behavior, and Immunity*, vol. 22, no. 3, pp. 285–298, 2008.
- [68] A. G. Abdou, A. H. Maraee, and H. F. Abd-Elsattar Saif, "Immunohistochemical evaluation of COX-1 and COX-2 expression in keloid and hypertrophic scar," *The American Journal of Dermatopathology*, vol. 36, no. 4, pp. 311–317, 2014.
- [69] M. Cano Sanchez, S. Lancel, E. Boulanger, and R. Neviere, "Targeting oxidative stress and mitochondrial dysfunction in the treatment of impaired wound healing: a systematic review," *Antioxidants*, vol. 7, no. 8, p. 98, 2018.
- [70] A. Phaniendra, D. B. Jestadi, and L. Periyasamy, "Free radicals: properties, sources, targets, and their implication in various diseases," *Indian Journal of Clinical Biochemistry : IJCB*, vol. 30, no. 1, pp. 11–26, 2015.
- [71] A. Weidinger and A. V. Kozlov, "Biological activities of reactive oxygen and nitrogen species: oxidative stress versus signal transduction," *Biomolecules*, vol. 5, no. 2, pp. 472–484, 2015.
- [72] G. Zhu, Q. Wang, S. Lu, and Y. Niu, "Hydrogen peroxide: a potential wound therapeutic target?," *Medical Principles and Practice: international journal of the Kuwait University, Health Science Centre*, vol. 26, no. 4, pp. 301–308, 2017.
- [73] D. André-Lévigne, A. Modarressi, M. S. Pepper, and B. Pittet-Cuénod, "Reactive oxygen species and NOX enzymes are emerging as key players in cutaneous wound repair," *International Journal of Molecular Sciences*, vol. 18, no. 10, p. 2149, 2017.
- [74] D. Pitocco, F. Zaccardi, E. di Stasio et al., "Oxidative stress, nitric oxide, and diabetes," *The Review of Diabetic Studies: RDS*, vol. 7, no. 1, pp. 15–25, 2010.
- [75] N. S. Bryan and M. B. Grisham, "Methods to detect nitric oxide and its metabolites in biological samples," *Free Radical Biology & Medicine*, vol. 43, no. 5, pp. 645–657, 2007.
- [76] C. Csonka, T. Páli, P. Bencsik, A. Görbe, P. Ferdinandy, and T. Csont, "Measurement of NO in biological samples," *British Journal of Pharmacology*, vol. 172, no. 6, pp. 1620–1632, 2015.
- [77] I. Marrocco, F. Altieri, and I. Peluso, "Measurement and clinical significance of biomarkers of oxidative stress in humans," *Oxidative Medicine and Cellular Longevity*, vol. 2017, Article ID 6501046, 32 pages, 2017.

- [78] A. Rahal, A. Kumar, V. Singh et al., "Oxidative stress, prooxidants, and antioxidants: the interplay," *BioMed Research International*, vol. 2014, Article ID 761264, 19 pages, 2014.
- [79] H. Bian, Q. Yang, T. Ma et al., "Beneficial effects of extracts from *Lucilia sericata* maggots on burn wounds in rats," *Molecular Medicine Reports*, vol. 16, no. 5, pp. 7213–7220, 2017.
- [80] C. R. A. Nogueira, F. M. Damasceno, M. R. de Aquino-Neto et al., "Doxycycline protects against pilocarpine-induced convulsions in rats, through its antioxidant effect and modulation of brain amino acids," *Pharmacology Biochemistry and Behavior*, vol. 98, no. 4, pp. 525–532, 2011.
- [81] B. Gryszczyńska, D. Formanowicz, M. Budzyń et al., "Advanced oxidation protein products and carbonylated proteins as biomarkers of oxidative stress in selected atherosclerosis-mediated diseases," *BioMed Research International*, vol. 2017, Article ID 4975264, 9 pages, 2017.
- [82] R. Serra, L. Gallelli, G. Buffone et al., "Doxycycline speeds up healing of chronic venous ulcers," *International Wound Journal*, vol. 12, no. 2, pp. 179–184, 2015.
- [83] R. L. Kraus, R. Pasieczny, K. Lariosa-Willingham, M. S. Turner, A. Jiang, and J. W. Trauger, "Antioxidant properties of minocycline: neuroprotection in an oxidative stress assay and direct radical-scavenging activity," *Journal of Neurochemistry*, vol. 94, no. 3, pp. 819–827, 2005.
- [84] C. Espinosa-Diez, V. Miguel, D. Mennerich et al., "Antioxidant responses and cellular adjustments to oxidative stress," *Redox Biology*, vol. 6, pp. 183–197, 2015.
- [85] P. Patlevič, J. Vašková, P. Švorc, L. Vaško, and P. Švorc, "Reactive oxygen species and antioxidant defense in human gastrointestinal diseases," *Integrative Medicine Research*, vol. 5, no. 4, pp. 250–258, 2016.
- [86] H. Younus, "Therapeutic potentials of superoxide dismutase," *International Journal of Health Sciences*, vol. 12, no. 3, pp. 88–93, 2018.
- [87] N. Di Marzo, E. Chisci, and R. Giovannoni, "The role of hydrogen peroxide in redox-dependent signaling: homeostatic and pathological responses in mammalian cells," *Cell*, vol. 7, no. 10, p. 156, 2018.
- [88] E. M. Jones, C. A. Cochrane, and S. L. Percival, "The effect of pH on the extracellular matrix and biofilms," *Advances in Wound Care*, vol. 4, no. 7, pp. 431–439, 2015.
- [89] M. Krampert, W. Bloch, T. Sasaki et al., "Activities of the matrix metalloproteinase stromelysin-2 (MMP-10) in matrix degradation and keratinocyte organization in wounded skin," *Molecular Biology of the Cell*, vol. 15, no. 12, pp. 5242–5254, 2004.
- [90] L. P. Singh, A. Mishra, D. Saha, and S. Swarnakar, "Doxycycline blocks gastric ulcer by regulating matrix metalloproteinase-2 activity and oxidative stress," *World Journal of Gastroenterology*, vol. 17, no. 28, pp. 3310–3321, 2011.

Research Article

Apelin/APJ-Manipulated CaMKK/AMPK/GSK3 β Signaling Works as an Endogenous Counterinjury Mechanism in Promoting the Vitality of Random-Pattern Skin Flaps

Zhi-Ling Lou ^{1,2,3} Chen-Xi Zhang,^{3,4,5} Jia-Feng Li,^{3,4,5} Rui-Heng Chen,^{1,3,5} Wei-Jia Wu,^{1,3} Xiao-Fen Hu,⁶ Hao-Chun Shi,^{1,2,3} Wei-Yang Gao,^{4,5} and Qi-Feng Zhao ^{1,2}

¹Department of Cardiovascular and Thoracic Surgery, The Second Affiliated Hospital and Yuying Children's Hospital of Wenzhou Medical University, Wenzhou 325000, China

²Children's Heart Center, Institute of Cardiovascular Development and Translational Medicine, The Second Affiliated Hospital and Yuying Children's Hospital of Wenzhou Medical University, Wenzhou 325000, China

³The Second School of Medicine, Wenzhou Medical University, Wenzhou 325000, China

⁴Department of Orthopaedic Surgery, The Second Affiliated Hospital and Yuying Children's Hospital of Wenzhou Medical University, Wenzhou 325000, China

⁵Key Laboratory of Orthopaedics of Zhejiang Province, Wenzhou 325000, China

⁶Zhejiang Chinese Medical University, Hangzhou 310000, China

Correspondence should be addressed to Qi-Feng Zhao; zhaoqf1862@163.com

Received 20 August 2020; Accepted 28 December 2020; Published 27 January 2021

Academic Editor: Reggiani Vilela Gon alves

Copyright © 2021 Zhi-Ling Lou et al. This is an open access article distributed under the Creative Commons Attribution License, which permits unrestricted use, distribution, and reproduction in any medium, provided the original work is properly cited.

A random-pattern skin flap plays an important role in the field of wound repair; the mechanisms that influence the survival of random-pattern skin flaps have been extensively studied but little attention has been paid to endogenous counterinjury substances and mechanism. Previous reports reveal that the apelin-APJ axis is an endogenous counterinjury mechanism that has considerable function in protecting against infection, inflammation, oxidative stress, necrosis, and apoptosis in various organs. As an *in vivo* study, our study proved that the apelin/APJ axis protected the skin flap by alleviating vascular oxidative stress and the apelin/APJ axis works as an antioxidant stress factor dependent on CaMKK/AMPK/GSK3 β signaling. In addition, the apelin/APJ-manipulated CaMKK/AMPK/GSK3 β -dependent mechanism improves HUVECs' resistance to oxygen and glucose deprivation/reperfusion (OGD/R), reduces ROS production and accumulation, maintained the normal mitochondrial membrane potential, and suppresses oxidative stress *in vitro*. Besides, activation of the apelin/APJ axis promotes vascular migration and angiogenesis under relative hypoxia condition through CaMKK/AMPK/GSK3 β signaling. In a word, we provide new evidence that the apelin/APJ axis is an effective antioxidant and can significantly improve the vitality of random flaps, so it has potential be a promising clinical treatment.

1. Introduction

Wound repair is a common clinical problem in surgery. A skin flap has been proven to be one of the most common and effective methods for wound repair in surgical practice. Random-pattern skin flap replantation is increasingly being selected to close large surficial tissue defects caused by various reasons such as trauma, cancer excisions, and congenital deformity corrective surgery [1–3]. Obviously, wound heal-

ing is a coordinated, complex process involving oxidative stress, inflammation, cell proliferation, cell migration, and angiogenesis [4]. During skin flap replantation, especially with the purpose of treating large-area wounds, blood supply interruption, oxidative stress, inflammation, and postoperative infection make the distal flap vulnerable to necrosis and to a great extent limit the clinical application of a random skin flap [5–8]. Blood supply recovery is a consequence of vascular stump's initiation, growth, and recanalization

from the pedicle to the distal area [3, 9]. During neovascularization, the ischemia-reperfusion injury (IRI) process is inevitable and necessary, in which effective and reasonable artificial intervention can greatly improve the survival of the skin flap by diminishing the accumulation of acute inflammatory cells [10] and suppressing oxidative stress [11]. As it is a main factor resulting from necrosis of grafts [12–14], IRI is frequently targeted by a series of medicine, treatments, and even biomaterials [15–18].

Considering all of the above, discovery of the substances with both proangiogenesis and antioxidant stress may play positive roles in the clinical application of a skin flap. Apelin, a group of peptides initially isolated from the bovine stomach, is an endogenous ligand of the G protein-coupled APJ receptor [19–21]. Only by binding to the APJ receptor could apelin exert their biologic function [19, 22, 23]; while apelin and the APJ receptor are widely distributed in different organs and tissues [22, 23], the apelin/APJ signal axis may play a role in diseases of different organs including pulmonary fibrosis, kidney inflammation [24], acute lung injury (ALI) [25], ischemic heart failure [26], and even osteoporosis [27, 28]. What we are interested in is that the apelin/APJ signal axis is especially related to vascular pathophysiology [24, 29, 30]. In addition, the apelin/APJ axis regulates IRI and antioxidant stress through different mechanisms such as regulating FoxO3 trafficking [31], maintaining the Ca²⁺ transient [32], attenuating excessive mitochondrial ROS production [21], and restoring the metabolic defects of lipid oxidation [33]. Existing researches lay the foundation for our hypothesis that apelin can be selected as an adjuvant therapy of skin flap transplantation by regulating angiogenesis and treating oxidative stress.

AMP-activated protein kinase (AMPK) is described as the “energy sensor” or “gauge” and expressed in all cell types and is closely related to IRI and oxidative stress. Since a previous study has proven that apelin protected against IRI-involved ROS-mediated inflammation via the AMPK/GSK3 β pathway activated by apelin receptor/G α /PLC/IP3/CaMKK signaling and further upregulated downstream Nrf2-related antioxidant components in the central nervous system [34], skin vessels act as peripheral terminal vessels, and whether a similar mechanism can be established and further improve the survival of a random skin flap is still not clear. Considering this, we carry out our study to verify and increase the feasibility for clinical application. The apelin family is a peptide family, including apelin12, apelin13, apelin17, and apelin36. Our study preliminarily explored the antioxidant stress response and mechanism of the apelin/APJ axis. As a signal axis is damaged under pathological conditions, the apelin/APJ axis has potential therapeutic target value for further research.

2. Materials and Methods

2.1. Animals and Grouping. 6~8-week-old C57BL/6 mice (22–28 g, male) were obtained from the laboratory animal center of Wenzhou Medical University (license no. SCXK [ZJ] 2005-0019). All animal handling procedures (surgery, treatments, and postoperation care) were strictly in accor-

dance with the Guide for the Care and Use of Laboratory Animals of the China National Institutes of Health. All procedures involving mice were approved by the Animal Research Committee of Wenzhou Medical University (wydw2017-0022). Enormous efforts were made to alleviate the pain of the mice during experiments. All mice were housed in standard experimental cages and given free access to food and water at a room temperature of 25°C with a 12 h light/dark cycle. At the beginning of the experiment, 44 C57BL/6 mice were randomly divided into four groups: normal control group ($n = 8$): purely healthy mice without any trauma treatment; random flap group ($n = 12$): treated with 20 μ l saline from day 1~day 7 after skin flap operation; random flap+apelin13 group ($n = 12$): treated with apelin13 (50 μ g/kg weight) in a volume of 20 μ l by tail intravenous injection from day 1~day 7 after skin flap operation; and random flap+apelin13+ML221 group ($n = 12$): treated with apelin13 (50 μ g/kg weight) together with ML221 (50 μ g/kg weight) in a volume of 20 μ l by tail intravenous injection from day 1~day 7 after skin flap operation.

2.2. Reagents and Antibodies. Apelin13 (C₆₉H₁₁₁N₂₃O₁₆S, purity $\geq 95\%$) was bought from Cayman (catalog 2A-13523-1). ML221 (C₁₇H₁₁N₃O₆, purity: 99.25%) was bought from MedChemExpress (CAS. no. 877636-42-5, Shanghai, China). STO-609 (C₁₉H₁₀N₂O₃, purity $\geq 98.0\%$) was purchased from MedChemExpress (CAS no. 52029-86-4; Monmouth Junction, NJ, USA). Dorsomorphin (compound C: C₂₄H₂₅N₅O, purity: 99.65%) was purchased from MedChemExpress (CAS. no. 866405-64-3; Monmouth Junction, NJ, USA). BX795 (C₂₃H₂₆IN₇O₂S, purity: 99.33%) was purchased from MedChemExpress (CAS. no. 702675-74-9; Monmouth Junction, NJ, USA). The primary antibodies against glycogen synthase kinase 3 β (GSK3 β), phospho-glycogen synthase kinase 3 β (p-GSK3 β) (Ser-9), superoxide dismutase 2 (SOD2), APJ, vascular endothelial growth factor (VEGF), and CD34 were acquired from Proteintech Group (22104-1-AP, 67558-1-Ig, 24127-1-AP, 20341-1-AP, 19003-1-AP, and 14486-1-AP, respectively), and an apelin primary antibody was obtained from Novus Biologicals (H00008862-M01). Primary antibodies against heme oxygenase-1 (HO-1), B-cell-lymphoma-2 (Bcl2), and nuclear factor E2-related factor 2 (Nrf2) were obtained from Abcam (ab13243, ab196495, and ab137550, respectively). Rabbit monoclonal anti-BCL2-associated X (Bax) was purchased from Cell Signaling Technology (Beverly, MA, USA). Secondary antibodies HRP-conjugated AffiniPure goat anti-mouse IgG (H+L), HRP-conjugated AffiniPure goat anti-rabbit IgG (H+L), CoraLite488-conjugated goat anti-mouse IgG (H+L), CoraLite488-conjugated goat anti-rabbit IgG (H+L), CoraLite594-conjugated goat anti-mouse IgG (H+L), and CoraLite594-conjugated goat anti-rabbit IgG (H+L) were purchased from Proteintech Group (SA00001-1, SA00001-2, SA00013-1, SA00013-2, SA00013-3, and SA00013-4, respectively). The Lipid Peroxidation MDA Assay Kit, diamidino-2-phenylindole (DAPI) solution, the BCA Kit, and the BeyoECL Moon Reagent Kit were purchased from Beyotime Biotechnology (Jiangsu, China). IL-1 and TNF α detection kits were purchased from Jiancheng Biotechnology (Nanjing, China).

2.3. Random Skin Flap Animal Model. Mice were anesthetized with pentobarbital sodium 1% (50 mg/kg, intraperitoneally injection) before operation. An electric shaver and hair removal ointment were used to remove the dorsal fur of mice. Then, a random-pattern, caudal-based skin flap (size: $1.5 \times 4.5 \text{ cm}^2$) was elevated in the mouse dorsum (in the same position in each mouse) beneath the panniculus carnosus as reported previously. The left and right sacral arteries were excised to block bilateral blood supply of the skin flap. By confirming that the blood vessels were amputated, separated flaps were inserted to the original position and sutured with a 7-0 nonabsorbable suture. The random skin area was equally separated into three zones from the pedicle to the distal: proximal (area I), intermediate (area II), and distal (area III) [3, 9].

2.4. Cell Culture. The human umbilical vein endothelial cells (HUVECs) are obtained from the American Type Culture Collection (Manassas, VA, USA) and cultured in RPMI 1640 medium containing 10% fetal bovine serum and 1% antibiotics (penicillin, 100 IU/ml; streptomycin, 100 $\mu\text{g}/\text{ml}$) at 37°C at 5% CO_2 in a constant-temperature incubator.

2.5. Oxygen and Glucose Deprivation/Reperfusion (OGD/R) Model. The OGD/R model was established to simulate IRI. HUVECs were cultured in glucose-free and serum-free DMEM containing apelin13 and inhibitors in a hypoxia chamber (Thermo Scientific, USA) containing a gas mixture of 95% N_2 and 5% CO_2 for 6 hours; after 6 hours, the medium was replaced by RPMI 1640 medium containing 10% fetal bovine serum, and HUVECs were transferred back to the previous normoxic culture environment for another 6 hours. As for migration and angiogenesis, the culture medium cannot be changed due to the experimental operation; we only arranged a 4-hour short-time glucose oxygen deprivation (OGD) to observe cell migration and tube formation better.

2.6. Cell Grouping and Drug Administration. HUVECs were divided into the following groups: normal control group, OGD/R group, OGD/R+apelin13 group, OGD/R+apelin13+ML221 group, OGD/R+apelin13+STO-609 group, OGD/R+apelin13+DM group, and OGD/R+apelin13+BX795 group. OGD/R+apelin13 group: HUVECs were treated with apelin13 (0.5 μM); OGD/R+apelin13+ML221 group: HUVECs were treated with apelin13 (0.5 μM)+ML221 (0.5 μM); OGD/R+apelin13+STO-609 group: HUVECs were treated with apelin13 (0.5 μM)+STO-609 (0.5 μM); OGD/R+apelin13+DM group: HUVECs were treated with apelin13 (0.5 μM)+DM (50 ng/ml); OGD/R+apelin13+BX795 group: HUVECs were treated with apelin13 (0.5 μM)+BX795 (2 μM); OGD/R+ML221 group: HUVECs were treated with ML221 (0.5 μM); OGD/R+STO-609 group: HUVECs were treated with STO-609 (0.5 μM); OGD/R+DM group: HUVECs were treated with DM (50 ng/ml); OGD/R+BX795 group: HUVECs were treated with BX795 (2 μM); and normal control group: HUVECs were simply treated with saline.

2.7. Flap Macroscopic Evaluation. After operation, the viability of skin flaps was tracked macroscopically by necrotic area, edema, colour, and hair conditions on day 1, day 3, and day 7.

Then, on day 7, high-resolution photos of the random flaps were obtained to evaluate the viability. All photos were processed by using the Image-Pro Plus imaging software (ver 6.0; Media Cybernetics) to determine the survival area, and the survival percentage of the skin flap was determined as follows: extent of the survival area \times 100%/total area (survival and necrotic).

2.8. Laser Doppler Blood Flow (LDBF) Measurement. LDBF measurement was performed to evaluate vascular flow and blood supply in whole skin flaps. On day 3, day 5, and day 7, all mice were anesthetized and placed in a warm and quiet room, and the laser Doppler instrument (Moor Instruments, Axminster, UK) was used to scan mice in each group. The infrared Doppler scanning probe scanned the area of the skin flap to record the blood flow distribution as described in the previous literature [3, 9]. Blood flow of the skin flap was visualized with the strong signal (green, yellow, and red shown in pictures) and quantified with Moor LDI Review software (ver 6.1; Moor Instruments). Measurement of each mouse was performed three times at least, and the mean value was used.

2.9. Tissue Edema Measurement. Water content reflects edema of the skin flap. As previously described [3, 9], on day 7, skin flap tissue specimens were obtained and weighed and wet weight was recorded. Then, all specimens were dehydrated in an autoclave at a temperature of 50°C and weighed every day; finally, the stabilized weight was recorded as dry weight. The content of water was calculated as follows: percentage of tissue water content = $([\text{wet weight} - \text{dry weight}]/\text{wet weight}) \times 100\%$.

2.10. Hematoxylin Eosin (HE) Staining. Skin flap samples (1 cm \times 1 cm) of area II were obtained after sacrifice. The extracted skin flap samples were first fixed in 4% paraformaldehyde for 24 hours and then embedded in paraffin wax for transverse sectioning. Sections were sliced at the thickness of 4 μm with a microtome and mounted on adhesion microscope slides (CITOGlas, Taizhou, China) for HE staining. We calculated the number of microvessels per unit area (1 mm^2) under a light microscope (Olympus Corp, Tokyo, Japan), which was described as the microvascular density.

2.11. Immunohistochemistry (IHC). Skin flap sections in each group were baked at 65°C for 2 hours, then dewaxed twice in xylene, and hydrated with gradient ethanol baths. After washing, we blocked tissue sections with 3% hydrogen peroxide solution and performed antigen retrieval (20 min, 95°C) with 10.2 mM sodium citrate buffer (pH 6.0). Then, after blocking tissue sections with 10% goat serum albumin phosphate-buffered saline (10 min, 37°C), the sections were incubated with primary antibodies against CD34 (1:200), apelin (1:200), and APJ (1:200) overnight at 4°C. The second day, these sections were incubated with an HRP-conjugated secondary antibody and counterstained with hematoxylin. Finally, these slices were sealed with neutral resin and placed in a ventilation cupboard overnight. Stained flap sections were pictured at $\times 200$ magnification using a DP2-TWAN image-acquisition system (Olympus Corp, Tokyo, Japan). IHC images were evaluated with Image-Pro

Plus software (Media Cybernetics) for integral absorbance quantitation of apelin-, APJ-, and CD34-positive blood vessel counting.

2.12. Reactive Oxygen Species (ROS) Measurement. HUVECs were cultured on glass creep plates at a seeding density of 1×10^5 . After all stimulations, a reactive oxygen species (DCFH-DA) assay kit (Beyotime, China) was used to measure the cellular ROS level according to the manufacturer's instructions. Images were pictured by using an Olympus microscope. The average fluorescence intensity of the fluorescence emitted by DCF is measured by using Image-Pro Plus software, which reflects the accumulation level of ROS in a positive correlation.

2.13. Immunofluorescence Staining. HUVECs were cultured on 12-well culture plates containing glass creep plates at a seeding density of 1×10^5 . After all stimulations, remove medium and wash creep plates with aseptic phosphate buffer; then, cells were fixed in 4% paraformaldehyde for 20 min and permeabilized with 0.1% Triton X-100 for 20 min. 10% goat serum albumin was used to block plates (10 min, 37°C), and cell creep plates were incubated with primary antibodies against Nrf2 (1:200), HO-1 (1:200), and SOD2 (1:200) overnight at 4°C. For tissue sections, procedures before primary antibody incubation are the same as described in IHC; then, sections were incubated with primary antibodies against apelin (1:200) and APJ (1:200) overnight at 4°C. The second day, all sections and plates were washed three times with aseptic phosphate buffer, incubated with a Cora-Lite488/594-conjugated second antibody for 1 hour at 37°C, and finally stained with DAPI. All images were evaluated under a fluorescence microscope (Olympus, Tokyo, Japan). The percentage of Nrf2-, HO-1-, and SOD2-positive cells in the dermal layer was calculated, and apelin- and APJ- positive areas were colocalized.

2.14. Western Blotting. After being euthanized, samples (0.5 × 0.5 cm) from the middle of area II flaps in each group were removed from mice and stored at -80°C for Western blotting. In vitro, discard the culture medium of each group of cells, wash it with aseptic phosphate buffer, and harvest the cells with cell scrapers on ice. After extracting total protein from the flap tissues and cells with RIPA lysis buffer, protein concentration was measured by using the BCA protein assay kit. An equal amount of 60 µg tissue protein (30 µg cellular protein) was separated by 10-15% gel electrophoresis and transferred to polyvinylidene difluoride membranes (Roche Applied Science, Indianapolis, IN, USA). After blocking with 5% nonfat milk for 2 hours at room temperature, the membranes were incubated with the subsequent primary antibodies at 4°C overnight: VEGF (1:1000), CD34 (1:1000), APJ (1:1000), apelin (1:1000), Bcl2 (1:1000), Bax (1:1000), Nrf2 (1:1000), SOD2 (1:1000), HO-1 (1:1000), t-AMPK (1:1000), p-AMPK (1:1000), t-GSK3β (1:1000), p-GSK3β (1:1000), and GAPDH (1:3000). Then, the membranes were incubated with an HRP-conjugated IgG secondary antibody (1:1000) for 2 hours at room temperature. The bands on the membranes

were imaged using the ECL Moon Reagent Kit. Protein bands' signal intensity was quantified using Image Lab 3.0 software (Bio-Rad, Hercules, CA, USA).

2.15. JC-1 Staining. The mitochondrial membrane potential in each group was determined by staining with JC-1 (Beyotime, China) according to the manufacturer's guidelines. Stained cells were observed under a fluorescence microscope (Olympus; Tokyo, Japan).

2.16. MDA and Carbonylated Protein Measurements. Cellular lipid peroxidation in each group was measured by using the Lipid Peroxidation MDA Assay Kit (Beyotime, China). Carbonylated protein level was measured by using the Micro Protein Carbonyl Assay Kit (Solarbio, China). All measurements were performed according to the manufacturer's instructions.

2.17. Catalase (CAT) and Glutathione (GSH) Measurements. Catalase was measured by using the CAT Assay Kit (Solarbio, China), and GSH was measured by using the GSH Assay Kit (Solarbio, China) according to the manufacturer's instructions.

2.18. IL-1 and TNFα Measurements. HUVECs were homogenized by using RIPA buffer, and proteins were collected. IL-1 and TNFα levels inside HUVEC cells were measured by using, respectively, the IL-1 ELISA kit (Boyun, China) and TNFα ELISA kit (Boyun, China) according to the manufacturer's instructions.

2.19. Cell Migration and Tube Formation. Transwell assays (8 µm) (Corning, USA) were used to evaluate the HUVECs' migration ability. Briefly, 2×10^5 cells were seeded into the upper chamber in a volume of 200 µl, while the lower chamber contained glucose-free DMEM culture medium (Gibco) with 1% fetal bovine serum (FBS, Gibco) and different components (saline, apelin13, ML221, STO-609, DM, and BX795); then, cells were placed in a hypoxia chamber. Cells treated with RPMI 1640 medium (Meilunbio) with 1% FBS and placed in a normoxic incubator were used as a normal control group. 4 hours after incubation, cells on the upper surface of the upper chamber membrane were carefully wiped off with cotton swabs, fixed in 4% paraformaldehyde for 30 min at room temperature, and then stained with crystal violet to quantify the migrated cells. The migrated cells were pictured using an inverted microscope (Nikon, Japan). A tube formation assay on Matrigel (BD Biosciences, USA) was performed to evaluate the HUVECs' morphogenesis and tube formation capacity. Briefly, Matrigel solution was thawed at 4°C overnight and placed in a µ-Slide (10 µl per well, IBIDI, Germany) in a cell incubator for 30 min to solidify. A total of 5000 cells, which were treated with serum-free and glucose-free DMEM culture medium containing different components (saline, apelin13, ML221, STO-609, DM, and BX795), were seeded onto the Matrigel surface and placed in a hypoxia chamber, and cells treated with RPMI 1640 medium with 10% FBS and placed in a normoxic incubator were used as the normal control. Tube formation was

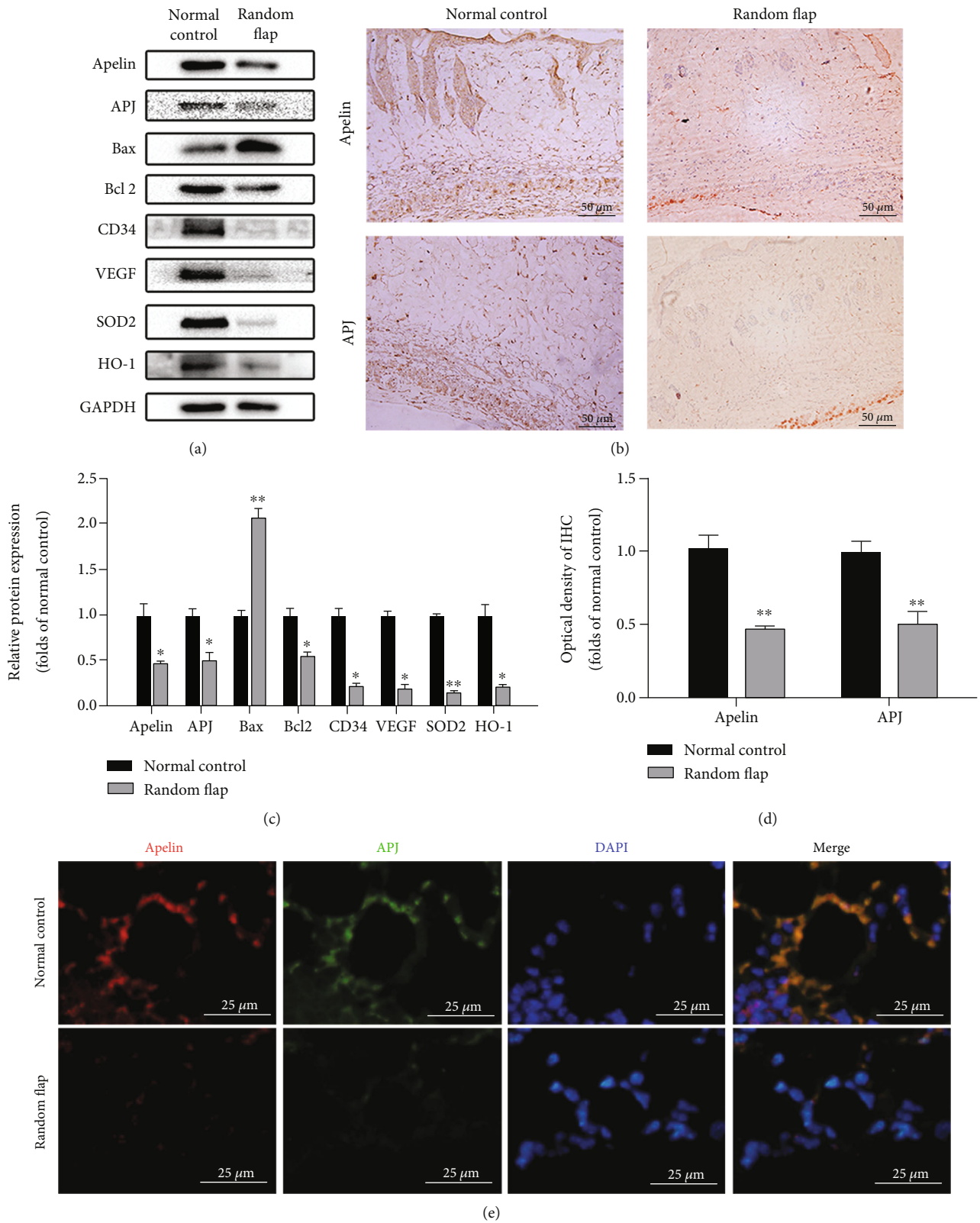
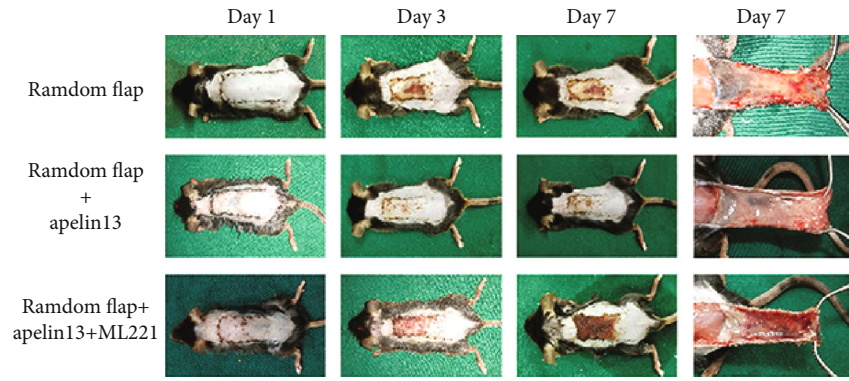
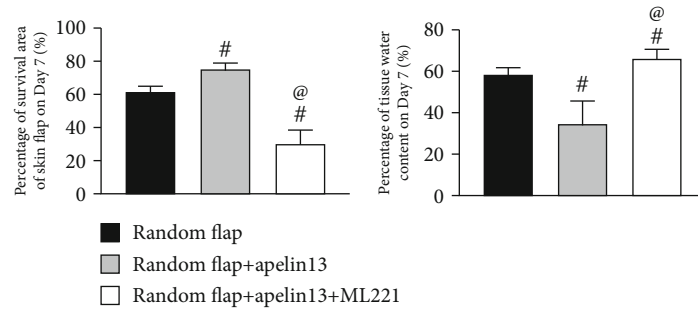


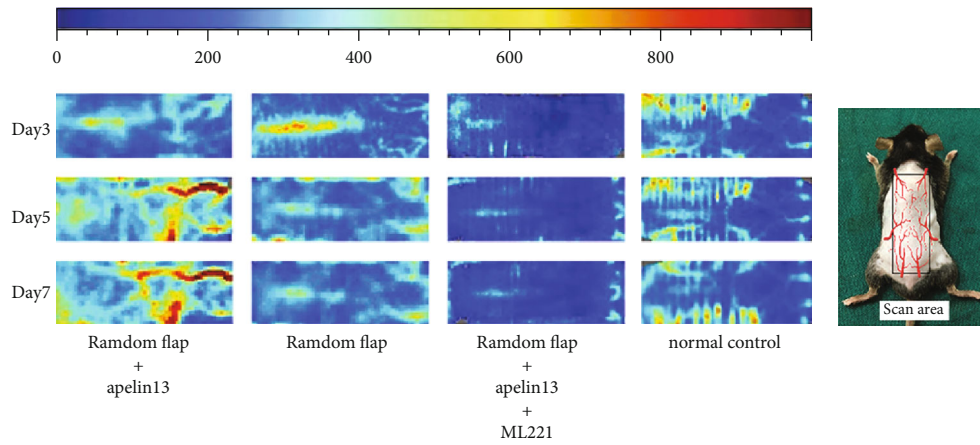
FIGURE 1: The apelin/APJ axis was shut down after random flap operation. (a, c) Western blot results of skin tissue suggest that apelin, APJ, CD34, VEGF, SOD2, and HO-1 were significantly downregulated and apoptosis was upregulated (Bcl2 decreased while Bax increased) after random flap operation. (b, d) IHC staining indicated that the apelin- and APJ-positive area almost halved (scale bar: 50 μm). (e) Immunofluorescence colocalization showed that the codistribution of apelin and APJ in skin microvessels decreased significantly after operation (scale bar: 25 μm). The densitometric analysis of all Western blot bands was normalized to GAPDH. $n = 4$ independent experiments. “*” means compared with the normal control group. * $p < 0.05$, ** $p < 0.01$.



(a)

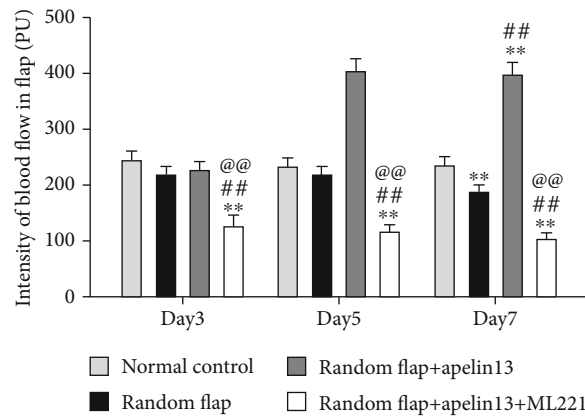


(b)



(c)

(d)



(e)

FIGURE 2: Continued.

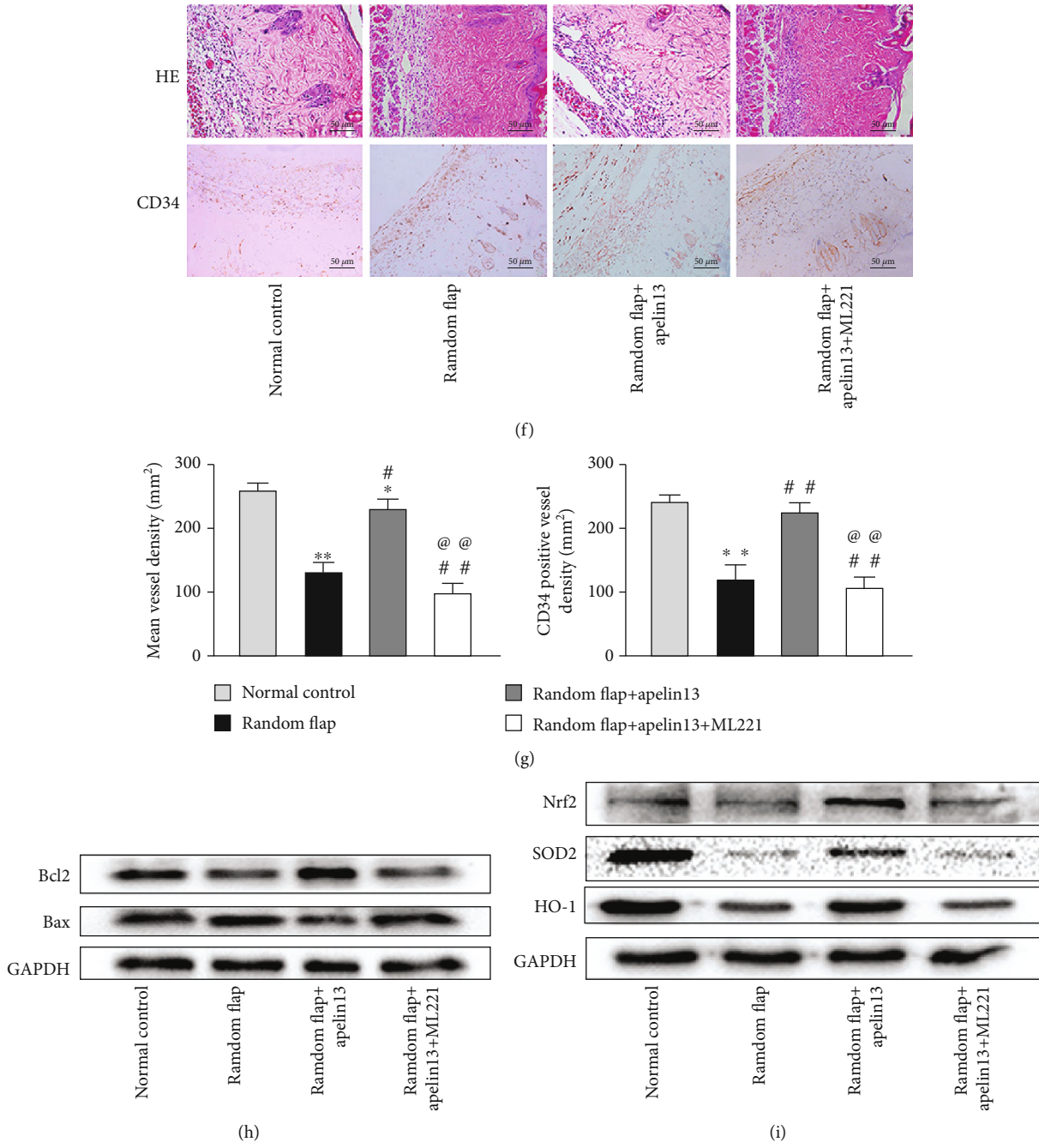


FIGURE 2: Continued.

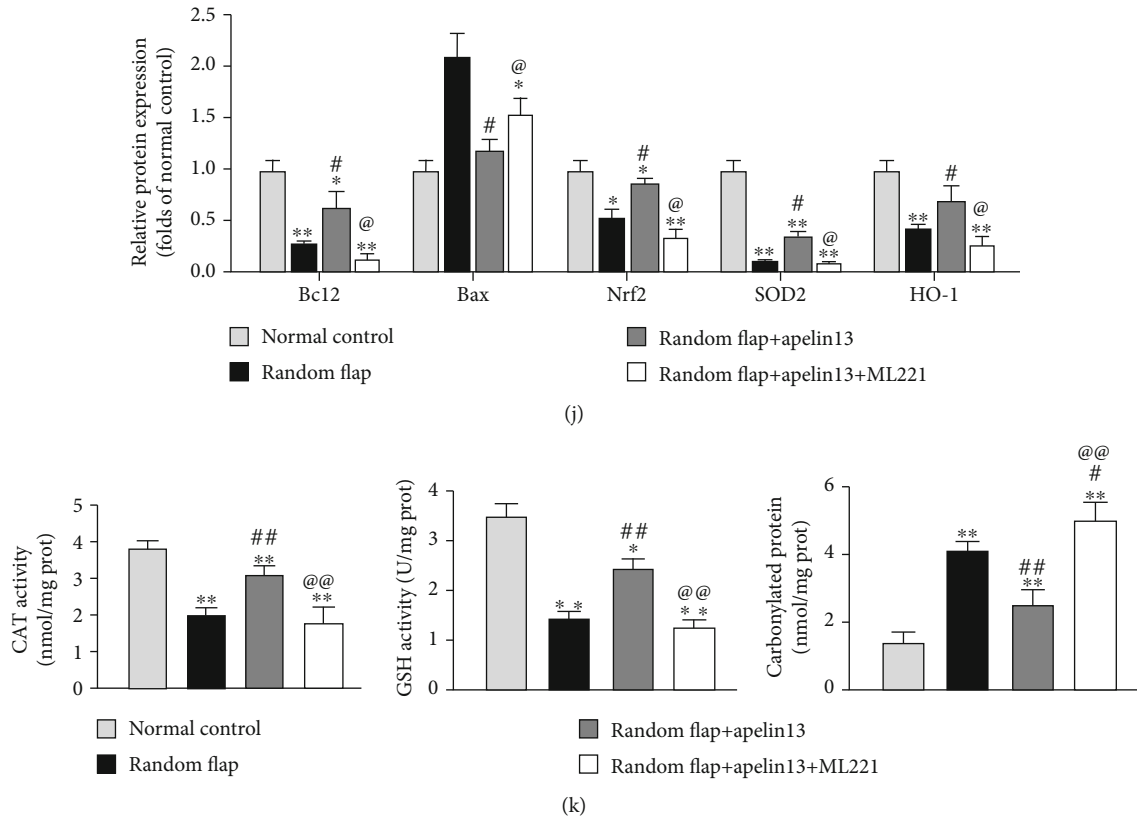


FIGURE 2: Apelin13 treatment promoted the viability of a random flap. (a) Digital photographs of flap appearances of the random flap group, random flap+apelin13 group, and random flap+apelin13+ML221 groups on day 1, day 3, and day 7 and their inner side photos on day 7 were recorded. (b) The percentages of the survival area and edema degree in three groups were quantified and analyzed. (c) Full-field LDBF images of flaps in each group on day 3, day 5, and day 7. (d) A schematic diagram of a rectangular area (1.5 cm × 4.5 cm) of surgery and scanning. (e) The signal intensity of blood flow of flaps was quantified and analyzed. (f) HE staining showed vessels in area II of flaps in all groups (original magnification ×200; scale bar: 50 μm). IHC staining showed CD34-positive vessels in area II in all groups (original magnification ×200; scale bar: 50 μm). (g) Histogram of mean vessel density and CD34-positive vessel density in each group. Western blot bands of apoptosis indexes (h), antioxidant stress proteins (i), and statistical results (j). The densitometric analysis of all Western blot bands was normalized to GAPDH. Antioxidant enzymes such as CAT and GSH and oxidative marker carbonylated protein levels in all groups of random flaps were measured (k). $n = 4$ independent experiments. “*” means compared with the normal control group; “#” means compared with the random flap group; “@” means compared with the random flap+apelin13 group. * $p < 0.05$, ** $p < 0.01$.

observed and quantified under an inverted microscope (Nikon, Japan) after 4 hours.

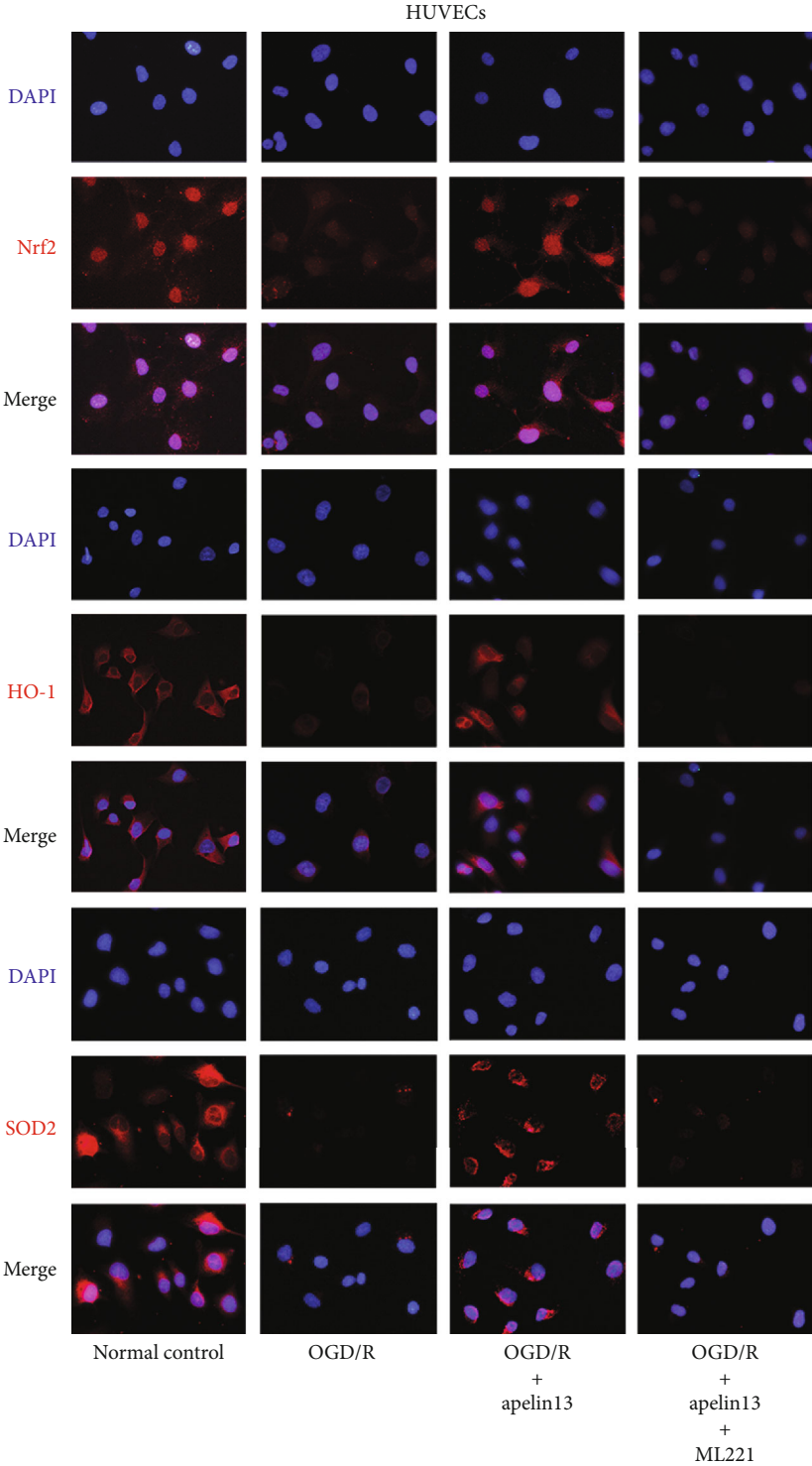
2.20. Statistical Analyses. Statistical analyses and statistical graphs were implemented using GraphPad Prism 8.0 (GraphPad Software, La Jolla, CA, USA). All data are presented as mean ± SD. Comparisons of mean values between two groups were performed using the independent-sample t -test. Mean value comparisons among multigroups were performed using one-way ANOVA followed by the Tukey test. $p < 0.05$ was considered significant.

3. Results

3.1. Apelin and APJ Were Downregulated in Random Skin Flap Tissue. At first, we examined whether the expression of endogenous apelin and its receptor APJ would change in random skin flap tissue. Western blot analysis and immunohistochemistry staining were used to evaluate the expression of apelin and APJ in normal skin tissue and random skin flap

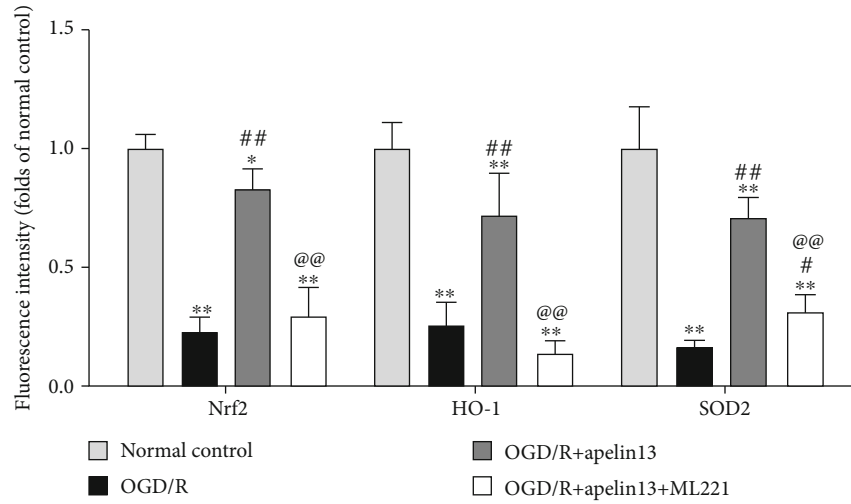
tissue. The corresponding results indicated that both apelin and APJ were significantly decreased in random skin flap tissue at day 7 as shown in Figures 1(a) and 1(b). Similarly, compared with normal skin tissue, VEGF, CD34, SOD2, and HO-1 were downregulated synchronously as shown in Figure 1(a). The proapoptotic protein Bax increased while the antiapoptotic factor Bcl2 decreased. Figures 1(c) and 1(d) show the statistical results of Western blot and immunohistochemistry, respectively. Furthermore, the colocalized immunofluorescence double staining of apelin and APJ (Figure 1(e)) in skin vessels showed an appropriate combination of apelin and APJ under normal conditions, which was greatly reduced in a skin flap. After operation, the ability of antioxidative stress of the skin flap decreased and showed an obvious trend of promoting apoptosis.

3.2. Apelin13 Protected the Skin Flap from IRI. We tracked the skin flap necrosis status on day 1, day 3, and day 7 after operation in each group and measured tissue edema, and Figures 2(a) and 2(b) suggested that by supplementing with



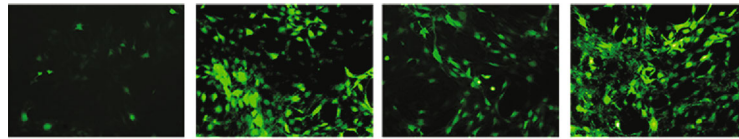
(a)

FIGURE 3: Continued.

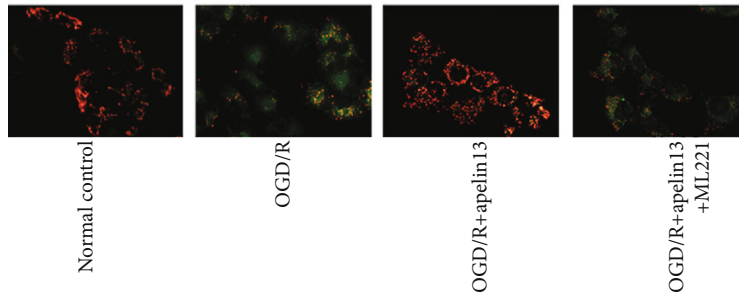


(b)

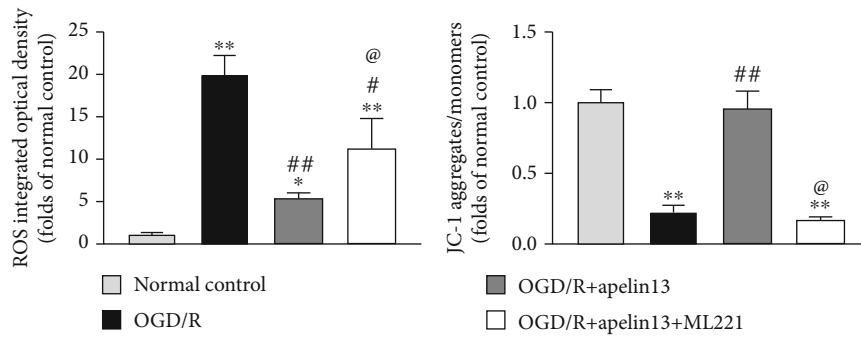
ROS



JC-1 aggregates/monomers



(c)



(d)

FIGURE 3: Continued.

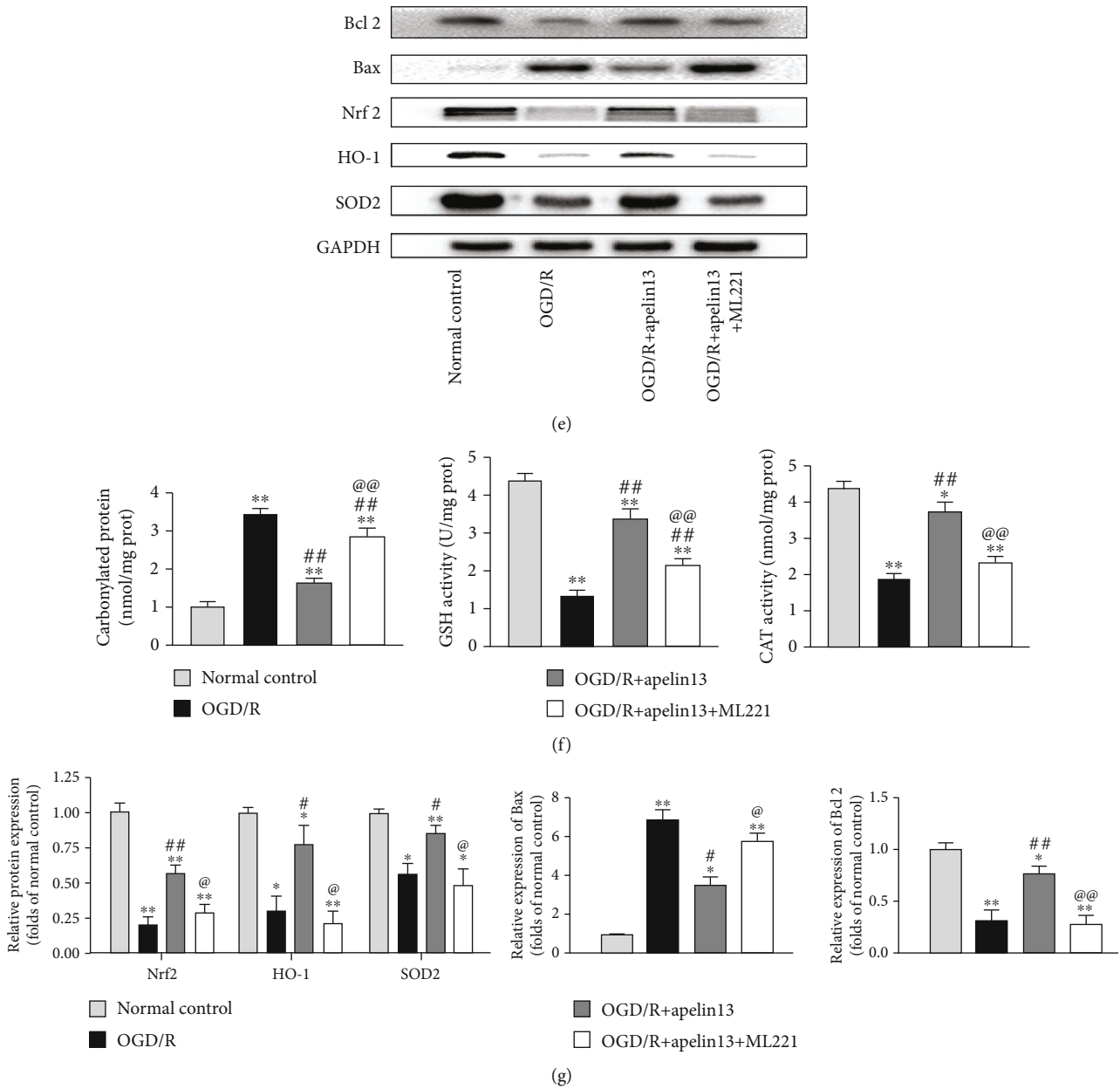


FIGURE 3: Apelin13 treatment protected the viability of HUVECs against OGD/R. (a, b) Immunofluorescence of Nrf2, HO-1, and SOD2 of HUVECs in all groups (scale bar: 20 μ m) and fluorescence intensity quantification. (c, d) Representative images showing ROS levels and JC-1 intensity in the differentially treated and quantified groups. (e) Western blot bands and relative protein levels (Bcl2, Bax, Nrf2, HO-1, and SOD2). (g) The densitometric analysis of all Western blot bands was normalized to GAPDH. (f) CAT, GSH, and carbonylated protein levels in all groups of HUVECs were measured. $n = 4$ independent experiments. “*” means compared with the normal control group; “#” means compared with the OGD/R group; “@” means compared with the OGD/R+apelin13 group. * $p < 0.05$, ** $p < 0.01$.

exogenous apelin13 after operation, the necrotic area of the skin flap reduced significantly and skin edema was also much milder. On the contrary, administration of ML221, an inhibitor of APJ, strongly reversed the protective effect of apelin13. Western blot showed that apelin13 enhanced the antioxidative stress ability of the skin flap, upregulated Nrf2, SOD2, and HO-1, promoted better entry to the nucleus of Nrf2, and resisted the apoptosis tendency while ML221 is reversed (Figures 2(h)–2(j)). Laser Doppler scanning imaging reflected the recovery of a vascular bed in the whole area of

the random skin flap, and administration of apelin13 visibly promoted the continuation of the vascular stump of the pedicle and wound edge and increased the blood supply of the skin flap (Figures 2(c) and 2(e)). In addition to the positive effect on visible vascular stumps, the apelin13-treated group has richer microvessel distribution than both the random flap group and apelin13+ML221-treated group (Figures 2(f) and 2(g)). Of all the vascular-related indicators, whether it was the abundance of microvessels and the regeneration of vascular stumps, the addition of the inhibitor ML221 made

it worst. In addition, apelin protected the random skin flaps from oxidative stress caused by ischemia-reperfusion to a great extent by increasing the level of GSH and CAT; then, oxidative stress marker carbonylated protein level was relatively few (Figure 2(k)).

3.3. Apelin13 Protected the HUVECs from OGD/R. As mentioned before, we adopt OGD/R to simulate the IRI after skin flap transplantation. Immunofluorescence and Western blot showed that OGD/R successfully reproduced oxidative stress and apoptosis of the vascular endothelium in vitro. The protective effect of apelin13 on HUVECs was consistent with that in vivo. Apelin13 upregulated Nrf2, SOD2, HO1, and Bcl2, suppressed the expression of Bax, and improved the ability of antioxidant stress and antiapoptosis of HUVECs (Figures 3(a), 3(b), 3(e), and 3(g)). The DCFH-DA fluorescence probe detected a large amount of ROS production and accumulation inside vascular endothelial cells after OGD/R, and treatment with apelin13 helped suppress it and reduced the cell damage caused by ROS during OGD/R (Figures 3(c) and 3(d)). The accumulation of ROS inside cells damages mitochondrial membrane potential and hinders cell energy metabolism. The changes of mitochondrial membrane potential indirectly reflect the state of energy metabolism under oxidative stress. The red and green fluorescence directly revealed the proportion of normal mitochondria. After OGD/R stimulation, mitochondrial membrane potential dropped but apelin13 treatment maintained relatively normal membrane potential (Figures 3(c) and 3(d)). The decrease in mitochondrial membrane potential can be easily detected by the transition of JC-1 from red fluorescence to green fluorescence, which can also be used as an early detection index of apoptosis. Similar to the results of experiments in vivo, GSH and CAT levels were upregulated while carbonylated protein levels were suppressed after apelin13 treatment (Figure 3(f)); thus, the treatment of apelin13 also increased the cellular CAT and GSH and enhanced the ability of vascular endothelial cells to resist OGD/R-induced injury; on the contrary, ML221 reversed the antioxidant function of apelin13.

3.4. Apelin13 Activated AMPK/GSK3 β Signaling In Vivo and In Vitro. In vivo, compared with normal skin tissue, the content of phosphorylated and activated AMPK together with its downstream GSK3 β phosphorylation ratio decreased significantly in the random flap (Figures 4(a) and 4(b)). We can see that phosphorylated AMPK remains at a high level in the apelin13-treated group, and apelin13 effectively resists the impairment of AMPK phosphorylation involved in IRI of the random flap. While suppressing APJ by ML221, the activation effect of apelin13 on AMPK and GSK3 β disappeared (Figures 4(c)–4(e)). HUVECs were stimulated by OGD/R in vitro and treated with apelin13 and apelin13+ML221, and we can see that the changes of phosphorylated AMPK and phosphorylated GSK3 β are consistent with those in vivo (Figures 4(f)–4(h)). AMPK and GSK3 β played a significant role in protecting the random flap from IRI. This proved once again that there is good consistency between the HUVECs' OGD/R model and the skin flap's IRI.

3.5. CaMKK Contributed to Apelin13-Dependent AMPK/GSK3 β Signaling Activation in HUVECs. The selective and cellular permeable CaMKK inhibitor STO-609 was used to identify the upstream relationship between the G α subunit of the G protein-coupled receptor APJ and AMPK after apelin13 activation. By inhibiting CaMKK by STO-609, the phosphorylation activation of downstream AMPK dropped, the phosphorylation of GSK3 β decreased (Figures 5(a)–5(c)), and the expression antioxidant factors Nrf2, HO-1, and SOD2 decreased (Figures 5(a), 5(f), 5(g), and 5(h)) which largely counteracted the protective effect of apelin. GSH and CAT declined (Figures 5(i) and 5(j)). Oxidative stress marker carbonylated protein (Figure 5(k)), lipid oxidation product MDA (Figure 5(l)), and inflammatory mediators IL-1 and TNF α (Figures 5(m) and 5(n)) became much higher in STO-609 treatment groups. At the same time, STO-609 also made the cells show an obvious trend of apoptosis during OGD/R (Figures 5(a), 5(d), and 5(e)).

3.6. Dorsomorphin (DM) Blocking Apelin13-Mediated AMPK/GSK3 β /Nrf2 Signaling Activation in HUVECs. DM is also known as compound C, a selective AMPK inhibitor, which was used to inhibit apelin13-mediated phosphorylation activation of AMPK. Downregulated phosphorylated AMPK led to the decrease in phosphorylated GSK3 β (Figures 6(a)–6(c)); the same as described before, cellular CAT (Figure 6(i)) and GSH (Figure 6(j)) declined, and the expression levels of antioxidant proteins Nrf2, HO-1, and SOD2 were downregulated parallelly (Figures 6(a), 6(f), 6(g), and 6(h)), which largely counteracted the protective effect of apelin. Accumulation of carbonylated protein (Figure 6(k)), MDA (Figure 6(l)), and inflammatory mediators IL-1 and TNF α (Figures 6(m) and 6(n)) increased significantly in DM treatment groups. The inhibition of AMPK by DM also made HUVECs no longer have physiological antiapoptosis ability when they were undergoing OGD/R stimulation (Figures 6(a), 6(d), and 6(e)).

3.7. Inhibition of GSK3 β Phosphorylation Counteracts Apelin13-Induced Nrf2/SOD2 Signaling Activation in HUVECs. BX795 can reduce the phosphorylation of GSK3 β at Ser9, and GSK3 β is highly phosphorylated in an inactive configuration under normal physiological conditions. GSK3 β was activated, and phosphorylation decreased under the stimulation of OGD/R. BX795's inhibition reversed phospho-Ser9-GSK3 β upregulation mediated by apelin13. BX795 could not reduce phospho-AMPK content obviously (Figures 7(a)–7(c)). BX795 treatment suppressed CAT (Figure 7(i)) and GSH (Figure 7(j)) and downregulated Nrf2, HO-1, and SOD2 (Figures 7(a), 7(f), 7(g), and 7(h)). Synchronously, BX795 treatment aggravated the production and accumulation of carbonylated protein (Figure 7(k)), MDA (Figure 7(l)), and IL-1 and TNF α (Figures 7(m) and 7(n)) compared with the apelin13 treatment group. The inhibition of GSK3 β phosphorylation aggravated oxidative stress inside HUVECs and promoted apoptosis in the pathological environment made by OGD/R (Figures 7(a), 7(d), and 7(e)).

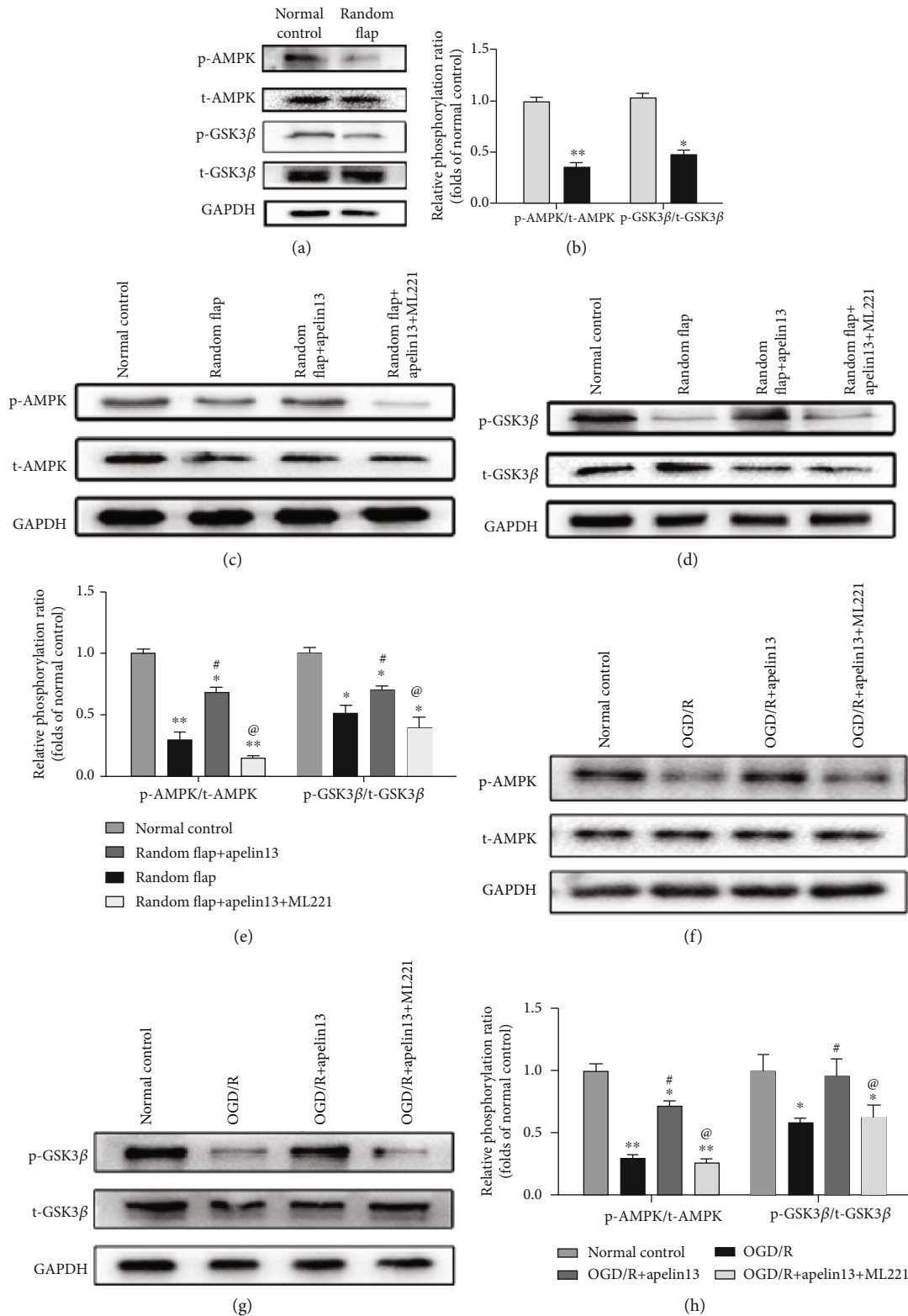


FIGURE 4: Apelin13 enhanced random flaps' viability through AMPK/GSK3 β signaling in vivo and in vitro. (a) Western blot bands suggested phosphorylation difference of GSK3 β and AMPK between normal skin and random flap. (b) Ratio of phosphorylated AMPK/total AMPK and phosphorylated GSK3 β /total GSK3 β . (c–e) Phosphorylation of AMPK and GSK3 β in all groups after apelin13 with or without ML221 in vivo. (f–h) Phosphorylation of AMPK and GSK3 β in all groups after apelin13 with or without ML221 in vitro. The densitometric analysis of all Western blot bands was normalized to total protein and GAPDH. $n = 4$ independent experiments. “*” means compared with the normal control group; “#” means compared with the random flap group (or OGD/R group); “@” means compared with the random flap+apelin13 group (or OGD/R+apelin13 group). * $p < 0.05$, ** $p < 0.01$.

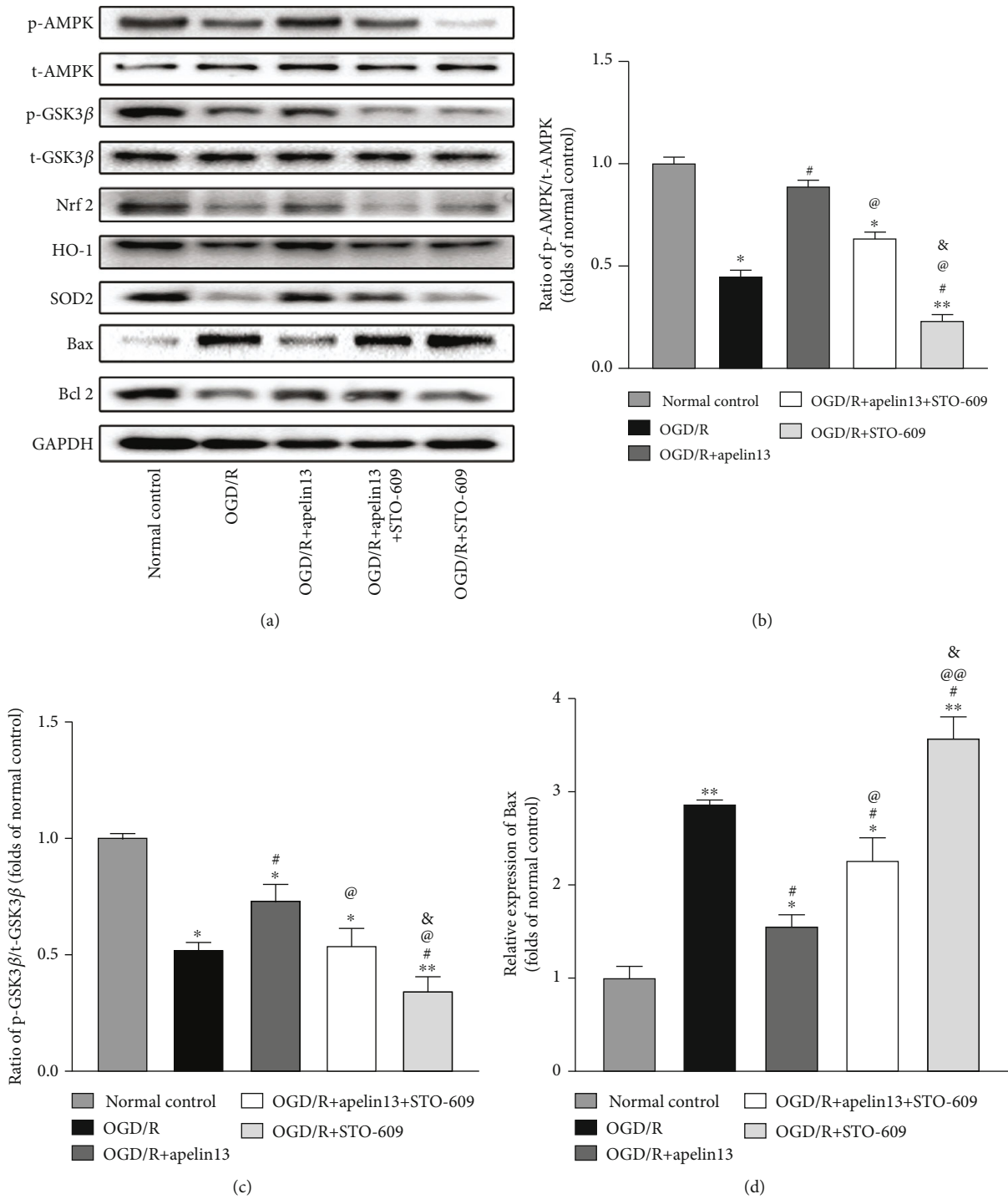


FIGURE 5: Continued.

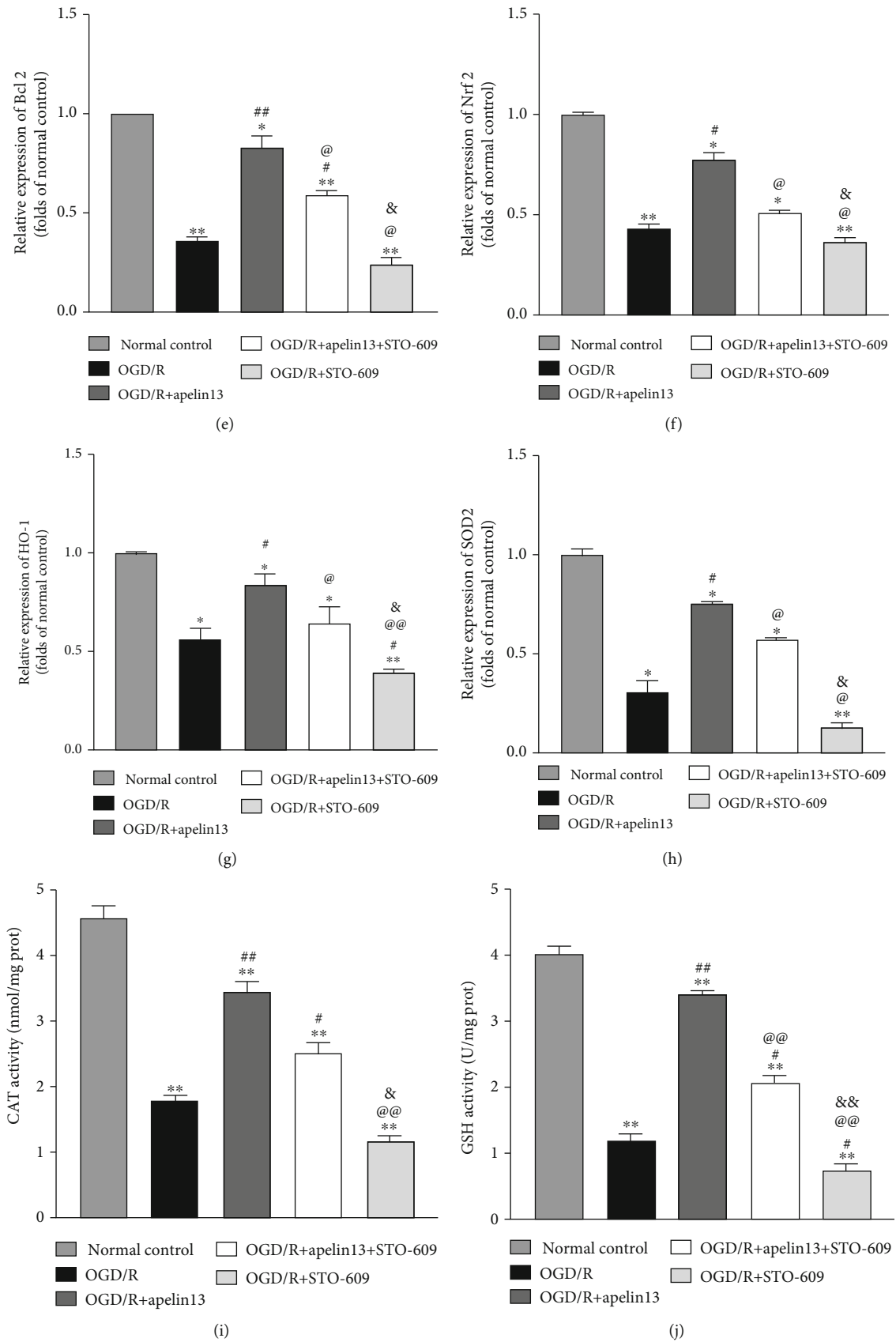


FIGURE 5: Continued.

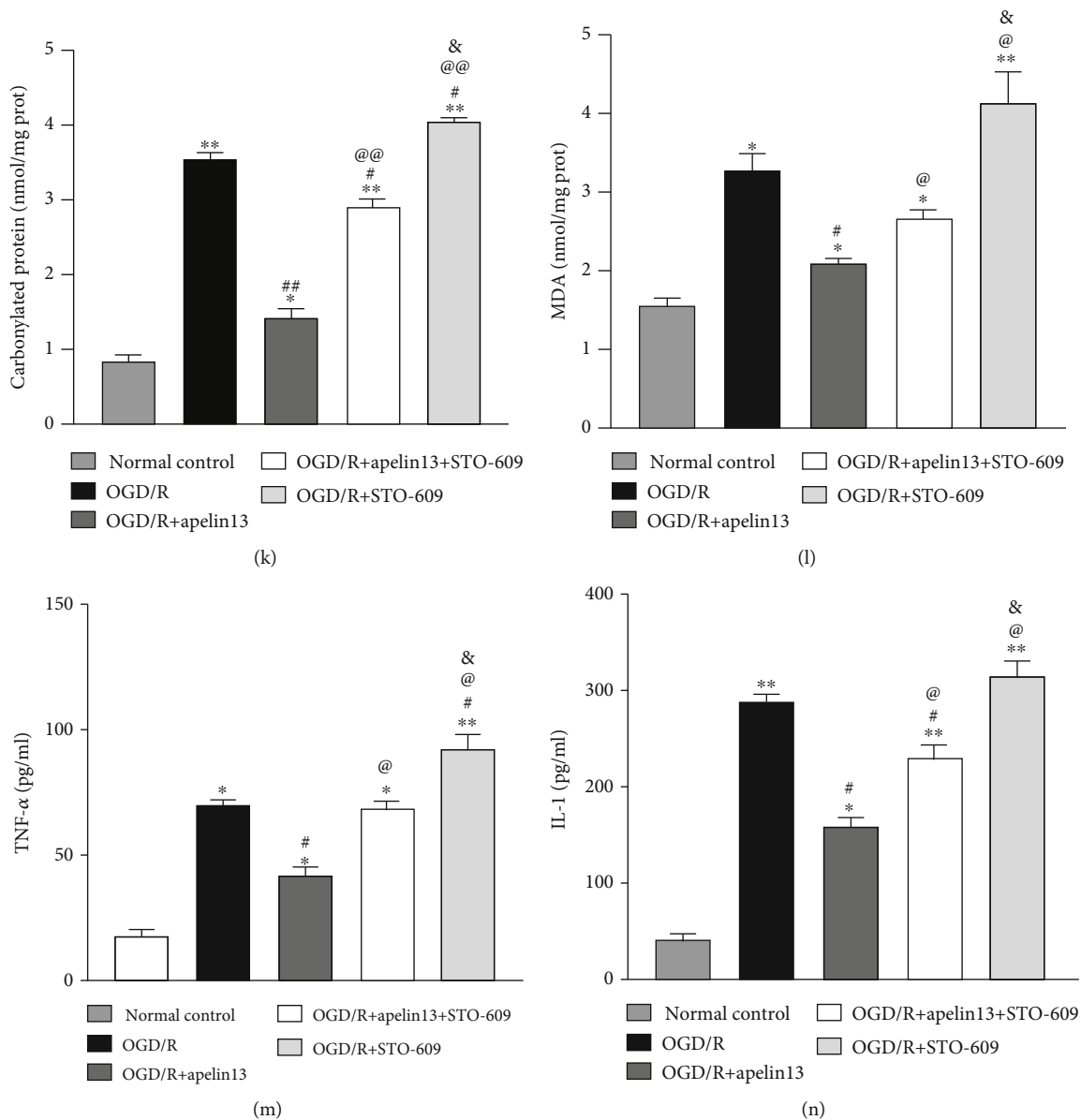


FIGURE 5: Apelin13 protected HUVECs from OGD/R by activating CaMKK-dependent AMPK/GSK3 β and downstream Nrf2/HO-1/SOD2. (a) Representative Western blot bands of p-AMPK, t-AMPK, p-GSK3 β , t-GSK3 β , Nrf2, HO-1, SOD2, Bax, and Bcl2 in different groups. (b–h) Relative expression and phosphorylation ratio. (i–l) CAT, GSH, MDA, and carbonylated protein levels were measured. (m, n) Inflammatory factors IL-1 and TNF α measured by using specific detection kits. The densitometric analysis of all Western blot bands was normalized to total protein and GAPDH. $n = 4$ independent experiments. The grouping legends are placed at the bottom of this figure. “*” means compared with the normal control group; “#” means compared with the OGD/R group; “@” means compared with the OGD/R+apelin13 group; “&” means compared with the OGD/R+apelin13+STO-609 group. * $p < 0.05$, ** $p < 0.01$.

3.8. Apelin13 Promoted the Migration of HUVECs and Angiogenesis by CaMKK/AMPK/GSK3 β Signaling. The migration of vascular endothelial cells is the foundation of angiogenesis. In our study, the Transwell experiment was used to quantify the migrated HUVECs. The tube formation experiment was used to assess the capacity of angiogenesis. When HUVECs are exposed to glucose and oxygen deprivation, both the number of migrated cells and the number of tubes formed decreased visibly. Apelin13 promoted cell migration and tube formation by combining with APJ; contrary to this, ML221 blocked APJ activation and further

inhibited apelin13's promotion (Figures 8(a)–8(c)). When we introduced STO-609 into the treatment, apelin13-mediated cell migration and angiogenesis were reversed (Figures 8(d)–8(f)). Similarly, DM inhibiting AMPK phosphorylation (Figures 8(g)–8(i)) and BX795 inhibiting GSK3 β Ser-9 phosphorylation (Figures 8(j)–8(l)) inhibited cell migration and reduced the tube number in fields. In addition to the antioxidant stress effect mediated by apelin13, CaMKK/AMPK/GSK3 β signaling also played an important role in promoting HUVEC migration and angiogenic capacity retroactively.

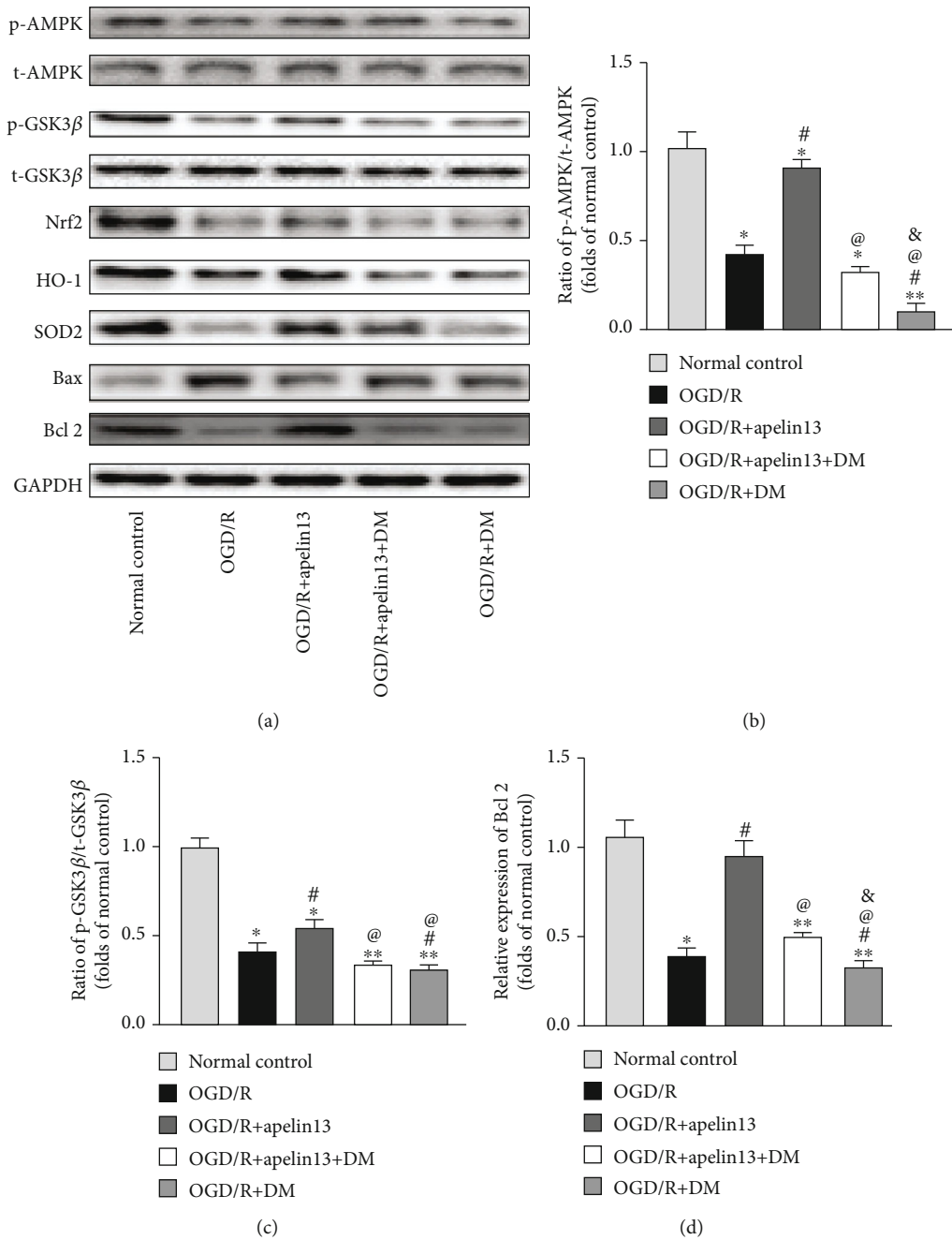


FIGURE 6: Continued.

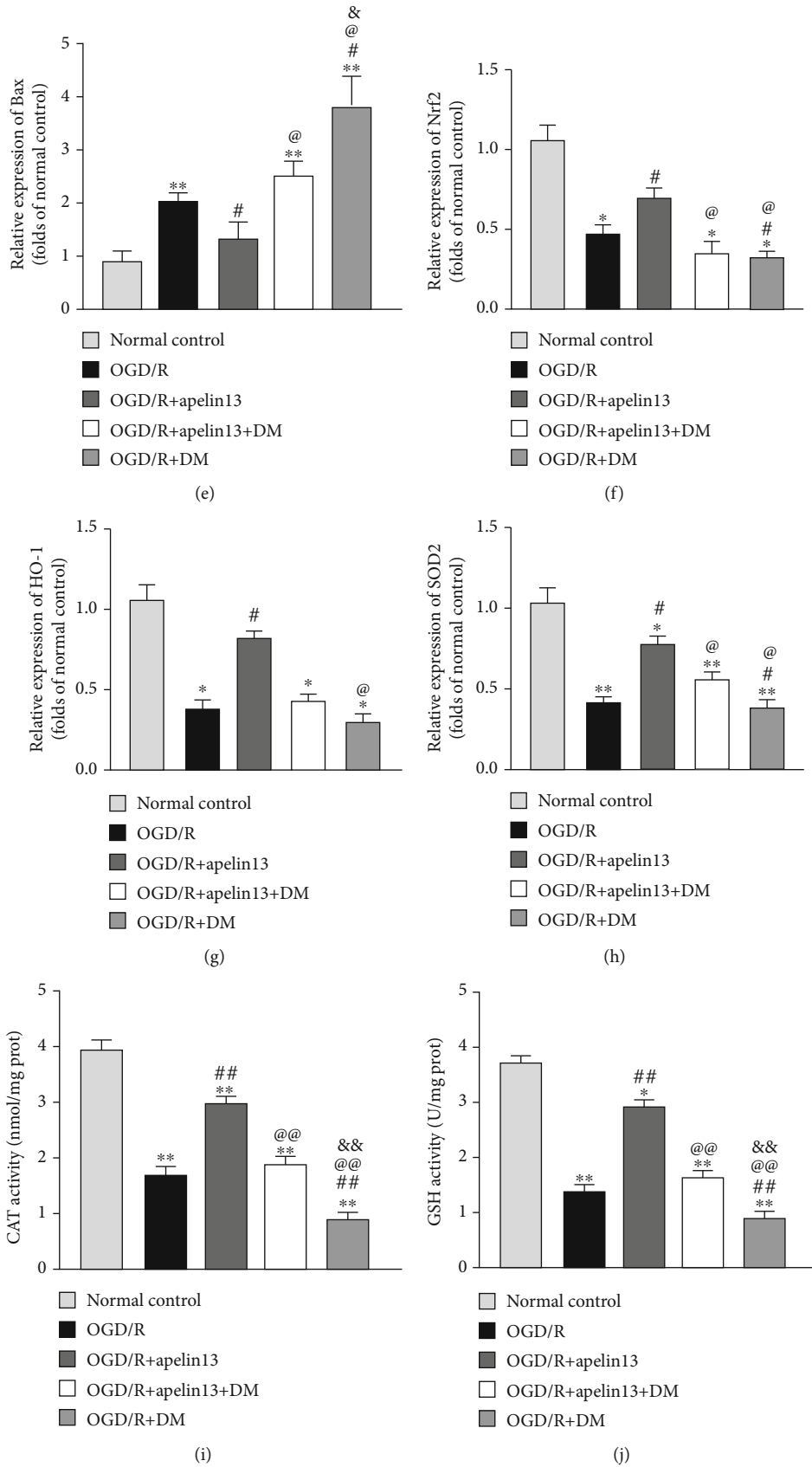


FIGURE 6: Continued.

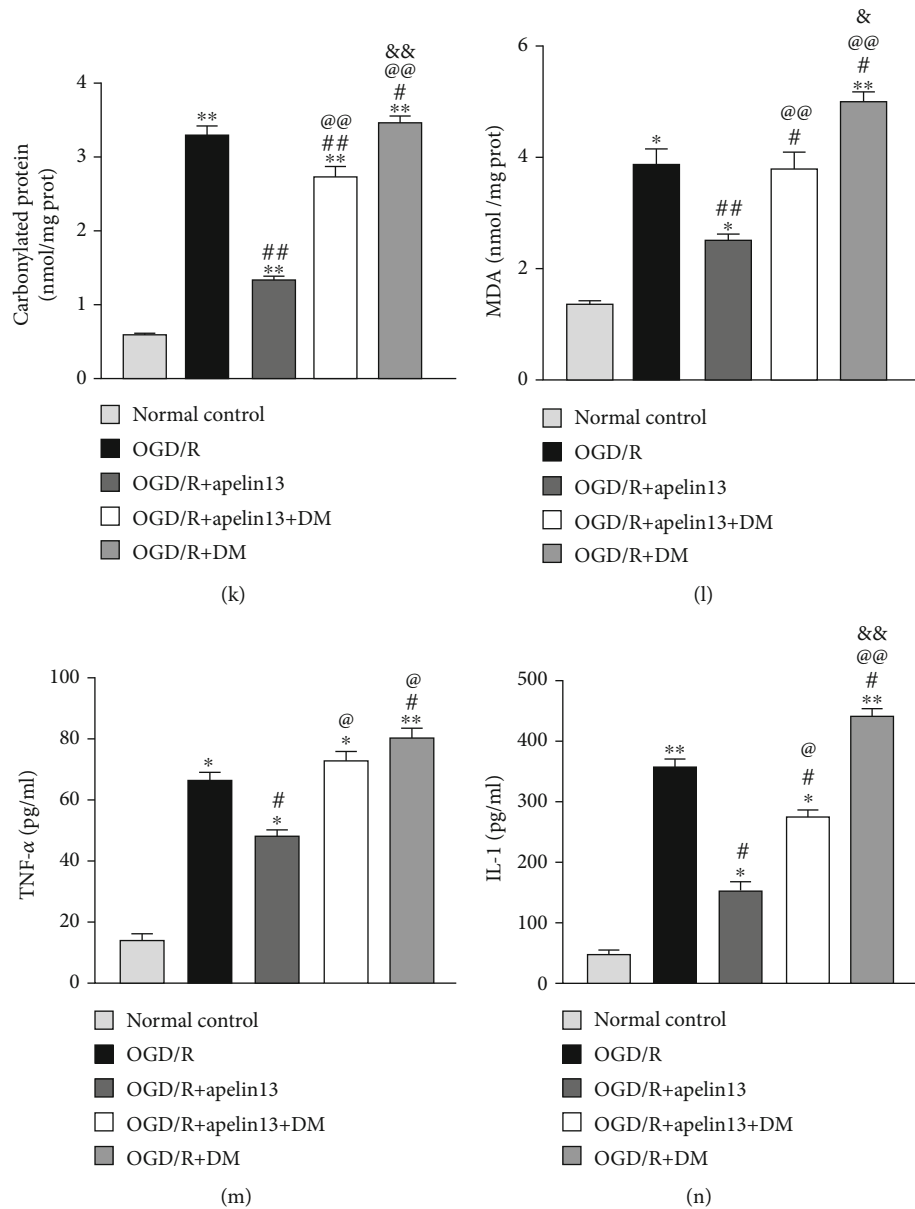


FIGURE 6: DM blocking apelin13-mediated AMPK/GSK3 β /Nrf2 signaling activation in HUVECs. (a) Representative Western blot bands of p-AMPK, t-AMPK, p-GSK3 β , t-GSK3 β , Nrf2, HO-1, SOD2, Bax, and Bcl2 in different groups. (b–h) Relative expression and phosphorylation ratio. (i–l) CAT, GSH, MDA, and carbonylated protein levels were measured. (m, n) Inflammatory factors IL-1 and TNF α measured by using specific detection kits. The densitometric analysis of all Western blot bands was normalized to total protein and GAPDH. $n = 4$ independent experiments. The grouping legends are placed at the bottom of this figure. “*” means compared with the normal control group; “#” means compared with the OGD/R group; “@” means compared with the OGD/R+apelin13 group; “&” means compared with the OGD/R+apelin13+DM group. * $p < 0.05$, ** $p < 0.01$.

4. Discussion

Large-area skin defects caused by severe trauma, burns, tumor resection, and ulcers often need to be repaired by a skin flap, but the occurrence of potential area necrosis limits the scope of the skin flap. Although delayed operation, pressurization, or drug intervention can improve the survival of the skin flap, the survival of the potential area is still different under different interventions and it is still difficult to guarantee the survival of potential areas. So far, there are many studies on promoting the survival of random skin flap trans-

plantation. In order to enhance skin flap viability, a variety of attempts have been made in the postoperation medicine treatment [3], the biomaterial development [7], herbal extract treatment [9], and even acupuncture treatment [35]. However, in clinical application, the curative effect of these methods is not accurate due to potential toxic side effects and unclear therapeutic targets, and many theoretical treatment schemes are not feasible yet. So, it is imperative to further explore its pathogenesis and seek effective therapeutic targets. A random skin flap, lacking a vessel pedicle, and its blood supply mainly come from the regenerated microvessels

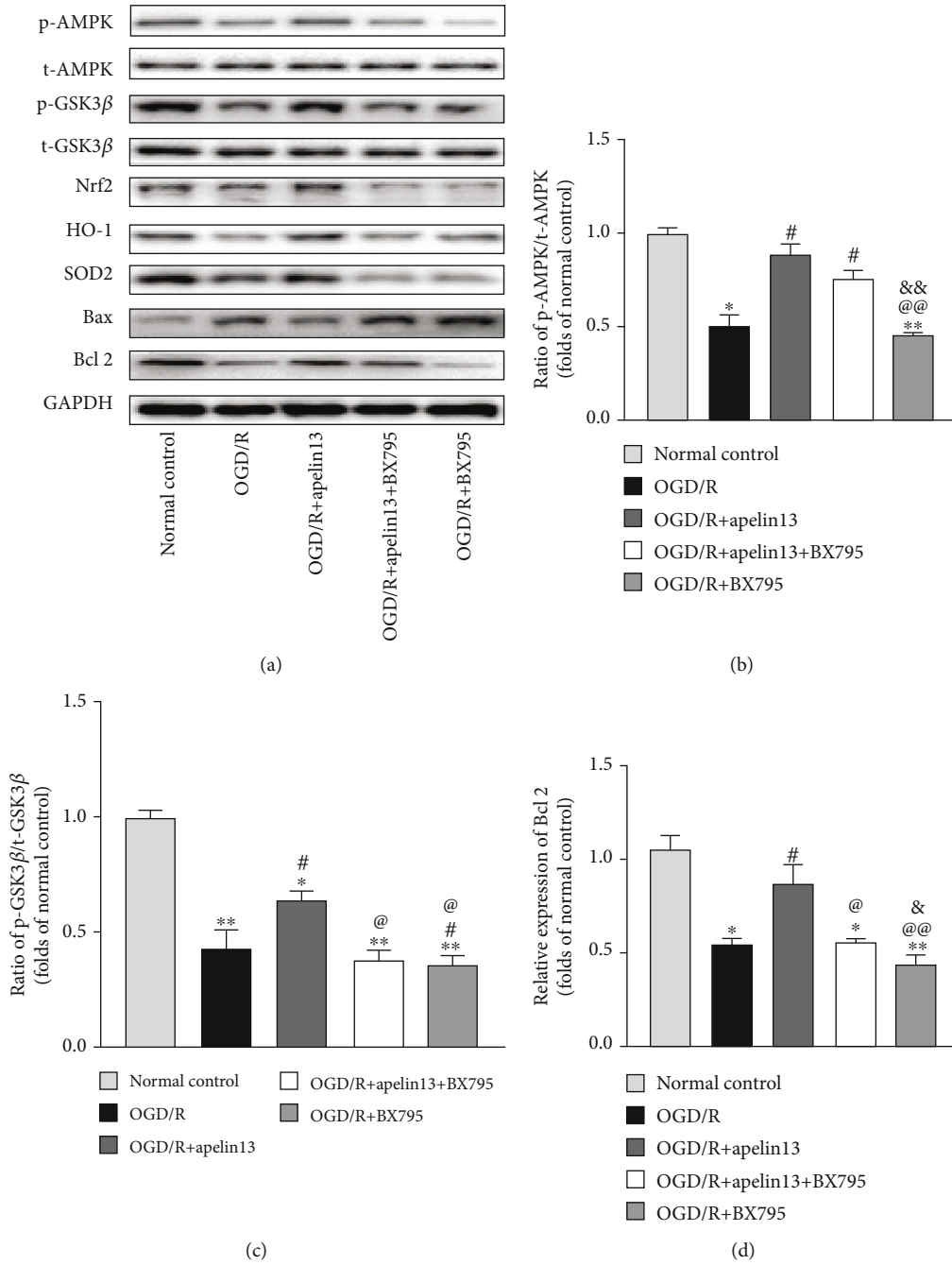


FIGURE 7: Continued.

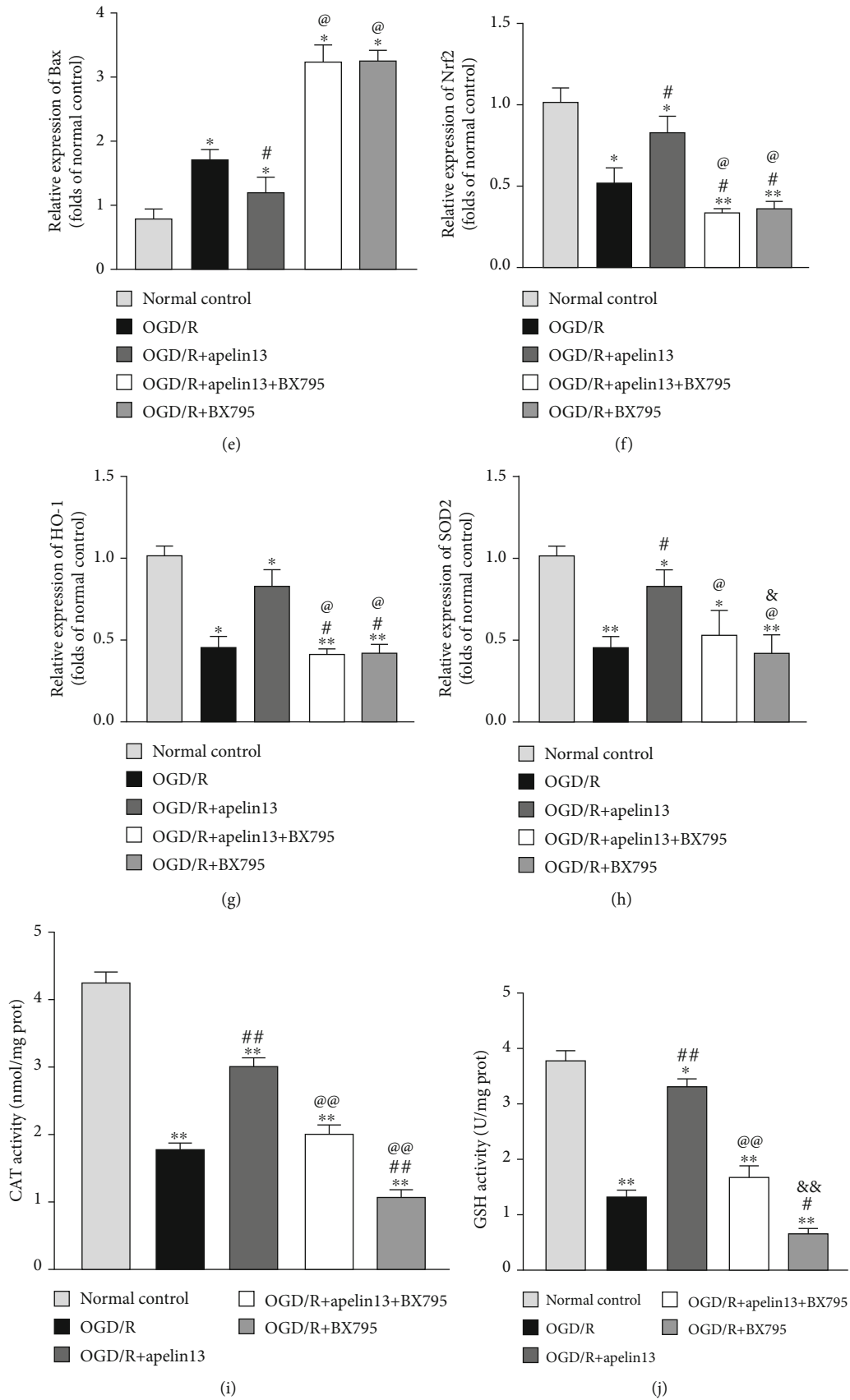


FIGURE 7: Continued.

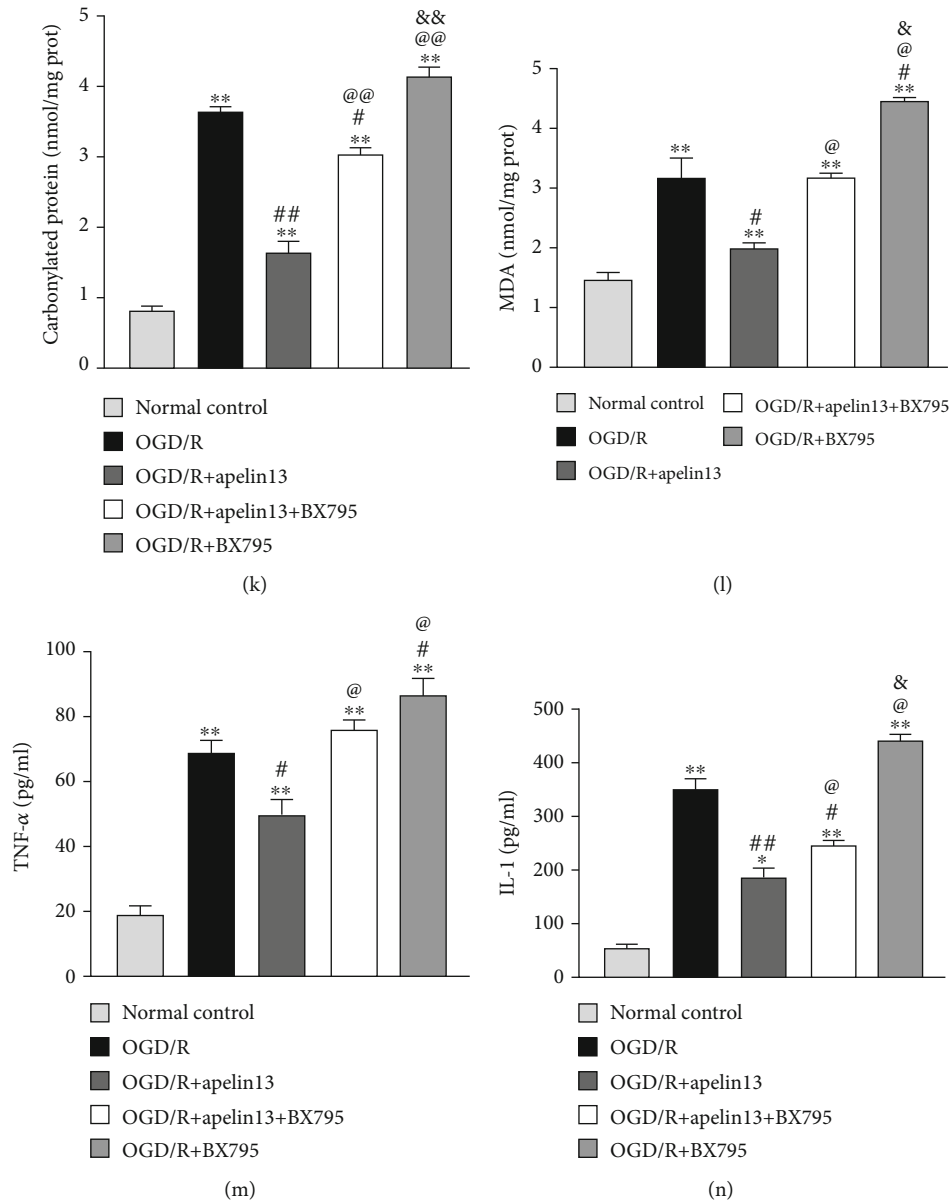


FIGURE 7: Inhibition of GSK3 β Ser-9 phosphorylation counteracts apelin13-induced Nrf2/SOD2 signaling activation in HUVECs. (a) Representative Western blot bands of p-AMPK, t-AMPK, p-GSK3 β , t-GSK3 β , Nrf2, HO-1, SOD2, Bax, and Bcl2 in different groups. (b–h) Relative expression and phosphorylation ratio. (i–l) CAT, GSH, MDA, and carbonylated protein levels were measured. (m, n) Inflammatory factors IL-1 and TNF α measured by using specific detection kits. The densitometric analysis of all Western blot bands was normalized to total protein and GAPDH. $n = 4$ independent experiments. The grouping legends are placed at the bottom of this figure. “*” means compared with the normal control group; “#” means compared with the OGD/R group; “@” means compared with the OGD/R+apelin13 group; “&” means compared with the OGD/R+apelin13+BX795 group. * $p < 0.05$, ** $p < 0.01$.

and small vessel stumps around the wound. It makes ischemia-reperfusion a definite and inevitable pathological process for a random skin flap. Our preexperiments show that the expression abundance of apelin and its receptor APJ decreased in the skin flap after operation. Our study focused on the significant loss of both the orphan receptor APJ and its ligand apelin in the random pattern skin flap. In order to clarify whether apelin plays a protective role in the survival of the skin flap, we try a short-term exogenous apelin supplementation after skin flap operation. The expected result is that the ischemic necrosis of the random

skin flap will decrease after apelin treatment. In fact, after apelin treatment, the degree of edema of the flap is reduced, the necrotic area is reduced, and the blood flow signal intensity of LDBF is increased. Our results suggest the administration of exogenous apelin can improve the viability of the skin flap by enhancing the growth of vascular stumps and microangiogenesis in the ischemic area, attenuating oxidative stress and subsequent apoptosis. Fortunately, as we expected and proved, apelin does have both antioxidant stress and angiogenic effects by activating its receptor APJ. We believe that postoperative exogenous supplementation of apelin to

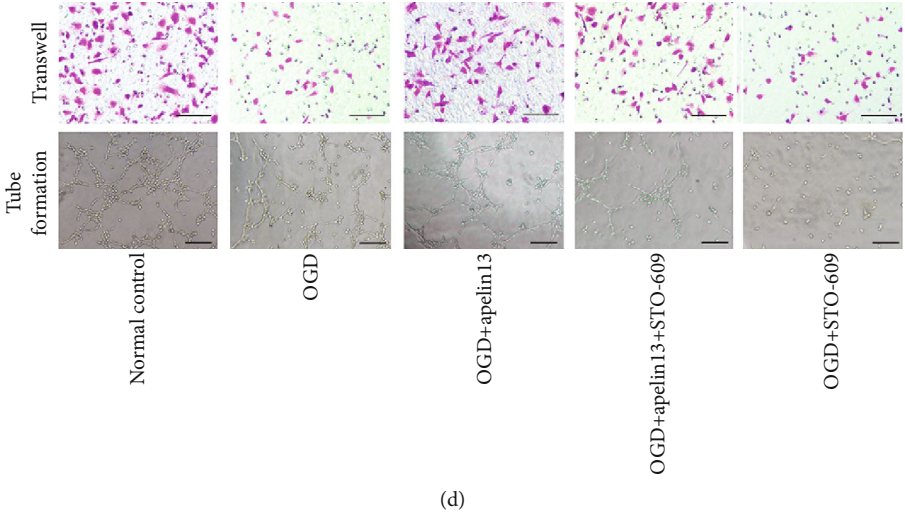
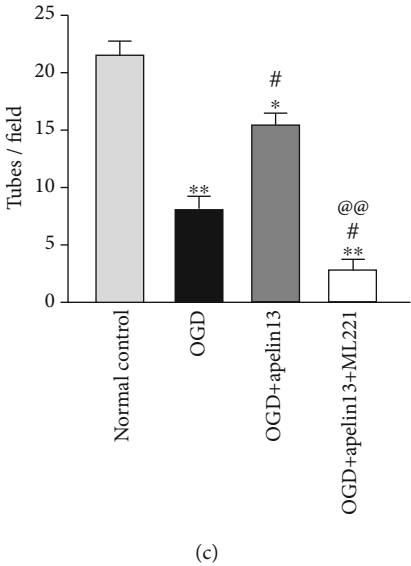
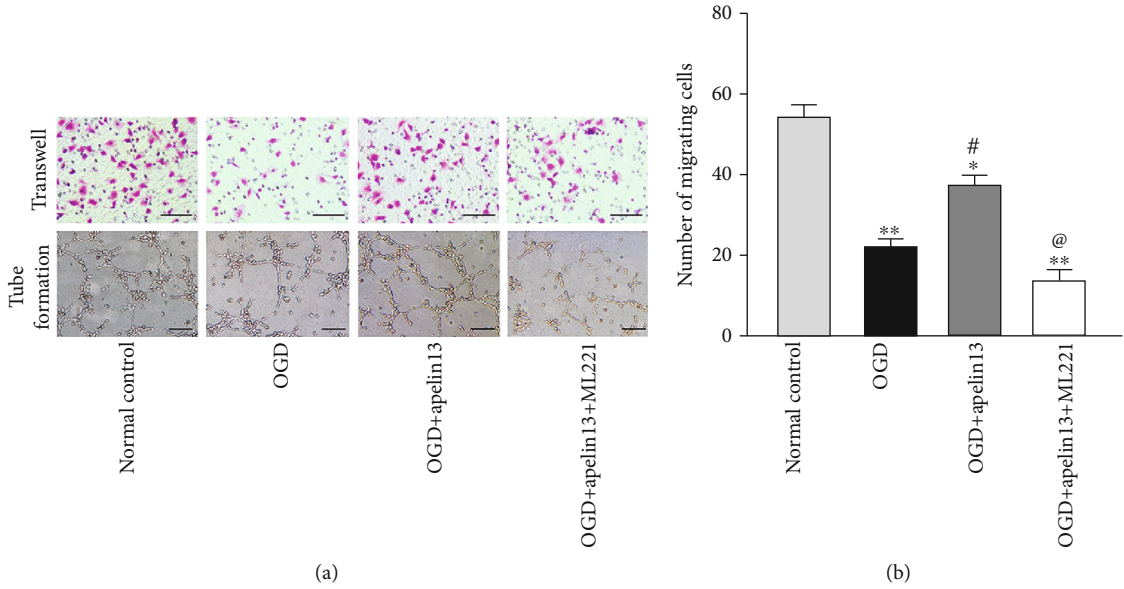


FIGURE 8: Continued.

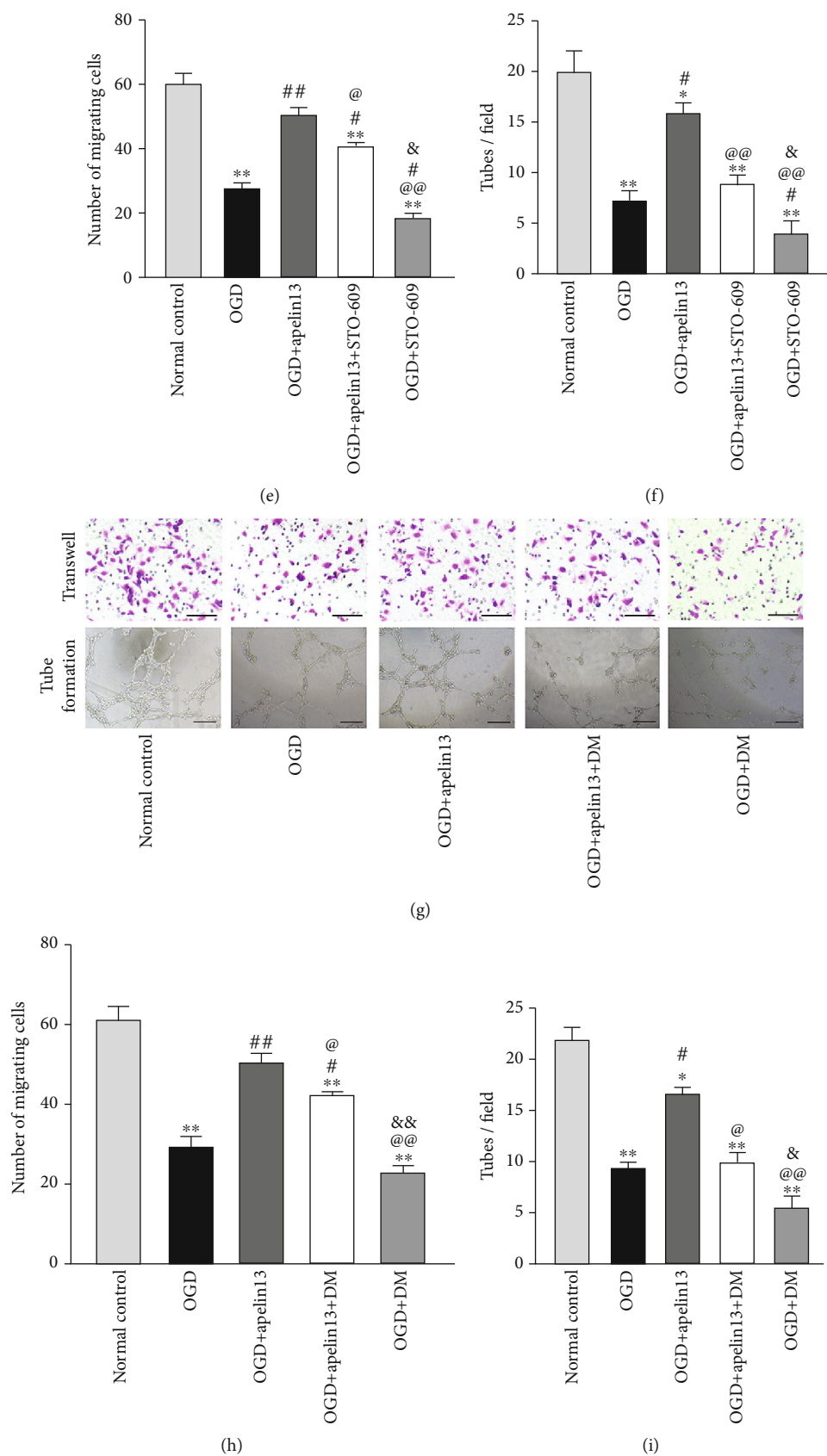


FIGURE 8: Continued.

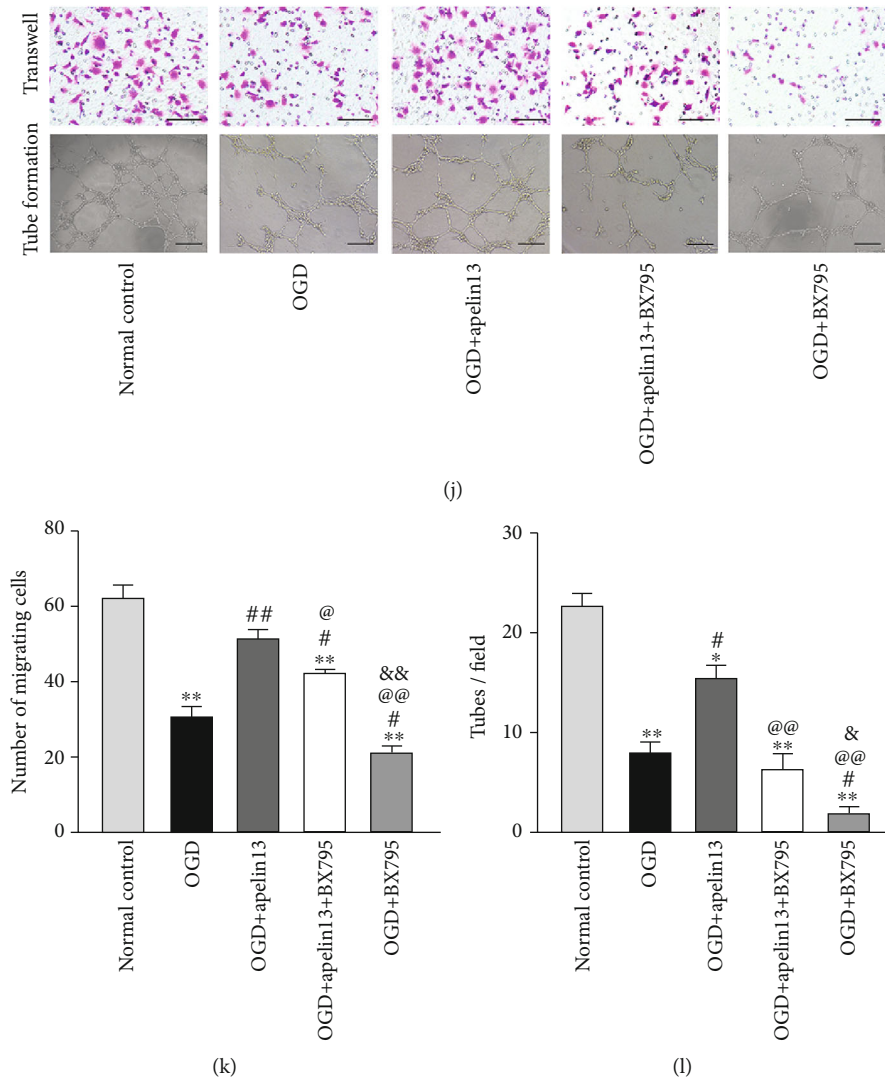


FIGURE 8: Apelin13 enhanced the migration and tube formation of HUVECs under short-time OGD via CaMKK/AMPK/GSK3 β signaling. (a, d, g, j) Transwell migration assay and tube formation images of HUVECs with different treatments. (b, e, h, k) Statistical histograms of cell migration. (c, f, i, l) Histogram of tube formations in all different groups. $n = 4$ independent experiments. “*” means compared with the normal control group; “#” means compared with the OGD group; “@” means compared with the OGD+apelin13 group; “&” means compared with the OGD+apelin13+STO-609 or DM and BX795 groups. * $p < 0.05$, ** $p < 0.01$.

awaken the apelin/APJ axis of vessels is a convenient way to ensure the survival of a random flap and apelin is an effective accelerator for flap survival.

It has been proven that apelin attenuates IRI in organs by a variety of mechanisms such as reducing acute injury through suppression of TGF- β 1 [36], protecting against myocardial IRI by inactivating GSK3 β [37]. In these studies, the levels of inflammation and oxidative stress are suppressed by apelin. Similarly, our experimental results in vivo showed that the expression of Nrf2, SOD2, and HO-1 decreased, which indirectly reflected the high oxidative stress operation, and the treatment of apelin increased the expression of Nrf2, SOD2, and HO-1 to some extent. In vitro, we stimulated HUVEC cells with OGD/R which was consistent with the ischemia/reperfusion process in vivo to simulate the pathophysiological changes in vessels. Free from any harmful stimulations, the expression of Nrf2 inside cells remained quite

satisfying. Immunofluorescence showed a strong signal of Nrf2 in the nucleus. As far as we know, translocation of Nrf2 into the nucleus promotes the expression of ARE-dependent antioxidant genes [38]. As a result, the expression levels of SOD2 and HO-1 increased; in the meantime, the production and accumulation of ROS inside cells were not active and JC-1 staining showed that the mitochondrial membrane potential was not impaired. After OGD/R stimulation, production and accumulation of ROS increased, the content of Nrf2 decreased either at the overall level or in the nucleus, the expression of antioxidant proteins SOD2 and HO-1 was inhibited, and the mitochondrial membrane potential was damaged resulting in the energy metabolic disorder. By treating with apelin13 alone, stimulated HUVECs appeared to have incredible tolerance to OGD/R stimulation, which was manifested in many aspects such as reduction of intracellular ROS, maintenance of

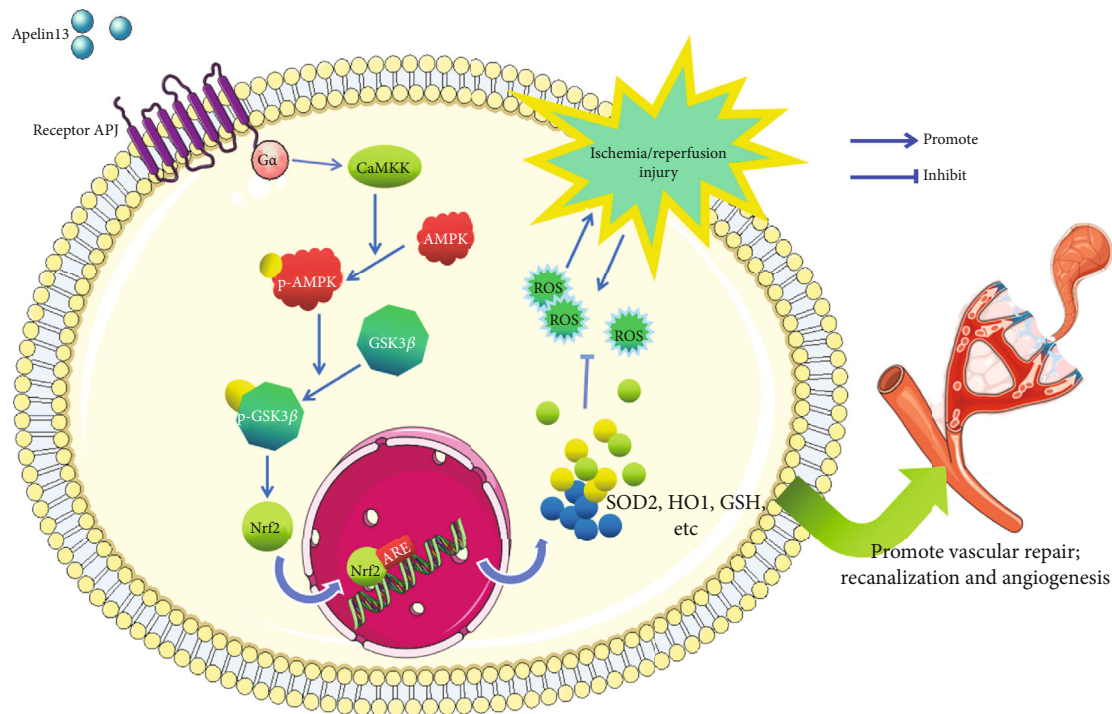


FIGURE 9: Potential mechanism underlying the wound healing promotion of apelin13 on IRI-induced skin flap injuries in mice and HUVECs. Apelin13 protected a random-pattern skin flap against IRI-induced oxidative stress and inflammation through AMPK-mediated inhibitory phosphorylation of GSK-3 β downstream of the G-coupled receptor (APJ), further inducing Nrf2-mediated antioxidant protein expressions and promoting angiogenesis.

intranuclear Nrf2, and a milder mitochondrial membrane potential damage. Given apelin13 treatment together with the inhibitor ML221, apelin13 can no longer activate the APJ receptor as usual, the protective effects were nearly reversed completely, and HUVECs showed a fragile side to OGD/R again.

APJ is an orphan receptor and a G protein-coupled receptor. Apelin13 binds to the APJ receptor and activates it, and the activation of its G α subunits (including G α i and G α q) can activate downstream CaMKK/AMPK/GSK3 β signaling, then promotes the translocation of Nrf2 into the nucleus, upregulates ARE-dependent antioxidants SOD, NQO1, and HO-1, suppresses oxidative stress, and protects brain and PC12 cells [39]. When the skin tissue is in a normal and healthy state, normal activation of apelin/APJ ensures a proper phosphorylation ratio of AMPK and GSK3 β which declined in a random flap. As shown in Figure 9, similar to the protective mechanism of the apelin/APJ axis in the brain, treatment with apelin13 restores the phosphorylation ratio of AMPK and GSK3 β greatly, which means that AMPK/GSK3 β signaling also exists as a potential protective mechanism in the skin flap in the same way in the brain.

As we all know, the regeneration of vessels and the recovery of blood supply are the essential problems in wound healing. In order to clarify the angiogenesis mechanism, we focus on the activation of apelin/APJ-dependent CaMKK/AMPK/GSK3 β signaling and the further effect including angiogenesis and antioxidant stress on HUVECs. The selective CaMKK inhibitor STO-609, selective AMPK inhibitor dorsomorphin, and selective GSK3 β phosphorylation inhib-

itor BX795 were given to cells separately. BX795 can inhibit Ser9-phosphorylation of GSK3 β while it cannot change the expression of total GSK3 β [40]. It is worth noting that phosphorylation of GSK3 β inactivates GSK3 β and the maintenance of GSK3 β activity increases glycogen degradation, glycolysis substrate oxidation, and lactate production, indicating decreased resistance of cells to oxidative stress [41–44]. All these three inhibitors inhibited apelin13's callback of Nrf2, SOD2, and HO-1. The similar changes of metabolite of lipid oxidation MDA and inflammatory mediators IL-1 and TNF α were observed, thus reversing apelin13's protective effect on HUVECs. These suggested that apelin13 protected HUVECs from oxidative stress through a CaMKK/AMPK/GSK3 β signaling-dependent mechanism during OGD/R.

As for the mechanism of angiogenesis, apelin, AMPK, and GSK3 β have been separately reported to be associated with angiogenesis [45–48]. However, the relationship among apelin, AMPK, and GSK3 β in angiogenesis has rarely been reported, especially in the environment of ischemia-reperfusion. In view of the fact that apelin13 can protect HUVECs from oxidative stress in vitro, in a CaMKK/AMPK/GSK3 β -dependent manner after activating the receptor APJ, we are also interested in whether apelin13 promotes angiogenesis in this CaMKK/AMPK/GSK3 β -dependent manner. Therefore, the model of short-term glucose and oxygen deprivation was established in vitro, and the quantity of migrated cells in Transwell migration assays and tubules' number in tube formation assays were used to comprehensively evaluate angiogenesis capacity. When cells

were exposed to OGD, both migrated cells and tubes formed sharply decreased. Apelin13 increased migrated cells and tubes formed. Administration of inhibitors STO-609, dorsomorphin, and BX795 reversed apelin13's angiogenesis promotion; thus, inhibition of CaMKK, AMPK-phosphorylation, and Ser9-phosphorylation of GSK3 β declined angiogenesis, indicating that apelin13/APJ promoted angiogenesis capacity at least through a CaMKK/AMPK/GSK3 β signaling-dependent mechanism.

Regarding prospect and deficiency, our study is precisely focused on skin flap vessels. Through this study, we prove that the apelin/APJ signal axis is suppressed in postoperative skin flap vessels, and postoperative supplementation of apelin can not only help skin flap resist the IRI but also promote angiogenesis, ultimately enhancing random skin flap viability through a CaMKK/AMPK/GSK3 β -dependent mechanism. Apelin is also a kind of widespread inherent polypeptides in animals, which has good compatibility with animals and can effectively reduce the risk of toxicity and side effects. With increasing clinical trials over time, apelin treatment can be expected to be a convenient and efficient clinical application in the field of wound healing. Besides, we also realize that there are still many limitations in our research, and we have yet to show whether apelin/APJ-manipulated CaMKK/AMPK/GSK3 β -dependent mechanism is the only mechanism of apelin's therapeutic work. Other therapeutic targets of apelin are not known yet. The study focuses on vessels but ignores exploring the function of other tissue components in the skin flap.

5. Conclusion

In conclusion, *in vivo*, our study proved that the apelin/APJ axis protected the skin flap by alleviating vascular oxidative stress and the apelin/APJ axis works as an antioxidant stress factor dependent on CaMKK/AMPK/GSK3 β signaling. Besides, an apelin/APJ-manipulated CaMKK/AMPK/GSK3 β -dependent mechanism improves the tolerance of HUVECs to OGD/R, reduces ROS production and accumulation, maintained the normal mitochondrial membrane potential, and suppresses oxidative stress *in vitro*. It is worth mentioning that activation of the apelin/APJ axis promotes vascular migration and angiogenesis under relative hypoxia condition through CaMKK/AMPK/GSK3 β signaling. The awakening of the apelin/APJ axis may play a dual role in both antioxidant stress and angiogenesis in wound healing.

Data Availability

The data used to support the findings of this study are available from the corresponding author upon request.

Conflicts of Interest

The authors have no conflicts of interest.

Authors' Contributions

Qifeng Zhao conceived the study and helped in modifying the manuscript. Zhi-Ling Lou performed the animal model experiments and collected the samples. Chen-Xi Zhang and Wei-Yang Gao participated in the experimental design and contributed to reagents, materials, and analytical tools. Rui-Heng Chen and Jia-Feng Li were also involved in the experiments. Zhi-Ling Lou wrote the manuscript. Zhi-Ling Lou, Chen-Xi Zhang, and Jia-Feng Li participated in the statistical analysis. Zhi-Ling Lou, Wei-Jia Wu, Xiao-Fen Hu, and Hao-Chun Shi prepared all figures. All authors read and approved the final manuscript. Zhi-Ling Lou, Chen-Xi Zhang, and Jia-Feng Li contributed equally.

Acknowledgments

This work was supported by the Zhejiang Provincial Natural Science Foundation of China (LY15H060010 and LY17H020012), the Key Supporting Discipline of Zhejiang Provincial Department of Health-Pediatric Surgery Research Project (11-ZC27), the Special Project for Significant New Drug Research and Development in the Major National Science and Technology Projects of China (2020ZX09201002), and the National Natural Science Foundation of China (Nos. 82070274 and 81973382).

References

- [1] A. Lyu and Q. Wang, "Dermatofibrosarcoma protuberans: a clinical analysis," *Oncology Letters*, vol. 16, no. 2, pp. 1855–1862, 2018.
- [2] G. Basu, H. Downey, S. Guo et al., "Prevention of distal flap necrosis in a rat random skin flap model by gene electrotransfer delivering VEGF165 plasmid," *The Journal of Gene Medicine*, vol. 16, no. 3-4, pp. 55–65, 2014.
- [3] H. Wu, J. Ding, S. Li et al., "Metformin promotes the survival of random-pattern skin flaps by inducing autophagy via the AMPK-mTOR-TFEB signaling pathway," *International Journal of Biological Sciences*, vol. 15, no. 2, pp. 325–340, 2019.
- [4] J. A. Winkles, "The TWEAK-Fn14 cytokine-receptor axis: discovery, biology and therapeutic targeting," *Nature Reviews Drug Discovery*, vol. 7, no. 5, pp. 411–425, 2008.
- [5] E. Gur, A. Chiodo, C. Y. Pang et al., "The vascularized pig fibula bone flap model: effects of multiple segmental osteotomies on growth and viability," *Plastic and Reconstructive Surgery*, vol. 103, no. 5, pp. 1436–1442, 1999.
- [6] S. C. Um, S. Suzuki, S. Toyokuni et al., "Involvement of nitric oxide in survival of random pattern skin flap," *Plastic and Reconstructive Surgery*, vol. 101, no. 3, pp. 785–792, 1998.
- [7] X. Mao, R. Cheng, H. Zhang et al., "Self-healing and injectable hydrogel for matching skin flap regeneration," *Advanced Science*, vol. 6, no. 3, article 1801555, 2019.
- [8] X. Mao, L. Liu, L. Cheng et al., "Adhesive nanoparticles with inflammation regulation for promoting skin flap regeneration," *Journal of Controlled Release*, vol. 297, pp. 91–101, 2019.
- [9] J. Li, G. Bao, E. ALyafeai et al., "Betulinic acid enhances the viability of random-pattern skin flaps by activating autophagy," *Frontiers in Pharmacology*, vol. 10, p. 1017, 2019.

- [10] M. A. Stotland and C. L. Kerrigan, "The role of platelet-activating factor in musculocutaneous flap reperfusion injury," *Plastic and Reconstructive Surgery*, vol. 99, no. 7, pp. 1989–1999, 1999.
- [11] J. Lin, C. Jia, Y. Wang et al., "Therapeutic potential of pravastatin for random skin flaps necrosis: involvement of promoting angiogenesis and inhibiting apoptosis and oxidative stress," *Drug Design Development and Therapy*, vol. Volume 13, pp. 1461–1472, 2019.
- [12] D. Marsolais and H. Rosen, "Chemical modulators of sphingosine-1-phosphate receptors as barrier-oriented therapeutic molecules," *Nature Reviews Drug Discovery*, vol. 8, no. 4, pp. 297–307, 2009.
- [13] M. Strüber, C. C. Hagl, S. W. Hirt, J. Cremer, W. Harringer, and A. Haverich, "C1-esterase inhibitor in graft failure after lung transplantation," *Intensive Care Medicine*, vol. 25, no. 11, pp. 1315–1318, 1999.
- [14] A. E. El-Desoky, A. M. Seifalian, and B. R. Davidson, "Effect of graded hypoxia on hepatic tissue oxygenation measured by near infrared spectroscopy," *Journal of Hepatology*, vol. 31, no. 1, pp. 71–76, 1999.
- [15] S. B. See, O. Aubert, A. Loupy et al., "Post-transplant natural antibodies associate with kidney allograft injury and reduced long-term survival," *Journal of the American Society of Nephrology*, vol. 29, no. 6, pp. 1761–1770, 2018.
- [16] H. Lin, M. Chen, F. Tian et al., "α1-Anti-trypsin improves function of porcine donor lungs during ex-vivo lung perfusion," *The Journal of Heart and Lung Transplantation*, vol. 37, no. 5, pp. 656–666, 2018.
- [17] M. J. Hernandez and K. L. Christman, "Designing acellular injectable biomaterial therapeutics for treating myocardial infarction and peripheral artery disease," *JACC: Basic to Translational Science*, vol. 2, no. 2, pp. 212–226, 2017.
- [18] G. Feng, J. Zhang, Y. Li et al., "IGF-1 C domain-modified hydrogel enhances cell therapy for AKI," *Journal of the American Society of Nephrology*, vol. 27, no. 8, pp. 2357–2369, 2016.
- [19] X. F. Fan, F. Xue, Y. Q. Zhang et al., "The apelin-APJ axis is an endogenous counterinjury mechanism in experimental acute lung injury," *Chest*, vol. 147, no. 4, pp. 969–978, 2015.
- [20] K. Tatemoto, M. Hosoya, Y. Habata et al., "Isolation and characterization of a novel endogenous peptide ligand for the human APJ receptor," *Biochemical and Biophysical Research Communications*, vol. 251, no. 2, pp. 471–476, 1998.
- [21] O. Pisarenko, V. Shulzhenko, I. Studneva et al., "Structural apelin analogues: mitochondrial ROS inhibition and cardiometabolic protection in myocardial ischaemia reperfusion injury," *British Journal of Pharmacology*, vol. 172, no. 12, pp. 2933–2945, 2015.
- [22] M. J. Klein and A. P. Davenport, "Emerging roles of apelin in biology and medicine," *Pharmacology & Therapeutics*, vol. 107, no. 2, pp. 198–211, 2005.
- [23] C. Galanthe, A. Hus-Citharel, B. Li, and C. Llorens-Cortès, "Apelin in the control of body fluid homeostasis and cardiovascular functions," *Current Pharmaceutical Design*, vol. 18, no. 6, pp. 789–798, 2012.
- [24] C. Read, D. Nyimanu, T. L. Williams et al., "International Union of Basic and Clinical Pharmacology. CVII. Structure and pharmacology of the apelin receptor with a recommendation that Elabela/Toddler is a second endogenous peptide ligand," *Pharmacological Reviews*, vol. 71, no. 4, pp. 467–502, 2019.
- [25] A. Mughal and S. T. O'Rourke, "Vascular effects of apelin: mechanisms and therapeutic potential," *Pharmacology & Therapeutics*, vol. 190, pp. 137–147, 2018.
- [26] M. F. Berry, T. J. Pirolli, V. Jayasankar et al., "Apelin has in vivo inotropic effects on normal and failing hearts," *Circulation*, vol. 110, pp. 187–193, 2004.
- [27] S. Liu, W. Wang, L. Yin, and Y. Zhu, "Influence of apelin-13 on osteoporosis in type-2 diabetes mellitus: a clinical study," *Pakistan Journal of Medical Sciences*, vol. 34, no. 1, pp. 159–163, 2018.
- [28] X. F. Han, X. X. Zhang, K. M. Liu, and Q. Zhang, "Apelin-13 deficiency alters cortical bone geometry, organic bone matrix, and inhibits Wnt/β-catenin signaling," *General and Comparative Endocrinology*, vol. 267, pp. 29–35, 2018.
- [29] H. Kidoya, H. Naito, F. Muramatsu et al., "APJ regulates parallel alignment of arteries and veins in the skin," *Developmental Cell*, vol. 33, no. 3, pp. 247–259, 2015.
- [30] R. O. Alabi, G. Farber, and C. P. Blobel, "Intriguing roles for endothelial ADAM10/Notch signaling in the development of organ-specific vascular beds," *Physiological Reviews*, vol. 98, no. 4, pp. 2025–2061, 2018.
- [31] F. Boal, J. Roumegoux, C. Alfarano et al., "Apelin regulates FoxO3 translocation to mediate cardioprotective responses to myocardial injury and obesity," *Scientific Reports*, vol. 5, no. 1, pp. 111–117, 2015.
- [32] L. Li, J. Xu, L. Chen, and Z. Jiang, "Apelin/APJ system: a novel promising therapy target for thrombotic diseases," *Acta Biochimica et Biophysica Sinica*, vol. 48, no. 6, pp. 589–591, 2016.
- [33] R. Stöhr, B. A. Kappel, D. Carnevale et al., "TIMP3 interplays with apelin to regulate cardiovascular metabolism in hypercholesterolemic mice," *Molecular Metabolism*, vol. 4, no. 10, pp. 741–752, 2015.
- [34] S. Le Lay, G. Simard, M. C. Martinez, and R. Andriantsitohaina, "Oxidative stress and metabolic pathologies: from an adipocentric point of view," *Oxidative Medicine and Cellular Longevity*, vol. 2014, Article ID 908539, 18 pages, 2014.
- [35] L. R. Wang, L. Y. Cai, D. S. Lin, B. Cao, and Z. J. Li, "Effect of electroacupuncture at the Zusanli point (Stomach-36) on dorsal random pattern skin flap survival in a rat model," *Dermatologic Surgery*, vol. 43, no. 10, pp. 1213–1220, 2017.
- [36] H. Chen, D. Wan, L. Wang et al., "Apelin protects against acute renal injury by inhibiting TGF-β1," *Biochimica et Biophysica Acta*, vol. 1852, no. 7, pp. 1278–1287, 2015.
- [37] P. Yang, J. J. Maguire, and A. P. Davenport, "Apelin, Elabela/Toddler, and biased agonists as novel therapeutic agents in the cardiovascular system," *Trends in Pharmacological Sciences*, vol. 36, no. 9, pp. 560–567, 2015.
- [38] C. Zhuang, W. Zhang, C. Sheng, W. Zhang, and Z. Y. Miao, "Chalcone: a privileged structure in medicinal chemistry," *Chemical Reviews*, vol. 117, no. 12, pp. 7762–7810, 2017.
- [39] J. Duan, J. Cui, Z. Yang et al., "Neuroprotective effect of apelin 13 on ischemic stroke by activating AMPK/GSK-3β/Nrf2 signaling," *Journal of Neuroinflammation*, vol. 16, no. 1, 2019.
- [40] R. I. Feldman, J. M. Wu, M. A. Polokoff et al., "Novel small molecule inhibitors of 3-phosphoinositide-dependent kinase-1," *The Journal of Biological Chemistry*, vol. 280, no. 20, pp. 19867–19874, 2005.
- [41] L. Gomez, P. A. Thiebaut, M. Paillard et al., "The SR/ER-mitochondria calcium crosstalk is regulated by GSK3β during reperfusion injury," *Cell Death & Differentiation*, vol. 23, no. 2, pp. 313–322, 2016.

- [42] L. Gomez, P. A. Thiebaut, M. Paillard et al., “The SR/ER-mitochondria calcium crosstalk is regulated by GSK3 β during reperfusion injury,” *Cell Death & Differentiation*, vol. 22, no. 11, pp. 1890–1890, 2015.
- [43] L. M. Delbridge, K. M. Mellor, D. J. Taylor, and R. A. Gottlieb, “Myocardial autophagic energy stress responses—macroautophagy, mitophagy, and glycophyagy,” *American Journal of Physiology-Heart and Circulatory Physiology*, vol. 308, no. 10, pp. H1194–H1204, 2015.
- [44] D. Yin, X. Yang, H. Li et al., “ β -Arrestin 2 promotes hepatocyte apoptosis by inhibiting Akt protein,” *Journal of Biological Chemistry*, vol. 291, no. 2, pp. 605–612, 2015.
- [45] R. Abdel Malik, N. Zippel, T. Frömel et al., “AMP-activated protein kinase α 2 in neutrophils regulates vascular repair via hypoxia-inducible factor-1 α and a network of proteins affecting metabolism and apoptosis,” *Circulation Research*, vol. 120, no. 1, pp. 99–109, 2017.
- [46] V. G. Zaha and L. H. Young, “AMP-activated protein kinase regulation and biological actions in the heart,” *Circulation Research*, vol. 111, no. 6, pp. 800–814, 2012.
- [47] Q. Duan, L. Ni, P. Wang et al., “Deregulation of XBP1 expression contributes to myocardial vascular endothelial growth factor-A expression and angiogenesis during cardiac hypertrophy in vivo,” *Aging Cell*, vol. 15, no. 4, pp. 625–633, 2016.
- [48] Y. P. Visser, F. J. Walther, E. H. Laghmani, A. Laarse, and G. T. Wagenaar, “Apelin attenuates hyperoxic lung and heart injury in neonatal rats,” *American Journal of Respiratory and Critical Care Medicine*, vol. 182, no. 10, pp. 1239–1250, 2010.

Research Article

The Effects of Hypoxia-Reoxygenation in Mouse Digital Flexor Tendon-Derived Cells

Chen Chen ¹, Wei Feng Mao ^{1,2} and Ya Fang Wu ¹

¹Department of Hand Surgery, Affiliated Hospital of Nantong University, Nantong, Jiangsu, China

²Department of Anatomy, Medical School, Nantong University, Nantong, Jiangsu, China

Correspondence should be addressed to Wei Feng Mao; maoweifeng@ntu.edu.cn and Ya Fang Wu; yafang.wu@ntu.edu.cn

Received 27 July 2020; Revised 12 November 2020; Accepted 25 November 2020; Published 15 December 2020

Academic Editor: Mariella B. Freitas

Copyright © 2020 Chen Chen et al. This is an open access article distributed under the Creative Commons Attribution License, which permits unrestricted use, distribution, and reproduction in any medium, provided the original work is properly cited.

Objective. Ischemia-reperfusion injury refers to the exacerbated and irreversible tissue damage caused by blood flow restoration after a period of ischemia. The hypoxia-reoxygenation (H/R) model in vitro is ideal for studying ischemia-reperfusion injury at the cellular level. We employed this model and investigated the effects of cobalt chloride- (CoCl₂-) induced H/R in cells derived from mouse digital flexor tendons. **Materials and Methods.** Various H/R conditions were simulated via treatment of tendon-derived cells with different concentrations of CoCl₂ for 24 h, followed by removal of CoCl₂ to restore a normal oxygen state for up to 96 h. Cell viability was measured using the Cell Counting Kit-8 (CCK-8) assay. Cell growth was determined via observation of cell morphology and proliferation. Oxidative stress markers and mitochondrial activity were detected. The expression levels of hypoxia-inducible factor- (HIF-) 1 α , vascular endothelial growth factor-A (VEGF-A), collagen I, and collagen III were determined using Western blot (WB), real-time PCR, and immunofluorescence staining. Cellular apoptosis was analyzed via flow cytometry, and the expression of apoptosis-related proteins Bax and bcl-2 was examined using WB. **Results.** The cells treated with low concentrations of CoCl₂ showed significantly increased cell viability after reoxygenation. The increase in cell viability was even more pronounced in cells that had been treated with high concentrations of CoCl₂. Under H/R conditions, cell morphology and growth were unchanged, while oxidative stress reaction was induced and mitochondrial activity was increased. H/R exerted opposite effects on the expression of HIF-1 α mRNA and protein. Meanwhile, the expression of VEGF-A was upregulated, whereas collagen type I and type III were significantly downregulated. The level of cellular apoptosis did not show significant changes during H/R, despite the significantly increased Bax protein and reduced bcl-2 protein levels that led to an increase in the Bax/bcl-2 ratio during reoxygenation. **Conclusions.** Tendon-derived cells were highly tolerant to the hypoxic environments induced by CoCl₂. Reoxygenation after hypoxia preconditioning promoted cell viability, especially in cells treated with high concentrations of CoCl₂. H/R conditions caused oxidative stress responses but did not affect cell growth. The H/R process had a notable impact on collagen production and expression of apoptosis-related proteins by tendon-derived cells, while the level of cellular apoptosis remained unchanged.

1. Introduction

Tendon injury is frequently accompanied by a lack of blood supply, exposing the tendon to a hypoxic condition. Oxygen tension, which is influenced by blood supply, is vital to cell survival and proliferation. In vitro studies have shown that low oxygen tension enhances the expansion capacity of newborn pig tenocytes without affecting the cellular phenotype and functions [1], and hypoxic conditions significantly improve the cell proliferation and self-renewal capacity of

human tendon stem cells [2, 3]. Other studies, however, have shown that hypoxia inhibits cell proliferation and alters the synthesis of matrix components in synovial tissue [4]. Cobalt chloride- (CoCl₂-) induced hypoxia has been shown to alter the expression of the bcl-2 family proteins and trigger caspase cascade apoptosis [5, 6]. Collectively, the conflicting results in these studies underscore the complicated effects of hypoxia on cell growth.

Most tissues subjected to oxygen deprivation after injury undergo reperfusion [7–10]. Reperfusion injury, which is

manifested by blood flow-deprived and oxygen-starved organs following blood flow restoration and tissue reoxygenation, is a tissue response to stimulate oxidative metabolism [11–15]. Tissues with reperfusion injury share some of the characteristic features of injury responses to oxygen deprivation and subsequent reoxygenation, such as necrosis, apoptosis, impaired microvascular function, and edema. It has been shown that considerable vascular remodeling takes place during tendon healing to enhance perfusion [16, 17]. Stange et al. reported a peak in changes of relative blood volume 7 days after *in situ* freezing-induced tendinopathy in a rat patellar tendon [18]. A significant uniform hypervascularization occurred during the healing process of chronic Achilles tendinopathy after operative tenolysis in rabbits [17]. The increased vascularization facilitates reoxygenation during tendon repair. Therefore, the process of ischemia/reperfusion after tendon injury, which causes hypoxia-reoxygenation (H/R) changes at the cellular level, presents a major impediment for tendon recovery [19]. However, the sensitivity of tendon-derived cells to hypoxia and the effect of H/R on cell growth and characteristics have been rarely addressed.

In this study, we aimed to establish an *in vitro* model of cobalt chloride- (CoCl_2 -) induced hypoxia-reoxygenation (H/R) in mouse digital flexor tendon-derived cells and investigate the effects of H/R on these cells [20]. Hypoxic conditions were simulated by treating cultured cells with CoCl_2 , whereas reoxygenation conditions were simulated by replacing the culture media following CoCl_2 treatment. The principle behind CoCl_2 -induced hypoxia is the replacement of Fe^{2+} by Co^{2+} in heme-based oxygen sensors, which prevents the oxygen sensor from combining with oxygen [21]. Compared with culturing cells in a low-oxygen incubator, the mimic of the hypoxic niche chemically exhibits several advantages, including simple preparation of CoCl_2 , flexible dosage adjustment, treatment suspension at any time, and no impact on oxygen levels for cells that require normal oxygen tension [22]. To have better control over the degree of hypoxia, we decided to employ different CoCl_2 concentrations. Following H/R, cell viability, cell growth, oxidative stress markers, mitochondrial activity, and expression of HIF-1 α , vascular endothelial growth factor-A (VEGF-A), collagen I, and collagen III were assessed. Cellular apoptosis and expression of apoptosis-related protein markers Bax and bcl-2 were analyzed.

2. Materials and Methods

2.1. Experiment Design. We first confirmed the success of the CoCl_2 -induced hypoxia model by examining the expression of HIF-1 α protein in tendon-derived cells treated with low-to-high concentrations of CoCl_2 (0.05, 0.1, 0.2, and 0.4 mM), according to previous studies [20, 23, 24]. Next, the cells were divided into the following groups: control (cells cultured in regular medium), H (cells treated with a concentration gradient of CoCl_2 for 24 h), and R (cells treated with CoCl_2 for 24 h, followed by culturing in regular culture medium for 24 h, 48 h, 72 h, and 96 h (R24h, R48h, R72h, and R96h)). Cell viability was compared across the control, H, and R groups, as well as among different concentrations

of CoCl_2 . Then, we determined an appropriate concentration of CoCl_2 for the hypoxia model to perform the following experiments: cell growth, oxidative stress markers, mitochondrial activity, mRNA and protein expression of HIF-1 α , VEGF-A, collagen I, and collagen III, cellular apoptosis, and expression of the apoptosis-related proteins Bax and bcl-2.

2.2. Isolation of Mouse Flexor Tendon Cells and H/R Model.

The animal procedures were approved by the Administration Committee of Experimental Animals of our university. All animal experiments were carried out in accordance with the Experimental Animal Management Ordinance (National Science and Technology Committee of China) and the Guide for the Care and Use of Laboratory Animals (National Institutes of Health (NIH), Bethesda, MD, USA). Tendon-derived cells were isolated from mouse flexor digitorum profundus (FDP) tendons (C57BL/6, female, 4 weeks old). The mice were sacrificed by cervical dislocation, and the FDP tendons of the index, middle, and ring fingers of the hind paws were harvested. The tendon samples were washed with sterile phosphate-buffered saline (PBS) and then cut into small pieces. The cut samples were digested in a mixture of 3 mg/ml type I collagenase (Gibco, Thermo Fisher Scientific, Grand Island, NY) and 4 mg/ml dispase (Gibco, Thermo Fisher Scientific) for 2 h at 37°C. Undigested tissues and debris were filtered through a 70 μm cell strainer (Merck Millipore, Cork, Ireland). The released cells in the filtrate were centrifuged at 600 g for 10 min and resuspended in low-glucose Dulbecco's modified Eagle's medium (LG-DMEM; Gibco, Thermo Fisher Scientific) supplemented with 10% fetal bovine serum (FBS), 100 U/ml penicillin, and 100 $\mu\text{g}/\text{ml}$ streptomycin. The isolated nucleated cells were plated as passage 0 (P0) at a seeding density of 500 cells/cm², as determined in a previous study [25]. The cells were cultured at 37°C with 5% CO₂. After 2 days, the cells were washed twice with PBS to remove nonadherent cells. After 10 days, the cells at 95% confluence were collected via local trypsin digestion and split 1:3 for subsequent passages. The medium was changed twice a week. Cells at P3 were used for all the experiments.

2.3. Cell Viability. The cells were seeded in 96-well plates at a density of 5000 cells/well and cultured in DMEM. After 48 h, different concentrations of CoCl_2 (0.05, 0.1, 0.15, 0.2, 0.25, 0.3, 0.35, and 0.4 mM) were added to the cells for 24 h. Subsequently, the cell media were replaced with regular DMEM, and the cells were cultured for 24 h, 48 h, 72 h, and 96 h. Cell Counting Kit-8 (CCK-8; meilunbio, China) was used to evaluate the viability of cells subjected to H/R. Briefly, fresh medium containing CCK-8 solution was added to the 96-well plates containing cells cultured for different time periods. The cells were then incubated for 1.5 h at 37°C. The absorbance of the supernatants (100 μl) was measured at 450 nm using an automatic microplate reader (Bio-Rad).

2.4. Cell Growth. The cells were seeded in a 6-well plate at 5000 cells/cm² and in a 96-well plate at 5000 cells/well. After 48 h, cells were treated with CoCl_2 (concentration determined by

above cell viability measurement) for 24 h, followed by reoxygenation for 24 h, 48 h, 72 h, and 96 h. The morphological changes of cells in the 6-well plate before and after H/R treatment were observed under a phase-contrast microscope (Olympus IX71). The cells in the 96-well plate were harvested using a 0.05% trypsin (Invitrogen) solution, and the cell numbers were counted for growth curve construction before and after H/R treatment.

2.5. Oxidative Stress Markers. The intracellular malondialdehyde (MDA) levels were measured using a Lipid Peroxidation MDA Assay Kit (Beyotime, Shanghai, China) following the manufacturer's instructions. First, cells were seeded in 6-well plates (5×10^4 cells/well) and continuously grew until the confluence reached 90%. After H/R treatment, cells were collected and lysed by cell lysis buffer (Beyotime, Shanghai, China) and centrifuged at 10,000 g for 15 min. The supernatants were reacted with the thiobarbituric acid (TBA), and the reaction products were measured spectrophotometrically at 532 nm.

A superoxide dismutase (SOD) assay was performed using the Total Superoxide Dismutase Assay Kit with WST-8 (Beyotime, Shanghai, China). Cells were seeded in 6-well plates (5×10^4 cells/well) and continuously grew until the confluence reached 90%. The cells were treated with H/R conditions₂. Cells were washed with cold PBS before the addition of SOD buffer solution. Protein concentration was measured using the Enhanced BCA Protein Assay Kit (Beyotime, Shanghai, China). The samples (20 μ l) were mixed with the WST-8/enzyme solution (160 μ l) and the reaction starting solution (20 μ l) and incubated at 37°C for 30 minutes. The absorbance at 450 nm was measured using a microplate reader (Bio-Rad).

2.6. MitoTracker Red Staining. Cells were stained with MitoSOX Red Mitochondrial Superoxide Indicator (Yeasen, Shanghai, China) and Hoechst 33342 (Cell Signaling Technologies, Danvers, MA). Cells at 80-90% confluence were treated with H/R conditions₂. Then, the cells were incubated with MitoSOX Red Mitochondrial Superoxide Indicator for 10 min at 37°C. Then, the cells were washed with PBS and stained with Hoechst 33342 labeling solution (1:10000) for 10 min at room temperature. The cells were observed under a fluorescence microscope (Olympus IX71).

2.7. Western Blot Analysis. The cells were rinsed twice with cold PBS and then lysed in RIPA buffer (Beyotime, Shanghai, China) containing 1% (v/v) phenylmethanesulfonyl fluoride (PMSF) (Beyotime, Shanghai, China) and 1% (v/v) protease and phosphatase inhibitor cocktails (Roche, Mannheim, Germany). The Enhanced BCA Protein Assay Kit (Beyotime, Shanghai, China) was used to measure protein concentrations. The samples were subjected to 10% SDS-polyacrylamide gel electrophoresis and subsequently transferred onto a polyvinylidene difluoride membrane (Millipore Corp., Billerica, Mass.) under 100 volts for 2 h. The membranes were incubated in Tris-buffered saline (TBS: 10 mM Tris-HCl, pH 7.4, 150 mM NaCl) and 0.1% (v/v) Tween 20 (TBS-Tween) containing 5% (w/v) dried milk

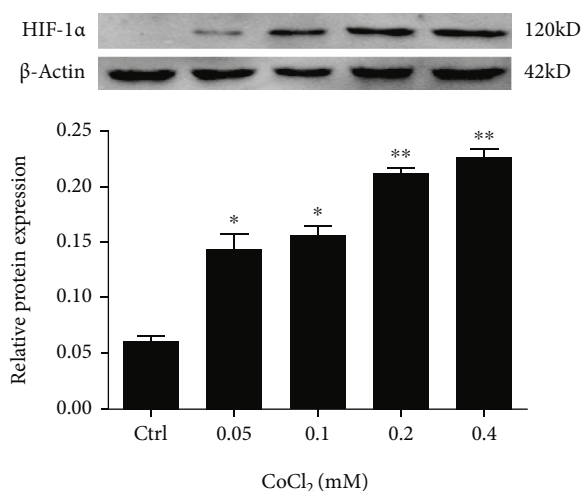


FIGURE 1: Protein expression of HIF-1 α after treatment with different concentrations of CoCl₂ for 24 h. * $P < 0.05$ vs. control group; ** $P < 0.005$ vs. control group.

for 1 h and then incubated with the respective primary antibody overnight at 4°C. The primary antibodies against HIF-1 α , VEGF-A, collagen I, collagen III, Bax, and bcl-2 are described in Table S1. Next, the filters were washed 3 times, 8 min each, with TBS-T and then incubated with a conjugated affinity-purified secondary antibody labeled with IRDye 800v for 1 h at room temperature. Afterwards, the membranes were washed again, and the protein bands were detected with an Odyssey imager (LI-COR, Inc., Lincoln, NE). The intensity of each band was quantified with ImageJ software (NIH, Bethesda, MD, USA). The expression levels of proteins were normalized to β -actin.

2.8. Real-Time PCR. Total RNA of cells was isolated using TRIzol[®] Reagent (Ambion, Life Technologies). First-strand cDNA were reverse-transcribed with HiScript II qRT Super-Mix plus gDNA wiper (R223-01, Vazyme, China). QRT-PCR was carried out using 1x AceQ qPCR SYBR Green Master Mix (Q111-02, Vazyme, China) according to the manufacturer's instructions. Specific primers were synthesized for the HIF-1 α , VEGF-A, collagen I, and collagen III mRNAs. GAPDH was used as an internal reference, and the geometric mean of its expression was used for normalization. The sequences of qPCR primers are listed in Table S2. Relative quantification of the target genes was performed in triplicate and analyzed using the $2^{-\Delta\Delta C_t}$ method.

2.9. Immunocytochemistry. The cells were plated at a density of 1×10^4 cells/well on coverglasses in 24-well plates for 2 days. The expression of 4 protein markers, including HIF-1 α , VEGF-A, collagen I, and collagen III, was measured using immunocytochemistry. Briefly, cells were fixed in 4% paraformaldehyde for 30 min at room temperature. Following washing, the cells were permeabilized with 0.25% Triton X-100 in PBS and blocked with 1% bovine serum albumin (BSA) for 1 h at room temperature. The cells were then incubated with antibodies against HIF-1 α , VEGF-A,

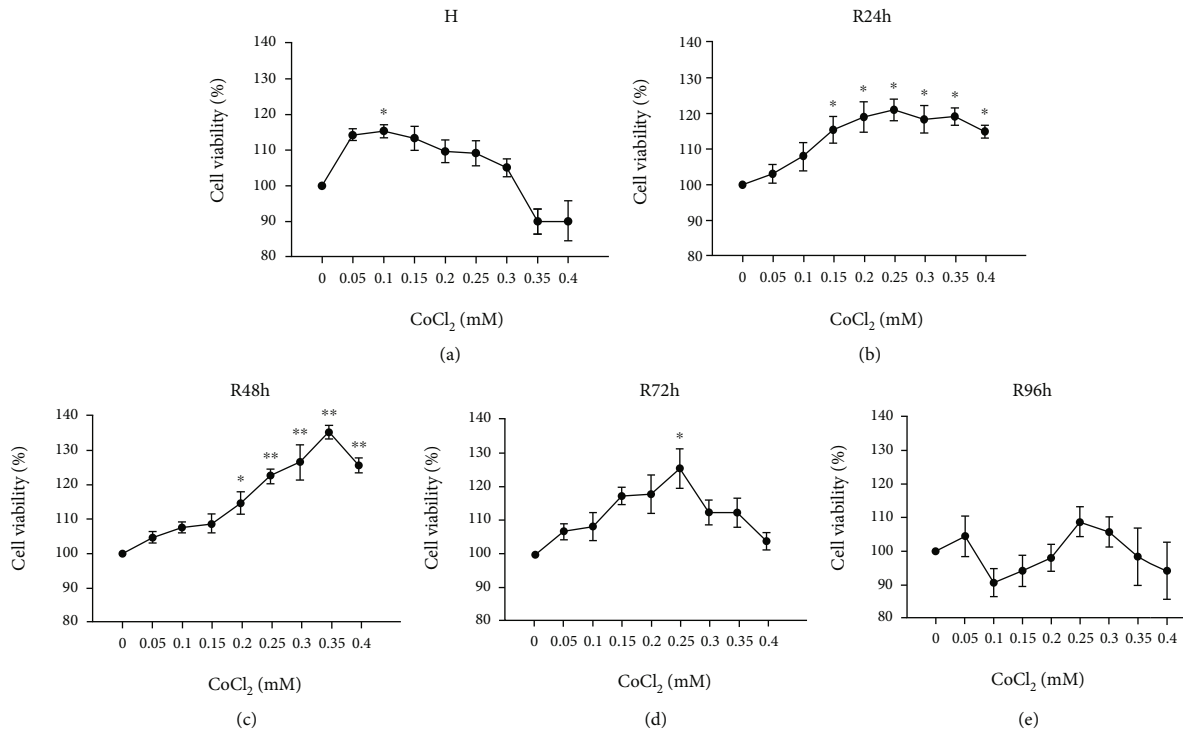


FIGURE 2: Changes in cell viability of tendon-derived cells under H/R conditions induced by a concentration gradient of CoCl₂. (a) Cell viability under CoCl₂-induced hypoxia. (b–e) Cell viability after reoxygenation for 24 h, 48 h, 72 h, and 96 h. **P* < 0.05 vs. control group; ***P* < 0.005 vs. control group.

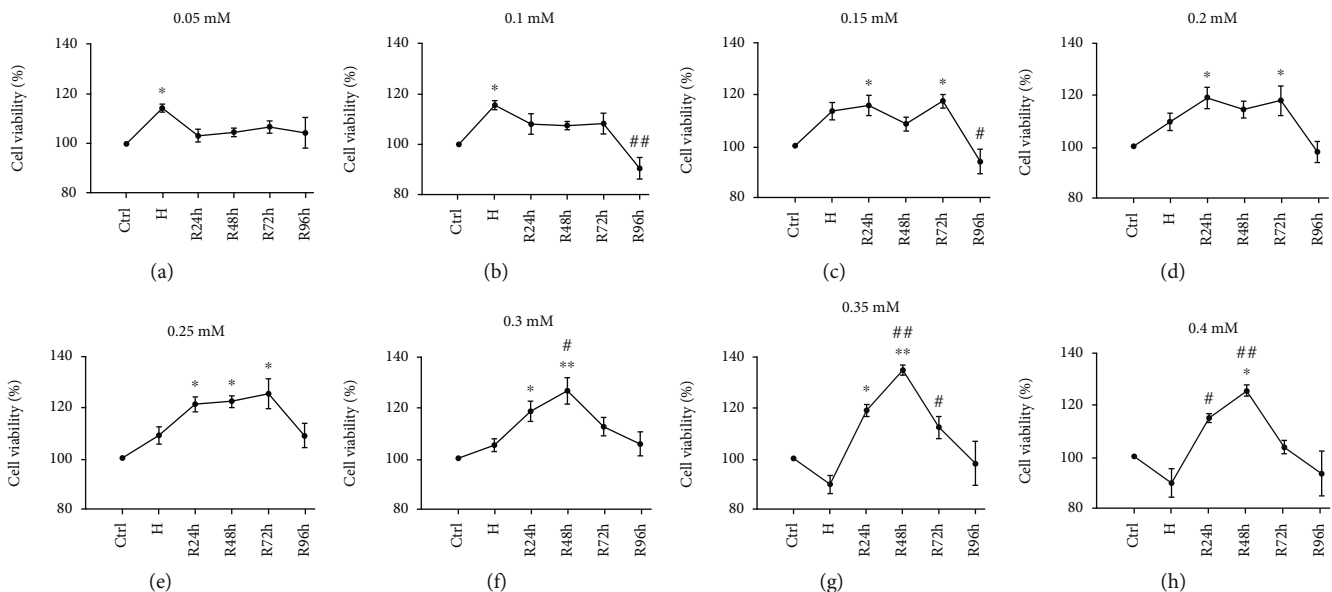


FIGURE 3: Changes in cell viability of tendon-derived cells under H/R at each concentration of CoCl₂. (a–h) Cell viability increases along the CoCl₂ concentration gradient (0.05–0.4 mM). **P* < 0.05 vs. control group; ***P* < 0.005 vs. control group; #*P* < 0.05 vs. H group; ##*P* < 0.005 vs. H group.

collagen I, and collagen III overnight at 4°C. After 3 washes with PBS, the cells were incubated with Alexa Fluor488 Goat anti-rabbit IgG (H+L) for 2 h at room temperature. Finally, cells were counterstained with Hoechst. The stained cells were then examined under a fluorescence microscope (Olympus IX71).

2.10. Flow Cytometry Analysis. Annexin V labeling was used in conjunction with flow cytometry to detect phosphatidylserine on the outer membrane of apoptotic cells. First, the binding buffer was diluted to 1: 4 with deionized water (4 ml binding buffer+12 ml deionized water). Then, the cells were harvested using 0.05% trypsin with no EDTA solution

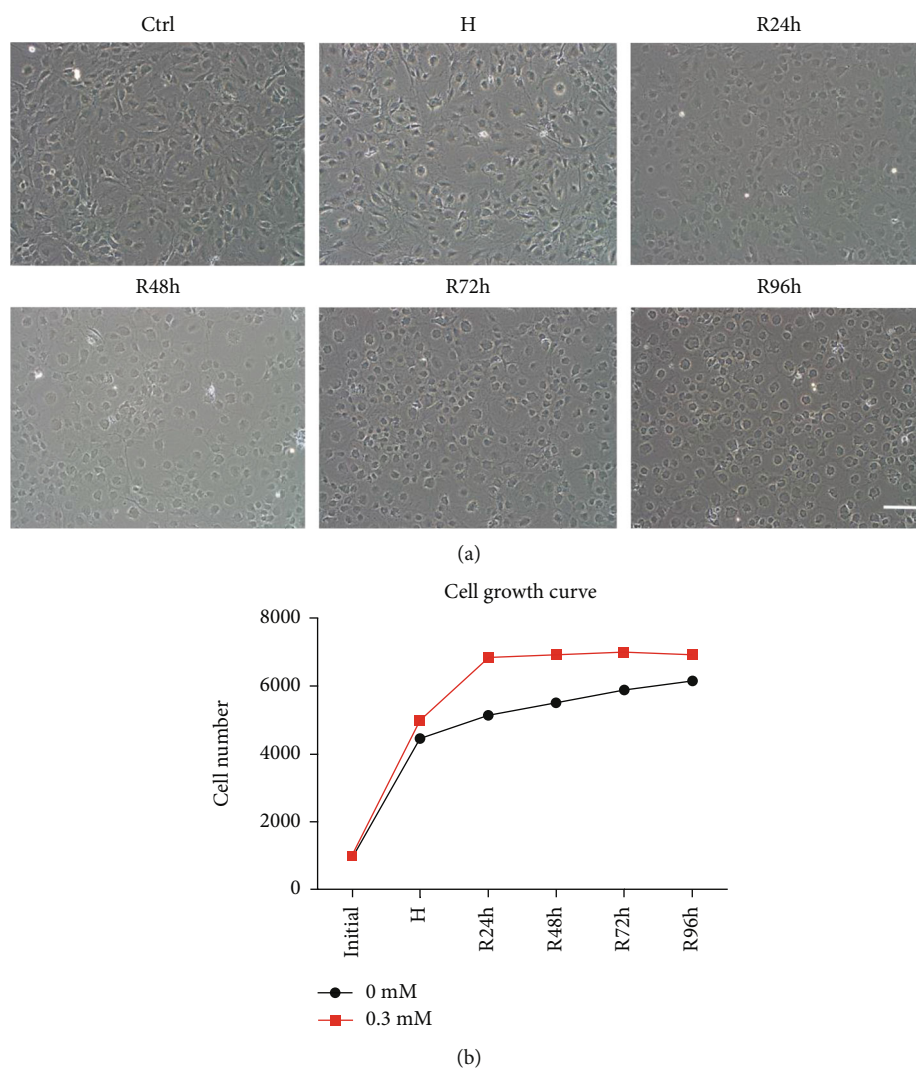


FIGURE 4: Cell morphology and growth curves of tendon-derived cells when treated with 0.3 mM CoCl_2 . (a) Cell morphology under H/R conditions. Scale bar: 200 μm . (b) Cell growth curves under H/R conditions.

(Invitrogen), washed twice with 4°C prechilled PBS, and resuspended with binding buffer. Next, the cell concentration was adjusted to 1×10^6 cells / ml. The cell suspension (100 μl) was placed in a 5 ml flow tube, and 5 μl annexin V/Alexa Fluor 488 and 10 μl propidium iodide solution were added. After mixing, the mixture was incubated away from light for 15 min at room temperature. After incubation, 400 μl of PBS was added to the reaction tube, and the cells were analyzed using flow cytometry (Attune NxT, Applied Biosystems, CA, USA). For each sample, approximately 10,000 events were counted and analyzed using the FlowJo software (FlowJo, Ashland, OR, USA).

2.11. Statistical Analysis. All experiments were repeated at least 3 times for replication. The data were expressed as mean \pm SD. The results were analyzed by one-way ANOVA with post hoc Tukey testing or by the *t*-test for pairwise comparisons. All data were analyzed using Prism 5.0b (GraphPad

Software, La Jolla, CA, USA). $P < 0.05$ was considered statistically significant.

3. Results

3.1. CoCl_2 -Induced Hypoxia Elevates HIF-1 α Expression. The protein expression of HIF-1 α significantly increased in cells treated with CoCl_2 at concentrations of 0.05 and 0.1 mM ($P < 0.05$) and further increased with higher CoCl_2 concentrations of 0.2 and 0.4 mM ($P < 0.005$) (Figure 1), which confirmed the success of the CoCl_2 -induced hypoxia model in tendon-derived cells.

3.2. H/R Increases Cell Viability. Under hypoxic conditions induced by different concentrations of CoCl_2 , the viability of tendon-derived cells showed an initial increase followed by a gradual decrease with the increased CoCl_2 concentrations. A significant difference was observed only at 0.1 mM of CoCl_2 when compared with the control group ($P < 0.05$)

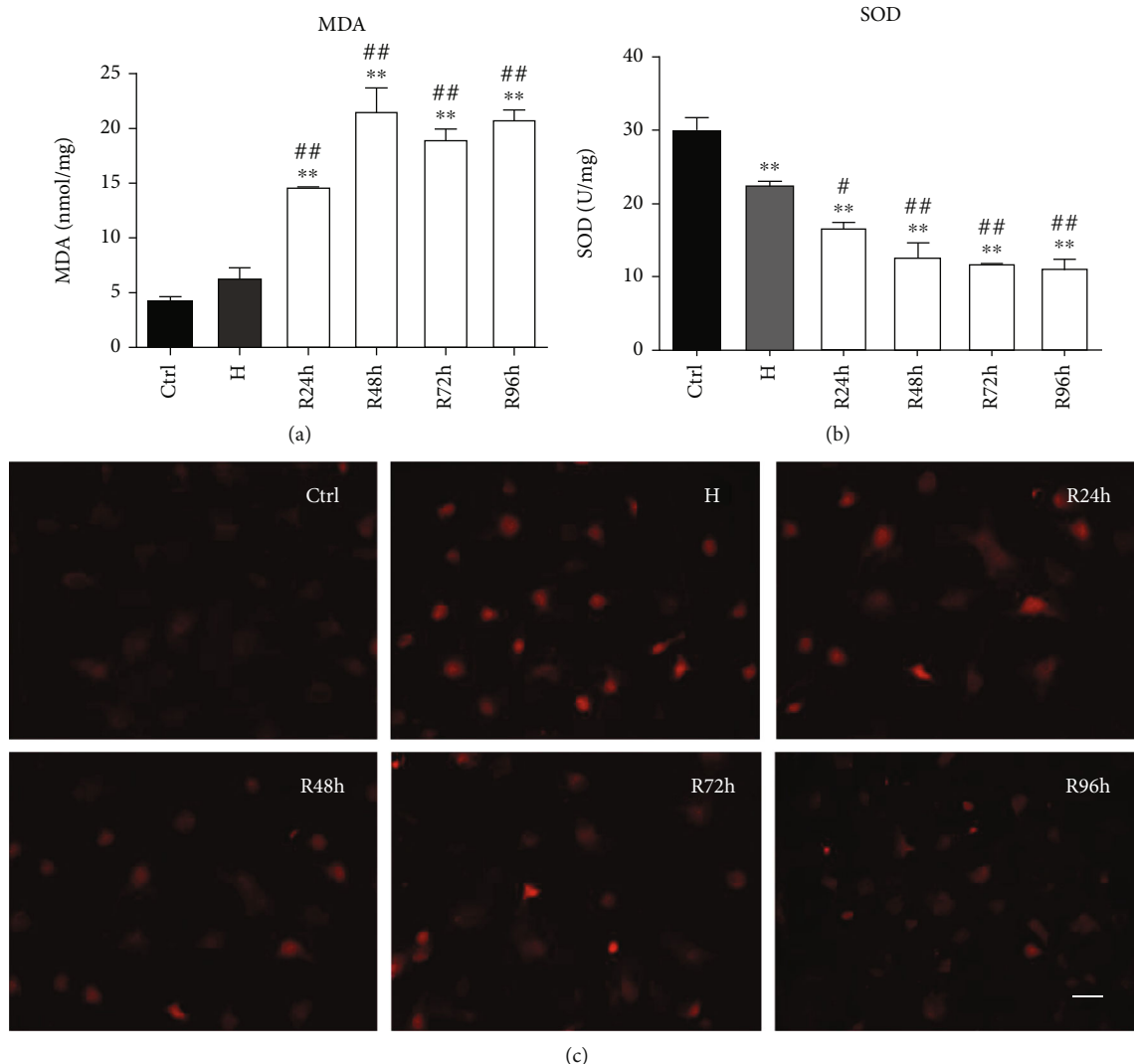


FIGURE 5: (a) Cellular malondialdehyde (MDA) levels. (b) Superoxide dismutase (SOD) activity. (c) The intensity of mitochondria in different groups. Scale bar: 100 μ m. * $P < 0.05$ vs. control group; ** $P < 0.005$ vs. control group; # $P < 0.05$ vs. H group; ## $P < 0.005$ vs. H group.

(Figure 2(a)). After reoxygenation for 24 h (R24h), cell viability significantly increased in cells treated with 0.15 mM and higher CoCl_2 concentrations ($P < 0.05$) (Figure 2(b)). At R48h, cell viability significantly increased in cells treated with 0.2–0.4 mM CoCl_2 ($P < 0.05$ or $P < 0.005$) (Figure 2(c)). At R72h, a significant increase in cell viability was only observed in cells treated with 0.25 mM of CoCl_2 ($P < 0.05$) (Figure 2(d)). The cell viability of all CoCl_2 -treated cells was similar to that in the control group at R96h (Figure 2(e)).

At each concentration, cell viability was compared across the control, hypoxia, and reoxygenation groups. Compared with the control group, the cells treated with low concentrations of CoCl_2 showed significant increases in cell viability under hypoxia, with a 14% increase at 0.05 mM and 15% at 0.1 mM ($P < 0.05$) (Figures 3(a) and 3(b)). The cells treated with higher concentrations of CoCl_2 at 0.15, 0.2, 0.25, and 0.3 mM exhibited significantly enhanced cell viability after reoxygenation for 24 h–72 h ($P < 0.05$ or $P < 0.005$) (Figures 3(c)–3(f)). At the 2 highest CoCl_2 concentrations, cell viability significantly increased at R48h compared with

those in the control and H groups ($P < 0.005$) (Figures 3(g) and 3(h)).

3.3. H/R Does Not Inhibit Cell Growth. During the experiment, we observed relatively healthy growth of cells treated with 0.3 mM CoCl_2 after reoxygenation. The cells were shrunk slightly when under hypoxic conditions, but the morphology returned to normal after reoxygenation (Figure 4(a)). Therefore, we selected 0.3 mM CoCl_2 to simulate hypoxia for subsequent experiments. Cell growth curves revealed a slightly increased cell proliferation under H/R compared with that of the control group (Figure 4(b)).

3.4. H/R Mediates Oxidative Stress and Mitochondrial Activity. To determine the impact of H/R on oxidative stress, the intracellular levels of MDA and SOD were measured. The MDA levels significantly increased during reoxygenation compared with those in the control and H groups ($P < 0.005$) (Figure 5(a)). The SOD levels significantly decreased under H/R compared with that in the control group

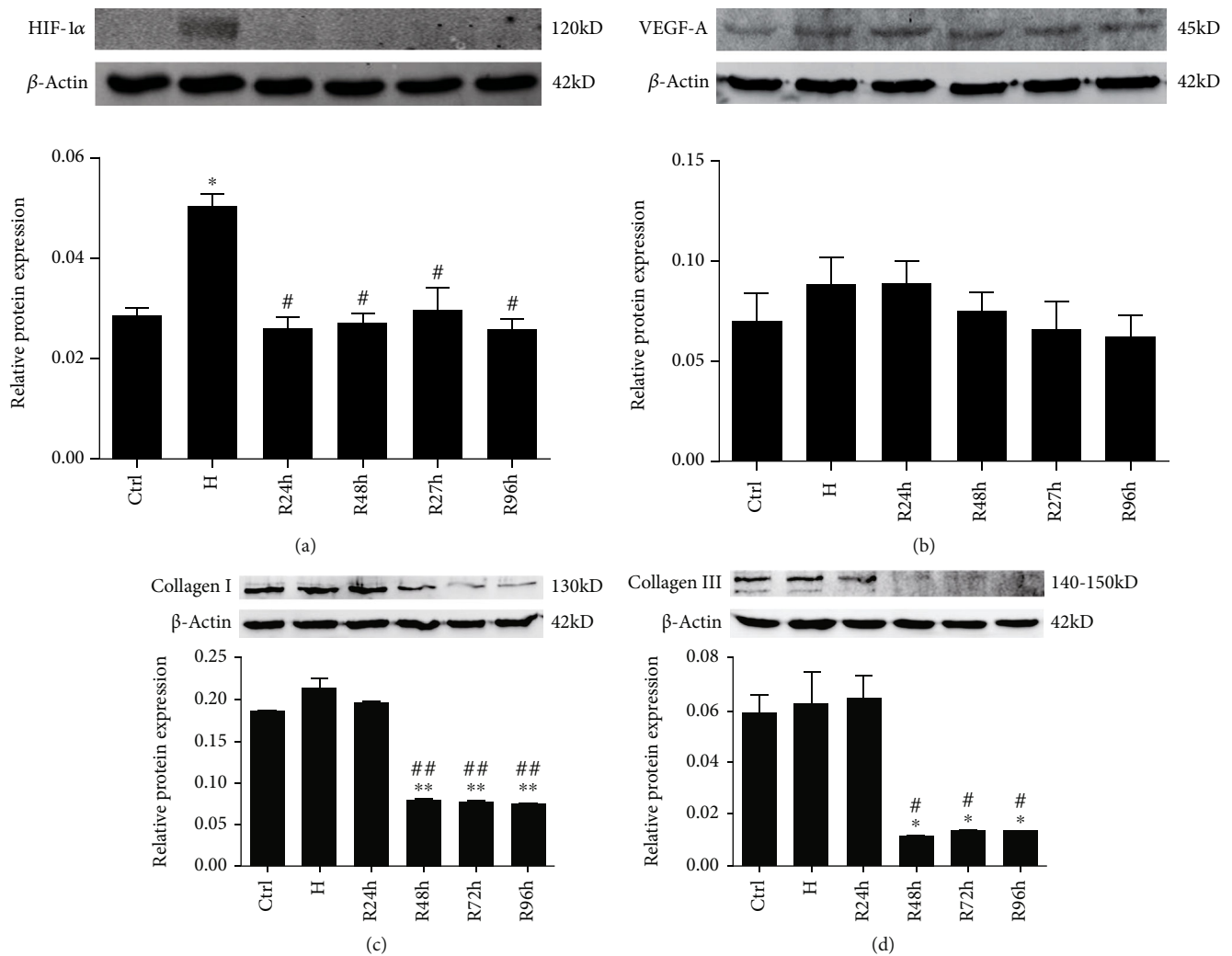


FIGURE 6: Protein expression of (a) HIF-1 α , (b) VEGF-A, (c) collagen I, and (d) collagen III when cells were under H/R conditions at 0.3 mM CoCl₂. * $P < 0.05$ vs. control group; ** $P < 0.005$ vs. control group; # $P < 0.05$ vs. H group; ## $P < 0.005$ vs. H group.

($P < 0.005$) (Figure 5(b)). The MitoTracker Red staining showed that the intensity of bioactive mitochondria was higher in the H and R groups than in the control group (Figure 5(c)).

3.5. H/R Enhances Protein Expression of HIF-1 α and VEGF-A and Decreases Expression of Collagens I and III. The protein expression of HIF-1 α significantly increased when the cells were under hypoxia and returned to normal levels after reoxygenation ($P < 0.05$) (Figure 6(a)). By comparison, VEGF-A levels showed a similar but not significant increase under hypoxia and at R24h and returned to normal from R48h and after (Figure 6(b)). Both collagen I and collagen III protein levels significantly decreased at R48h, R72h, and R96h compared with those of the control group and H group ($P < 0.05$ or $P < 0.005$) (Figures 6(c) and 6(d)).

3.6. H/R Regulates mRNA Expression of HIF-1 α , VEGF-A, Collagen I, and Collagen III. Under H/R conditions, the mRNA expression of HIF-1 α was significantly suppressed (Figure 7(a)). The VEGF-A mRNA level significantly

increased when the cells were under hypoxia and at R24h compared with that of the control group ($P < 0.05$) but significantly decreased when the cells were at R72h and R96h compared with that of the H group ($P < 0.05$) (Figure 7(b)). The mRNA expression of collagen I significantly increased under hypoxia, returned to normal levels at R24h, and significantly decreased from R48h to R96h compared with those of the control and H groups ($P < 0.05$ or $P < 0.005$) (Figure 7(c)). The collagen III mRNA levels also significantly increased under hypoxia compared with that of the control group but remained at normal levels with different periods of reoxygenation ($P < 0.05$) (Figure 7(d)).

3.7. Immunocytochemical Staining. Figure 8(a) shows the representative fluorescence micrographs of HIF-1 α , VEGF-A, collagen I, and collagen III when the cells were under H/R conditions. We calculated the percentage of positive cells via cell counting Figure 8(b). Compared with the control group, the percentage of HIF-1 α -positive cells significantly increased under hypoxia (Figure 8), whereas that of VEGF-A-positive cells was significantly increased under hypoxia,

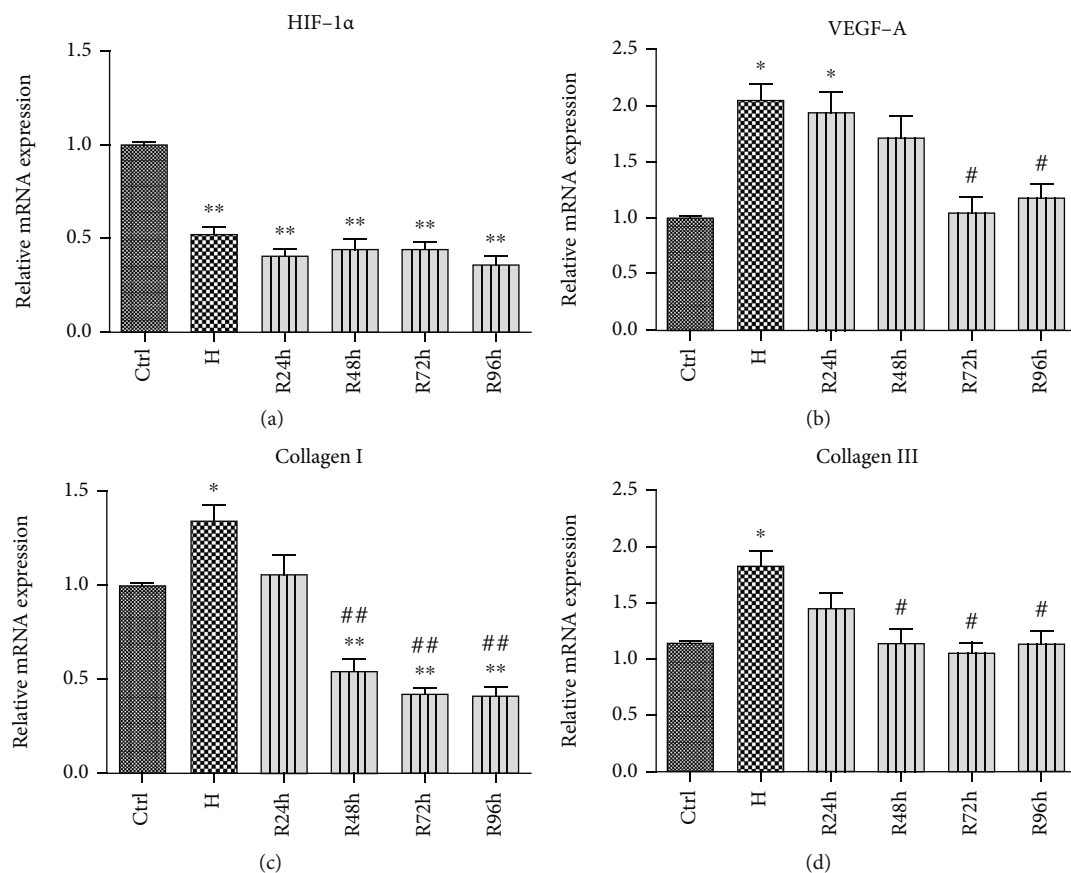


FIGURE 7: mRNA expression of (a) HIF-1 α , (b) VEGF-A, (c) collagen I, and (d) collagen III when cells were under H/R conditions induced by 0.3 mM CoCl₂. * $P < 0.05$ vs. control group; ** $P < 0.005$ vs. control group; # $P < 0.05$ vs. H group; ## $P < 0.005$ vs. H group.

at R24h, and at R48h ($P < 0.05$) (Figure 8(CID="C002" value="B")). The percentages of collagen I- and collagen III-positive cells were significantly lower at R48h, R72h, and R96h compared with those in the control and H groups ($P < 0.05$ or $P < 0.005$) (Figures 8(CID="C004" value="C") and 8(CID="C006" value="D")).

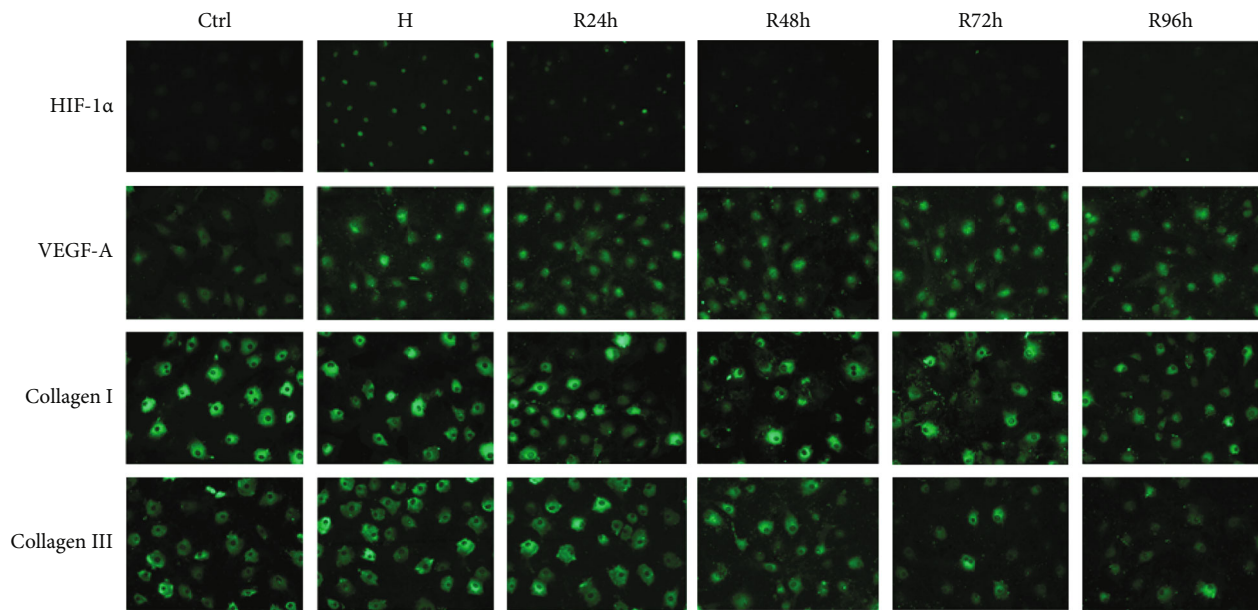
3.8. H/R Does Not Affect Cellular Apoptosis but Alters Protein Expression of Bax and bcl-2. value="Flo" value="w" cytometry was conducted to investigate the apoptotic levels of cells under H/R conditions. The flow cytometric analysis showed that no significant differences in the number of apoptotic cells were found across the control, hypoxia, and reoxygenation groups (Figures 9(a) and 9(b)). Meanwhile, the ratio of Bax/bcl-2 protein expression was significantly upregulated after reoxygenation compared with those of the control and hypoxia groups ($P < 0.05$), with a peak at R48h (Figure 9(c)).

4. Discussion

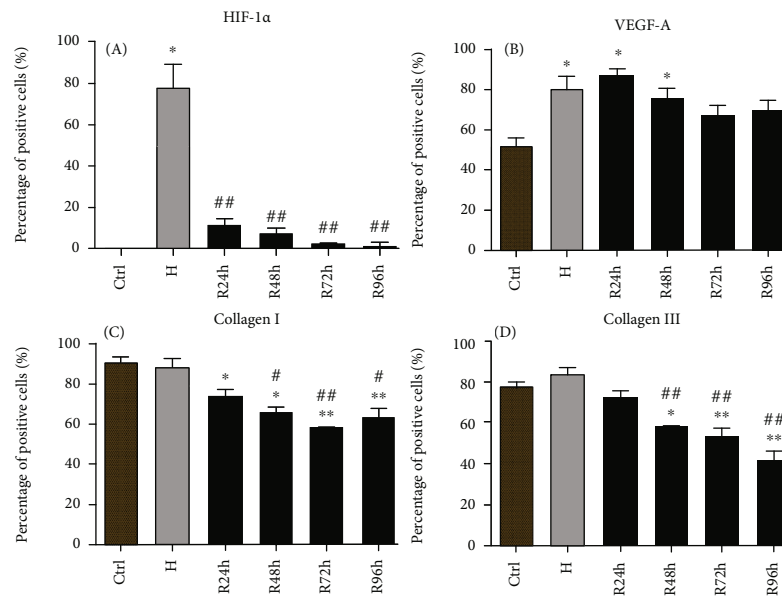
The current study uncovered the cellular responses of tendon-derived cells to hypoxia and subsequent reoxygenation. Our results showed that different concentrations of CoCl₂ exerted distinct effects on cell viability. Hypoxia induced by low CoCl₂ concentrations (0.05 and 0.1 mM) enhanced cell viability, while further increases in CoCl₂ con-

centrations (0.15–0.4 mM) led to a gradual decrease in cell viability. With 24 h–72 h of reoxygenation, cell viability increased in cells treated with high concentrations of CoCl₂. Cell viability returned to the same level as the control group after 96 h of reoxygenation, irrespective of the initial CoCl₂ concentrations.

Previous studies have demonstrated that different cell lines show diverse tolerance profiles to CoCl₂-induced H/R. Zhang et al. demonstrated that CoCl₂ did not promote or attenuate the viability of A498 cells at low concentrations (0.05–0.2 mM), but when the concentration was increased to 0.25 mM, cell activity gradually declined [20]. The study by Shi et al. in a human ovarian carcinoma cell line showed that CoCl₂-induced (0.15 mM) hypoxia inhibited cell proliferation, which was subsequently recovered with reoxygenation [23]. Tong et al. showed that HepG2 cells treated with different concentrations of CoCl₂ (0.05, 0.1, 0.15, and 0.2 mM) exhibited significantly repressed cell viability in a concentration-dependent manner [24]. However, our data showed that cell viability was enhanced by CoCl₂-induced hypoxia, even when the concentration of CoCl₂ reached 0.3 mM. Furthermore, during the early period of reoxygenation, cell viability further increased, especially in cells treated with high concentrations of CoCl₂ (0.25–0.4 mM). In addition, H/R had no obvious negative effects on cell growth. These results suggested that tendon-derived cells



(a)



(b)

FIGURE 8: (a) Representative fluorescence micrographs of HIF-1 α , VEGF-A, collagen I, and collagen III in cells under H/R conditions induced by 0.3 mM CoCl₂. (b) Percentages of positive cells stained with HIF-1 α (A), VEGF-A (B), collagen I (C), and collagen III (D). Scale bar: 100 μ m. * P < 0.05 vs. control group; ** P < 0.005 vs. control group; # P < 0.05 vs. H group; ## P < 0.005 vs. H group.

were highly tolerant to CoCl₂-induced hypoxia and the reoxygenation.

H/R conditions can cause oxidative stress, which is a major mechanism involved in the pathogenesis of H/R injury [26–29]. Therefore, we examined the levels of two oxidative stress markers, MDA and SOD, and the activity of bioactive mitochondria in cells under H/R. MDA, a byproduct of lipid oxidation, is a biomarker of oxidative stress of cells [30]. SOD is the main antioxidant enzyme in cells that plays important roles in scavenging oxygen free radicals and resisting the damage of oxygen free radicals

[31]. Mitochondria, accounting for the majority of oxygen consumption, can help to tune cellular and organismal hypoxia responses [32]. Our results showed that the MDA level increased, the SOD level decreased, and the activity of bioactive mitochondria was enhanced under H/R, indicating that H/R induced notable oxidative stress in the tendon-derived cells. However, the oxidative stress did not affect the cell growth in this study. We speculate that the increased mitochondrial activity may retain the metabolic demand of the cells and induce an adaptive response to oxidative stress [33–36].

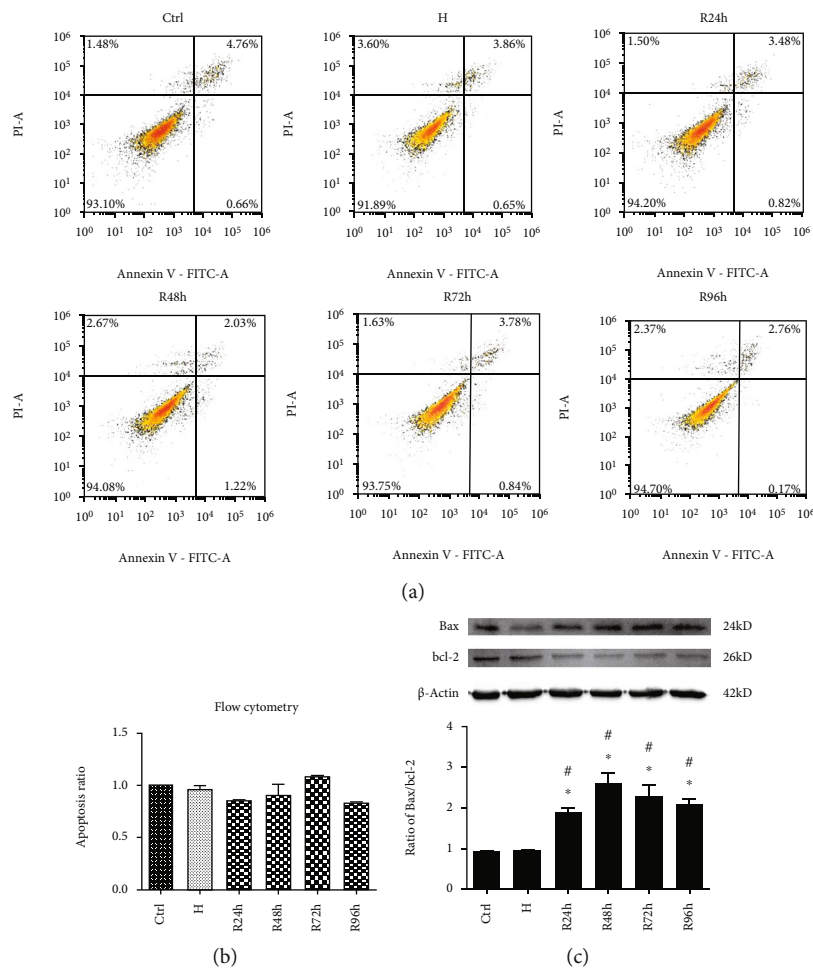


FIGURE 9: Flow cytometric analysis of cellular apoptosis and ratios of Bax/bcl-2 proteins: (a) representative graphs of flow cytometric assays showing the apoptosis of different groups; (b) the histogram showing the ratio of apoptotic cells; (c) expression ratio of Bax/bcl-2 protein. * $P < 0.05$ vs. control group; ** $P < 0.005$ vs. control group. # $P < 0.05$ vs. H group; ## $P < 0.005$ vs. H group.

HIF-1 α is a key transcription factor in response to hypoxic stress and is widely expressed in mammals, including humans, under hypoxic conditions [37, 38]. In the present study, the HIF-1 α protein level increased notably in the cells under hypoxia and then returned to the same level in the control cells immediately after reoxygenation. We noted, however, that the changes in HIF-1 α mRNA and protein expression were inconsistent. Specifically, HIF-1 α mRNA expression decreased significantly during hypoxia and reoxygenation, which is inconsistent with previous studies [39, 40]. A possible explanation is that the expression of HIF-1 α mRNA changes prior to the expression of protein, and the peak of mRNA expression occurred in less than 24 hours. Then, the inhibited HIF-1 α mRNA expression caused the recovery of the HIF-1 α protein level in the cells under reoxygenation. These results indicate that tendon-derived cells can regulate the expression of HIF-1 α rapidly under H/R conditions. It may be beneficial to the adaptation of tendon-derived cells to oxygen deprivation, leading to the high tolerance of this type of cells to H/R.

VEGF-A is an essential growth factor for most tissues in their response to traumatic injuries involving disrupted blood supply. Previous studies demonstrated that the expres-

sion of the VEGF gene significantly increased during the early period of tendon healing and that intraoperative delivery of VEGF notably enhanced tendon healing in a chicken model, indicating the importance of VEGF in tendon healing [41, 42]. In our study, we found that VEGF-A was upregulated under hypoxia when HIF-1 α was activated, and its levels returned to normal during reoxygenation along with the passage of time. Our results were consistent with previous studies investigating the role of the HIF-1 α /VEGF pathway in hypoxia. Liang et al. showed that hypoxia markedly upregulated VEGF-A and that appropriate vascular response might be essential for normal repair and remodeling. VEGF-A elevation is a rapid and strong response to hypoxic insult typically seen in most tissues [43]. Therefore, hypoxia-promoted expression of VEGF may be a self-protective mechanism after tendon injury.

Collagen is the major substance secreted by tendon cells. It is the main component of tendon ECM, and thus, synthesis of collagen is essential for maintaining tendon structure [44, 45]. A normal tendon comprises 65%–85% of collagen I, which is the most abundant collagen, followed by collagen III [46, 47]. Collagen III is highly upregulated during tendon healing [48]. Collagen III primarily forms an abundant but

disorganized collagen matrix in the proliferative phase of tendon healing. Webster et al. showed that when tendon-derived cells were cultured at low oxygen tensions, cellular metabolism was depressed and both total protein and collagen production were reduced [49]. It was hypothesized that the hypoxic environment might not have satisfied the physiological oxygen requirements of the cells, and it may have deleterious effects on collagen production [50]. A study also reported that there was an abrupt reduction of collagens I and III in the early stages of Achilles tendinitis; the tendon subsequently developed substantial impairment and Achilles tendinitis eventually occurred [51]. Our results showed that the expression of collagens I and III was downregulated during reoxygenation. Therefore, the in vitro reoxygenation process may correspond to the in vivo repair process after ischemia. Interestingly, the decline in the expression of collagen appears to contradict the increased cell viability. We speculate that although cell growth is not affected, other cellular functions are inhibited under hypoxic stress.

Apoptosis plays a critical role in the homeostasis of normal tissue [52]. In human rotator cuff tendinopathy, HIF-1 α accumulation was associated with cellular apoptosis, which provided an early support for the role of hypoxia-induced damage to cell loss via apoptosis [53]. However, Sasabe et al. reported that forced expression of HIF-1 α suppressed hypoxia-induced apoptosis of human oral squamous cell carcinoma cell lines [54]. Based on flow cytometry analysis in the present study, CoCl₂-induced H/R had a minimal effect on the cellular apoptosis. However, the protein expression of Bax was upregulated while that of bcl-2 was downregulated, resulting in a significant increase in the Bax/bcl-2 ratio during reoxygenation. The Bax/bcl-2 ratio reached its peak at 48 h after reoxygenation and began to decrease thereafter. This suggested that although the apoptotic pathway was activated, the cells did not actually undergo apoptosis within the observed period. We speculate that tendon-derived cells are highly resistant to H/R-induced apoptosis, and their inherent cell characteristics may prevent or even reverse the occurrence of apoptosis. Another possibility is that the initiation of the apoptotic mechanism precedes the occurrence of apoptosis. To this regard, extending the observation time may allow us to obtain a more complete picture of apoptotic events after H/R.

5. Conclusions

Collectively, the present study successfully established a CoCl₂-induced H/R model in tendon-derived cells, which provided a framework for future studies to understand the tendon-specific features of this widely observed stress response mechanism. The data in this study showed that hypoxia followed by reoxygenation for a certain period of time promoted cell viability in a concentration-dependent manner. Tendon-derived cells exhibited considerable tolerance to hypoxia. H/R caused oxidative stress responses but did not affect cell growth. H/R altered the expression of HIF-1 α , VEGF-A, collagen I, and collagen III. Cellular apo-

ptosis was not affected by H/R, but the Bax/bcl-2 ratio increased during reoxygenation.

Data Availability

All data generated or analyzed during this study are included in this published article.

Conflicts of Interest

All authors have read the journal's policy on disclosure of potential conflicts of interest and declare no conflict of interest.

Acknowledgments

This work was supported by the Jiangsu Provincial Medical Youth Talent (grant number QNRC2016701), Natural Science Foundation of Jiangsu Province (grant number BK20181203), and Six Talent Peaks Project in Jiangsu Province (grant number WSW-048).

Supplementary Materials

Table S1: antibodies used in the Western blot assay and immunocytochemical staining. Table S2: sequences of qPCR primers. (*Supplementary Materials*)

References

- [1] Y. Zhang, B. Wang, W. J. Zhang, G. Zhou, Y. Cao, and W. Liu, "Enhanced proliferation capacity of porcine tenocytes in low O₂ tension culture," *Biotechnology Letters*, vol. 32, no. 2, pp. 181–187, 2010.
- [2] J. Zhang and J. H. Wang, "Human tendon stem cells better maintain their stemness in hypoxic culture conditions," *PLoS One*, vol. 8, no. 4, article e61424, 2013.
- [3] Y. Yu, L. Lin, Y. Zhou et al., "Effect of hypoxia on self-renewal capacity and differentiation in human tendon-derived stem cells," *Medical Science Monitor*, vol. 23, pp. 1334–1339, 2017.
- [4] D. Rempel and S. O. Abrahamsson, "The effects of reduced oxygen tension on cell proliferation and matrix synthesis in synovium and tendon explants from the rabbit carpal tunnel: an experimental study in vitro," *Journal of Orthopaedic Research*, vol. 19, no. 1, pp. 143–148, 2001.
- [5] F. K. Fung, B. Y. Law, and A. C. Lo, "Lutein attenuates both apoptosis and autophagy upon cobalt (II) chloride-induced hypoxia in rat Müller cells," *PLoS One*, vol. 11, no. 12, article e0167828, 2016.
- [6] H. Song, I. Y. Han, Y. Kim et al., "The NADPH oxidase inhibitor DPI can abolish hypoxia-induced apoptosis of human kidney proximal tubular epithelial cells through Bcl 2 up-regulation via ERK activation without ROS reduction," *Life Sciences*, vol. 126, pp. 69–75, 2015.
- [7] S. Guo, A. Tjärnlund-Wolf, W. Deng et al., "Comparative transcriptome of neurons after oxygen-glucose deprivation: potential differences in neuroprotection versus reperfusion," *Journal of Cerebral Blood Flow and Metabolism*, vol. 38, no. 12, pp. 2236–2250, 2018.
- [8] Y. Zhang, Q. Pan, and Y. Liu, "CXCL16 silencing alleviates hepatic ischemia reperfusion injury during liver transplantation

- by inhibiting p 38 phosphorylation," *Pathology, Research and Practice*, vol. 216, no. 5, p. 152913, 2020.
- [9] W. Hou, X. Zhu, J. Liu, and J. Map, "Inhibition of miR-153 ameliorates ischemia/reperfusion-induced cardiomyocytes apoptosis by regulating Nrf2/HO-1 signaling in rats," *Biomedical Engineering Online*, vol. 19, no. 1, p. 15, 2020.
- [10] D. Fang, Z. Li, Q. Zhong-ming et al., "Expression of bystin in reactive astrocytes induced by ischemia/reperfusion and chemical hypoxia in vitro," *Biochimica et Biophysica Acta*, vol. 1782, no. 11, pp. 658–663, 2008.
- [11] J. M. Downey, "Free radicals and their involvement during long-term myocardial ischemia and reperfusion," *Annual Review of Physiology*, vol. 52, no. 1, pp. 487–504, 1990.
- [12] J. E. Jung, G. S. Kim, H. Chen et al., "Reperfusion and neurovascular dysfunction in stroke: from basic mechanisms to potential strategies for neuroprotection," *Molecular Neurobiology*, vol. 41, no. 2-3, pp. 172–179, 2010.
- [13] Y. Zhai, H. Petrowsky, J. C. Hong, R. W. Busuttil, and J. W. Kupiec-Weglinski, "Ischaemia-reperfusion injury in liver transplantation—from bench to bedside," *Nature Reviews. Gastroenterology & Hepatology*, vol. 10, no. 2, pp. 79–89, 2013.
- [14] W. Z. Wang, R. C. Baynosa, and W. A. Zamboni, "Update on ischemia-reperfusion injury for the plastic surgeon: 2011," *Plastic and Reconstructive Surgery*, vol. 128, no. 6, pp. 685e–692e, 2011.
- [15] D. N. Granger and P. R. Kvietys, "Reperfusion injury and reactive oxygen species: the evolution of a concept," *Redox Biology*, vol. 6, pp. 524–551, 2015.
- [16] P. Sharma and N. Maffulli, "Tendon injury and tendinopathy: healing and repair," *The Journal of Bone and Joint Surgery. American Volume*, vol. 87, no. 1, pp. 187–202, 2005.
- [17] T. Friedrich, W. Schmidt, D. Jungmichel, L. C. Horn, and C. Josten, "Histopathology in rabbit Achilles tendon after operative tenolysis (longitudinal fiber incisions)," *Scandinavian Journal of Medicine & Science in Sports*, vol. 11, no. 1, pp. 4–8, 2001.
- [18] R. Stange, H. Sahin, B. Wieskötter et al., "In vivo monitoring of angiogenesis during tendon repair: a novel MRI-based technique in a rat patellar tendon model," *Knee Surgery, Sports Traumatology, Arthroscopy*, vol. 23, no. 8, pp. 2433–2439, 2015.
- [19] M. Aslam, K. D. Schluter, S. Rohrbach et al., "Hypoxia-reoxygenation-induced endothelial barrier failure: role of RhoA, Rac1 and myosin light chain kinase," *The Journal of Physiology*, vol. 591, no. 2, pp. 461–473, 2013.
- [20] N. Zhang, B. Hong, C. Zhou et al., "Cobalt chloride-induced hypoxia induces epithelial-mesenchymal transition in renal carcinoma cell lines," *Annals of Clinical and Laboratory Science*, vol. 47, no. 1, pp. 40–46, 2017.
- [21] T. Kietzmann, H. Schmidt, I. Probst, and K. Jungermann, "Modulation of the glucagon-dependent activation of the phosphoenolpyruvate carboxykinase gene by oxygen in rat hepatocyte cultures. Evidence for a heme protein as oxygen sensor," *FEBS Letter*, vol. 311, no. 3, pp. 251–255, 1992.
- [22] A. Menon, P. Creo, M. Piccoli et al., "Chemical activation of the hypoxia-inducible factor reversibly reduces tendon stem cell proliferation, inhibits their differentiation, and maintains cell undifferentiation," *Stem Cells International*, vol. 2018, Article ID 9468085, 13 pages, 2018.
- [23] J. Shi, Y. Wan, and W. Di, "Effect of hypoxia and reoxygenation on cell invasion and adhesion in human ovarian carcinoma cells," *Oncology Reports*, vol. 20, no. 4, pp. 803–807, 2008.
- [24] Y. Tong, K. Tong, Q. Zhu et al., "Cobalt chloride induced apoptosis by inhibiting GPC3 expression via the HIF-1 α /c-Myc axis in HepG2 cells," *Oncotargets and Therapy*, vol. Volume 12, pp. 10663–10670, 2019.
- [25] Y. F. Wu, C. Chen, J. B. Tang, and W. F. Mao, "Growth and stem cell characteristics of tendon-derived cells with different initial seeding densities: an in vitro study in mouse flexor tendon cells," *Stem Cells and Development*, vol. 29, no. 15, pp. 1016–1025, 2020.
- [26] N. Ming, H. S. T. Na, J. L. He, Q. T. Meng, and Z. Y. Xia, "Propofol alleviates oxidative stress via upregulating lncRNA-TUG1/Brg1 pathway in hypoxia/reoxygenation hepatic cells," *Journal of Biochemistry*, vol. 166, no. 5, pp. 415–421, 2019.
- [27] Y. Hu, Z. Mao, L. Xu et al., "Protective effect of dioscin against intestinal ischemia/reperfusion injury via adjusting miR-351-5p-mediated oxidative stress," *Pharmacological Research*, vol. 137, pp. 56–63, 2018.
- [28] N. E. Hoffman, B. A. Miller, J. F. Wang et al., "Ca²⁺ entry via Trpm 2 is essential for cardiac myocyte bioenergetics maintenance," *American Journal of Physiology. Heart and Circulatory Physiology*, vol. 308, no. 6, pp. H637–H650, 2015.
- [29] M. J. Berridge, P. Lipp, and M. D. Bootman, "The versatility and universality of calcium signalling," *Nature Reviews. Molecular Cell Biology*, vol. 1, no. 1, pp. 11–21, 2000.
- [30] P. Eschwege, V. Paradis, M. Conti et al., "In situ detection of lipid peroxidation by-products as markers of renal ischemia injuries in rat kidneys," *The Journal of Urology*, vol. 162, no. 2, pp. 553–557, 1999.
- [31] H. Chen, P. H. Chow, S. K. Cheng, A. L. M. Cheung, L. Y. L. Cheng, and W. S. O, "Male genital tract antioxidant enzymes: their source, function in the female, and ability to preserve sperm DNA integrity in the golden hamster," *Journal of Andrology*, vol. 24, no. 5, pp. 704–711, 2003.
- [32] G. S. McElroy and N. S. Chandel, "Mitochondria control acute and chronic responses to hypoxia," *Experimental Cell Research*, vol. 356, no. 2, pp. 217–222, 2017.
- [33] K. M. Porter, B. Y. Kang, S. E. Adesina, T. C. Murphy, C. M. Hart, and R. L. Sutliff, "Chronic hypoxia promotes pulmonary artery endothelial cell proliferation through H2O2-induced 5-lipoxygenase," *PLoS One*, vol. 9, no. 6, article e98532, 2014.
- [34] F. G. Thankam, I. S. Chandra, A. N. Kovilam et al., "Amplification of mitochondrial activity in the healing response following rotator cuff tendon injury," *Scientific Reports*, vol. 8, no. 1, article 17027, 2018.
- [35] B. H. Jiang, G. L. Semenza, C. Bauer, and H. H. Marti, "Hypoxia-inducible factor 1 levels vary exponentially over a physiologically relevant range of O2 tension," *The American Journal of Physiology*, vol. 271, no. 4, pp. C1172–C1180, 1996.
- [36] H. F. Burgers, D. W. Schelshorn, W. Wagner, W. Kuschinsky, and M. H. Maurer, "Acute anoxia stimulates proliferation in adult neural stem cells from the rat brain," *Experimental Brain Research*, vol. 188, no. 1, pp. 33–43, 2008.
- [37] S. Cao, S. Yang, C. Wu, Y. Wang, J. Jiang, and Z. Lu, "Protein expression of hypoxia-inducible factor-1 alpha and hepatocellular carcinoma: a systematic review with meta-analysis," *Clinics and Research in Hepatology and Gastroenterology*, vol. 38, no. 5, pp. 598–603, 2014.

- [38] A. J. Majmundar, W. J. Wong, and M. C. Simon, "Hypoxia-inducible factors and the response to hypoxic stress," *Molecular Cell*, vol. 40, no. 2, pp. 294–309, 2010.
- [39] H. Li, X. Li, X. Jing et al., "Hypoxia promotes maintenance of the chondrogenic phenotype in rat growth plate chondrocytes through the HIF-1 α /YAP signaling pathway," *International Journal of Molecular Medicine*, vol. 42, no. 6, pp. 3181–3192, 2018.
- [40] L. Liu, W. Liu, L. Wang, T. Zhu, J. Zhong, and N. Xie, "Hypoxia-inducible factor 1 mediates intermittent hypoxia-induced migration of human breast cancer MDA-MB-231 cells," *Oncology Letters*, vol. 14, no. 6, pp. 7715–7722, 2017.
- [41] C. H. Chen, Y. Cao, Y. F. Wu, A. J. Bais, J. S. Gao, and J. B. Tang, "Tendon healing in vivo: gene expression and production of multiple growth factors in early tendon healing period," *The Journal of Hand Surgery*, vol. 33, no. 10, pp. 1834–1842, 2008.
- [42] W. F. Mao, Y. F. Wu, Q. Q. Yang et al., "Modulation of digital flexor tendon healing by vascular endothelial growth factor gene transfection in a chicken model," *Gene Therapy*, vol. 24, no. 4, pp. 234–240, 2017.
- [43] M. Liang, H. R. Cornell, N. Zargar Baboldashti, M. S. Thompson, A. J. Carr, and P. A. Hulley, "Regulation of hypoxia-induced cell death in human tenocytes," *Advances in Orthopedics*, vol. 2012, no. 984950, 12 pages, 2012.
- [44] J. Zhang, C. Keenan, and J. H. Wang, "The effects of dexamethasone on human patellar tendon stem cells: implications for dexamethasone treatment of tendon injury," *Journal of Orthopaedic Research*, vol. 31, no. 1, pp. 105–110, 2013.
- [45] R. James, G. Kesturu, G. Balian, and A. B. Chhabra, "Tendon: biology, biomechanics, repair, growth factors, and evolving treatment options," *The Journal of Hand Surgery*, vol. 33, no. 1, pp. 102–112, 2008.
- [46] G. Riley, "The pathogenesis of tendinopathy. A molecular perspective," *Rheumatology*, vol. 43, no. 2, pp. 131–142, 2004.
- [47] Y. Bi, D. Ehrchiou, T. M. Kilts et al., "Identification of tendon stem/progenitor cells and the role of the extracellular matrix in their niche," *Nature Medicine*, vol. 13, no. 10, pp. 1219–1227, 2007.
- [48] K. Ueda, O. Shimizu, S. Oka, M. Saito, M. Hide, and M. Matsumoto, "Distribution of tenascin-C, fibronectin and collagen types III and IV during regeneration of rat submandibular gland," *International Journal of Oral and Maxillofacial Surgery*, vol. 38, no. 1, pp. 79–84, 2009.
- [49] D. F. Webster and H. C. Burry, "The effects of hypoxia on human skin, lung and tendon cells in vitro," *British Journal of Experimental Pathology*, vol. 63, no. 1, pp. 50–55, 1982.
- [50] E. A. Makris, D. J. Responde, N. K. Paschos, J. C. Hu, and K. A. Athanasiou, "Developing functional musculoskeletal tissues through hypoxia and lysyl oxidase-induced collagen cross-linking," *Proceedings of the National Academy of Sciences of the United States of America*, vol. 111, no. 45, pp. E4832–E4841, 2014.
- [51] S. M. Mosier, G. Pomeroy, and A. Manoli 2nd., "Pathoanatomy and etiology of posterior tibial tendon dysfunction," *Clinical Orthopaedics and Related Research*, vol. 365, pp. 12–22, 1999.
- [52] J. Yuan, G. A. Murrell, A. Q. Wei, and M. X. Wang, "Apoptosis in rotator cuff tendonopathy," *Journal of Orthopaedic Research*, vol. 20, no. 6, pp. 1372–1379, 2002.
- [53] R. T. Benson, S. M. McDonnell, H. J. Knowles, J. L. Rees, A. J. Carr, and P. A. Hulley, "Tendinopathy and tears of the rotator cuff are associated with hypoxia and apoptosis," *Journal of Bone and Joint Surgery. British Volume*, vol. 92-B, no. 3, pp. 448–453, 2010.
- [54] E. Sasabe, Y. Tatemoto, D. Li, T. Yamamoto, and T. Osaki, "Mechanism of HIF-1 α -dependent suppression of hypoxia-induced apoptosis in squamous cell carcinoma cells," *Cancer Science*, vol. 96, no. 7, pp. 394–402, 2005.

Research Article

Effects of Strong Acidic Electrolyzed Water in Wound Healing via Inflammatory and Oxidative Stress Response

Ailyn Fadriquela ^{1,2}, Ma Easter Joy Sajo ^{1,3}, Johny Bajgai ¹, Dong-Heui Kim ¹,
Cheol-Su Kim ¹, Soo-Ki Kim ⁴, and Kyu-Jae Lee ^{1,5}

¹Department of Environmental Medical Biology, Wonju College of Medicine Yonsei University, Wonju, Gangwon 26426, Republic of Korea

²Department of Laboratory Medicine, Wonju College of Medicine Yonsei University, Wonju, Gangwon 26426, Republic of Korea

³Department of Biology, College of Science, University of the Philippines Baguio, 2600, Philippines

⁴Department of Microbiology, Wonju College of Medicine Yonsei University, Wonju, Gangwon 26426, Republic of Korea

⁵Institute for Poverty Alleviation and International Development, Yonsei University, Wonju, Gangwon 26493, Republic of Korea

Correspondence should be addressed to Kyu-Jae Lee; medbio9@gmail.com

Received 27 July 2020; Revised 26 November 2020; Accepted 3 December 2020; Published 14 December 2020

Academic Editor: Reggiani Vilela Gon alves

Copyright © 2020 Ailyn Fadriquela et al. This is an open access article distributed under the Creative Commons Attribution License, which permits unrestricted use, distribution, and reproduction in any medium, provided the original work is properly cited.

Strong acidic electrolyzed water (StAEW) is known to inactivate microorganisms but is not fully explored in the medical field. This study is aimed at exploring StAEW as a potential wound care agent and its mechanism. StAEW (pH: 2.65, ORP: 1159 mV, ACC: 32.1 ppm) was sprayed three times a day to the cutaneous wounds of hairless mice for seven days. Wound morphological and histological features and immune-redox markers were compared with saline- (Sal-) and alcohol- (Alc-) treated groups. Results showed that the StAEW group showed a significantly higher wound healing percentage than the Sal group on days 2, 4, 5, and 6 and the Alc group on day 4. The StAEW group also showed earlier mediation on proinflammatory cytokines such as tumor necrosis factor- α , interleukin- (IL-) 6, IL-1 β , and keratinocyte chemoattractant. In addition, basic fibroblast growth factor and platelet-derived growth factor were found to be significantly changed in favor of the fibroblast synthesis and angiogenesis. In line, the StAEW group showed a controlled amount of ROS and significantly decreased compared to the Alc group. The StAEW group also favored oxidative stress balance through antioxidant responses. Additionally, matrix metalloproteinases (MMP) 9 and MMP1 were also modulated for keratinocyte and cell migration. Taken together, this study has proven the wound healing effect of StAEW and its earlier mediation through oxidative and inflammatory responses.

1. Introduction

Acidic electrolyzed water (AEW) or also known as electrolyzed oxidizing water is produced by a machine through electrolysis of water where a diluted salt solution and water pass through and produces water with oxygen gas, chlorine gas, hypochlorite ion, hypochlorous acid, and hydrochloric acid as components. The general characteristics of acidic water are as follows: low pH (2.2-6.5), high oxidation-reduction potential (ORP) (800-1100 mV), high available chlorine concentration (ACC) (10-60 ppm), and high content of dissolved

oxygen [1]. Because of its wide range in pH, researchers in this field came up with the classification of AEW: slightly AEW (SAEW), weak AEW (WAEW), and strong AEW (StAEW). Since the discovery of the production of acidic water, several studies have been conducted over the years that prove its efficacy in killing microbes, fungus, viruses, and inactivating toxins [1]. It has also been studied for its effect on disinfecting food equipment, vegetables, fruits, poultry, and meat; on hand washing; and on hospital bactericidal effect [2–4]. Recent studies in AEW concluded its damage to cell membranes and cell homeostasis of *Pseudomonas*

fluorescens biofilms [5] and was also found to enhance the reactive oxygen species (ROS) scavenging capacity of fruits for its enhanced storability [6].

To understand how AEW may potentially facilitate wound healing, it is important to know the wound healing process. Wound healing is a complex, overlapping but systemic mechanism that is strongly controlled for restoring the integrity of the skin. The process consists of four phases namely: haemostasis, inflammation, proliferation, and remodeling phases. Because it is a complex mechanism, several factors are involved such as nutrition, hypoxia, infection, immunosuppression, chronic disease, wound management, age, and genetics [7]. In addition, pH has a great influence in wound healing because of its effect on controlling wound infection, increasing antimicrobial activity, altering protease activity such as matrix metalloproteinases (MMPs) and tissue inhibitor of MMPs (TIMPs), releasing oxygen, reducing toxicity of bacterial end products, and enhancing epithelialization and angiogenesis [8–11]. Thus, there are increasing studies on the use of wound care agents or dressings that control and alter wound pH to accelerate the healing process. The progression of the wound stages depends on the wound type and its pathological condition as well as the type of dressing material. Some of the criteria for dressing selection are its ability to provide protection against bacterial infection, enhance epidermal migration, and promote angiogenesis and connective tissue synthesis, and it must be sterile, nontoxic, and nonallergic [12]. However, the safety of some wound healing agents can still pose a threat due to their possible side effects. StAEW has been reported as generally safe both *in vitro* and *in vivo*. A biocompatibility study of StAEW concluded that acidic water did not show cytotoxicity even in a dose-dependent manner, and a skin irritation test on a human epidermal model reported StAEW as nonirritant [13]. Additionally, another study concluded that electrolyzed waters are generally safe as evidenced by cytotoxicity assay and phospholipid leakage examination [14]. Furthermore, the involvement of the oxidative stress response and immune responses in wound healing has been one of the keys in studying wound care treatment. The good balance of reactive oxygen species (ROS) and antioxidant enzymes also known as redox balance leads to a normal and successful wound healing process [15].

Immunological and oxidative stress regulation has been shown to mediate skin diseases such as atopic dermatitis [16]. Since the development of AEW production, a few studies have been done over the years exploring its function in the medical field. Due to its widely known antibacterial effect, some studies have concluded that it can be effective in wound healing [17, 18]. However, these studies did not fully explore how AEW facilitates cutaneous wound healing. Knowing the different properties and characteristic of this water, and the complexity and factors involved in wound healing, we then hypothesized that StAEW can be an effective wound healing agent, and we tried to find out the mechanism of how StAEW facilitate wound healing by measuring oxidative stress and immune response markers and compared its effect with other potent wound care agents.

2. Materials and Methods

2.1. Preparation of StAEW, Saline, and Alcohol. StAEW was generated from a water electrolyzing machine (HDR, IONIA Co., Ltd. Bucheon, Korea), wherein tap water and 1% NaCl solution was added to the machine and StAEW was collected in the anode area. Tap water had the properties of pH: 7.62, ORP: 500 mV, and ACC: 0.2 mg/mL, and StAEW had pH: 2.65, ORP: 1159 mV, and ACC: 32.1 mg/mL. Saline (Sal) solution (0.9% NaCl, Life Science Co., Ltd., Dangjin, Korea) and 70% alcohol (Alc) (SK Chemical, Ulsan, Korea) were prepared as control groups.

2.2. Animal Groupings. Seven-week-old female hairless mice (18 ± 2 g) were purchased from Orient Bio Inc., Seongnam, South Korea, and were placed in a plastic cage (W 172 mm \times D 240 mm \times H 129 mm, five mice per cage). First, the mice were acclimatized for one week and kept at room condition of 22°C and 40–60% humidity in 12:12 h light and dark. Animals were randomly assigned into four groups with ten mice each: NC: normal control, no wound induction group; and wound-induced groups: Sal: saline-treated groups; Alc: alcohol-treated group; and StAEW: strong acidic electrolyzed water-treated group. Institutional Animal Care and Use Committee (IACUC), Yonsei University Wonju Campus (YWC-170907-1), approved the animal use and protocol done in this study.

2.3. Wound Induction and Treatment. To induce the wounds, a total of six wounds were created at the back part of each hairless mouse following protocols [19] by using a 5 mm biopsy punch (Integra-Miltex, PA, USA). Wounds were treated by spraying 2 mL of treatment solutions on the wounded areas, three times a day for seven days.

2.4. Wound Area Measurement and Gross Examination. Wound size was measured using a digital caliper vernier scale (Mitutoyo Corp., Japan) to measure the length and width of the two wounds located on the middle part of the mice, and the wound area was computed. Wound healing percentage was measured using the following formula [20]:

$$\text{Wound healing\%} = \left[\frac{\left[\text{wound area}_{(\text{day } 0)} - \text{wound area}_{(\text{day desired})} \right]}{\text{wound area}_{(\text{day } 0)}} \right] \times 100. \quad (1)$$

Wounds were observed macroscopically, and a digital photograph was taken every day to check and compare the wound state of each mouse.

2.5. Blood Collection and Serum Preparation. Upon sacrifice on the seventh day, blood samples were collected from the retroorbital plexus puncture by using EDTA (Ethylenediamine Tetra-Acetic Acid) and BD Microtainer®. Approximately, blood was collected in each tube per mouse in a microcontainer and used for hematological and biochemical analyzer. Briefly, EDTA microcontainer blood was used for white blood cell (WBC) analysis by mixing thoroughly for

3-5 minutes with an automatic rolling mixer and was counted by hematology analyzer (Hemavet® HV950 FS; Drew Scientific, Erba Diagnostics, Inc., Dallas, Texas, USA). BD Microtainer® blood samples from each mouse were further centrifuged at $700 - 1,000 \times g$ for 10 min at 4°C to get the serum and were kept at -80°C until analysis.

2.6. Skin Lysate Preparation. Equal size of skin tissue from the dorsal area was cut and was placed in ice-cold RIPA buffer (Pierce Biotechnology, Inc.) with protease and proteinase inhibitor cocktail (Sigma Chemical Co., St Louis, MO, USA). The crude skin lysate then was homogenized at 25 rpm for 15 min using a Tissue Lyser II (Qiagen, MD, USA). The lysate was then centrifuged for 5 minutes, and the supernatant was collected and transferred to a new epi-tube and was kept at -80°C until further use. Pierce BCA Assay Kit (Thermo Scientific, Rockford, IL, U.S.A.) was used to check the total protein concentration.

2.7. Histological Examination. The representative skin of each group was cut from the wound area and was fixed in 10% buffered formalin (0.1 M phosphate buffer, pH 7.4), dehydrated through a graded ethanol series, cleared by xylene, and embedded in paraffin wax (Polyscience, WA, USA). The paraffin section was cut into $4 \mu\text{m}$ thick by microtome (Reichert, Inc. New York, USA), stained by hematoxylin and eosin stains, and was observed under the light microscope (BA300, Motic Ltd., Hongkong, China).

2.8. WBC and Its Differential Counts Examination. Total WBC, lymphocytes, monocytes, and neutrophil counts were measured by an automatic blood analyzer (HEMAVET HV950 FS, Drew Scientific Inc., Dallas, TX, USA).

2.9. Total ROS Detection. Total ROS was measured using DCFH-DA (Abcam, Cambridge, MA, USA) following the manufacturer's manual. In brief, $25 \mu\text{L}$ of serum and $50 \mu\text{L}$ of skin lysate were plated into a 96-well plate. Then, $100 \mu\text{L}$ of $10 \mu\text{M}$ DCFH-DA was added to the wells, and the plate was incubated in the dark for 30 minutes. Fluorescence reading of the plate at 488 nm excitation/525 nm emission using DTX-880 multimode microplate reader (Beckman Counter Inc., Fullerton, CA, USA) was obtained.

2.10. Antioxidant Enzyme Assays. The activity of glutathione peroxidase (GPx) and catalase (CAT) in skin lysate was measured using Biovision kits (Milpitas, CA, USA) following the manufacturer's instructions. In brief, protein concentrations from skin lysate were normalized using Pierce™ BCA Protein Assay Kit by Thermo Scientific (Illinois, USA), the standards of each assay were prepared, the reagents from each assay were mixed in a 96-well microtiter plate, and absorbance was read at 340 nm (GPx) and 510 nm (CAT).

2.11. Cytokine and Growth Factor Analysis. Serum cytokines such as interleukin- (IL-) 1β , IL-6, tumor necrosis factor (TNF)- α , keratinocyte chemoattractant (KC), and growth factors such as platelet-derived growth factor (PDGF) and basic fibroblast growth factor (bFGF) were measured using Bead Array Suspension Multiplex Kit (Bio-Rad, San Diego,

CA, USA) according to the manufacturer's instructions. Standard curves for each cytokine were generated using the reference concentrations given in the kit. Standards and samples were read in a multiplex bead suspension array system (Bio-Plex 200, BIO-RAD®, CA, USA).

2.12. Western Blot Analysis. The protein expression of MMP1, MMP3, and MMP9 (Abcam, Cambridge, MA, USA) was measured by performing western blotting. The prepared normalized skin lysate was equally loaded and separated by electrophoresis on SDS-polyacrylamide gels. It was then transferred to nitrocellulose membranes which were blocked in 5% skim milk in tris-buffered saline (TBS) containing 0.1% Tween 20 for 1 h at room temperature. After blocking, the membranes were incubated with primary antibodies at 4°C with agitation. It was followed by incubation with horseradish peroxidase-conjugated secondary antibodies for 1 h at room temperature. The blots were developed using the Chemiluminescence Western Blot Detection System (BioSpectrum®600 Imaging System, Upland, CA, USA).

2.13. Statistical Analysis. The mean values among the groups were analyzed by the GraphPad Prism version 5.0 software packages (GraphPad, La Jolla, CA, USA) and were compared using one-way analysis of variance (ANOVA) followed by subsequent multiple comparison test (Tukey). A p value ≤ 0.05 was considered statistically significant.

3. Results

The effects of StAEW on wound healing percentage and wound morphology and histology wound healing percentage of StAEW were compared with saline (Sal) and alcohol (Alc) treatment on wounded mice. The wound healing percentage of the StAEW group was significantly higher than the Sal group on days 2, 4, 5, and 6 and the Alc group on day 4 (Figure 1(a)). At the end of seven days, the wound healing percentage was highest in the StAEW group as compared to the Sal and Alc groups, which shows that wounds are in 71-77% healed on day 7. Figure 1(b) showed the morphological change of the representative wounds of mice from each group from day 0 to day 7 of treatment. In the histological analysis, the thickness of the epidermis of the StAEW group was more pronounced similar to the NC group and followed by the Sal group, while the epidermis of the Alc group showed markedly increased proliferation of the epidermis layer (Figure 1(c)). In addition, the presence of immune cells was observed more in the Alc group and lesser in the StAEW group.

3.1. Effects of StAEW in Total WBC and Its Differential Counts. We examined the changes in total WBC and its differential counts. Table 1 shows that compared to the NC group, the Sal ($p < 0.05$) and Alc ($p < 0.05$) groups had reduced total WBC, but there was no statistically significant reduction in the StAEW group. We found that neutrophil counts were similar among all treated groups. However, lymphocyte counts were found to be reduced in the StAEW-treated groups ($p < 0.05$), and the Sal- and Alc-treated groups ($p < 0.01$) as compared to the NC group. Similarly,

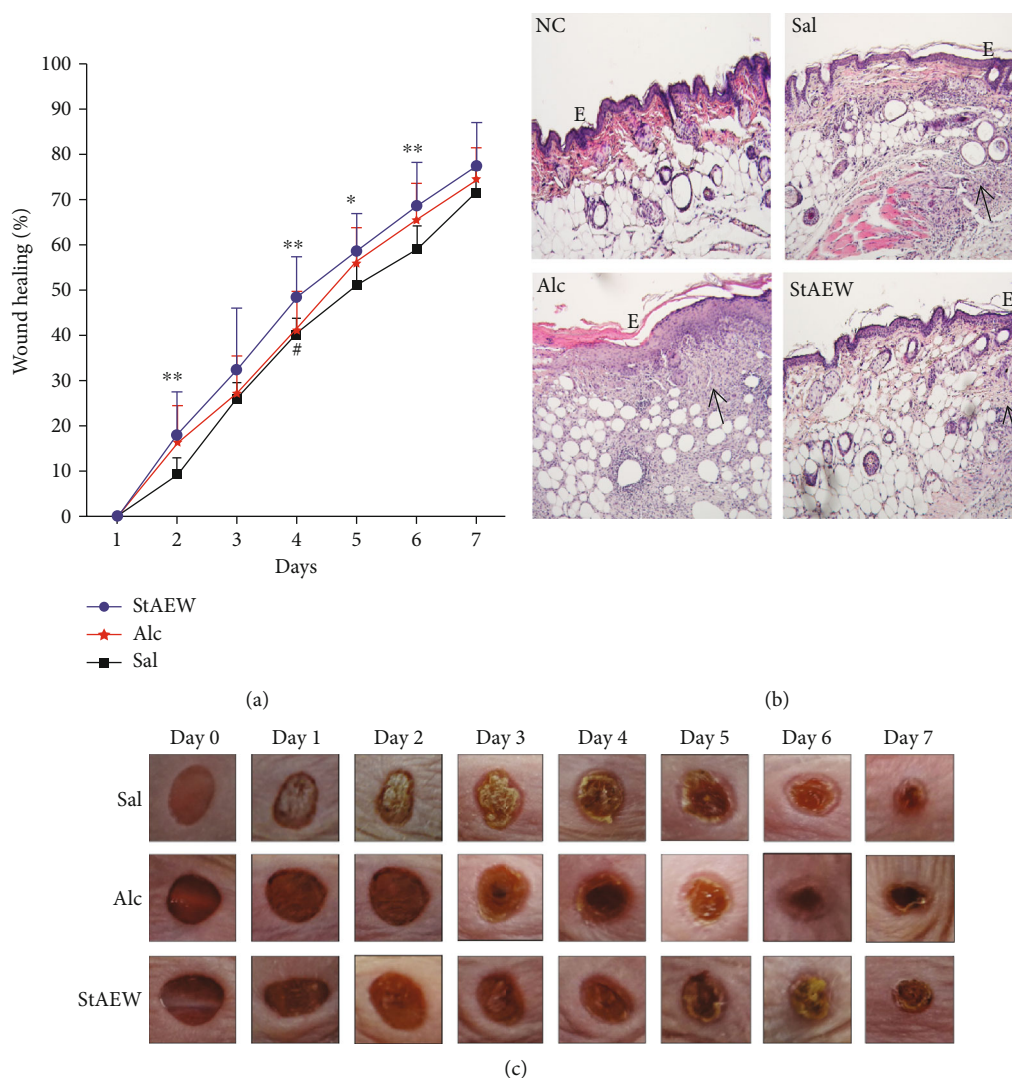


FIGURE 1: Effects of StAEW on (a) wound healing percentage, (b) wound morphology, and (c) histological appearance from day 1 to day 7 of different treatment groups. Wound size was measured using a digital caliper vernier scale (Mitutoyo Corp., Japan) to measure the length and width of the two wounds located on the middle part of the mice, and the wound area and wound healing percentage were computed. The wounds were observed macroscopically, and a digital photograph was taken every day to check and compare the wound state of each mouse. The histological appearance of cutaneous wounds stained with hematoxylin and eosin. All values are presented as mean \pm SD, $n = 10$. * $p < 0.05$, ** $p < 0.01$ vs. Sal group, # $p < 0.05$ vs. StAEW group. StAEW: strong acidic electrolyzed water; Sal: saline; Alc: alcohol.

TABLE 1: Total white blood cells (WBC) and its differential counts.

WBC count (K/ μ L)	NC	Sal	Alc	StAEW
Total WBC	5.14 \pm 0.95	4.04 \pm 0.40*	4.02 \pm 0.63*	4.54 \pm 0.55
Neutrophils	1.50 \pm 0.28	1.66 \pm 0.13	1.77 \pm 0.39	1.80 \pm 0.28
Lymphocytes	3.24 \pm 0.80	2.12 \pm 0.34**	2.04 \pm 0.39**	2.47 \pm 0.48*
Monocytes	0.41 \pm 0.09	0.26 \pm 0.07***	0.19 \pm 0.05***	0.22 \pm 0.05***

Data were expressed as mean \pm SD, $n = 10$. NC: normal control; StAEW: strong acidic electrolyzed water. * $p < 0.05$, ** $p < 0.01$, and *** $p < 0.001$ compared with the NC group indicate significant differences with ANOVA. Tukey's test was used for post hoc tests.

monocytes were significantly reduced in the StAEW, Sal, and Alc groups ($p < 0.001$) as compared to the NC group.

3.2. Effect of StAEW in ROS and Antioxidant Enzymes Generation. To explore its effect on oxidative stress, the

results showed that the ROS level in the serum of the StAEW group had the lowest level of ROS and also showed a significant decrease than the Alc group ($p < 0.001$). In skin lysate, the ROS level showed a similar trend wherein the Alc group consistently have significantly higher ROS level as compared

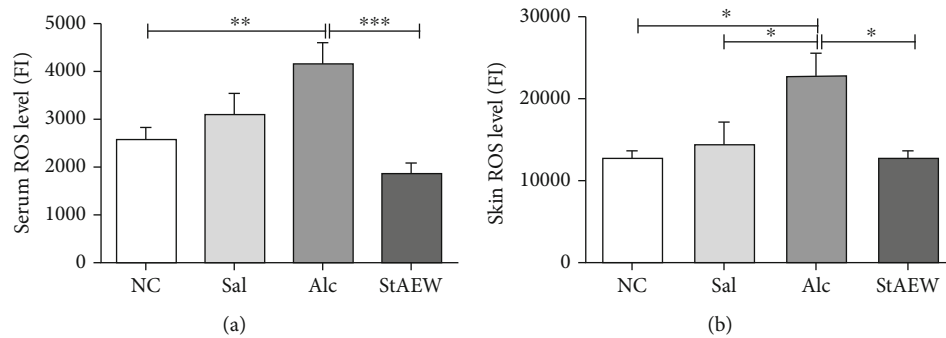


FIGURE 2: ROS levels in serum (a) and skin lysate (b) among the treatment groups. Total ROS was measured using DCFH-DA. All values are presented as mean \pm SD., $n = 10$. * $p < 0.05$, ** $p < 0.01$, and *** $p < 0.001$. NC: normal control; Sal: saline; Alc: alcohol; StAEW: strong acidic electrolyzed water.

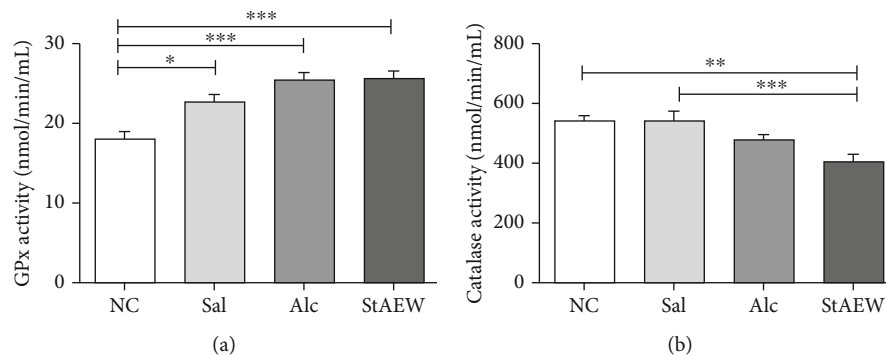


FIGURE 3: Skin lysate's GPx (a) and catalase (b) levels among the treatment groups. The normalized protein concentration of the skin lysate from each group and standards of each assay were prepared, and reagents were added and were read at 340 nm (GPx) and 510 nm (CAT), respectively. All values are presented as mean \pm SD., $n = 10$. * $p < 0.05$, ** $p < 0.01$, and *** $p < 0.001$ indicate significant differences when tested with ANOVA. Tukey's test was used for post hoc tests. NC: normal control; Sal: saline; Alc: alcohol; StAEW: strong acidic electrolyzed water.

to the NC ($p < 0.05$), Sal ($p < 0.05$), and StAEW groups ($p < 0.05$) (Figure 2). For antioxidant enzyme activities, the GPx level showed a significant increase in the Sal ($p < 0.05$), Alc ($p < 0.001$), and StAEW ($p < 0.001$) groups as compared to the NC group. Catalase activity, on the other hand, was found to be lower in StAEW as compared to the NC ($p < 0.01$) and Sal ($p < 0.001$) groups (Figure 3).

3.3. Effects of StAEW in Inflammatory Cytokines. To explore the mediation of StAEW on various inflammatory mediators such as cytokine production, we measured the concentration of IL-1 β , IL-6, KC, and TNF- α . Our results showed that the IL-1 β , IL-6, KC, and TNF- α concentrations of the StAEW group were significantly decreased as compared to NC (Figure 4). In detail, the IL-1 β of both the Alc and StAEW-treated groups were significantly reduced as compared to the NC ($p < 0.001$) and Sal groups ($p < 0.001$). On the other hand, only StAEW showed a significant reduction in IL-6 concentration as compared to the NC ($p < 0.001$) and Sal groups ($p < 0.01$). It was also observed that the IL-6 concentration of the Alc group was significantly lower than the NC group ($p < 0.05$). Likewise, TNF- α showed a similar trend with IL-1 β wherein both the Alc and StAEW groups were significantly reduced as compared to the NC

group (both $p < 0.001$) and Sal group ($p < 0.05$, $p < 0.01$, respectively). KC concentration showed a similar trend of significant reduction of all treatment groups as compared to NC ($p < 0.01$). A reduction in KC concentration was also observed between the Sal and StAEW groups ($p < 0.05$).

3.4. Effects of StAEW in Growth Factors. We also measured the concentration of PDGF and bFGF and found that they significantly changed as compared to the NC group. As compared to NC, PDGF showed a significantly increased level in the Sal ($p < 0.01$) and Alc ($p < 0.001$) groups but not as much as the increase in the StAEW group ($p < 0.05$). Moreover, a significant increase in the bFGF expression was seen in the StAEW group as compared to the NC and Sal groups ($p < 0.01$) (Figure 5).

3.5. Effects of StAEW in MMP Expression. Another important modulator of wound healing is the MMP activity. Our results show that the MMP1 and MMP9 expressions were upregulated in all groups but were not observed in MMP3 as compared to the NC group. The relative expression of MMP9 showed that there was a significant upregulation on the Sal ($p < 0.001$), Alc ($p < 0.01$), and StAEW ($p < 0.001$) groups while the Sal group showed the highest expression and was

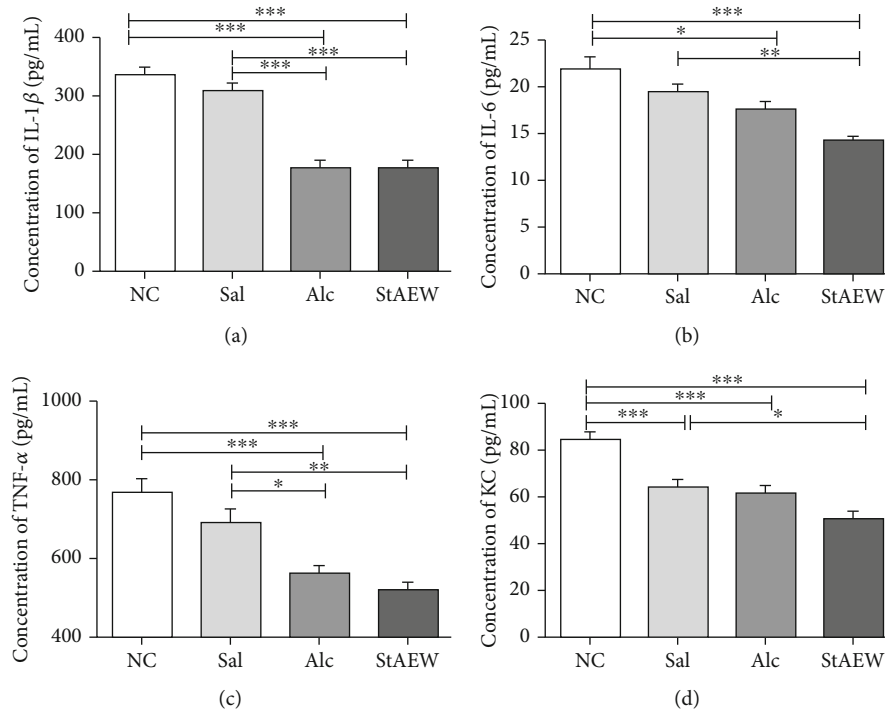


FIGURE 4: Effect of the treatment groups on IL-1 β (a), IL-6 (b), TNF- α (c), and KC (d). Cytokines were carefully selected and were measured using a multiplex bead suspension array system. All values are presented as mean \pm SD., $n = 10$. * $p < 0.05$, ** $p < 0.01$, and *** $p < 0.001$ indicate significant differences when tested with ANOVA. Tukey's test was used for post hoc tests. NC: normal control; StAEW: strong acidic electrolyzed water.

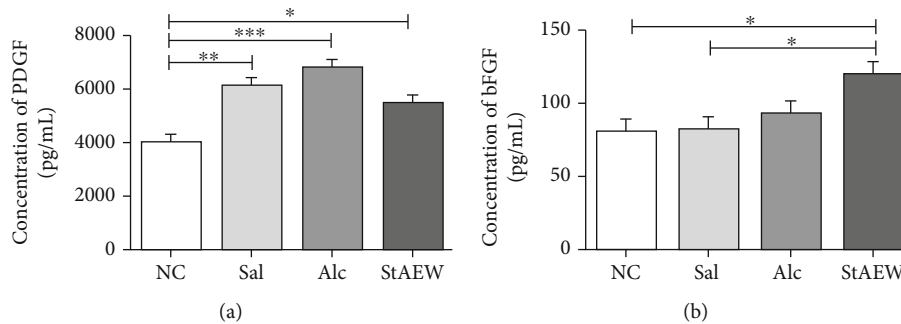


FIGURE 5: Effect of the treatment groups PDGF (a) and bFGF (b). Growth factors were carefully selected and were measured using a multiplex bead suspension array system. All values are presented as mean \pm SD., $n = 10$. * $p < 0.05$, ** $p < 0.01$, and *** $p < 0.001$ indicate significant differences when tested with ANOVA. Tukey's test was used for post hoc tests. NC: normal control; StAEW: strong acidic electrolyzed water.

significantly higher than the Alc ($p < 0.01$) and StAEW ($p < 0.001$) groups. Similarly, the MMP1 expression was also significantly upregulated in the Sal ($p < 0.01$), Alc ($p < 0.001$), and StAEW ($p < 0.001$) groups as compared with the NC group (Figure 6).

4. Discussion

Acidic water has been known first to inactivate different microorganisms. We confirmed the efficacy of our experimental water in killing microbes such as *Staphylococcus aureus* and *Pseudomonas aeruginosa* as compared to other kinds of water (Supplementary Figure 1). With this

background, this study proved that StAEW could also enhance skin wound healing effects in SKH-1 hairless mice through alleviating inflammatory and oxidative response, thus promoting earlier wound contraction and angiogenesis in wound tissue. This was first supported by the higher wound healing percentage of the StAEW-treated groups after 7 days of treatment especially on the earlier days (days 2 to 6). Our histological results showed that with StAEW treatment, the wounded epidermal area was highly intact than other available conventional wound cleaning agents and showed lesser infiltration of inflammatory cells. Exploring further the possible mechanism of this healing efficacy, it is important to know the involvement of the

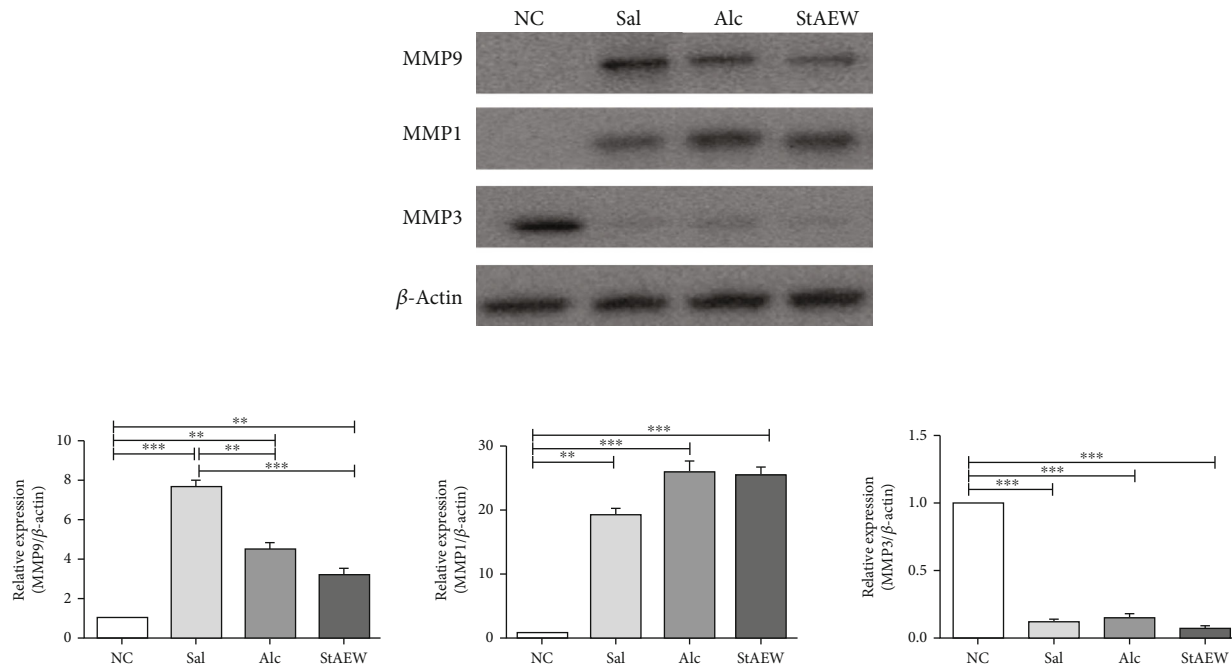


FIGURE 6: MMP1, MMP3, and MMP9 expressions of the treatment groups. The protein expressions were measured by performing western blotting. Relative intensity was compared to the housekeeping gene, β -actin, using ImageJ. All values are presented as mean \pm SD., $n = 10$. ** $p < 0.01$ and *** $p < 0.001$ indicate significant differences when tested with ANOVA. Tukey's test was used for post hoc tests. NC: normal control; Sal: saline; Alc: alcohol; StAEW: strong acidic electrolyzed water.

inflammatory and oxidative response in the wound healing process and its markers.

It is well known that WBCs play an essential role in wound healing and tissue repairing process especially in the earlier stage of wound healing. Upon injury, inflammatory cells migrate into the injury area and promote the inflammatory phase, which is further exemplified by the sequential but overlapping infiltration of neutrophils, macrophages, and lymphocytes [21, 22]. In our study, the reduction of the WBC counts especially the lymphocytes and monocytes indicates the mediation of the treatment groups in wound healing. This mediation of StAEW was also supported histologically by the presence of lesser inflammatory cells at this wound stage compared to other groups.

To continue exploring the immune and oxidative stress response in wound healing, we also explored the oxidative stress response mediated by StAEW. A controlled amount of ROS is well-studied to play an important role in a normal wound-healing response. Some of their roles include actions as the host's defense through phagocytosis, acting as second messengers to immune cells and also regulating angiogenesis [23]. This controlled amount of ROS is attained by the antioxidant's role in scavenging ROS, in a process called redox homeostasis [15]. Consistently, the controlled amount of ROS upon the StAEW treatment in both serum and wound area may suggest its beneficial mediation on the wound healing process, while the significant increase of ROS in both serum and skin lysate in Alc-treated group may suggest its oxidative stress damage upon its treatment. Overproduction of ROS causes oxidative stress thereby causing cytotoxicity and delayed wound healing process, and elimination of these

contributing ROS could be an important strategy in wound healing. To support this, the production of antioxidant enzymes seems to be mediated earlier by StAEW. It is essential to note that the functions of antioxidant enzymes in wound healing are in a temporal and spatial expression pattern [24]. Hence, the estimation of antioxidant enzymes like GPx and CAT in granulation tissues is relevant because the antioxidant activities have been reported to accelerate wound healing effect through decreasing the free radicals [25–27]. Therefore, the antioxidant levels obtained after StAEW treatment, along with reduced total ROS, may seem to prevent oxidative damage and promote the healing process.

To further confirm the mediation of StAEW in immune response, cytokines and growth factors involved in the healing process were screened and assayed. Upon careful screening, cytokines, IL-1 β , IL-6, TNF- α , and KC were investigated for the mediation of the treatment groups in response to wound healing. Proinflammatory cytokines IL-1 β , IL-6, and TNF- α are released by neutrophils, macrophages, and keratinocytes and trigger inflammatory cell proliferation and are also involved in promoting angiogenesis [28]. Moreover, the significant change of a chemokine, KC, may attribute to its function on the epithelialisation, angiogenesis, and tissue remodelling [29]. The significant reduction of these cytokines in the StAEW-treated groups shows the potential earlier mediation of StAEW in these cytokines to facilitate the healing process. Our results showed that the Alc-treated groups have a similar effect with StAEW on these cytokines; however, a more decreasing trend was observed in the StAEW groups. In addition to cytokines, growth factors also play essential roles in accelerating the healing process. At this

wound stage, mediation of StAEW in PDGF, which is important in the earlier stage of wound healing and functions in inflammation, granulation tissue formation, reepithelialisation, matrix formation, and remodelling [30], was less as compared to the Sal and Alc groups. On the other hand, bFGF, which plays an important role in the late remodelling stage and functions in angiogenesis and granulation tissue formation [31], showed to be significantly mediated by StAEW. Our results revealed that at this wound stage, StAEW seems to mediate the decreased production of PDGF and increased production of bFGF faster than the other conventional wound healing agents.

During the late proliferation and remodelling stages of wound healing, MMPs and their inhibitors play a critical role in irreversible remodelling wherein MMPs mainly degrade substances in the extracellular matrix. Recently, MMPs are known to be also responsible in inflammation, epithelial repair, and resolution. It is also important to note that there is a specific location and wound stages that MMP actions are upregulated and downregulated [32]. Our results showing the upregulation of MMP1 and MMP9 protein expression in wounded mice groups and the downregulation of MMP3 expression may imply the wound stage upon mice sacrifice. It is known that MMP9 produced by keratinocytes at the wound edge facilitates cell migration and reepithelialisation and is also involved in angiogenesis through the activation of TNF- α and VEGF [32] while MMP1 facilitates keratinocyte migration [33]. Moreover, MMP3 is known to be not necessary for keratinocyte proliferation or migration, collagen synthesis, and remodelling of the extracellular matrix but has a significant effect on wound contraction [34]. Our results showing the upregulation of MMP9 and MMP3 proves the mediation of StAEW on these proteins, and its decreasing level may suggest its faster mediation on these MMPs than in the Sal and Alc groups.

Taken together, it is certain that along with the known and potent antiseptic agents, such as Sal and Alc, StAEW is not only shown to be effective but also shows its earlier mediation in the wound healing process. This is done through its mediation on the immune response, as evidenced by the lesser inflammatory cells, the reduction of inflammatory cytokine and wound-stage-dependent growth factor release, and oxidative response, through providing a redox environment essential to the wound healing process, shown by the controlled amount of ROS and the significant difference of antioxidant enzymes and also through the crosslink of wound-stage-dependent MMP expressions. As more evidences and studies prove the efficacy of StAEW not only in killing microorganisms but also in the wound healing process, it is important to make sure that StAEW is retained in the wound site. One way is by freshly preparing StAEW and the repeated applications on the wound site. Our study showed that application three times a day was found effective. However, further studies might be necessary to check on the frequency of application as well as the possible use of gauzes or the development of hydrogels to retain the StAEW. However, as a recent report showed that physical properties such

as pH, ORP, and available chlorine concentration of electrolyzed waters might be affected by storage, temperature, and light exposure [35], it is important to make sure that the StAEW is prepared and stored well to maximize its full healing efficacy. In conclusion, StAEW can be used as an antiseptic agent in wounds and as a wound dressing. This result is consistent with the previous study that our lab reported on the immune-redox modulation of slightly acidic water (pH: 5–6.50, ORP: 800 mV, ACC:25 ppm) on cutaneous wounds [36]. Over the years, several disinfectants such as Alc and Sal have been used in wound care agents. However, due to its compound chemical properties, it may be possible that these agents can have side effects. The advantages of using StAEW as wound dressing include its faster healing efficacy than Alc and Sal. Moreover, because acidic water has been generally recognized as a safe compound as shown in the biocompatibility studies [13, 14], including toxicity and mutagenicity study in wound healing [35] and even on the application on the skin [37], the use of this agent in wound care can be more advantageous and better alternative to harsh chemical disinfectants. In addition, StAEW is also well-known for its cost-effectiveness due to its economical set-up generation using salt and tap water.

More studies are needed to explore the crosslink of immune response and inflammation factors and other potential parameters such as gender and use of other mice strains, which may affect the earlier mediation of StAEW in the healing process. An in-depth study of checking the effect of StAEW on each wound stage would be a great future study to fully understand its effect in wound healing responses and to take full advantage of the application of StAEW.

Data Availability

Data will be provided upon request to the corresponding author.

Conflicts of Interest

The authors declare no conflict of interest.

Acknowledgments

This work is part of the Doctoral Thesis of Ailyn Fadriqela [38]. The authors would also like to acknowledge the help of Dr. Jesmin Ara and Soon-Bong Song for the histological analysis done in this study. This work was supported by the Ministry of Education of the Republic of Korea and the National Research Foundation of Korea (NRF-2016S1A5B8925203).

Supplementary Materials

Supplementary Figure 1. Staphylococcus aureus (A) and Pseudomonas aeruginosa (B)-culture treated with different kinds of water. PW: purified water; TW: tap water; DW: distilled water; StAEW: strong acidic electrolyzed water. (*Supplementary Materials*)

References

- [1] Y. R. Huang, Y. C. Hung, S. Y. Hsu, Y. W. Huang, and D. F. Hwang, "Application of electrolyzed water in the food industry," *Food Control*, vol. 19, no. 4, pp. 329–345, 2008.
- [2] C. Zhang, B. Li, R. Jadeja, and Y. C. Hung, "Effects of electrolyzed oxidizing water on inactivation of *Bacillus subtilis* and *Bacillus cereus* spores in suspension and on carriers," *Journal of Food Science*, vol. 81, no. 1, pp. M144–M149, 2016.
- [3] Q. Han, X. Song, Z. Zhang et al., "Removal of foodborne pathogen biofilms by acidic electrolyzed water," *Frontiers in Microbiology*, vol. 8, p. 988, 2017.
- [4] V. N. Bui, K. V. Nguyen, N. T. Pham et al., "Potential of electrolyzed water for disinfection of foot-and-mouth disease virus," *Journal of Veterinary Medical Science*, vol. 79, no. 4, pp. 726–729, 2017.
- [5] L. L. Cai, H. J. Hu, Q. Lu et al., "Morphophysiological responses of detached and adhered biofilms of *Pseudomonas fluorescens* to acidic electrolyzed water," *Food Microbiology*, vol. 82, pp. 89–98, 2019.
- [6] Y. Chen, Y. C. Hung, M. Chen, M. Lin, and H. Lin, "Enhanced storability of blueberries by acidic electrolyzed oxidizing water application may be mediated by regulating ROS metabolism," *Food Chemistry*, vol. 270, pp. 229–235, 2019.
- [7] A. Young and C. E. McNaught, "The physiology of wound healing," *Surgery (Oxford)*, vol. 29, no. 10, pp. 475–479, 2011.
- [8] B. S. Nagoba, N. M. Suryawanshi, B. Wadher, and S. Selkar, "Acidic environment and wound healing: a review," *Wounds: a Compendium of Clinical Research and Practice*, vol. 27, no. 1, pp. 5–11, 2015.
- [9] S. L. Percival, S. McCarty, J. A. Hunt, and E. J. Woods, "The effects of pH on wound healing, biofilms, and antimicrobial efficacy," *Wound Repair and Regeneration*, vol. 22, no. 2, pp. 174–186, 2014.
- [10] S. Schreml, R.-M. Szeimies, S. Karrer, J. Heinlin, M. Landthaler, and P. Babilas, "The impact of the pH value on skin integrity and cutaneous wound healing," *Journal of European Academy of Dermatology and Venereology*, vol. 24, no. 4, pp. 373–378, 2010.
- [11] L. A. Schneider, A. Korber, S. Grabbe, and J. Dissemmond, "Influence of pH on wound-healing: a new perspective for wound-therapy?," *Archives of Dermatological Research*, vol. 298, no. 9, pp. 413–420, 2007.
- [12] S. Dhivya, V. V. Padma, and E. Santhini, "Wound dressings—a review," *BioMedicine*, vol. 5, no. 4, 2015.
- [13] H. Sipahi, R. Reis, O. Dinc, T. Kavaz, A. Dimoglo, and A. Aydin, "In vitro biocompatibility study approaches to evaluate the safety profile of electrolyzed water for skin and eye," *Human & Experimental Toxicology*, vol. 38, no. 11, pp. 1314–1326, 2019.
- [14] T. Kitamura, H. Todo, and K. Sugibayashi, "Effect of several electrolyzed waters on the skin permeation of lidocaine, benzoic acid, and isosorbide mononitrate," *Drug Development and Industrial Pharmacy*, vol. 35, no. 2, pp. 145–153, 2009.
- [15] T. Kurahashi and J. Fujii, "Roles of antioxidative enzymes in wound healing," *Journal of Developmental Biology*, vol. 3, no. 2, pp. 57–70, 2015.
- [16] J. Ara, J. Bajgai, M. E. J. Sajo et al., "The immunological and oxidative stress regulation of non-thermal plasma-aided water on atopic dermatitis-like lesion in dinitrochlorobenzene-induced SKH-1 hairless mice," *Molecular & Cellular Toxicology*, vol. 15, no. 2, pp. 199–208, 2019.
- [17] H. Nakae and H. Inaba, "Effectiveness of electrolyzed oxidized water irrigation in a burn-wound infection model," *Journal of Trauma and Acute Care Surgery*, vol. 49, no. 3, pp. 511–514, 2000.
- [18] N. Yahagi, M. Kono, M. Kitahara et al., "Effect of electrolyzed water on wound healing," *Artificial Organs*, vol. 24, no. 12, pp. 984–987, 2008.
- [19] A. Grada, J. Mervis, and V. Falanga, "Research techniques made simple: animal models of wound healing," *Journal of Investigative Dermatology*, vol. 138, no. 10, article e2091, pp. 2095–2105.e1, 2018.
- [20] D. Cukjati, S. Reberšek, and D. Miklavčič, "A reliable method of determining wound healing rate," *Medical and Biological Engineering and Computing*, vol. 39, no. 2, pp. 263–271, 2001.
- [21] J. E. Park and A. Barbul, "Understanding the role of immune regulation in wound healing," *The American Journal of Surgery*, vol. 187, no. 5, pp. S11–S16, 2004.
- [22] T. A. Wilgus, S. Roy, and J. C. McDaniel, "Neutrophils and wound repair: positive actions and negative reactions," *Advances in Wound Care*, vol. 2, no. 7, pp. 379–388, 2013.
- [23] C. Dunnill, T. Patton, J. Brennan et al., "Reactive oxygen species (ROS) and wound healing: the functional role of ROS and emerging ROS-modulating technologies for augmentation of the healing process," *International Wound Journal*, vol. 14, no. 1, pp. 89–96, 2017.
- [24] H. Steiling, B. Munz, S. Werner, and M. Brauchle, "Different types of ROS-scavenging enzymes are expressed during cutaneous wound repair," *Experimental Cell Research*, vol. 247, no. 2, pp. 484–494, 1999.
- [25] M. Barbara, S. Frank, G. Hübner, E. Olsen, and S. Werner, "A novel type of glutathione peroxidase: expression and regulation during wound repair," *Biochemical Journal*, vol. 326, no. 2, pp. 579–585, 1997.
- [26] S. Roy, S. Khanna, K. Nallu, T. K. Hunt, and C. K. Sen, "Dermal wound healing is subject to redox control," *Molecular Therapy*, vol. 13, no. 1, pp. 211–220, 2006.
- [27] A. Hasmann, E. Wehrschoetz-Sigl, A. Marold et al., "Analysis of myeloperoxidase activity in wound fluids as a marker of infection," *Annals of Clinical Biochemistry*, vol. 50, no. 3, pp. 245–254, 2013.
- [28] C. Qing, "The molecular biology in wound healing & non-healing wound," *Chinese Journal of Traumatology*, vol. 20, no. 4, pp. 189–193, 2017.
- [29] J. Ding and E. E. Tredget, "The role of chemokines in fibrotic wound healing," *Advances in Wound Care*, vol. 4, no. 11, pp. 673–686, 2015.
- [30] S. Barrientos, O. Stojadinovic, M. S. Golinko, H. Brem, and M. Tomic-Canic, "Perspective article: growth factors and cytokines in wound healing," *Wound Repair and Regeneration*, vol. 16, no. 5, pp. 585–601, 2008.
- [31] M. Okumura, T. Okuda, T. Nakamura, and M. Yajima, "Effect of basic fibroblast growth factor on wound healing in healing-impaired animal models," *Arzneimittel-Forschung*, vol. 46, no. 5, pp. 547–551, 1996.
- [32] M. P. Caley, V. L. C. Martins, and E. A. O'Toole, "Metalloproteinases and wound healing," *Advances in Wound Care*, vol. 4, no. 4, pp. 225–234, 2015.
- [33] M. G. Rohani and W. C. Parks, "Matrix remodeling by MMPs during wound repair," *Matrix Biology*, vol. 44–46, pp. 113–121, 2015.

- [34] K. M. Bullard, L. Lund, J. S. Mudgett et al., “Impaired wound contraction in stromelysin-1-deficient mice,” *Annals of Surgery*, vol. 230, no. 2, pp. 260–265, 1999.
- [35] R. Reis, H. Sipahi, O. Dinc et al., “Toxicity, mutagenicity and stability assessment of simply produced electrolyzed water as a wound healing agent in vitro,” *Human & Experimental Toxicology*, 2020.
- [36] H. S. You, A. Fadriquela, M. E. J. Sajo et al., “Wound healing effect of slightly acidic electrolyzed water on cutaneous wounds in hairless mice via immune-redox modulation,” *Biological and Pharmaceutical Bulletin*, vol. 40, no. 9, pp. 1423–1431, 2017.
- [37] A. Desai, C. Tam, K. Bhakta, T. Desai, R. Sarkar, and N. B. Desai, “The efficacy and tolerability of electrolyzed oxidized water in treating mild to moderate acne,” *Cosmetic Dermatology*, vol. 17, no. 2, pp. 93–105, 2004.
- [38] A. Fadriquela, *Effects of Strong Acidic Electrolyzed Water in Wound Healing Via Oxidative Stress and Inflammatory Response ([UCI]1804:11046-000000518283)*, [Ph.D. thesis], Institutional Repository at RISS, South Korea, 2019, http://www.riss.or.kr/search/Search.do?queryText=znSubject,%EC%82%B0%ED%99%94+%EC%A0%84%EC%9C%84&searchGubun=true&colName=bib_t&detailSearch=true#redirect.

Research Article

What Is the Impact of Depletion of Immunoregulatory Genes on Wound Healing? A Systematic Review of Preclinical Evidence

Bárbara Cristina Félix Nogueira ¹, **Artur Kanadani Campos** ¹, **Raul Santos Alves** ²,
Mariáurea Matias Sarandy ², **Rômulo Dias Novaes** ³, **Debora Esposito** ⁴,
and Reggiani Vilela Gonçalves ²

¹Department of Veterinary Medicine, Federal University of Viçosa, Viçosa, Minas Gerais, Brazil

²Department of General Biology, Federal University of Viçosa, Viçosa, Minas Gerais, Brazil

³Department of Structural Biology, Federal University of Alfenas, Alfenas, Minas Gerais, Brazil

⁴Department of Animal Science, North Carolina State University, USA

Correspondence should be addressed to Reggiani Vilela Gonçalves; reggysvilela@yahoo.com.br

Received 25 August 2020; Revised 4 November 2020; Accepted 16 November 2020; Published 7 December 2020

Academic Editor: Sander Bekeschus

Copyright © 2020 Bárbara Cristina Félix Nogueira et al. This is an open access article distributed under the Creative Commons Attribution License, which permits unrestricted use, distribution, and reproduction in any medium, provided the original work is properly cited.

Cytokines and growth factors are known to play an important role in the skin wound closure process; however, in knockout organisms, the levels of these molecules can undergo changes that result in the delay or acceleration of this process. Therefore, we systematically reviewed evidence from preclinical studies about the main immunoregulatory molecules involved in skin repair through the analysis of the main mechanisms involved in the depletion of immunoregulatory genes, and we carried out a critical analysis of the methodological quality of these studies. We searched biomedical databases, and only original studies were analyzed according to the PRISMA guidelines. The included studies were limited to those which used knockout animals and excision or incision wound models without intervention. A total of 27 studies were selected; data for animal models, gene depletion, wound characteristics, and immunoregulatory molecules were evaluated and compared whenever possible. Methodological quality assessments were examined using the ARRIVE and SYRCLE's bias of risk tool. In our review, the extracellular molecules act more negatively in the wound healing process when silenced and the metabolic pathway most affected involved in these processes was TGF- β /Smad, and emphasis was given to the importance of the participation of macrophages in TGF- β signaling. Besides that, proinflammatory molecules were more evaluated than anti-inflammatory ones, and the main molecules evaluated were, respectively, TGF- β 1, followed by VEGF, IL-6, TNF- α , and IL-1 β . Overall, most gene depletions delayed wound healing, negatively influenced the concentrations of proinflammatory cytokines, and consequently promoted a decrease of inflammatory cell infiltration, angiogenesis, and collagen deposition, compromising the formation of granulation tissue. The studies presented heterogeneous data and exhibited methodological limitations; therefore, mechanistic and highly controlled studies are required to improve the quality of the evidence.

1. Introduction

Cutaneous wounds, according to the World Health Organization (WHO), represent a public problem that affects a major part of the world population and entails elevated costs for health systems. It is estimated that billions of dollars are spent on the acquisition of preventive material and complication treatment every year [1]. About 85% of amputations in diabetic patients are preceded by ulcers, and around 70% of

these patients die after five years of amputation [2–4]. Usually, patients with cutaneous wounds present not only pain but also difficulties in everyday activities and loss of function on the affected limb [5]. The efforts to intervene in the wound healing process include ionizing radiation, chemical products, and wound dressings. However, the majority of these efforts have not obtained the desired results, since the pathways through which the skin repair process could be accelerated are still unclear. This is probably why current therapies

fail to accelerate wound closure and promote a fast infection-free recovery.

The repair process occurs when the skin is damaged and the connective tissue is exposed [6–8]. The wound healing process is multifaceted and composed of a phase that can be sequential or overlapping [9]. This process is divided into four phases: hemostasis, inflammation, proliferation, and remodeling [6]. These phases involve the action of molecules of cell adhesion, growth factors, and cytokines, besides several other molecules present in the extracellular matrix for it to be efficient [10, 11]. The cytokines and growth factors are important in all phases of the wound healing process. At the beginning of the process, activated platelets release Transforming Growth Factor- β (TGF- β) and Platelet-Derived Growth Factor (PDGF) resulting in the platelet plugs [12]. Besides that, the degranulation products of the platelet diffused to the extracellular matrix forming a chemotactic gradient of orientation for leukocyte diapedesis [13]. Proinflammatory molecules are released in the inflammatory phase such as interleukins IL-1, IL-2, IL-6, IL-17, and Tumor Necrosis Factor (TNF) that promote the activation of macrophages, neutrophils, and mast cells and stimulate the expression of adhesion molecules [14]. Therefore, macrophages suffer hypertrophy and metabolic increase releasing other growth factors such as TGF- β , PDGF, and Vascular endothelial growth factor (VEGF) that are responsible for the activation of endothelial cells and adhesion of molecule and recruitment of more phagocytes in a cyclical process. Besides, these molecules promote the division and differentiation of keratinocytes and fibroblasts, stimulating the production of collagen early in the repair process [15, 16]. In the proliferative phase, TNF- α controls the angiogenesis and formation of the tissue granulation; this is composed of cells and a network of blood vessels responsible for reestablishing regional circulation [17, 18]. The remodeling phase corresponds mainly to changes in the extracellular matrix of the scar tissue, where collagen type III is replaced by collagen type I and occurs the release of mediators such as TGF- β , which stimulate the differentiation of myofibroblasts and promote the closure of the wound [19–21]. Also, occurs the release of IL-1, IL-6, and TNF that act through the Nuclear Factor- κ B (NF- κ B) and signal transducers and activators of transcription-3 (STAT3) pathways, which act to prevent cell death and promote cell proliferation, differentiation, and inflammation [22, 23]. However, many more cytokines and growth factors are present at the wound site, and their dynamic expressions show important temporal and spatial characteristics in the regulation of wound healing processes. Besides that, it is known that important changes in the levels of these molecules affect the production of other cytokines and growth factors [24], and this highlights the complex interactions that occur between these compounds during wound healing. Therefore, these interactions should be considered when interpreting results obtained from the overexpression or elimination of a single immunoregulatory molecule at the wound site.

Currently, the most common and desirable animal model for studying the effect of depletion of specific genes during the repair process are knockout mice [25]. These animal

models are important for understanding the role of specific genes in tissue repair, and consequently, for understanding the mechanisms that are involved in the activation of specific cells and the interruption of the repair process [25–29]. Despite this, some questions about the use of this animal model may arise, mainly because this animal is not normally exposed to cytokines and growth factors, and some of these molecules may control more than one cellular activity [25, 30]. However, as it presents the correct ontogenesis process and the normal phenotype, the use of knockout mice is considered successful in the presentation of the physiological and pathophysiological roles of cytokines and growth factors, and it even allows observing the compensation of these molecules activity or the exclusion of receptors excluded by their performance. Therefore, the utilization of genetically altered mice is a powerful method for exploring signal transduction cascades, and it allows more clarification in studies on the impact of single genes in wound healing [25, 30].

It is already known that cytokines and growth factors play an important role in the closure of skin wounds, however, little is known about the design and bias of molecular knockout studies of these small proteins and the impact that this molecular knockout has on skin repair. In addition, typical incisional and excisional wound models in mice are simplistic and at best semiquantitative when used in wound healing analysis. Moreover, a comprehensive analysis of the impact of these molecules that may have proinflammatory and/or anti-inflammatory function over the modulation of important wound healing parameters has never been evaluated by a systematic review. Therefore, we believe that the results of this study will help to understand the main mechanisms involved in the wound healing process and provide a guideline for decision-makers or even researchers in the development of new products and treatments that can accelerate skin wound closure. Based on a detailed analysis of methodological bias, we also evaluated the force of the current evidence by analyzing the advances and limitations of the studies carried out in this field.

2. Methods

2.1. Focus Question and Registration on the Prospero Platform. This systematic review was based on the following focus question: How can gene depletion related to cytokines and growth factors compromise skin repair? Second, what are the main cytokines and growth factors analyzed in the studies? And what are the main consequences of this depletion? Third, what are the main methodological parameters used to evaluate the evolution of the repair process in the knockout model?

The registration number on the Prospero platform is CRD42020163197.

2.2. Bibliographic Search. This systematic review was developed according to the Preferred Reporting Items for Systematic Reviews and Meta-Analysis (PRISMA) guidelines [31], which was used as a guide for the selection, screening, and eligibility of studies. The bibliographic search was performed on September 30, 2019, and was conducted in the following

databases: PubMed/Medline (<https://www.ncbi.nlm.nih.gov/pubmed>), Scopus (<https://www.scopus.com/home.uri>), and Web of Science (<https://www.webofknowledge.com>). The descriptors were structured based on search filters built for three domains: (i) animals, (ii) wound healing, and (iii) skin. Inside the animal domain, it was possible to select the knockout animals using this theme (knockout animal) as an eligibility criterion.

The filters on the PubMed/Medline platform were constructed using a hierarchical distribution of the MeSH Terms (Medical Subject Headings) and by the algorithm TIAB (Title and Abstract). These filters were adapted for research in the Scopus platform and Web of Science; however, the filter for animal studies was provided by the Scopus platform (Table S1). The studies were filtered considering the languages: English, Portuguese, and Spanish. Two reviewers (BCFN and RSA) manually searched the reference lists of studies selected in the previous step independently to find additional relevant articles.

2.3. Selection of Relevant Studies. After an exhaustive reading of the abstracts, we began to preselect the studies that corresponded to the focus question answers. Studies that were not primary studies, such as brief reports, literature reviews, comments, notes, book chapters, and non-indexed studies, were excluded. Studies with other approaches (i.e., bacteria, virus, radiation, wound suture studies, infected wound, treated wound, wound repair in diabetic mice, or other pathologies) were also excluded. Studies that used only *in vitro* and *ex vivo* studies, knockout for receptor gene, and studies that not evaluated cytokines and growth factors were excluded. Double knockouts were also excluded due to the difficulty of isolating the effect of each gene on cytokines and growth factors and consequently on the wound closure process.

Only studies that met the following eligibility criteria were selected:

- (1) *In vivo* studies of skin wound healing with knockout animals whose gene depletion is immunoregulatory molecules
- (2) Studies that evaluate changes in cytokines and growth factor expression from the analysis performed on the biopsy

2.4. Data Extraction and Management. Three independent researchers (BCFN, MMS, and RVG) selected eligible studies following the analysis of their titles and abstracts. The level of agreement between these reviewers was assessed using Kappa (Kappa = 0.914). When there was doubt, an arbitration was requested from other independent researchers (RDN, RSA, DE, and AKC) to decide whether any given study met the eligibility criteria previously defined, likewise to discard subjectivity in the data collection and selection process, the information was extracted independently and analyzed separately.

The data of the publications were extracted using standardized information such as (1) Publication characteristics and animal models (authorship, country, ethics committee, statistical analysis, lineage, gene depletion, sex, age, and weight); (2) cutaneous wounds (antisepsis, anesthesia, instrument used for biopsy, biopsy collection days, wound area,

number of wounds per animal, and wound healing assessment period); and (3) cytokine and growth factor evaluation (cytokine and growth factor analyzed, evaluation methods, and biological material used to evaluate). After this, the data were compared between the reviewers, and the conflict information was corrected. The characteristics that we collected from the studies and used for their evaluation were presented in Table S2. Cytokines and growth factors were classified according to their inflammatory action based on the source cell and the mechanism of action.

2.5. Bias Analysis. The quality of the studies was assessed by the criteria described on the SYRCLE's Risk of Bias (RoB) tool (Systematic Review Centre for Laboratory animal Experimentation) [32] and ARRIVE (Animal Research: Reporting of *In Vivo* Experiments) guideline [33]. In relation to SYRCLE's, to facilitate the judgment of scientific articles through the use of characteristics of all studies using animal models, we made questions divided into the following subtopics: Q1-Q3 consider selection bias, Q4-Q5 consider performance bias, Q6-Q7 consider detection bias, Q8 considers attrition bias, Q9 considers reporting bias, and Q10 considers other biases. The articles in the RoB tool were marked with "yes" (low risk of bias), "no" (high risk of bias), or "unclear" (indicating that the item was not reported, and therefore, the risk of bias was unknown). Moreover, we made three additional questions that contributed to the judgment of the studies: Q11: "Was the number of animals per group and the number of animals per cage presented?" We marked "yes" whenever the study mentioned the number of animals per group and per cage. We marked "unclear" for incomplete answers, and "no" whenever nothing was mentioned. Q12: "What conditions were the animals kept in?" Whenever the answer was yes, we analyzed if the author had mentioned the temperature, humidity, light/dark cycles, water, and food. If the author does not mention these parameters (temperature, humidity, light/dark cycles, water, and food), we stated the study as "unclear." And whenever this topic was not mentioned at all, we answered "no" for that study. Q13: "Wound closure data were presented with follow-up days, photos, and graphs?" We answered "yes" when the study mentioned the method of wound evaluation in the methodology and presented graphs and photos of wound follow-ups in the results. We answered "unclear" to just some of the information and "no" when nothing was mentioned. The SYRCLE chart was built using Review Manager 5.3 software system. The ARRIVE strategy requires the complete screening of all manuscript sections (abstract to acknowledgments and funding) to evaluate the completeness of scientific reports on animal studies. The screening strategy was based on short descriptions of essential characteristics such as baseline measurements, sample size, animal allocation, randomization, experimental concealment, statistical methods, ethical statement, and generalizability. A table summarizing all relevant and applicable aspects was constructed considering the specificity and aims of the systematic review. The individual adherence to bias criteria and the overall mean adherence were expressed as absolute and relative values [34].

3. Results

3.1. Characteristics of Publications. The initial research resulted in 1130 studies on the PubMed/Medline, 850 on the Scopus, and 297 on the Web of Science platform, totaling 2277 studies, of which 1048 were excluded because they were duplicates. After reading the titles and abstracts, other 896 studies were excluded, and 333 studies were selected and read in full. Of these studies, only 27 fully met the inclusion criteria and were included in the systematic review (Figure 1).

The studies were conducted in United States of America (25.9%) [27, 35–40]; Japan (18.5%) [26, 41–44]; Germany (11.1%) [45–47]; Brazil, Canada, and China (7.4%, each) [28, 29, 48–51]; and Australia, Singapore, Netherlands, Spain, Taiwan, and Switzerland (3.7%, each) [52–57]. The approval for the use of animals in experimental procedures by the Animal Use and Care Committee was mentioned in 85.2% of the studies, and the statistical analyses performed were specified in 81.5% of the studies.

3.2. Characteristics of Experimental Animals. All studies used mice as the animal model and wild type as the control group (100.0%). The animal sex was neglected in 51.9% of the studies, and 33.3% of the studies used males and just 14.8% used females. The age was presented in months and weeks, varying between four and 20 weeks, and 7.4% of the studies neglected this data. The animals' weight ranged from 19 to 30 grams and was reported in two (7.4%) of the studies (Table S2). Only 22.2% [29, 36, 41–43, 51] of the studies allocated the animals individually in cages. Among the strains found in this review, C57BL/6 (29.6%) [27, 35, 43, 46, 47, 51, 54, 55] and BALB/c (14.8%) [26, 41, 56, 57] were the most frequent, besides, 14.8% of the studies [38, 39, 44, 45] omitted this information (Table S2). We found studies with other animal models during the study selection process, such as the rat, but these were discarded due to not meeting the requirements of the other selection criteria.

3.3. Characteristics of Wounds. Dorsal skin wounds were made in all 27 studies, 85.2% of studies with excision wounds, and 14.8% with incision wounds (Table S2). There were no similarities in the studies of excisional and incisional wounds in relation to the days when cytokines and growth factors were analyzed. We found other studies that analyzed wounds in other parts of the animal body, but these studies were not considered in this systematic review because they did not meet the requirements of the other selection criteria.

3.3.1. Excision Wounds. Specifications on hygiene and asepsis were reported in 39.1% of the studies, and most of the studies used alcohol as antiseptics (30.4%). Two forms of anesthesia were found in the studies, being ketamine and xylazine as the most common by intraperitoneal injection (26.0%) [27, 45, 46, 48, 55, 56] and isoflurane inhalation as the other compound used (13.0%) [44, 50, 54]. The biopsy punch was the surgical instrument most used to make the wounds (52.2%). Eighteen studies (78.3%) presented data regarding the number and size of wounds, and 21.7% did not provide clear information regarding the number of wounds. The

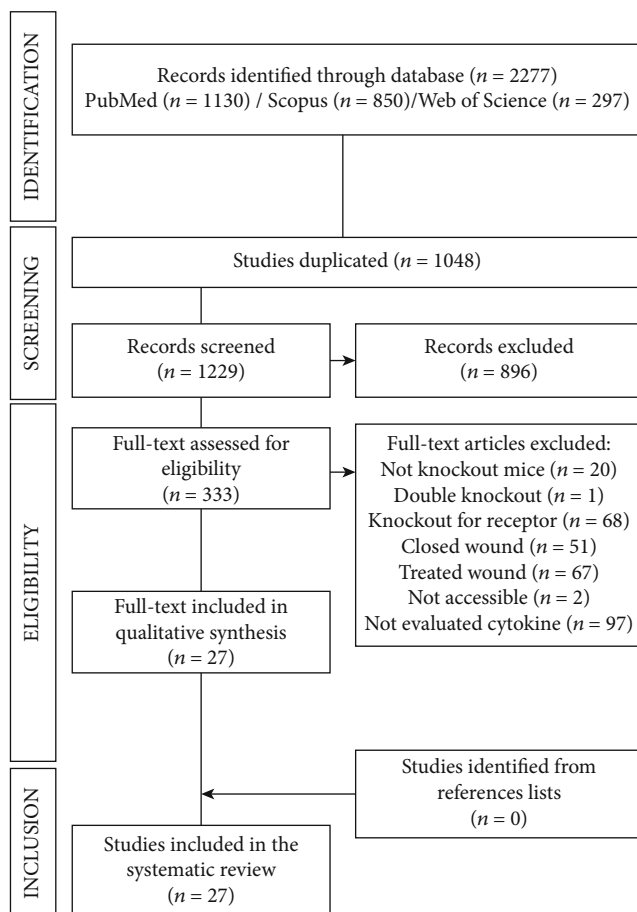


FIGURE 1: PRISMA diagram. Different phases of the selection of studies for conducting qualitative and quantitative analyses. Flow diagram of the systematic review literature search results. Based on “Preferred Reporting Items for Systematic Reviews and Meta-Analyses: The PRISMA Statement.” <http://www.prisma-statement.org>. From: Moher D, Liberati A, Tetzlaff J, Altman DG, The PRISMA Group (2009).

most common size of the wounds was 6 mm (33.3%), and the number of wounds found per animal was two (29.6%). Just 43.5% of studies presented data about the days of wounds biopsy, only 8.7% of the studies [26, 41] carried out the collection of material on 1, 3, 6, 10, and 14 days. The period of evaluation and presentation of data related to wound closure follow-up was presented in 82.6% of studies, and this information was neglected by 17.4% of the studies, as shown in Table S2.

3.3.2. Incision Wounds. Among the studies that evaluated incision wounds, antisepsis, and anesthesia, specifications were reported just in 50.0% [39, 40] of the studies. Regarding the instrument used to perform the wounds, 25.0% of the studies used a scalpel to make the wounds; and this information was omitted in 75.0% of the studies. Half of these studies presented data regarding the number and size of wounds, one study [57] with two wounds per animal, and another study [39] with four wounds per animal; in addition, these studies showed wounds of similar size, 1 cm. Two studies (50.0%) [39, 40] presented the collection days of wounds

but there was no similarity. The period of evaluation of wound healing was presented in all studies (100.0%), as shown in Table S2.

3.4. Gene Depletion on Wound Healing. Considering the 27 studies evaluated, a total of 30 gene depletions were analyzed. Most of the gene depletion analyzed (60.0%) showed negative effects in the wound healing process, and seven gene depletions showed accelerated wound healing. This probably occurred due to the anti-inflammatory and proinflammatory characteristics of some molecules, and in some cases, the same molecule presented both functions. Moreover, five gene depletions showed no interference in the healing process. The predicted location of the depleted genes was defined based on the location of the corresponding protein, so we found eight genes located exclusively in the extracellular matrix (Interferon-gamma (*IFN- γ*), Granulocyte-Macrophage Colony-Stimulating Factor (*GM-CSF*), Thrombospondin (*TSP1* and *TSP2*), Matrix Metalloproteinase (*MMP9* and *MMP13*), Lumican (*Lum*), and Myostatin (*Mstn*)). Eight genes were located in the intracellular space (Transcription factor NF-E2-related factor 2 (*Nrf2*), Mitogen-Activated Protein Kinase-2 (*MK2*), Serine/threonine kinase (*Akt1*), *Smad3*, Neuronal protein 3.1 (*P311*), Transcription factor proto-oncogene *c-Myb* (*c-Myb*), Peroxiredoxin 6 (*Prdx6*), and 5-Lipoxygenase (*5-LO*)). Three proteins were located in the plasma membrane (Natural resistance-associated macrophage proteins (*Nramp1*), Connexin 43 (*Cx43*), and Inducible Costimulator (*ICOS*)). Other genes expressed proteins located in different regions of the cells, as in the extracellular matrix and intracellular space (basic Fibroblast Growth Factor (*bFGF*), Interleukins (*IL-6* and *IL-10*), Keratinocyte Growth Factor (*KGF*), and *MMP8*), two were located in the intracellular space and plasma membrane (*MMP14* and Inducible Costimulator Ligand (*ICOSL*)), and one alpha-klotho (*α -kl*) was located in the extracellular matrix and plasma membrane, while one Heme Oxygenase 2 (*HO-2*) was present in these three locations (Table 1).

Among the studies, twenty-one (77.8%) corresponds to the depletion of immunoregulatory genes that influence cytokine and growth factor expression. We can highlight *P311* (*TGF- β* and *VEGF*); *TSP*: (*TGF- β* and *VEGF*); *MK2* (*GM-CSF*, *IFN*, *IL-6*, *IL-1 β* , and *TNF*); *ICOS*, and *ICOSL* (*IL-6*, *TNF- α* , Connective Tissue Growth Factor (*CTGF*), *TGF- β* , *PDGF*, *VEGF*, and *IFN- γ*). Six (22.2%) [26, 35, 38, 41, 46, 51] studies analyzed the depletion of cytokines and growth factors; among them, we can point *IL-6*, *IL-10*, *bFGF*, *IFN- γ* , *KGF*, and *GM-CSF*. Although all the studies included in this review have analyzed the depletion of immunoregulatory genes, just 25.9% studies presented clear data on tests performed to verify the absence of the depleted molecules, since some molecules can be produced by other stimuli (Table 1). Some studies evaluated more than one gene depletion (11.1%) [36, 42, 43], and different studies that analyzed the same depletion (14.8%), for example, two studies analyzed the effects of the *TSP2* depletion [36, 37] and two studies analyzed the effects of the *P311* depletion [27, 28].

Thirteen (48.1%) studies were related to gene depletion that influenced the organization and deposition of collagen

fibers; among them, 29.6% of the studies showed a reduction of collagen fibers at the wound site, 14.8% of the studies showed an increase in collagen deposition, and 7.4% presented results similar to wild type (Table 1). Fourteen studies (51.8%) presented clear data on the presence of inflammatory cells in the wound area, being that eight studies presented a reduction, four presented similar results to wild type, and just two presented an increase in these cells. Another mechanism that has been thoroughly analyzed was angiogenesis and vascularization. Six (22.3%) studies presented reduction for these important parameters in the wound healing process, four (14.8%) presented an increase, and two (7.4%) did not present alterations on these markers (Table 1).

Furthermore, some individual study results were somewhat conflicting, for example, *P311* gene depletion, in which one study showed that the depletion of this gene resulted in delayed wound closure, while in the others, the changes were not significant when compared to the wild type. In addition, these results demonstrated that direct gene depletion of immunoregulatory molecules that indirectly control the cytokines and growth factors can influence one specific or several cellular pathways and consequently proinflammatory and anti-inflammatory molecules reflecting a delay or acceleration of the wound healing process (Table 1). Therefore, we observed that the depletion of some genes delays the healing process because it promotes a decrease in cellular activity in the inflammatory, proliferative, and remodeling phases. On the other hand, the gene depletions related to improvements in the repair process are mainly related to the proliferation and remodeling phases of skin repair.

3.5. Main Characteristics and Methodologies Applied in the Investigation of Immunoregulatory Molecules in Wound Healing. All studies selected in this systematic review used wound tissue for cytokines and growth factors evaluation, and the predominant evaluation methods were Enzyme-Linked Immunosorbent Assay (ELISA) (29.6%), followed by Reverse Transcription Polymerase Chain Reaction (RT-PCR) (18.5%) (Table S2). The materials extracted from the wound tissues used for these analyses were RNA (55.5%) and protein (37.0%) (Table S2 and Figure 2).

3.5.1. Cytokines and Growth Factors Analyzed. The gene depletion using exclusively proinflammatory molecules was done in 22.2% of the studies, we can highlight *IL-1 α* , *IL-1 β* , *IL-12*, *IL-18*, *GM-CSF*, Acid Fibroblastic Growth Factor (*aFGF*), Basic Fibroblastic Growth Factor (*bFGF*), Epidermal Growth Factor (*EGF*), *CTGF*, *PDGF*, *VEGF*, *VEGF-A*, *TNF*, *TNF- α* , and *TGF- β 2*. Most of the studies (81.4%) analyzed molecules with both functions (*IL-6*, Angiopoietin (*Ang-2*), *IFN- γ* , *TGF- β* , and *TGF- β 1*). Only four studies (14.8%) analyzed the effect of gene depletion exclusively in anti-inflammatory molecules (*IL-4*, *IL-10*, *Ang-1*, and *TGF- β 3*) (Table 1).

Among the most studied cytokines and growth factors, we can highlight *TGF- β 1* (40.7%), followed by *VEGF* (33.3%), *IL-6* (18.5%), *TNF- α* (18.5%), and *IL-1 β* (14.8%) (Figure 2). These molecules are involved in the different phases of the wound healing process, such as inflammation,

TABLE 1: Main results of the gene depletion on immunoregulatory molecules involved with wound healing of knockout mice compared to the wild type.

References	Gene depletion	Predicted location	WH	Proinflammatory function	Anti-inflammatory function	Both function	Healing mechanisms
Ortega et al. (1998) [35]	<i>bFGF</i>	EC/I	D	∅ bFGF			(D) crust thickness, reepithelization
Lin et al. (2003) [26]	<i>IL-6</i>	EC/I	D	↓IL-1 α , IL-1 β , VEGF		↓TGF- β 1	↓Neutrophil, macrophage, collagen production, angiogenesis = fibrinogen, platelet
Ishida et al. (2004) [41]	<i>IFN-γ</i>	EC	A	= IL-12, IL-18 ↑VEGF		↑TGF- β 1	↓Macrophages ↑angiogenesis, collagen deposition
Guo et al. (1996) [38]	<i>KGF</i>	EC/ I	U	∅ KGF, = aEGF, bFGF, EGF, TNF- α			(U) reepithelization
Fang et al. (2007) [51]	<i>GM-CSF</i>	EC	D			↓IL-6 = level of constitutive expression	↑(D) collagen deposition ↓acute inflammatory response = microvessel number
Yamauchi et al. (2016) [44]	<i>α-kl</i>	EC/M	D	↑IL-1 β , TNF- α		↑IL-6	↓Collagen fibers, formation of the granulation tissue
Thuraisingam et al. (2006) [50]	<i>Nramp1</i>	M	D			↑TGF- β	—
Cogliati et al. (2015) [48]	<i>Cx43</i>	M	A			↑TGF- β 1	= Collagen deposition ↑proliferation and activation of dermal fibroblasts
Braun et al. (2002) [56]	<i>Nrf2</i>	I	U	↓IL-1 β , TNF- α		↓IL-6	(D) EC molecules
Thuraisingam et al. (2010) [49]	<i>MK2</i>	I	D	↓GM-CSF, VEGF, TNF, IL-1 β		↓IL-6, IFN- γ	↓Angiogenesis, collagen deposition = neutrophils and macrophages
Somanath et al. (2008) [40]	<i>Akt1</i>	I	U	↓VEGF			↓Vascularization, collagen fibers, macrophages
Ashcroft et al. (1999) [39]	<i>Smad3</i>	I	A			↓TGF- β 1	(A) reepithelization, ↓fibroblasts, and inflammatory cells
Kopecki et al. (2007) [57]	<i>c-Myb</i>	I	D			↑TGF- β 1	↓Collagen deposition, cell proliferation
Wang et al. (2017) [28]	<i>P311</i>	I	D	↓VEGF		↓TGF- β 1	↓Neangiogenesis, tissue granulation remodeling, neocapillaries, reepithelization, length of the neopeithelium
Cheng et al. (2017) [27]	<i>P311</i>	I	U	↓TGF- β 2	↓TGF- β 3	↓TGF- β 1	↓Collagen deposition, stiffness, and tensile strength in scars
Agah et al. (2002) [36]	<i>TSP1</i> and <i>TSP2</i>	EC	<i>TSP1</i> = D <i>TSP2</i> = A			<i>TSP1</i> = ↓TGF- β 1 <i>TSP2</i> = TGF- β 1	<i>TSP1</i> = ↓collagen fibers, macrophages = vascularization <i>TSP2</i> = ↓organization collagen fibers, matrix metalloproteinase expression ↑neovascularization

TABLE 1: Continued.

References	Gene depletion	Predicted location	WH	Proinflammatory function	Anti-inflammatory function	Both function	Healing mechanisms
MacLauchlan et al. (2009) [37]	<i>TSP2</i>	EC	A	↑VEGF			= Collagen fibers, tensile strength, proliferation, myofibroblast differentiation
Gutiérrez-Fernández et al. (2007) [54]	<i>MMP8</i>	EC/I	D			↓TGF-β1	(D) reepithelization
Hattori et al. (2009) [42]	<i>MMP9</i> and <i>MMP13</i>	EC	<i>MMP9</i> = D <i>MMP13</i> = D	<i>MMP9</i> = ↓intact CTGF <i>MMP13</i> = ↓intact CTGF			(D) reepithelization = infiltration of inflammatory cells
Yeh et al. (2010) [55]	<i>Lum</i>	EC	D			↑TGF-β1 just was at day 6	↑Macrophages, inflammatory cells ↓skin thickness
Zhang et al. (2012) [52]	<i>Mstn</i>	EC	D			↓TGF-β	(D) reepithelization and wound contraction ↓collagen deposition, fibroblast-to-myofibroblast transformation
Zigrino et al. (2012) [47]	<i>MMP14</i>	I/M	D	= VEGF			= Formation of the granulation tissue, epidermal differentiation, formation ↑vascularization
Maeda et al. (2011) [43]	<i>ICOS</i> and <i>ICOSL</i>	<i>ICOS</i> = M <i>ICOSL</i> = I/M	<i>ICOS</i> = D <i>ICOSL</i> = D	↓TNF-α, CTGF = PDGF, VEGF	↓IL-4, IL-10	↓IL-6 = TGF-β, IFN-γ	↓Granulation tissue formation, vascularization, myofibroblasts proliferation, neutrophils, and macrophages infiltration
Kümin et al. (2007) [45]	<i>Prdx6</i>	I	U	= VEGF, IL-1β		= TGF-β1	= Area of hyperproliferative
Lundvig et al. (2014) [53]	<i>HO-2</i>	EC/I/M	D	= TNF	= Ang-1	= Ang-2	↓Collagen deposition
Guimarães et al. (2018) [29]	<i>5-LO</i>	I	A	↓TNF-α	= IL-10	↓TGF-β	↓Inflammatory infiltrate, mast cells, lymphocytes, matrix metalloproteinase expression ↑collagen deposition
Eming et al. (2007) [46]	<i>IL-10</i>	EC/I	A	↑VEGF-A-expressing mononuclear cells			(A) reepithelization ↑angiogenesis, myofibroblast differentiation, macrophages infiltration, collagen deposition ↓breakdown force

EC: extracellular; M: membrane; I: intracellular; WH: wound healing; ↑: increase; ↓: reduction; =: similar; Ø: absence; (D): delayed; (A): accelerated; (U): unchanged; 5-LO: 5-Lipoxygenase; aFGF: acid Fibroblastic Growth Factor; α-kl: alpha-Klotho; (Ang-1, Ang-2): Angiopoietin; bFGF: basic Fibroblastic Growth Factor; CTGF: Connective Tissue Growth Factor; Cx43: Connexin 43; EGF: Epidermal Growth Factor; GM-CSF: Granulocyte-Macrophage Colony-Stimulating Factor; HO-2: Heme Oxygenase 2; ICOS: Inducible Costimulator; ICOSL: Inducible Costimulator Ligand; IFN-γ: Interferon-γ; IL-4, IL-6, IL-10, IL-12, IL-18, IL-1β, IL-1α: interleukins; KGF: Keratinocyte Growth Factor; Lum: Lumican; (MMP8, MMP9, MMP13, MMP14): Matrix Metalloproteinase; MK2: Mitogen-Activated Protein Kinase-2; Mstn: Myostatin; Nrapm: Natural resistance-associated macrophage proteins; P311: Neuronal protein 3.1; Prdx6: Peroxiredoxin 6; PDGF: Platelet-Derived Growth Factor; Akt1: Serine/threonine kinase; (TPS1, TPS2): Thrombospondin; Nr1z: Transcription factor NF-E2-related factor 2; c-Myb: Transcription factor proto-oncogene c-Myb; (TGF-β, TGF-β1, TGF-β2, TGF-β3): Transforming Growth Factor; (TNF, TNF-α): Tumor Necrosis Factor; (VEGF, VEGF-A): Vascular Endothelial Growth Factor.

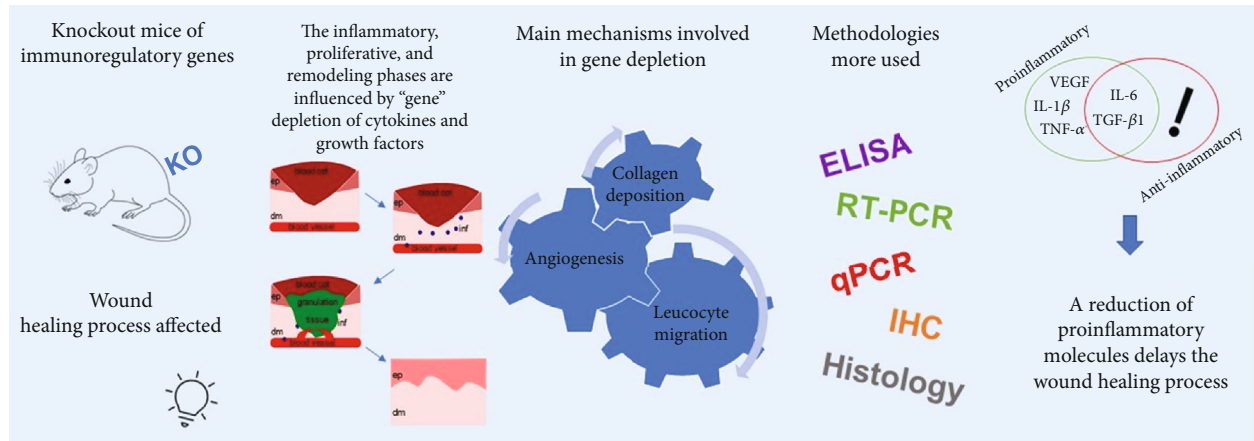


FIGURE 2: A schematic diagram showing the influence of different immunoregulatory genes of knockout mice on the wound healing process, the main phases affected by genetic silencing, and consequently the main mechanisms involved in this process, and the most common techniques used for this type of analysis. KO: Knockout; ELISA: Enzyme-Linked Immunosorbent Assay; RT-PCR: Reverse Transcription Polymerase Chain Reaction; qPCR: Real-Time quantitative Polymerase Chain Reaction; IHC: Immunohistochemistry; TGF- β 1: Transforming Growth Factor beta 1; VEGF: Vascular Endothelial Growth Factor; TNF- α : Tumor Necrosis Factor-alpha; IL-6: Interleukin-6; IL-1 β : Interleukin-1 beta; ep: epidermis; dm: dermis; inf: inflammatory molecules.

cell migration, granulation tissue synthesis, and reorganization and synthesis of the Extracellular Matrix (ECM), and reepithelization. Seven studies (25.92%) showed reductions in these molecules, consequently, a delay in wound closure and a decrease in the wound healing process (Table 1). Another important studied molecule was IFN- γ (11.1%), whose direct depletion promoted an accelerated wound healing, with increased angiogenesis and collagen deposition, but curiously, when IFN- γ was indirectly evaluated as the result of the depletion of other genes, for example, ICOS and ICOSL, the reduction of these molecules contributed to delaying the wound healing process. These findings indicate that the depletion mechanisms are complex, able to interfere with various cytokines and growth factors, and capable of acting on several pathways, and this reflected on the phases of the wound healing process.

Among the anti-inflammatory cytokines studied, we can highlight gene depletion related to IL-10 cytokine (11.1%) [29, 43, 46]. The studies showed that the reduced expression of IL-10 promoted a fast-wound closure and decreased granulation tissue formation and proliferation of the myofibroblasts, neutrophils, and macrophages. However, only one study (3.7%) [46] demonstrated that this cytokine was depleted in the tissue, which increased angiogenesis, high myofibroblast differentiation, macrophage infiltration, and collagen deposition (Table 1), reinforcing the role that anti-inflammatory modulation molecules play on the inflammatory phase during skin wound.

3.6. Other Analyses. In general, studies identified in this review support the evidence that the depletion of immunoregulatory genes did affect the wound healing process. Although all studies have performed histological and quantification of cytokine in the wound tissues, some studies have also performed other techniques, some of which have caught our attention due to the relevance of this process. One study [45] (3.7%) performed oxidative analyses and observed that

the knockout of *Prdx6* left endothelial cells more sensitive to the occurrence of oxidative stress during inflammation resulting in severe hemorrhage in the granulation tissue. Two studies (7.4%) [26, 41] performed Myeloperoxidase (MPO) assay to assess neutrophil infiltration and observed lower MPO activity and neutrophil infiltration in the knockout mice. Four studies (14.8%) [29, 36, 51, 54] performed chemokines analyses and observed the reduction of Monocyte Chemoattractant Protein (MCP-1) and Macrophage Inflammatory Protein (MIP-1 and MIP-2) in the knockout mice. These findings showed that markers of oxidative stress are important tools in evaluating the redox balance of healthy and damaged tissues, mainly in the inflammatory phase, indicating in general, damage in tissue, and a delay in wound closure.

3.7. Risk of Bias and Methodological Quality Assessments. The reporting bias based on SYRCL analysis was detailed in Figures 3 and 4. None of the studies fulfilled all methodological criteria of bias risk (100.0%). The sequence generation process (Q1) was not reported in any of the studies (100.0%). The similarity of animal characteristics to each other (Q2) was not reported clearly in 26 studies (96.3%). The information about allocation concealment (Q3), random housing (Q4), blinding of caregivers (Q5), and random outcome assessment for detection bias (Q6) were not clear in any of the studies (100.0%). Moreover, the outcome assessor was not reported to have been blinded (Q7) in 21 studies (77.7%). Incomplete outcome data (Q8) were shown in 17 studies (62.9%). Nine studies (33.3%) presented a high risk for reporting bias (Q9), and ten studies (37.0%) did not present other potential sources of bias (Q10). Three other quality indicators were used to assess the methodological quality of the studies, just 3.7% of the studies reported the distribution of animals by group and cage (Q11), nine (33.3%) studies presented unclear data about animal conditions (Q12), and 51.8% of studies presented clear data on wound closure

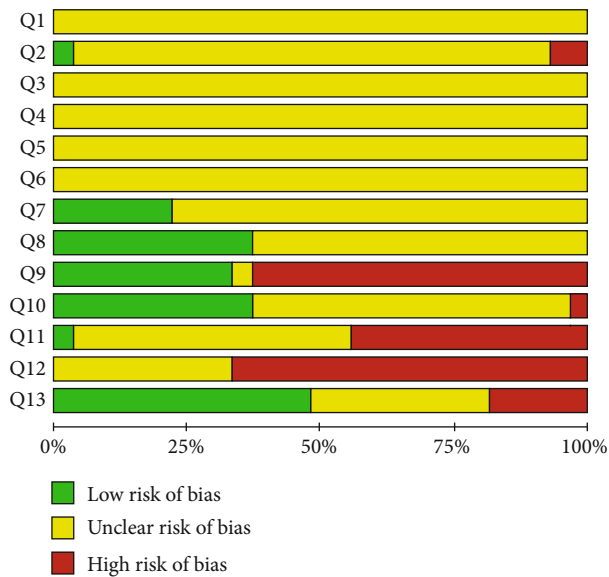


FIGURE 3: Bias risk results and methodological quality indicators for all studies included in this systematic review that evaluated the effect of gene depletion on excisional and incisional wounds. Q1: Was the allocation sequence adequately generated and applied? Q2: Were the groups similar at baseline or were they adjusted for confounders in the analysis? Q3: Was the allocation to the different groups adequately concealed? Q4: Were the animals randomly housed during the experiment? Q5: Were the caregivers and/or investigators blinded from knowledge regarding which intervention each animal received during the experiment? Q6: Were animals selected at random for outcome assessment? Q7: Was the outcome assessor-blinded? Q8: Were incomplete outcome data adequately addressed? Q9: Are reports of the study free of selective outcome reporting? Q10: Was the study free of other problems that could result in a high bias risk? Q11: Was the number of animals per group and number of animals per cage presented? Q12: What conditions were the animals kept in? and Q13: Wound closure data were presented with follow-up days, photos, and graphs?

follow-up (Q13). The results of the ARRIVE analysis show that the most recent studies have better met the methodological quality criteria analyzed (Table S3 and Figure 5). None of the studies fulfilled all methodological criteria, and the mean quality score of all studies reviewed was 46.3 ± 9.1 . No study reported the number of animals per group, blinding and randomization of the experiment, total number of animals, how to choose the sample size and repetitions, complete details of how the animals were allocated to the experimental groups, or the health status of the animals. Most studies presented analysis results carried out with precision measurements (96.3%), data on authorizations for use of animals (85.2%), and statistical analyses (81.5%). The characteristics of the animals that were most mentioned were the age (92.6%) followed by the strain (85.2%). Anesthesia (63.0%) was more addressed among the important items of surgical procedures, and the absence of pathogens (37.0%) was the most mentioned characteristic about accommodation place.

4. Discussion

4.1. General Characteristics of the Studies. In our study, we conducted a systematic review to investigate the direct influence of gene depletion of immunoregulatory molecules in the wound healing process. In addition, we analyzed the methodological quality of the studies that address this theme. We found 27 studies that met all the selection criteria. Optimism in this field has been tempered by some limitations of this animal model usage in wound healing studies; mainly, they required a substantial amount of the resources in terms of time and expense to be developed. This type of research requires laboratories with sufficient technology to identify changes in the cytokines and growth factors profile, and this condition is easily found in economically strong countries. Moreover, there are high costs for acquiring knockout animals since few laboratories are equipped for generating to create their knockouts. These points may justify our findings for the predominance of the studies in countries such as the United States of America, Germany, and Japan. Another interesting result about characteristics in the studies was that the gene depletion of the proinflammatory molecules was preferably analyzed when compared to that of the anti-inflammatory molecules. Probably, this has occurred because there is no consensus about the time-independent and concentration-dependent responses to individual proinflammatory cytokines. Furthermore, proinflammatory molecules are involved in the initial phase of the cutaneous healing process and are important to modulate all phases of this process. Within these phases, we can highlight the following points: hemostasis phase, characterized by the clearing of wound debris by inflammatory cells, and it occurs during the initial response. Granulation tissue formation and angiogenesis start the generation of a new provisional wound matrix. Both extracellular matrix synthesis and its appropriate degradation are necessary, especially during proliferation and remodeling. Therefore, the depletion of these molecules can compromise the whole healing process.

4.2. Animal Characteristics. Mice were the main animal model used for the study of gene depletion on the wound healing process. These results were expected since mice share many genes with humans, and consequently, knockout mice give crucial information that can be used to better understand this disease in humans. Additionally, rats and mice are popular experimental models because of their low cost, availability, and ease of care and handling, allowing researchers to use a relatively large number of animals for their experiments, thereby generating a greater degree of reliability in the results [58–65]. On the other hand, knockout mice also offer a biological context in which drugs and other therapies can be developed and tested [66]. Therefore, knockout mice still offer one of the most powerful means today for studying gene functions in a living animal. About the wound healing process, mice are organisms applied in studies for wound healing because this model allows the histological monitoring of the process [67]. Moreover, this model allows the realization of macroscopic, biochemical, and biomechanical measurements [68]. Despite

	Q1	Q2	Q3	Q4	Q5	Q6	Q7	Q8	Q9	Q10	Q11	Q12	Q13
Agah et al 2002	?	?	?	?	?	?	?	?	-	?	?	-	-
Ashcroft et al 1999	?	?	?	?	?	?	?	?	-	?	-	-	?
Braun et al 2002	?	?	?	?	?	?	?	?	-	?	-	?	-
Cheng et al 2017	?	?	?	?	?	?	?	+	+	?	-	?	?
Cogliati et al 2015	?	+	?	?	?	?	?	+	+	?	-	?	+
Eming et al 2007	?	?	?	?	?	?	+	+	+	+	?	?	?
Fang et al 2007	?	?	?	?	?	?	+	+	+	+	?	?	+
Guimarães et al 2018	?	?	?	?	?	?	?	+	+	+	?	?	+
Guo et al 1996	?	-	?	?	?	?	?	?	-	?	-	-	-
Gutiérrez-Fernández et al 2007	?	?	?	?	?	?	?	?	-	+	-	-	?
Hattori et al 2009	?	?	?	?	?	?	?	?	-	?	+	-	+
Ishida et al 2004	?	?	?	?	?	?	?	?	-	+	?	-	+
Kopecki et al 2007	?	?	?	?	?	?	?	+	?	-	?	-	?
Kümin et al 2007	?	-	?	?	?	?	?	?	-	?	?	?	-
Lin et al 2003	?	?	?	?	?	?	?	?	-	+	-	?	?
Lundvig et al 2014	?	?	?	?	?	?	+	?	-	+	?	?	?
MacLauchlan et al 2009	?	?	?	?	?	?	+	+	+	?	-	-	-
Maeda et al 2011	?	?	?	?	?	?	?	?	-	+	?	-	+
Ortega et al 1998	?	?	?	?	?	?	?	?	-	?	?	-	+
Somanath et al 2008	?	?	?	?	?	?	?	?	-	?	?	-	?
Thuraisingam et al 2006	?	?	?	?	?	?	+	?	-	+	-	-	+
Thuraisingam et al 2010	?	?	?	?	?	?	+	?	-	+	?	-	+
Wang et al 2017	?	?	?	?	?	?	?	+	+	?	?	-	+
Yamauchi et al 2016	?	?	?	?	?	?	?	+	+	?	-	-	+
Yeh et al 2010	?	?	?	?	?	?	?	+	+	?	?	-	+
Zhang et al 2012	?	?	?	?	?	?	?	?	-	?	-	-	+
Zigrino et al 2012	?	?	?	?	?	?	?	?	-	?	-	-	?

FIGURE 4: Risk of bias summary: review authors’ judgments about the risk of bias items for each included study. Green: low risk of bias; Yellow: unclear risk of bias; and Red: high risk of bias.

the advantages of mice models, there are also some negative points to the use of this animal model, such as skin characteristics. Rodents are loose-skinned animals with a panniculus carnosus layer and lack well-developed deep attachments to the skin compromising the study of important phases of the wound healing process, like granulation tissue formation and reepithelization. However, the positive points outweigh the negative ones for this model because mice, rats, and humans exhibit the same stages of wound healing, with immunoinflammatory and microstructural convergences,

based mainly on similar profiles of regulatory molecules (i.e., cytokines and growth factors) and composition of extracellular matrix (i.e., glycosaminoglycan’s, collagen, and noncollagen proteins).

Most studies founded in this review did not provide sufficient information on methodology development. For example, most of the studies did not present data regarding the sex of the animals although this is a very important piece of information since studies using females are subject to more variation due to their hormonal changes [67]. Another

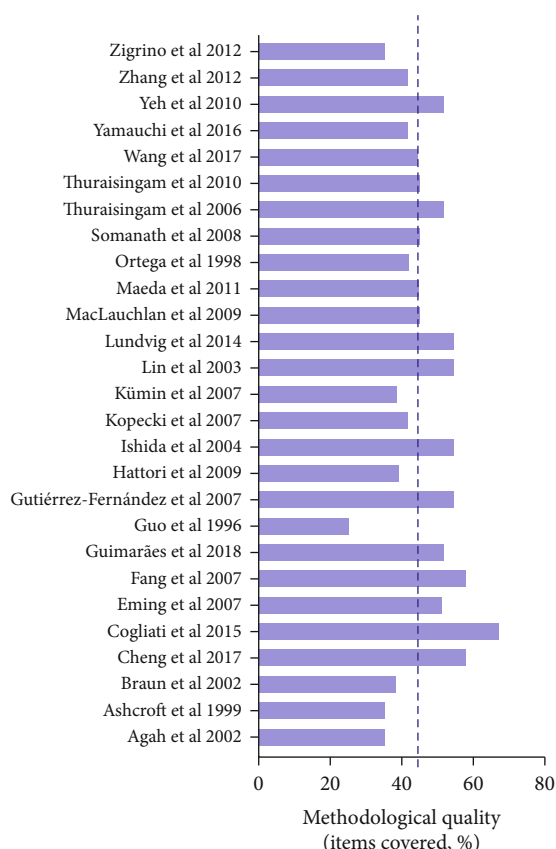


FIGURE 5: Analysis of methodological bias (reporting quality) for each study included in the review. Based on Animal Research: Reporting of In Vivo Experiments (ARRIVE) guidelines (<http://www.nc3rs.org.uk/arrive-guidelines>). The dotted line indicated the mean quality score (%). Detailed bias analysis stratified by domains and items evaluated is presented in Table S3.

interesting point is related to age, although some variations were reported, the experiments used animals within similar age ranges; this is an important feature of the studies that evaluate wound healing because the aging of mice influences wound closure, reepithelization, and filling of granulation tissue [69]. Surprisingly, only six studies mention that the mice were housed individually in cages. This is an important point because when placed in individual cages, there is no interference from the saliva of other animals in the wound closure process, and also, there is a reduction of injury risk and aggravation of the wound under analysis [67]. As shown, the lack of information about animals and their care, or even the neglect of certain characteristics of the experimental design, can compromise the results, thus increasing the bias of the studies, and consequently, reducing the reliability of the results found.

4.3. Wound Healing Characteristics. Considering the characteristics of the wound, most studies used an excisional wound, a model that generally presents high precision and few variations for wound healing evaluation, so in general, this model is efficient in comparing wild type and genetically modified animals [70]. Besides that, another important parameter that must be analyzed is the spatial position of

the wounds because the choice of the proper location allows minimizing differences and interferences, mainly about tensile strength and skin tissue resistance [67]. In our revision, all studies made dorsal wounds on the mice. Probably, this location was chosen because, in this location, the mice cannot lick the lesion area, which could interfere with the reliability of the results, since it has been confirmed that licking behavior can promote wound healing because the salivary gland is a reservoir for many growth factors in rodents [71]. Furthermore, the dorso is an appropriate area to perform a biopsy because it is easy to manipulate and allows obtaining of a sufficient quantity of tissues to study the contraction index of wound and reepithelization rates, and consequently, total tissue repair [72].

Among the surgical instruments used to perform skin excision biopsies, the punch was the most used, possibly due to this instrument presenting defined measures, and thus, ensuring that all wounds are the same size. As mentioned earlier, the evaluation periods of the wound healing process were different for excision and incision models, this must-have occurred because the models have distinct characteristics. Incision wounds heal by primary intention, and excision wounds heal by second intention [73]. Moreover, we observed that the biopsy collections for histological analysis and immunoregulatory molecules did not performed daily to accompany the wound healing process. This probably occurred because performing biopsies every day may be impracticable due to a large number of animals and to the fact that the wound healing phases occur in several phases for several days. Although the repair phases are not mutually exclusive but overlapped over time. It is possible to estimate the days for each phase. Approximately, the inflammatory phase will occur from day 1 to day 3, the proliferative phase from day 2 to day 14, and the remodeling phase would start on day 13 [74]. Based on this, the researchers can select the best moments to perform the analyses to attend all phases of the wound repair, since the moment of the analyses are critical and must include clear information not only for macroscopic closure but also for histological analysis and immunoregulatory molecules.

4.4. Analysis of Cytokines and Growth Factors in Skin Wound Healing Process. Cytokines and growth factors are considered biomarkers that make it possible to understand the progression of repair processes because, in high concentrations, they indicate activation of inflammation and proliferation-related pathways, which is very important for the wound healing process [75, 76]. Currently, several tests allow measuring the concentration of cytokines and growth factors, being ELISA tests and PCR technologies widely used. However, ELISA has limitations as it does not provide information on the biological potency of the detected proteins and fails to provide information to indicate the identities and frequencies of the individual cytokine and growth factor producing cells [77]. Whereas the RT-PCR, which was the most used PCR type in the studies found in this review, use the specific mRNA expression of the molecule evaluated for the analysis of cytokines for the minimum amount of molecules released by cells [78]. This allows the quantitative comparison of these

molecules in different targets [79]. This test is widely used for this type of analysis, and its execution is considered as quick and easy, although its results may differ from those found by the ELISA test and do not provide exact information on the concentration of cytokines [78]. Thus, it is necessary that when performing the analysis of cytokines, the person in charge evaluates the available methodologies and chooses the one that meets their demands with a greater degree of sensitivity to obtain reliable data.

The important role that cytokines and growth factors play in the wound healing process is already known. However, this systematic review is the first to investigate and compare the most studied cytokines and growth factors as well as their behavior in different pathways. Our findings showed that the depletion of the most studied immunoregulatory genes was TGF- β 1 followed by VEGF. TGF- β 1 has important functions in the wound healing process mainly in the regulation of inflammation and also in the accumulation of collagen and resistance of ECM [80]. Additionally, VEGF has played an important role during the skin repair process, as it stimulates angiogenesis, which is essential for the transport of oxygen and nutrients to the wound site. It influences the recruitment of inflammatory cells, granulation tissue formation, fibroblasts proliferation, and remodeling tissue [81]. Overall, the depletion of these genes negatively influenced the production of other proinflammatory cytokines and consequently promoted the decrease of inflammatory cell infiltration, angiogenesis, and collagen deposition. These genes are important in the regulation of keratinocytes and fibroblasts proliferation and consequently on the recovery of the skin tissue which justifies the fact that most studies evaluated the action of these molecules in the cutaneous lesions. Interestingly, there were conflicting results when other genes were analyzed, for example, our findings indicated that the reduction or silencing of proinflammatory cytokines and growth factors like GM-CSF, bFGF, and IL-1 β showed a negative impact on the skin repair process. These findings corroborate with previous evidence that GM-CSF influences important phases of the repair process because it promotes neovascularization and collagen deposition and contributes to the composition of the vascular collagenous matrix [81], and consequently, represents important markers to understand the main proinflammatory mechanisms involved in the wound healing process.

Other constantly studied molecules were the interleukins, and the signaling pathway IL-1 β cytokine was one of the most frequently analyzed in studies, and its action is related to the activation of the pathway of NF- κ B and Mitogen-activated protein kinases (MAPK) [82–84]. Both survival and proliferation pathways promote the activation of Toll-like receptors, which contribute to the activation and regulation of the immune response [85]. The NF- κ B corresponds to a family of inducible transcription factors, which regulates genes involved in the immune and inflammatory responses [86]. It induces the expression of various proinflammatory genes, like cytokines, and regulates the survival, activation, and differentiation of inflammatory and innate immune cells [87]. The MK2 is a serine/threonine kinase of the p38 MAPK pathway, and it was a genic depletion studied in this review.

This depletion resulted in delayed wound healing, a decrease of angiogenesis, and collagen deposition. This probably occurs because the MK2 phosphorylation is important for cell cycle regulation, acting on remodeling, cell development and migration, and cytokine production [88–91], and in their absence, these processes can be affected. The IFN- γ is an important cytokine in the activation of pathways involved with the cell cycle; interestingly, this depletion promoted accelerated wound healing. The interferon family is divided into three types of IFN, with IFN- γ being a cytokine involved in the adaptive immune response. These cytokines have been playing a key role in the activation of proinflammatory macrophages [92, 93] and act with anti-inflammatory function modulating proinflammatory cytokines and apoptosis [94].

In our review, the lack of studies and analyses performed with cytokines and growth factors exclusively anti-inflammatory functions was evident, and this calls into question the accuracy of the presentation of the effect of these molecules in the wound healing process. However, gene depletion of IL-10 showed beneficial effects for the repair process with increased epithelization, macrophages infiltration, angiogenesis, collagen production, and myofibroblasts differentiation. Besides, the depletion of these cytokines stimulated the expression of other cytokines such as VEGF-A, important for skin wound healing. In addition, IL-10 acts as balancing cellular signaling by inhibiting proinflammatory cytokines, inhibiting the antigen presentation by dendritic cells, or inhibiting macrophage activation and infiltration into the site of the wound [95]. Another interesting point was that few studies in this review have evaluated cytokine isoforms and growth factors such as three isoforms of TGF- β (TGF- β 1, TGF- β 2, and TGF- β 3) [27], isoform VEGF-A [46], and isoforms Ang-1 and Ang-2 [53]. However, the study of different isoform assessment whenever possible is important because these may be antagonistic to each other, have different functions, and applications in the wound healing process. Based on these findings, we see the importance of evaluating cytokines and growth factors, including their isoforms, since they have important functions for each phase of the wound healing process and act in different pathways in the entire process.

4.5. Other Analyses. Analyses of oxidative stress are very relevant when we study the wound closure process because inflammation occurs in skin lesions, thus macrophages produce free radicals through the respiratory burst process, such as Reactive Oxygen Species (ROS) that promote changes in lipids, proteins, and cellular DNA impairing cellular longevity [96, 97]. As mentioned previously, in some studies, we found the oxidative analysis of wound tissues and analyses associated with free radicals in these same tissues; however, in some cases, the participation of the molecules analyzed in the oxidative processes is not clear. The MPO is an enzyme that catalyzes the formation of ROS because it reacts with hydrogen peroxide forming free radicals, which results in oxidative damage to the tissue in case of imbalance with antioxidant enzymes [98–100]. While MCP-1, MIP-1, and MIP-2 are chemokines related to inflammation. MCP-1 in high concentrations generates respiratory explosion and

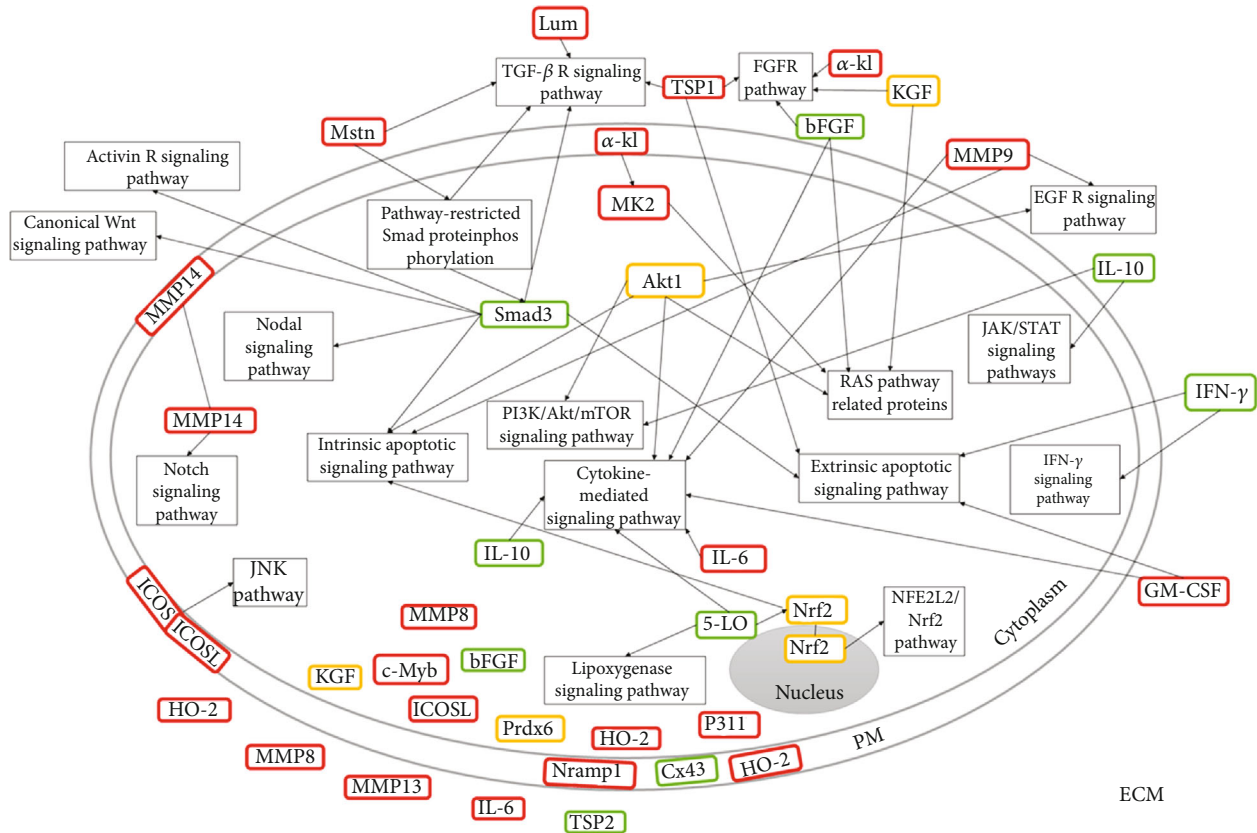


FIGURE 6: Location of the molecules of depleted genes addressed in this review and their participation in metabolic pathways involved in the wound repair. The effect of depleted genes on wound closure was shown by the colors: red (delayed), green (accelerated), and yellow (unchanged). PM: plasma membrane; ECM: extracellular matrix; 5-LO: 5-Lipoxygenase; α -kl: alpha-Klotho; bFGF: basic Fibroblastic Growth Factor; Cx43: Connexin 43; GM-CSF: Granulocyte-Macrophage Colony-Stimulating Factor; HO-2: Heme Oxygenase 2; ICOS: Inducible Costimulator; ICOSL: Inducible Costimulator Ligand; IFN- γ : Interferon-gamma; (IL-10, IL-6): Interleukins; KGF: Keratinocyte Growth Factor; Lum: Lumican; (MMP8, MMP9, MMP13, MMP14): Matrix Metalloproteinase; MK2: Mitogen-Activated Protein Kinase-2; Mstn: Myostatin; Nramp: Natural resistance-associated macrophage proteins; P311: Neuronal protein 3.1; Prdx6: Peroxiredoxin 6; Akt1: Serine/threonine kinase; (TPS1, TPS2): Thrombospondin; Nrf2: Transcription factor NF-E2-related factor 2; c-Myb: Transcription factor proto-oncogene c-Myb. Signaling pathways: Activin R: Activin Receptor; FGF R: Fibroblast Growth Factor Receptor; EGF R: Epidermal Growth Factor Receptor; TGF- β R: Transforming Growth Factor- β Receptor; NFE2L2/Nrf2: Nuclear Factor, Erythroid 2 Like 2; JNK: c-Jun N-terminal kinase; IFN- γ : Interferon-gamma; JAK/STAT: Janus Kinase Signal Transducer and Activator of Transcription.

consequently the release of ROS [101]. MIP-1 and MIP-2 are produced by various inflammatory cells, recruit and activate neutrophils [102], and these produce ROS which under normal conditions, eliminate damaged tissue, but in excess cause tissue injuries [103].

As seen, there are several possibilities to estimate the occurrence of oxidizing activity in tissues, and these analyses are extremely important to rule out factors that interfere with the wound healing process, as it is known that the excessive production of ROS impairs healing [97].

4.6. *Synthesis of the Mechanistic Theory of Studies.* Although all studies have analyzed the influence of the depletion of immunoregulatory genes on the wound healing process, not all of them make clear the main mechanisms involved in this process after specific gene depletions, even though this information is important to justify the analysis. In addition, it is important to consider that the depletion of a gene can generate a chain reaction and impair the entire repair metabolic

process [52]. However, our findings showed that there were three points based on the location of the corresponding protein that directly interferes in the wound healing process, which are (1) extracellular molecules; (2) intracellular molecules; and (3) membrane molecules. Although all molecular locations have distinct and important functions in cellular processes, we can see that extracellular molecules act more negatively in skin wound healing when silenced (Figure 6), probably because they act as signals for several important metabolic pathways. In addition, some molecules that have different locations may do different functions depending on their location and not participate in repair-related metabolic pathways, for example, bFGF in the extracellular space acts on metabolic pathways that result in cell proliferation, migration, differentiation, and apoptosis, while in the intracellular environment, this molecule acts on antiviral immunity [104].

As the studies are quite heterogeneous and the type of gene depletions is different in most of the studies, it has been difficult to determine the real impact of depletion

of immunoregulatory genes on wound healing. However, we observed that extracellular molecules act more negatively in the wound healing process when silenced, and the TGF- β family of growth factors has been addressed frequently in studies and mechanistic theories, which suggests that this molecule is very important for the wound healing process, mainly due to its participation in the TGF- β /Smad pathway that has so many other linked metabolic pathways. TGF- β /Smad signaling pathway is involved in the regulation of proliferation, differentiation, and survival or apoptosis of many cells. In addition, Smads are phosphoproteins, which when phosphorylated start signaling the TGF- β family, which results in a cascade of protein-protein and protein-DNA interactions [105]. Macrophages and TGF- β 1 were frequently mentioned in explaining these processes, this is probably because macrophages play an important role in the repair process, since they act by secreting growth factors like TGF- β and inflammatory mediators important for collagen deposition, wound contraction, and angiogenesis, while TGF- β 1 performs functions at all phases of the repair process, is essential for regulating collagen deposition [106], and can stimulate VEGF transcription in various cells [80, 107]. In addition, there are reports of changes in TGF- β levels of different forms, either by kidnapping by competition for the receptor or by sequestering TGF- β by other molecules, as Decorin [108].

Although the other metabolic pathways were less affected (Figure 6), they are also important for the occurrence of the repair process and can act in several biological processes, such as inflammation, proliferation, remodeling, growth and cell differentiation, on the immune system, and tissue repair [109–112]. We also found molecules related to pathways that result in apoptosis, such as extrinsic and intrinsic apoptotic signaling pathways. The activation of these pathways results in a cascade of proteases, the caspases, resulting in cell death [113] and acts in removing unwanted cells [114]. In addition to the pathways that act directly on the wound healing process, we had depleted genes that are involved in pathways related to ROS, such as 5-LO in Lipoxygenase signaling pathway and Nrf2 in Nuclear factor, erythroid 2 like 2 (NFE2L2/Nrf2) signaling pathway. Even 5-LO can activate Nrf2 which has a cytoprotective effect [115, 116]. Some molecules, such as matrix metalloproteinases, were not linked to metabolic pathways involved in the wound healing process, but they play an extremely important role in this process, their silencing results in prolonged inflammation and delayed wound closure.

5. Methodological Quality of the Animal Studies

Genetic advancements in recent years have made mouse models of human disease processes increasingly popular considering their numerous other advantages. However, no systematic review has been reported to investigate the impact of depletion of immunoregulatory genes on wound healing. The main strength of this study is its novelty and the applied findings that can be useful to provide a direction for future studies in this field and the development of decision-making for therapeutic alternatives. Also, the metabolic network descrip-

tion of this study may help to understand the main mechanisms involved in the alterations triggered by gene depletion and, consequently, the translation to the human health assessment. Therefore, systematic reviews are essential tools for summarizing evidence accurately and reliably, assisting risk assessment, and providing evidence of the benefits of health-related interventions [117].

This review also has some limitations. The bias analysis demonstrated that fundamental characteristics, such as random sequence generation or random outcome assessment and blinding of participants (caregivers and outcome assessor), were not reported in the studies. In addition, some records provided incomplete outcome data and insufficient information, which affect the accuracy of the results. Overall, the evidence of the individual studies showed wide heterogeneity and so it was not possible to compare the data statistically. This kind of comparison should be avoided because it generates evidence that presupposes an apparent external validity (generalizability), which is not supported by the available data set. In this sense, we identified that each study presented marked differences regarding the experimental model and methods of data collection, analysis, and interpretation, as well as biopsy procedures, wound monitoring, evaluation of immunoregulatory molecules, and mechanisms involved in the healing process contributing to the increased risk of bias. In individual studies, each element of methodological bias is associated with some degree of variability in the research outcomes, with a direct impact on the quality of evidence. However, it is important to emphasize that all types of reviews have limitations, and these limitations are more evident in systematic review studies once flaws in methodological and incomplete reports can produce inaccurate and unreliable conclusions. In our case, the major limitation was the heterogeneity of the studies, which makes it an arduous task to compare them. Therefore, considering these analytical limitations, we developed a systematic review admitting its intrinsic qualitative nature by describing important points of bias, and we hope to contribute to future studies on avoiding those elements of bias that impair the quality of evidence.

6. Conclusion

Despite these limitations, our results support that is very important to evaluate and understand the role of cytokines and growth factors during the wound healing process, once these molecules have specific and important functions for each phase of the process acting in different pathways. In our review, we observed that extracellular molecules act more negatively in the wound healing process when silenced compared to intracellular and membrane molecules and the metabolic pathway more studied in the cutaneous process was TGF- β /Smad, and emphasis was given to the importance of the participation of macrophages in TGF- β signaling. In addition, the main molecules studied in knockout models in the healing process were the inflammatory cytokines and growth factors TGF- β 1, VEGF, IL-6, TNF- α , and IL-1 β and, consequently, the most investigated wound healing mechanisms were inflammation, angiogenesis, and

consequently granulation tissue formation and collagen deposition. Besides that, some studies do not mention the participation of the molecules of gene depletion in metabolic pathways, which hinders the understanding of their role in wound healing mechanism. By using the right methodologies with the minimum risk of bias, we will be closer to finding specific biomarkers for wound healing. Overall, our findings provide new insights into the mechanisms of gene depletion in the wound healing process. However, the fragility of the current studies was evident, given that the majority presented unclear results, which can prevent the reproducibility of most of the studies considered in this review.

Data Availability

The data can be made available upon request through the email: barbaracfn28@gmail.com.

Conflicts of Interest

The authors declare that there are no conflicts of interest.

Acknowledgments

The authors are grateful to the support provided by Fundação do Amparo à Pesquisa do Estado de Minas Gerais (FAPEMIG, processes APQ-01895-16, PPM-00687-17, and PPM-00077-18), Conselho Nacional de Desenvolvimento Científico e Tecnológico (CNPq, processes 303972/2017-3, 423594/2018-4, 305093/2017-7, and MCTIC 408503/2018-1), and Coordenação de Aperfeiçoamento de Pessoal de Nível Superior - Brazil (CAPES, finance code 001).

Supplementary Materials

Table S1: complete search strategy with search filters and the number of studies recovered in databases PubMed-Medline, Scopus, and Web of Science. Table S2: description of the main characteristics of studies of this systematic review that evaluated the effect of gene depletion on excision and incision wounds. Table S3: analysis of methodological bias of the studies founded in this systematic review that evaluated the effect of gene depletion on excision and incision wounds. (*Supplementary Materials*)

References

- [1] C. K. Sen, G. M. Gordillo, S. Roy et al., "Human skin wounds: a major and snowballing threat to public health and the economy," *Wound Repair and Regeneration*, vol. 17, no. 6, pp. 763–771, 2009.
- [2] A. Hingorani, G. M. LaMuraglia, P. Henke et al., "The management of diabetic foot: a clinical practice guideline by the Society for Vascular Surgery in collaboration with the American Podiatric Medical Association and the Society for Vascular Medicine," *Journal of Vascular Surgery*, vol. 63, no. 2, pp. 3S–21S, 2016.
- [3] B. Peter-Riesch, *The diabetic foot: the never-ending challenge* Novelties in Diabetes.
- [4] N. C. Schaper, J. J. Van Netten, J. Apelqvist, B. A. Lipsky, and K. Bakker, "Prevention and management of foot problems in diabetes: a Summary Guidance for Daily Practice 2015, based on the IWGDF Guidance Documents," *Diabetes/Metabolism Research and Reviews*, vol. 32, pp. 7–15, 2016.
- [5] S. Newbern, "Identifying pain and effects on quality of life from chronic wounds secondary to lower-extremity vascular disease," *Advances in Skin & Wound Care*, vol. 31, no. 3, pp. 102–108, 2018.
- [6] A. Oryan, A. Mohammadalipour, A. Moshiri, and M. R. Tabandeh, "Topical application of aloe vera accelerated wound healing, modeling, and remodeling," *Annals of Plastic Surgery*, vol. 77, no. 1, pp. 37–46, 2016.
- [7] N. Jabbari, G. H. Farjah, B. Ghadimi, H. Zanjani, and B. Heshmatian, "Acceleration of skin wound healing by low-dose indirect ionizing radiation in male rats," *The Kaohsiung Journal of Medical Sciences*, vol. 33, no. 8, pp. 385–393, 2017.
- [8] L. Marrot, "Pollution and sun exposure: a deleterious synergy. mechanisms and opportunities for skin protection," *Current Medicinal Chemistry*, vol. 25, pp. 5469–5486, 2019.
- [9] L. E. Lindley, O. Stojadinovic, I. Pastar, and M. Tomic-Canic, "Biology and biomarkers for wound healing," *Plastic and Reconstructive Surgery*, vol. 138, 3 Suppl, pp. 18S–28S, 2016.
- [10] I. Pastar, O. Stojadinovic, N. C. Yin et al., "Epithelialization in wound healing: a comprehensive review," *Advances in Wound Care*, vol. 3, no. 7, pp. 445–464, 2014.
- [11] P. Rousselle, F. Braye, and G. Dayan, "Re-epithelialization of adult skin wounds: cellular mechanisms and therapeutic strategies," *Advanced Drug Delivery Reviews*, vol. 146, pp. 344–365, 2019.
- [12] P. A. M. Everts, J. T. A. Knape, G. Weibrich et al., "Platelet-rich plasma and platelet gel: a review," *The Journal of extracorporeal technology*, vol. 38, no. 2, pp. 174–187, 2006.
- [13] G. Ed Rainger, M. Chimen, M. J. Harrison et al., "The role of platelets in the recruitment of leukocytes during vascular disease," *Platelets*, vol. 26, no. 6, pp. 507–520, 2015.
- [14] G. Arango Duque and A. Descoteaux, "Macrophage cytokines: involvement in immunity and infectious diseases," *Frontiers in Immunology*, vol. 5, 2014.
- [15] G. Y. Seo, Y. Lim, D. Koh et al., "TMF and glycerin act synergistically on keratinocytes and fibroblasts to promote wound healing and anti-scarring activity," *Experimental & Molecular Medicine*, vol. 49, no. 3, pp. e302–e302, 2017.
- [16] S. Barrientos, O. Stojadinovic, M. S. Golinko, H. Brem, and M. Tomic-Canic, "PERSPECTIVE ARTICLE: Growth factors and cytokines in wound healing," *Wound Repair and Regeneration*, vol. 16, no. 5, pp. 585–601, 2008.
- [17] Y. W. Kwon, S. C. Heo, G. O. Jeong et al., "Tumor necrosis factor- α -activated mesenchymal stem cells promote endothelial progenitor cell homing and angiogenesis," *Biochimica et Biophysica Acta (BBA) - Molecular Basis of Disease*, vol. 1832, no. 12, pp. 2136–2144, 2013.
- [18] P. Baluk, L.-C. Yao, J. Feng et al., "TNF- α drives remodeling of blood vessels and lymphatics in sustained airway inflammation in mice," *The Journal of Clinical Investigation*, 2009.
- [19] A. Desmoulière, A. Geinoz, F. Gabbiani, and G. Gabbiani, "Transforming growth factor-beta 1 induces alpha-smooth muscle actin expression in granulation tissue myofibroblasts and in quiescent and growing cultured fibroblasts," *The Journal of Cell Biology*, vol. 122, no. 1, pp. 103–111, 1993.

- [20] L. Ronnov-Jessen and O. W. Petersen, "Induction of alpha-smooth muscle actin by transforming growth factor-beta 1 in quiescent human breast gland fibroblasts. Implications for myofibroblast generation in breast neoplasia," *Laboratory Investigation*, vol. 68, no. 6, pp. 696–707, 1993.
- [21] R. Hosokawa, K. Nonaka, M. Morifuji, L. Shum, and M. Ohishi, "TGF- β 3 decreases type I collagen and scarring after labioplasty," *Journal of Dental Research*, vol. 82, pp. 558–564, 2016.
- [22] M. A. Nosenko, S. G. Ambaryan, and M. S. Drutskaya, "Pro-inflammatory cytokines and skin wound healing in mice," *Molecular Biology*, vol. 53, no. 5, pp. 653–664, 2019.
- [23] S. Rose-John, "IL-6 trans-signaling via the soluble IL-6 receptor: importance for the pro-inflammatory activities of IL-6," *International Journal of Biological Sciences*, vol. 8, no. 9, pp. 1237–1247, 2012.
- [24] J.-M. Zhang and J. An, "Cytokines, inflammation, and pain," *International Anesthesiology Clinics*, vol. 45, no. 2, pp. 27–37, 2007.
- [25] P. Martin, "Wound healing—aiming for perfect skin regeneration," *Science*, vol. 276, no. 5309, pp. 75–81, 1997.
- [26] Z.-Q. Lin, T. Kondo, Y. Ishida, T. Takayasu, and N. Mukaida, "Essential involvement of IL-6 in the skin wound-healing process as evidenced by delayed wound healing in IL-6-deficient mice," *Journal of Leukocyte Biology*, vol. 73, no. 6, pp. 713–721, 2003.
- [27] T. Cheng, M. Yue, M. N. Aslam et al., "Neuronal protein 3.1 deficiency leads to reduced cutaneous scar collagen deposition and tensile strength due to impaired transforming growth factor- β 1 to - β 3 translation," *The American Journal of Pathology*, vol. 187, pp. 292–303, 2017.
- [28] S. Wang, X. Zhang, W. Qian et al., "P311 deficiency leads to attenuated angiogenesis in cutaneous wound healing," *Frontiers in Physiology*, vol. 8, 2017.
- [29] F. R. Guimarães, H. Sales-Campos, V. Nardini et al., "The inhibition of 5-lipoxygenase (5-LO) products leukotriene B₄ (LTB₄) and cysteinyl leukotrienes (cysLTs) modulates the inflammatory response and improves cutaneous wound healing," *Clinical Immunology*, vol. 190, pp. 74–83, 2018.
- [30] M. J. Kluger, W. Kozak, L. R. Leon, and C. A. Conn, "The use of knockout mice to understand the role of cytokines in fever," *Clinical and Experimental Pharmacology & Physiology*, vol. 25, no. 2, pp. 141–144, 1998.
- [31] D. Moher, A. Liberati, J. Tetzlaff, and D. G. Altman, "Preferred reporting items for systematic reviews and meta-analyses: the PRISMA statement," *PLoS Medicine*, vol. 6, no. 7, article e1000097, 2009.
- [32] C. R. Hooijmans, M. M. Rovers, R. B. de Vries, M. Leenaars, M. Ritskes-Hoitinga, and M. W. Langendam, "SYRCLE's risk of bias tool for animal studies," *BMC Medical Research Methodology*, vol. 14, pp. 1471–2288, 2014.
- [33] C. Kilkenny, W. J. Browne, I. C. Cuthill, M. Emerson, and D. G. Altman, "Improving bioscience research reporting: the ARRIVE guidelines for reporting animal research," *PLoS Biology*, vol. 8, no. 6, 2010.
- [34] R. M. Pereira, G. M. Z. Greco, A. M. Moreira et al., "Applicability of plant-based products in the treatment of *Trypanosoma cruzi* and *Trypanosoma brucei* infections: a systematic review of preclinical in vivo evidence," *Parasitology*, vol. 144, no. 10, pp. 1275–1287, 2017.
- [35] S. Ortega, M. Ittmann, S. H. Tsang, M. Ehrlich, and C. Basilico, "Neuronal defects and delayed wound healing in mice lacking fibroblast growth factor 2," *Proceedings of the National Academy of Sciences*, vol. 95, no. 10, pp. 5672–5677, 1998.
- [36] A. Agah, T. R. Kyriakides, J. Lawler, and P. Bornstein, "The lack of thrombospondin-1 (TSP1) dictates the course of wound healing in double-TSP1/TSP2-null mice," *The American Journal of Pathology*, vol. 161, no. 3, pp. 831–839, 2002.
- [37] S. MacLauchlan, E. A. Skokos, A. Agah et al., "Enhanced angiogenesis and reduced contraction in thrombospondin-2-null wounds is associated with increased levels of matrix metalloproteinases-2 and -9, and soluble VEGF," *The Journal of Histochemistry and Cytochemistry*, vol. 57, no. 4, pp. 301–313, 2008.
- [38] L. Guo, L. Degenstein, and E. Fuchs, "Keratinocyte growth factor is required for hair development but not for wound healing," *Genes & Development*, vol. 10, no. 2, pp. 165–175, 1996.
- [39] G. S. Ashcroft, X. Yang, A. B. Glick et al., "Mice lacking Smad3 show accelerated wound healing and an impaired local inflammatory response," *Nature Cell Biology*, vol. 1, no. 5, pp. 260–266, 1999.
- [40] P. R. Somanath, J. Chen, and T. V. Byzova, "Akt1 is necessary for the vascular maturation and angiogenesis during cutaneous wound healing," *Angiogenesis*, vol. 11, no. 3, pp. 277–288, 2008.
- [41] Y. Ishida, T. Kondo, T. Takayasu, Y. Iwakura, and N. Mukaida, "The essential involvement of cross-talk between IFN- γ and TGF- β in the skin wound-healing process," *Journal of Immunology*, vol. 172, no. 3, pp. 1848–1855, 2004.
- [42] N. Hattori, S. Mochizuki, K. Kishi et al., "MMP-13 plays a role in keratinocyte migration, angiogenesis, and contraction in mouse skin wound healing," *The American Journal of Pathology*, vol. 175, no. 2, pp. 533–546, 2009.
- [43] S. Maeda, M. Fujimoto, T. Matsushita, Y. Hamaguchi, K. Takehara, and M. Hasegawa, "Inducible costimulator (ICOS) and ICOS ligand signaling has pivotal roles in skin wound healing via cytokine production," *The American Journal of Pathology*, vol. 179, no. 5, pp. 2360–2369, 2011.
- [44] M. Yamauchi, Y. Hirohashi, T. Torigoe et al., "Wound healing delays in α -Klotho-deficient mice that have skin appearance similar to that in aged humans – study of delayed wound healing mechanism," *Biochemical and Biophysical Research Communications*, vol. 473, no. 4, pp. 845–852, 2016.
- [45] A. Kümin, M. Schäfer, N. Epp et al., "Peroxiredoxin 6 is required for blood vessel integrity in wounded skin," *The Journal of Cell Biology*, vol. 179, no. 4, pp. 747–760, 2007.
- [46] S. A. Eming, S. Werner, P. Bugnon et al., "Accelerated wound closure in mice deficient for interleukin-10," *The American Journal of Pathology*, vol. 170, no. 1, pp. 188–202, 2007.
- [47] P. Zigrino, O. Ayachi, A. Schild et al., "Loss of epidermal MMP-14 expression interferes with angiogenesis but not with re-epithelialization," *European Journal of Cell Biology*, vol. 91, no. 10, pp. 748–756, 2012.
- [48] B. Cogliati, M. Vinken, T. C. Silva et al., "Connexin 43 deficiency accelerates skin wound healing and extracellular matrix remodeling in mice," *Journal of Dermatological Science*, vol. 79, no. 1, pp. 50–56, 2015.
- [49] T. Thuraisingam, Y. Z. Xu, K. Eadie et al., "MAPKAPK-2 signaling is critical for cutaneous wound healing," *The*







- Journal of Investigative Dermatology*, vol. 130, no. 1, pp. 278–286, 2010.
- [50] T. Thuraisingam, H. Sam, J. Moisan, Y. Zhang, A. Ding, and D. Radzioch, “Delayed cutaneous wound healing in mice lacking solute carrier 11a1 (formerly Nramp1): correlation with decreased expression of secretory leukocyte protease inhibitor,” *The Journal of Investigative Dermatology*, vol. 126, no. 4, pp. 890–901, 2006.
- [51] Y. Fang, S.-J. Gong, Y.-H. Xu, B. D. Hambly, and S. Bao, “Impaired cutaneous wound healing in granulocyte/macrophage colony-stimulating factor knockout mice,” *The British Journal of Dermatology*, vol. 157, no. 3, pp. 458–465, 2007.
- [52] C. Zhang, C. K. Tan, C. McFarlane, M. Sharma, N. S. Tan, and R. Kambadur, “Myostatin-null mice exhibit delayed skin wound healing through the blockade of transforming growth factor- β signaling by decorin,” *American Journal of Physiology-Cell Physiology*, vol. 302, no. 8, pp. C1213–C1225, 2012.
- [53] D. M. S. Lundvig, A. Scharstuhl, N. A. J. Cremers et al., “Delayed cutaneous wound closure in HO-2 deficient mice despite normal HO-1 expression,” *Journal of Cellular and Molecular Medicine*, vol. 18, no. 12, pp. 2488–2498, 2014.
- [54] A. Gutiérrez-Fernández, M. Inada, M. Balbín et al., “Increased inflammation delays wound healing in mice deficient in collagenase-2 (MMP-8),” *The FASEB Journal*, vol. 21, no. 10, pp. 2580–2591, 2007.
- [55] J.-T. Yeh, L.-K. Yeh, S.-M. Jung et al., “Impaired skin wound healing in lumican-null mice,” *The British Journal of Dermatology*, vol. 163, no. 6, pp. 1174–1180, 2010.
- [56] S. Braun, C. Hanselmann, and M. G. Gassmann, “Nrf2 transcription factor, a novel target of keratinocyte growth factor action which regulates gene expression and inflammation in the healing skin wound,” *Molecular and Cellular Biology*, vol. 22, no. 15, pp. 5492–5505, 2002.
- [57] Z. Kopecki, M. Luchetti, D. Adams et al., “Collagen loss and impaired wound healing is associated with c-Myb deficiency,” *The Journal of Pathology*, vol. 211, no. 3, pp. 351–361, 2007.
- [58] T. Yoshihara, H. Satake, T. Nishie et al., “Lactosylceramide synthases encoded by B4galt5 and 6 genes are pivotal for neuronal generation and myelin formation in mice,” *PLOS Genetics*, vol. 14, article e1007545, 2018.
- [59] O. Alshaarawy, E. Kurjan, N. Truong, and L. K. Olson, “Diet-induced obesity in cannabinoid-2 receptor knockout mice and cannabinoid receptor 1/2 double-knockout mice,” *Obesity*, vol. 27, no. 3, pp. 454–461, 2019.
- [60] J. Liao, X. Guo, M. Wang et al., “Scavenger receptor class B type 1 deletion led to coronary atherosclerosis and ischemic heart disease in low-density lipoprotein receptor knockout mice on modified Western-type diet,” *Journal of Atherosclerosis and Thrombosis*, vol. 24, no. 2, pp. 133–146, 2017.
- [61] A. Lugat, M. Joubert, and B. Cariou, “Au cœur de la cardiomyopathie diabétique,” *Médecine/Sciences*, vol. 34, no. 6-7, pp. 563–570, 2018.
- [62] Y. Jiang and Y. Yu, “Transgenic and gene knockout mice in gastric cancer research,” *Oncotarget*, vol. 8, no. 2, pp. 3696–3710, 2017.
- [63] W. Liu, H. Pan, Q. Wang, and Z. Zhao, “The application of transgenic and gene knockout mice in the study of gastric precancerous lesions,” *Pathology - Research and Practice*, vol. 214, no. 12, pp. 1929–1939, 2018.
- [64] E. Ahlqvist, M. Hultqvist, and R. Holmdahl, “The value of animal models in predicting genetic susceptibility to complex diseases such as rheumatoid arthritis,” *Arthritis Research & Therapy*, vol. 11, no. 3, p. 226, 2009.
- [65] A. W. Cheever, J. A. Lenzi, H. L. Lenzi, and Z. A. Andrade, “Experimental models of *Schistosoma mansoni* infection,” *Memórias do Instituto Oswaldo Cruz*, vol. 97, no. 7, pp. 917–940, 2002.
- [66] A. Zuberi and C. Lutz, “Mouse models for drug discovery. Can new tools and technology improve translational power?,” *ILAR Journal*, vol. 57, no. 2, pp. 178–185, 2017.
- [67] N. S. Tan and W. Wahli, “Studying wound repair in the mouse,” *Current Protocols in Mouse Biology*, vol. 3, no. 3, pp. 171–185, 2013.
- [68] H. Trøstrup, K. Thomsen, H. Calum, N. Hoiby, and C. Moser, “Animal models of chronic wound care: the application of biofilms in clinical research,” *Chronic Wound Care Manag Res.*, vol. Volume 3, pp. 123–132, 2016.
- [69] D. J. Kim, T. Mustoe, and R. A. Clark, “Cutaneous wound healing in aging small mammals: a systematic review,” *Wound Repair and Regeneration*, vol. 23, no. 3, pp. 318–339, 2015.
- [70] L. Chen, R. Mirza, Y. Kwon, L. A. DiPietro, and T. J. Koh, “The murine excisional wound model: contraction revisited,” *Wound Repair and Regeneration*, vol. 23, no. 6, pp. 874–877, 2015.
- [71] B. Abbasian, S. Azizi, and A. Esmaeili, “Effects of rat’s licking behavior on cutaneous wound healing,” *Iranian Journal of Basic Medical Sciences*, vol. 13, pp. 242–247, 2009.
- [72] H. E. Koschwanez and E. Broadbent, “The use of wound healing assessment methods in psychological studies: a review and recommendations,” *British Journal of Health Psychology*, vol. 16, no. 1, pp. 1–32, 2011.
- [73] A. Bieniek, Ł. Matusiak, I. Chlebicka, and J. C. Szepietowski, “Secondary intention healing in skin surgery: our own experience and expanded indications in hidradenitis suppurativa, rhinophyma and non-melanoma skin cancers,” *Journal of the European Academy of Dermatology and Venereology*, vol. 27, pp. 1015–1021, 2013.
- [74] A. C. D. O. Gonzalez, T. F. Costa, Z. D. A. Andrade, and A. R. A. P. Medrado, “Wound healing - a literature review,” *Anais Brasileiros de Dermatologia*, vol. 91, no. 5, pp. 614–620, 2016.
- [75] C. A. Dinarello, “Proinflammatory cytokines,” *Chest*, vol. 118, no. 2, pp. 503–508, 2000.
- [76] J. Bienvenu, G. Monneret, N. Fabien, and J. P. Revillard, “The clinical usefulness of the measurement of cytokines,” *Clinical Chemistry and Laboratory Medicine*, vol. 38, no. 4, pp. 267–285, 2000.
- [77] N. Sachdeva, “Cytokine quantitation: technologies and applications,” *Frontiers in Bioscience*, vol. 12, no. 8-12, p. 4682, 2007.
- [78] L. Potůčková, F. Franko, M. Bambousková, and P. Dráber, “Rapid and sensitive detection of cytokines using functionalized gold nanoparticle-based immuno-PCR, comparison with immuno-PCR and ELISA,” *Journal of Immunological Methods*, vol. 371, no. 1-2, pp. 38–47, 2011.
- [79] P. Boeuf, I. Vigan-Womas, D. Jublot et al., “CyProQuant-PCR: a real time RT-PCR technique for profiling human cytokines, based on external RNA standards, readily automatable for clinical use,” *BMC Immunology*, vol. 6, no. 1, p. 5, 2005.

- [80] K. K. Kim, D. Sheppard, and H. A. Chapman, "TGF- β 1 signaling and tissue fibrosis," *Cold Spring Harbor Perspectives in Biology*, vol. 10, no. 4, article a022293, 2018.
- [81] T. A. Wilgus, "Vascular endothelial growth factor and cutaneous scarring," *Advances in Wound Care*, vol. 8, no. 12, pp. 671–678, 2019.
- [82] J. Palomo, D. Dietrich, P. Martin, G. Palmer, and C. Gabay, "The interleukin (IL)-1 cytokine family – balance between agonists and antagonists in inflammatory diseases," *Cytokine*, vol. 76, no. 1, pp. 25–37, 2015.
- [83] C. A. Dinarello, "Overview of the IL-1 family in innate inflammation and acquired immunity," *Immunological Reviews*, vol. 281, no. 1, pp. 8–27, 2018.
- [84] C. Garlanda, C. A. Dinarello, and A. Mantovani, "The interleukin-1 family: back to the future," *Immunity*, vol. 39, no. 6, pp. 1003–1018, 2013.
- [85] M. J. Portou, D. Baker, D. Abraham, and J. Tsui, "The innate immune system, toll-like receptors and dermal wound healing: a review," *Vascular Pharmacology*, vol. 71, pp. 31–36, 2015.
- [86] A. Oeckinghaus and S. Ghosh, "The NF- κ B family of transcription factors and its regulation," *Cold Spring Harbor Perspectives in Biology*, vol. 1, no. 4, pp. a000034–a000034, 2009.
- [87] T. Liu, L. Zhang, D. Joo, and S.-C. Sun, "NF- κ B signaling in inflammation," *Signal Transduction and Targeted Therapy*, vol. 2, article 17023, 2017.
- [88] T. Thuraisingam, Y. Z. Xu, J. Moisan et al., "Distinct role of MAPKAPK-2 in the regulation of TNF gene expression by toll-like receptor 7 and 9 ligands," *Molecular Immunology*, vol. 44, no. 14, pp. 3482–3491, 2007.
- [89] M. Kobayashi, M. Nishita, T. Mishima, K. Ohashi, and K. Mizuno, "MAPKAPK-2-mediated LIM-kinase activation is critical for VEGF-induced actin remodeling and cell migration," *The EMBO Journal*, vol. 25, no. 4, pp. 713–726, 2006.
- [90] H. C. Reinhardt, A. S. Aslanian, J. A. Lees, and M. B. Yaffe, "p53-deficient cells rely on ATM- and ATR-mediated checkpoint signaling through the p38MAPK/MK2 pathway for survival after DNA damage," *Cancer Cell*, vol. 11, no. 2, pp. 175–189, 2007.
- [91] Z. Xiao, "Differential roles of checkpoint kinase 1, checkpoint kinase 2, and mitogen-activated protein kinase-activated protein kinase 2 in mediating DNA damage-induced cell cycle arrest: implications for cancer therapy," *Molecular Cancer Therapeutics*, vol. 5, no. 8, pp. 1935–1943, 2006.
- [92] J. R. Schoenborn and C. B. Wilson, *Regulation of interferon- γ during innate and adaptive immune responses*, *Advances in Immunology*, 2007.
- [93] H. Negishi, T. Taniguchi, and H. Yanai, "The interferon (IFN) class of cytokines and the IFN regulatory factor (IRF) transcription factor family," *Cold Spring Harbor Perspectives in Biology*, vol. 10, no. 11, article a028423, 2018.
- [94] H. Mühl and J. Pfeilschifter, "Anti-inflammatory properties of pro-inflammatory interferon- γ ," *International Immunopharmacology*, vol. 3, no. 9, pp. 1247–1255, 2003.
- [95] E. H. Steen, X. Wang, S. Balaji, M. J. Butte, P. L. Bollyky, and S. G. Keswani, "The role of the anti-inflammatory cytokine interleukin-10 in tissue fibrosis," *Advances in Wound Care*, vol. 9, pp. 184–198, 2020.
- [96] E. Birben, U. M. Sahiner, C. Sackesen, S. Erzurum, and O. Kalayci, "Oxidative stress and antioxidant defense," *World Allergy Organization Journal*, vol. 5, no. 1, pp. 9–19, 2012.
- [97] M. C. Sanchez, S. Lancel, E. Boulanger, and R. Neviere, "Targeting oxidative stress and mitochondrial dysfunction in the treatment of impaired wound healing: a systematic review," *Antioxidants*, vol. 7, no. 8, p. 98, 2018.
- [98] S. J. H. S. Nicholls, "Myeloperoxidase and cardiovascular disease," *Arteriosclerosis, Thrombosis, and Vascular Biology*, vol. 25, pp. 1102–1111, 2005.
- [99] M. Brennan and S. Hazen, "Emerging role of myeloperoxidase and oxidant stress markers in cardiovascular risk assessment," *Current Opinion in Lipidology*, vol. 14, no. 4, pp. 353–359, 2003.
- [100] E. Podrez, H. Abu-Soud, and S. Hazen, "Myeloperoxidase-generated oxidants and atherosclerosis," *Free Radical Biology & Medicine*, vol. 28, no. 12, pp. 1717–1725, 2000.
- [101] D. C. T. Palomino and L. C. Marti, "Chemokines and immunity," *Einstein*, vol. 13, no. 3, pp. 469–473, 2015.
- [102] C.-C. Qin, Y.-N. Liu, Y. Hu, Y. Yang, and Z. Chen, "Macrophage inflammatory protein-2 as mediator of inflammation in acute liver injury," *World Journal of Gastroenterology*, vol. 23, no. 17, pp. 3043–3052, 2017.
- [103] J. Peake and K. Suzuki, "Neutrophil activation, antioxidant supplements and exercise-induced oxidative stress," *Exercise Immunology Review*, vol. 10, pp. 129–141, 2004.
- [104] Y. Tan, Y. Qiao, Z. Chen et al., "FGF2, an immunomodulatory factor in asthma and chronic obstructive pulmonary disease (COPD)," *Frontiers in Cell and Development Biology*, vol. 8, 2020.
- [105] I. Yakymovych and S. Souchelnytskyi, "Regulation of Smad Function by Phosphorylation," in *Proteins and Cell Regulation*, Smad Signal Transduction, P. Dijke and C. H. Heldin, Eds., Springer, The Netherlands, 2006.
- [106] A. Okada, C. Tomasetto, Y. Lutz, J.-P. Bellocq, M.-C. Rio, and P. Basset, "Expression of matrix metalloproteinases during rat skin wound healing: evidence that membrane type-1 matrix metalloproteinase is a stromal activator of pro-gelatinase A," *The Journal of Cell Biology*, vol. 137, no. 1, pp. 67–77, 1997.
- [107] R. A. Dean, G. S. Butler, Y. Hamma-Kourbali et al., "Identification of candidate angiogenic inhibitors processed by matrix metalloproteinase 2 (MMP-2) in cell-based proteomic screens: disruption of vascular endothelial growth factor (VEGF)/heparin affinity regulatory peptide (pleiotrophin) and VEGF/connective tissue growth factor angiogenic inhibitory complexes by MMP-2 proteolysis," *Molecular and Cellular Biology*, vol. 27, no. 24, pp. 8454–8465, 2007.
- [108] Y. Li, J. Li, J. Zhu et al., "Decorin gene transfer promotes muscle cell differentiation and muscle regeneration," *Molecular Therapy*, vol. 15, no. 9, pp. 1616–1622, 2007.
- [109] M. Antsiferova and S. Werner, "The bright and the dark sides of activin in wound healing and cancer," *Journal of Cell Science*, vol. 125, no. 17, pp. 3929–3937, 2012.
- [110] J. R. Molina and A. A. Adjei, "The Ras/Raf/MAPK pathway," *Journal of Thoracic Oncology*, vol. 1, no. 1, pp. 7–9, 2006.
- [111] M. Bosch, F. Serras, E. Martín-Blanco, and J. Bagaña, "JNK signaling pathway required for wound healing in regenerating *Drosophila* wing imaginal discs," *Developmental Biology*, vol. 280, no. 1, pp. 73–86, 2005.
- [112] S. W. Jere, H. Abrahamse, and N. N. Houreld, "The JAK/STAT signaling pathway and photobiomodulation in chronic wound healing," *Cytokine & Growth Factor Reviews*, vol. 38, pp. 73–79, 2017.
- [113] K. Sakamaki, "Regulation of endothelial cell death and its role in angiogenesis and vascular regression," *Current Neurovascular Research*, vol. 1, no. 4, pp. 305–315, 2004.

- [114] N. F. Huang, S. Zac-Varghese, and S. Luke, "Apoptosis in skin wound healing," *Wounds*, vol. 15, pp. 182–194, 2003.
- [115] N. Nagahora, H. Yamada, S. Kikuchi, M. Hakozaki, and A. Yano, "Nrf2 activation by 5-lipoxygenase metabolites in human umbilical vascular endothelial cells," *Nutrients*, vol. 9, no. 9, p. 1001, 2017.
- [116] M. Pajares, A. I. Rojo, E. Arias, A. Díaz-Carretero, A. M. Cuervo, and A. Cuadrado, "Transcription factor NFE2L2/NRF2 modulates chaperone-mediated autophagy through the regulation of LAMP2A," *Autophagy*, vol. 14, no. 8, pp. 1310–1322, 2018.
- [117] A. Liberati, D. G. Altman, J. Tetzlaff et al., "The PRISMA statement for reporting systematic reviews and meta-analyses of studies that evaluate health care interventions: explanation and elaboration," *PLoS Medicine*, vol. 6, article e1000100, 2009.

Research Article

Were our Ancestors Right in Using Flax Dressings? Research on the Properties of Flax Fibre and Its Usefulness in Wound Healing

Tomasz Gębarowski ¹, Benita Wiatrak ^{1,2}, Maciej Janeczek ³, Magdalena Żuk ⁴,
Patrycja Pistor ⁵ and Kazimierz Gąsiorowski ¹

¹Department of Basic Medical Sciences, Wrocław Medical University, Borowska 211, 50-560 Wrocław, Poland

²Department of Pharmacology, Wrocław Medical University, Mikulicza-Radeckiego 2, 50-345 Wrocław, Poland

³Department of Biostructure and Animal Physiology, Wrocław University of Environmental and Life Sciences, Koźuchowska 1/3, 51-631 Wrocław, Poland

⁴Department of Genetic Biochemistry, University of Wrocław, Przybyszewskiego 63/77, 51-148 Wrocław, Poland

⁵Faculty of Veterinary Medicine, Wrocław University of Environmental and Life Sciences, Koźuchowska 1/3, 51-631 Wrocław, Poland

Correspondence should be addressed to Benita Wiatrak; benita.wiatrak@umed.wroc.pl

Received 21 July 2020; Revised 12 October 2020; Accepted 28 October 2020; Published 24 November 2020

Academic Editor: Mariella B. Freitas

Copyright © 2020 Tomasz Gębarowski et al. This is an open access article distributed under the Creative Commons Attribution License, which permits unrestricted use, distribution, and reproduction in any medium, provided the original work is properly cited.

Background. Despite the wide range of medical dressings available commercially, there is still a search for better biomaterials for use in the treatment of especially difficult-to-heal wounds. For several years, attention has been paid to the use of substances, compounds, and even whole plants in medicine. Flax is a plant that has been used as a dressing for thousands of years. Therefore, we decided to test flax fibres that had previously been genetically modified as a potential wound dressing. **Materials and Methods.** In this study, two modified flax fibres and their combinations were tested on cell lines (mice fibroblast, normal human dermal fibroblast, normal human epidermal keratinocytes, human dermal microvascular endothelial cell, epidermal carcinoma cancer cells, monocyte cells). In the tests, fibres of the traditional flax (Nike) were used as a control. Several experiments were performed to assess cell proliferation and viability, the number of apoptotic cells, the cell cycle, genotoxicity, the level of free oxygen radicals, and determination of the number of cells after 48 hours of incubation of cell cultures with the tested flax fibres. **Results.** The obtained results confirm the positive influence of flax on the used cell lines. Both traditional fibres (Nike) and genetically modified fibres increased the proliferation of fibroblast cells and keratinocytes, reduced the level of free oxygen radicals, and influenced the repair of DNA damage. At the same time, the tested flax fibres did not have a proproliferative effect on the neoplastic cell line. Interestingly, genetic modifications had a stronger impact on the proliferative activity of fibroblasts, keratinocytes, and microvascular endothelium compared to the traditional flax fibre used. **Conclusions.** In this study, the positive properties of the tested flax fibres on cell lines were proved. In the next stage, it is worth carrying out *in vivo* tests of tested genetically modified flax fibres.

1. Introduction

It is well known that linen was used in medicine in ancient times. It was used, among others, to dress wounds and stabilize fractures [1]. Wound care was important, for example, due to frequent armed conflicts. In Mesopotamia, linen was used as bandages and tampons. However, wool material was more popular [1]. Cotton wool, made from the cotton

tree, was known from the rules of Assyrian king Sennacherib [1]. Some texts give detailed instructions for surgery with a scalpel, including postoperative care such as the dressing of operations sites with oil-soaked linen bandages [2]. AMT 16/5 text describes the support of an infected purulent wound using honey-soaked linen compresses [3].

In Ancient Egypt, linen was the basic dressing material used in various forms. For example, it is mentioned in

medical Edwin Smyth Papyrus: "...thou shouldst make for him two swabs of linen, (and) thou shouldst clean out every worm of blood which has coagulated on the inside of his nostril" [4]. It seems to be that treatment with linen, oil, and honey was considered standard wound dressing for soft tissue injuries in Ancient Egypt as it is recommended in 30 out of the 48 cases in the Edwin Smith Papyrus. Linen was used for its absorptive properties, which is useful in drawing moisture and lymph away from the wound [4]. Similarly to Mesopotamia, it was also used to stabilize fractures. In Edwin Smith Papyrus, various kinds of splints with linen are described: (a) brace of wood padded with linen (Edwin Smith, case 7) inserted into the mouth to help in feeding the patient, (b) splint made of linen (Edwin Smith, case 35, fractured clavicle), (c) stiff post-like roll of linen (Edwin Smith, cases 11 and 12), and (d) it is possible that cartonnage was used, similar to our plaster of Paris to splint fractures, also made of linen [5].

The oldest information on the use of bandages in ancient Greece comes from Homer's *Iliad*.

Homer's *Iliad* and *Odyssey* are our first sources of information about trauma management in the Greek (and Western) world. This poet recorded some 147 wounds, of which 106 were caused by spears, 17 by swords, 12 by arrows, and another 12 by slings [6]. In *Corpus Hippocraticum*, the linen bandages are recommended, among others, for the stabilization of the fractured humerus [7]. As a result of Alexander the Great's conquests, Greek medicine has taken over and established many Middle Eastern treatments. Alexandria in Egypt became the center of world science including medicine.

The Roman Republic and later the Empire waged wars on an unprecedented scale.

The Roman army had professional medical and veterinary staff in each legion. On the other hand, the gladiator fights have also gained valuable experience in the treatment of injuries and wounds. In the first step of proceeding, a medicus cleansed the wound with rainwater or other freshwater mixed with ammoniacum. Then, if it was possible, the wound sutured the wound with silk, linen, or gut thread, and whenever possible, the wound was closed [8]. The linen bandages were the most common type of dressing used for binding wounds. However, Cornelius Celsus recommended covering the wound with a special mixture that contains copper acetate, lead oxide, alum, dried pitch, dried pine-resin, oil, and vinegar [8]. Cornelius Celsus and Claudius Galen advised using plasters and linen bandages in the treatment of limb ulcers [9]. In the Middle Ages, the same means were still used, as in antiquity, although surgeons were no longer medicine doctors.

A revolution in synthetic products took place in the 20th century. By the 1950s, the textile industry produced synthetic fibres and fabrics from polymers, including nylon, polyethylene, polypropylene, polyesters, polyvinyl, acrylics, and olefins [10]. In medical applications, linen has been replaced by synthetic materials—relatively cheap and easy to manufacture (with the current technology). Synthetics have generally replaced natural materials in the last decades. Recently, however, there has been a trend towards a return to the use of

natural materials in medicine. There are two companies in Poland that produce flax dressings, but they are still niche products on the market. Therefore, we drew attention to linen, which has been used as a dressing material since antiquity. Moreover, we currently have the possibility of influencing the properties of flax fibres by genetic modifications.

The study is aimed at investigating the effect of fibre from traditional cultivar of flax and fibres from two transgenic flax plants on cell cultures, commonly used as *in vitro* models of wound healing. The research results show that flax fibres have valuable properties in this field.

2. Materials and Methods

2.1. Tested Flax Fibres. The study examined the fibre obtained from a traditional fibrous cultivar of flax (Nike) and the fibres from two transgenic flax types (M50 and B14), and a combination of these two flax fibres (M50 +B14) [11]. Both transgenic plants are obtained from Nike cultivar. B14 plants transformed with a defence-related potato β -1,3-glucanase gene (PR-2). M50 plants have been enriched with *Ralstonia eutropha* genes coding for β -ketothiolase (phbA), acetoacetyl-CoA reductase (phbB), and PHB synthase (phbC) for poly- β -hydroxybutyrate (PHB) synthesis.

Flax fibres were prepared for cell culture studies by dividing the fibres into four different weights: 10, 20, 30, and 40 mg. The fibres prepared in this way were soaked in PBS for 48 h, sterilized for 60 min by irradiation with UV, and transferred to cell cultures for 48 h. The fibres were in direct contact with the cells during the experiments.

2.2. Cell Lines and Conditions. This study used three human cell lines that are an *in vitro* skin model and one line of mouse fibroblasts recommended by the National Institutes of Health (NIH) for a cytotoxic assay. Research has also been carried out on a cell line often used to study monocyte and macrophage differentiation, including inflammation.

Normal human dermal fibroblast (NHDF) was purchased from Lonza (Verviers, Belgium) and were grown in Dulbecco's modified Eagle medium (DMEM) without phenol red. Normal human epidermal keratinocytes (NHEK) were from PromoCell (Heidelberg, Germany) and cultured in the KBM-Gold medium (Keratinocyte Cell Basal Medium). Human Dermal Microvascular Endothelial Cells—Adult (HMVEC) were purchased from Lonza and were cultured in EGM medium, supplemented according to Lonza's procedure. Cancer cells A431, which are derived from epidermal carcinoma, received from ATCC (USA) were incubated in Dulbecco's modified Eagle's medium (DMEM). Mice fibroblast BALB/3T3 (cloneA31 from mouse embryo donor) were obtained from Sigma-Aldrich (St.Louis, MO, USA) and were cultured in Minimum Essential Medium (MEM). Monocyte cell line (THP-1), which was derived from acute monocytic leukemia, was in receipt of the Laboratory for Therapeutic Innovation, Faculty of Pharmacy, University of Strasbourg, France. These cells were grown in suspended in RPMI-1640 medium. All cell lines were cultured in 95% humidified, at 37°C and 5% CO₂ incubator, in the complete

culture medium. The MEM, DMEM, RPMI-1640, and DMEM without phenol red media were supplemented with penicillin (10000 U/ml), streptomycin (10mg/ml), L-glutamine (200mM), and 10% fetal bovine serum (FBS). The KGM medium was supplemented following the Promo-Cell company's recommendations.

The cells were evaluated at least twice a week under a microscope, and then, the cells were passaged using the TrypLE solution or the appropriate medium was changed. All assays were performed in five independent replicates.

2.3. Cell Viability. The impact of flax fibres on the viability of the Balb/3T3 cell line was evaluated. After 24-hour treatment of cells with the tested fibres, the fibres were rinsed with PBS, which was collected to preprepared centrifuge tubes. The culture supernatant was collected into the same tubes. The culture plates were washed with TrypLe solution, which was also harvested. The TrypLe solution was again added, and culture plates were incubated for 2min at 37°C. Finally, the solution with cells was collected into appropriate tubes, which was centrifuged at 600 g for 5min. After supernatant removal, the cells were resuspended in PBS, and propidium iodide was added. After 5min incubation in the dark, the samples were analyzed in the image-based cytometer Arthur (NanoEnTek Inc.).

2.4. Cell Proliferation. The sulforhodamine-B (SRB) assay was used to evaluate the effect of flax fibres on the total amount of cellular protein. All cell lines were seeded on 96-well plates at a density of 2×10^4 cell/ml per well. After 24-hour incubation, the tested fibres (with various weights: 10-40 mg) were put on cells for 48 h. Before the addition of the fibres, one plate from each cell line was fixed with cold 50% trichloroacetic acid (TCA) for the adherent cell line and 20% TCA for THP-1 cells at 4-8°C; these plates were the control. After 48-hour incubation, the culture plates were also fixed with 50% TCA for adherent cell line and 20% TCA for THP-1 cells for 1h at 4-8°C. In the next step, the plates were washed five times under running water. After air-drying, the sulforhodamine-B dye was added for a further 30 minutes to stained cellular proteins, and unbounded dye was removed by five washes with 1% acetic acid and again air-dried. In the last step, the SRB dye was dissolved with Trisma, and the absorbance was measured at 555nm, using a microplate reader (Victor2, PerkinElmer).

2.5. Evaluation of the Intracellular Free Radical Level. The intracellular reactive oxygen species (ROS) level was visualized by 2', 7'-dichlorofluorescein-diacetate (DCF-DA, BRAND) fluorescence. This assay was performed only for the NHDF cell line. These cells were seeded on 96-well plates at a density of 2.5×10^4 cell/ml per well. The next day, into the plates, there were put tested flax fibres for 24h incubation. The supernatant and fibre were then removed, and the DCF-DA solution was added to the culture for the last 1 hour of incubation. The following steps were performed in two different ways. In the first case, after incubation with DCF-DA solution, the fluorescence was measured ($\lambda_{ex} = 485\text{nm}$, $\lambda_{em} = 535\text{nm}$) using a microplate reader (Victor2, PerkinElmer).

In the second stage, during incubation with DCF-DA solution, for the last 30min, the cells were treated with $100\mu\text{M}$ H_2O_2 . In both cases, after incubation with the DCF-DA solution, before measuring, the supernatant was removed and cells were washed twice with PBS.

2.6. Total Number of Cells. An image-based cytometer, Arthur (NanoEnTek Inc.), was used to assess the effect of the tested flax fibres on cell proliferation. After 48 hours of incubation of Balb/3T3 and NHDF cell lines with the tested fibres, the supernatant was collected into previously prepared tubes, and the tested fibres were washed in PBS, which was also harvested into tubes. Cell cultures were washed with a TrypLE solution, which was also collected, and the TrypLE solution was added to the cells, and the plates were incubated at 37°C for 2min. The cell suspensions were harvested into the same tubes, which was then centrifuged at 600 g for 5min. The supernatant was removed, and the pellet was resuspended in PBS. In the last step, the cell suspensions were analyzed using a cytometer.

2.7. Apoptotic and Necrotic Cells. The effect of flax fibres on apoptosis and necrosis of NHDF and THP-1 cells was assessed. After 24-hour incubation of the cells with the tested flax fibres, the fibres were washed with PBS, and the washing solutions were collected in appropriate preprepared centrifuge tubes. The culture supernatant was also received into the same tubes. In the case of the NHDF cell line, all wells were then treated with the TrypLE solution and incubated at 37°C for 2min. In the next step, the solution with cells was harvested to the centrifuge tubes. For both cell lines, the tubes with cells were centrifuged at 600 g for 5min. After the supernatant was removed, the cell pellet was resuspended in $100\mu\text{l}$ of HEPES-NaOH buffer at pH 7.5. The mixture of fluorochromes Annexin V-FITC and propidium iodide was then added and left in the dark for 10 min. The samples were analyzed in the image-based cytometer Arthur (NanoEnTek Inc.).

2.8. Cell Cycle. The effect of the flax fibres on the cell cycle of NHDF cells after 24-hour incubation was evaluated. After the incubation of cells with the tested fibres, a standard procedure was performed (such as detached cells from the surface of wells, centrifuged, and removed supernatant). The cells were then fixed with 70% cold ethanol for 10min at room temperature and again centrifuged at 600 g for 5min. The supernatant was removed, and the cell pellet was resuspended in propidium iodide solution and left in the dark for 10min. The samples were analyzed in the image-based cytometer Arthur (NanoEnTek Inc.).

2.9. Genotoxicity Assessment. The comet assay was performed to assess the effect of flax fibres on genotoxic damage and repair after exposure to exogenous oxidative stress. After 48-hour incubation of NHDF cells with the tested flax fabrics, the cells were detached from the surface of the wells with the TrypLE solution, and they were collected in preprepared appropriate tubes and were added a medium with the serum to neutralize the effect of TrypLE. The tubes were centrifuged at 600 g for 5min. At this stage, DNA damage was

carried out according to the standard comet test procedure, or to assess the repair activity of the tested fibres after supernatant removal, the cell pellet was resuspended with 200 μ M H₂O₂ in PBS for 30 min at 4°C, and the cell suspension prepared in this way was subjected to the standard comet test procedure. In both cases, after slides were stained with 1 μ g/ml DAPI for 20 min, the samples were evaluated under a fluorescence microscope (Nikon Eclipse E-600) with UV 1A filter block and with a digital camera and CometPlus 2.5 software (ThetaSystem Electronics GmbH, Gröbenzell, Germany). The 75 photos of the first comets found on each slide were taken. Using the software, the DNA content in the comet's head (%) and comet's tail length were analyzed.

2.10. Statistical Analysis. All studies were performed in five independent replicates. Due to the normal distribution and equal variance of the obtained results, statistical calculations were performed with parametric tests. Using the Statistica v.13 software, statistical significance was calculated using Tukey's post hoc test. The significance point was set at * $p < 0.05$.

3. Results

3.1. Morphological Characterization of the Flax Fibres Used in the Experiment. The types of flax analysed did not differ significantly in the content of the basic polymers of the cell wall (cellulose, pectins, lignin, hemicellulose). Their differentiating parameter was the content of potentially bioactive substances such as phenolic compounds, polyhydroxybutyrate/hydroxybutyrate, and polyamines (Table 1).

3.2. Cell Viability. The Balb/3T3 cell line is recommended by the NIH for assessing the effect of substances on cytotoxicity. The cytotoxic effect of the studied fibres on mouse fibroblasts was performed by analyzing the number of necrotic cells after propidium iodide staining. All flax fibres tested did not increase the number of necrotic cells compared to the control cultures (incubated only in complete medium) (Figure 1). The highest number of necrotic cells was observed for 20 mg of traditional flax fibres (Nike), about 4% more than in the control culture. In other cases studied, the number of necrotic cells was not more than 1% compared to the control.

3.3. Cell Proliferation. Flax fibres affected the amount of total cellular protein in the cultures of mouse fibroblasts (Balb/3T3), as well as human fibroblasts (NHDF) after incubation (48h). In the Balb/3T3 cells, no significant reduction in the protein level was found, regardless of the flax fibre used, which proves the lack of cytotoxicity (Figure 2(a)). At weights of 20-40 mg, an increase in total cellular protein was observed for all flax fibres compared to the control. The increase was found at all doses tested after using the traditional flax fibre (Nike) for both fibroblast lines, and B14 fibre in human dermal fibroblast culture (Figure 2(b)). In the 10-40 mg concentration range, the increase in total Balb/3T3 cell protein was significant after incubation of the culture with M50 and B14 fibres (Figure 2(a)). In the same concentration range, the total growth of NHDF cell protein was observed after treatment with M50 fibre (Figure 2(b)).

The combination of both fibres (M50+B14) resulted in an increase in the total amount of cellular protein in both fibroblast lines (Figures 2(a) and 2(b)). However, this increase was statistically significant only at doses of 10 and 30 mg for mouse fibroblast culture (Figure 2(a)).

The first phase of wound healing preceding the proliferative phase is the inflammatory phase. Wound healing consists of three overlapping healing phases: inflammation, proliferation, and remodeling. In the inflammatory phase, there is an increase in the number of cytokines and immune cells that allow the wound to be cleansed. Inflammation should disappear in subsequent stages of the regeneration of the damaged skin. The model line in assessing inflammation is the THP-1 line. Therefore, the effect of the tested fibres on the total amount of THP-1 cell protein after 48 hours of incubation was evaluated. Nike fibre inhibits the total cellular protein over the entire range of concentrations tested (also, 10-40 mg statistically significant). An activity increasing the amount of cellular protein, M50 fibre, and a combination of M50 and B14 fibres at a dose of 10 mg (statistically significant), at the lowest concentration, this activity was comparable to the control culture (Figure 2(c)).

In comparison, at 20 mg (M50 fibre) and 20-30 mg (M50+B14 fibres), a decrease in the amount of cell protein was observed compared to control. Interestingly, at concentrations of 30-40 mg for the M50 fibre and the highest concentration of M50 and B14 combination fibres tested, the observed reduction in the amount of cellular protein compared to cell cultures before fibre addition indicates the cytotoxic effects of these fibres at high doses, which is important in the later stages of wound healing. The 48-hour incubation of THP-1 culture with B14 fibre strongly influences the increase in total protein in the concentration range of 5-30 mg. However, at the highest concentration tested, it has an inhibitory effect on cellular protein amount compared to the control (Figure 2(c)).

In wound healing, in the proliferation phase, an increase in the number of keratinocytes is the most important. Therefore, the effect of the flax fibres on the total amount of cellular protein in the culture of human keratinocytes was evaluated (Figure 2(d)). A statistically significant increase in the total amount of protein was observed for all tested fibres in the whole tested concentration range compared to the control. A concentration dependence was observed for all tested fibres, where the largest increase in protein was shown at the lowest concentrations (5 mg). The highest increase in protein was observed in cultures treated with fibre combination of both modified fibres (M50+B14) (Figure 2(d)).

A very important stage of the proliferative phase in wound healing is richly vascularized granulation tissue. An assessment of the influence of the studied fibres on the amount of cellular protein in HMVEC vascular cell culture was carried out. The highest increase in cellular protein was observed at 20 mg in all fibres examined. The traditional flax fibre (Nike) affected the growth of the total cellular protein over the entire concentration range studied. The M50 fibre at low doses (5 and 10 mg) increased the amount of cellular protein (statistically significant) (Figure 2(e)).

TABLE 1: Content of potentially bioactive substances in tested flax fibres.

Bioactive substance	Content (ng/g) in flax fibres		
	Nike	B14	M50
Vanillin	156.34 ± 10.45	169.73 ± 11.83	147.49 ± 9.09
4-Hydroxybenzoic acid	344.50 ± 25.60	318.75 ± 32.46	354.48 ± 31.25
Ferulic acid	221.65 ± 21.65	245.61 ± 12.55	227.34 ± 9.83
Coumaric acid	62.23 ± 12.45	53.28 ± 10.33	68.42 ± 12.24
Syringaldehyde	148.17 ± 18.33	143.67 ± 12.24	172.74 ± 19.95
Polyhydroxybutyrate/hydroxybutyrate	14.67 ± 3.05	15.45 ± 4.02	32.40 ± 9.95
Polyamines	357.04 ± 19.95	417.87 ± 22.92	836.76 ± 28.25

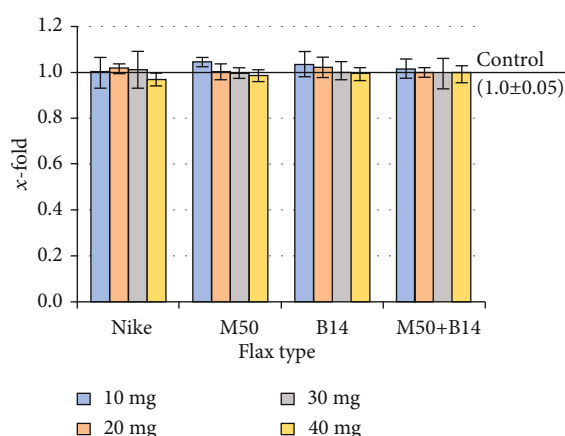


FIGURE 1: Cell viability of the Balb/3T3 cells after 48-hour incubation with the tested flax fibre in four different weights (10, 20, 30, and 40mg). The results are presented as x -fold-ratio to control culture (cells without fibres; x -fold = 1.0). The results are the means of 5 independent experiments \pm SEM. The statistical significance of the differences between the results for the tested flax fibres compared to the control was calculated using Tukey's post hoc test (* $p < 0.05$).

In comparison, in higher concentrations (20 and 40 mg), a decrease in the total amount of HMVEC protein was observed compared to the control. However, after using B14 fibre, an increase in total protein was found in doses of 10 mg and 20 mg, while in other doses used, a similar amount of cellular protein was shown as in the control culture. Interestingly, the largest increase in cellular protein was observed after combining both modified fibres (M50+B14), even compared to the cultures treated with Nike fibre (Figure 2(e)).

Epidermal neoplasms are one of the most common skin cancers. They constitute about 65–75% of all skin cancers (about 25% of all cancers). It is expected that the given dressing material will not increase the cell division of the tumour cells. Therefore, the influence of the tested materials on the amount of cellular protein in the culture of epidermal cancer cells was checked (A431). There was a significant inhibition of the total amount of cellular protein compared to the control cultures in all tested fibres and the whole range of the tested doses. The strongest effect was observed after 48 hours

of culture incubation in the presence of the Nike fibre (Figure 2(f)).

3.4. Total Number of Cells. An increase in the total cellular protein may indicate an increase in cell mass or increased cell division (proliferation). Due to the expectation of increased skin fibroblast proliferation during intense wound healing, the number of NHDF and Balb/3T3 cells was evaluated after incubation for 48 hours in the presence of test fibres (Figure 3(a) and 3(b)).

After 48-hour incubation of Balb/3T3 cells with Nike fibre in the concentration range of 5–20 mg, a similar number of cells was observed as in the control. However, at the highest concentration tested, a reduced cell number was shown. In the tested M50, B14 fibres, and combinations of these two types of fibres, a significant increase in the number of Balb/3T3 cells was observed compared to the control (except for the 5mg dose after treatment with M50 fibre) (Figure 3(a)). In contrast, the number of human dermal fibroblast cells was higher compared to the controls at all doses and all tested flax fibres (Figure 3(b)).

3.5. Evaluation of the Intracellular Free Radical Level. As the number of cells increases, the amount of free oxygen radicals increases as a result of metabolic processes through an increased number of cells. Therefore, the level of free radicals in the culture of NHDF cells treated with the tested fibres for 48 hours was evaluated. All the tested doses of all the tested fibres caused an increase in ROS levels of up to 20% compared to controls (except for the combination of M50 and B14 fibres, where the increase was significant only at the 40mg dose) (Figure 4(b)).

At the same time, a study was conducted to evaluate the effect of fibres on the ROS levels in cells that had previously exogenous oxidative stress by adding $100\mu\text{M}$ H_2O_2 . All the flax fibres tested reduced the level of free radicals compared to the control that was treated with $100\mu\text{M}$ H_2O_2 (Figure 4(a)).

3.6. Apoptotic and Necrotic Cells. To assess the number of cells in apoptosis and necrosis, Annexin V conjugated with FITC and propidium iodide staining was performed. After a 48-hour incubation of NHDF cells with the test fibres, the percentage of cells in necrosis did not exceed more than 5% (Figure 5). However, the sum of cells in the apoptosis and late

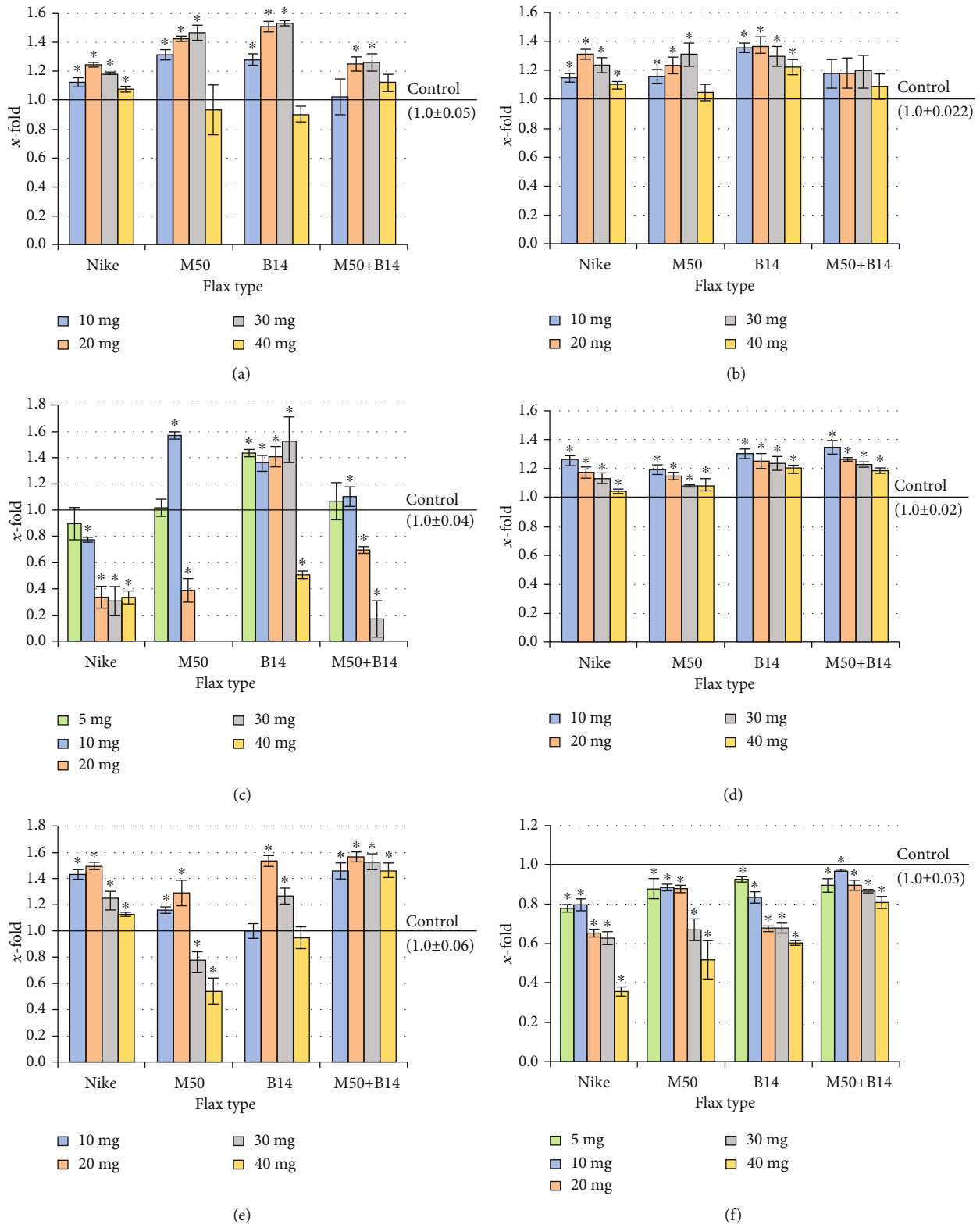


FIGURE 2: The proliferation of cells ((a) Balb/3T3, (b) NHDF, (c) THP-1, (d) NHEK, (e) HMVEK, (f) A431) after 48-hour incubation with the tested flax fibre in four different weights (10, 20, 30, and 40mg). The results are presented as x -fold-ratio to control culture (cells without fibres; x -fold = 1.0). The results are the means of 5 independent experiments \pm SEM. Statistical significance of differences between the results for the tested flax fibres compared to the control was calculated using Tukey's post hoc test ($*p < 0.05$). In THP-1 cells for weights of 30 and 40mg of the M50 flax fibre and 40 mg of M50+B14, there was complete inhibition of cell growth, and therefore, these results are not shown in the figure.

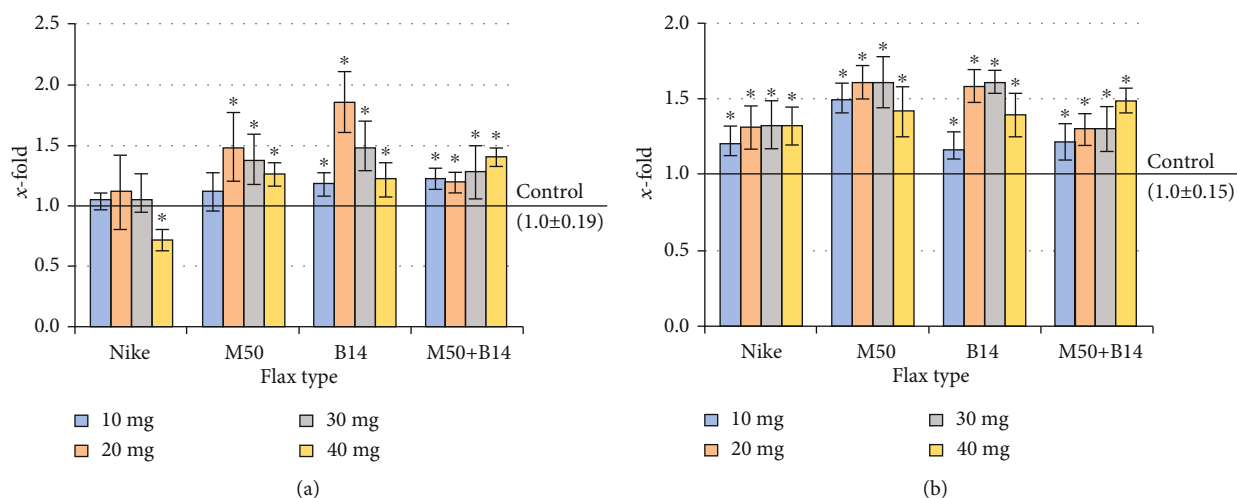


FIGURE 3: Total number of cells ((a) Balb/3T3, (b) NHDF) after 48-hour incubation with the tested flax fibres in four different weights (10, 20, 30, and 40 mg). The results are presented as x -fold-ratio to control culture (cells without fibres; x -fold = 1.0). The results are the means of 5 independent experiments \pm SEM. The statistical significance of differences between the results for the tested flax fibres compared to the control was calculated using Tukey's post hoc test ($*p < 0.05$).

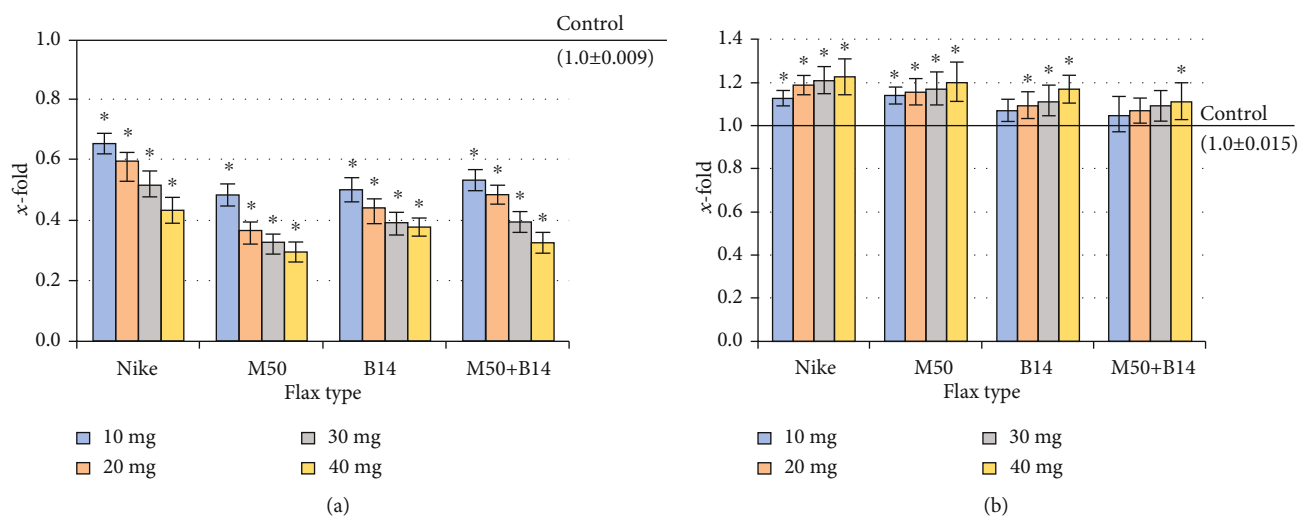


FIGURE 4: The level of ROS in NHDF cells cultured for 48 h with the presence of the tested flax fibres in four different weights (10, 20, 30, and 40 mg): (a) subsequently exposed to H_2O_2 (100 μ M, 30 min, 4°C); (b) not exposed to H_2O_2 . The results are presented as x -fold-ratio to control culture (cells without fibres; x -fold = 1.0). The results are the means of 5 independent experiments \pm SEM. The statistical significance of differences between the results for the tested flax fibres compared to the control was calculated using Tukey's post hoc test ($*p < 0.05$).

apoptosis was the highest at the highest doses tested and did not exceed more than 22%. The lowest number of cells in the phase of apoptosis was observed in cultures treated with M50 fibre. Moreover, the sum of necrotic and apoptotic cells was not up to 10% (Figure 5).

3.7. Cell Cycle. A cell cycle analysis was performed to check whether incubation of the culture with the examined fibres increased the number of cells in the proliferation phase (S phase). After a 48-hour incubation of NHDF cells with the tested fibres, an increase in the number of S phase cells at 20-30 mg was observed in all cases (Figure 6).

3.8. Genotoxicity Assessment. The effect on DNA damage in NHDF cells of the tested flax fibre was evaluated in the comet assay. The amount of DNA in the comet's head after incubation of NHDF cells with the tested fibres was compared to the amount of DNA in the control culture. No genotoxic effect has been demonstrated after applying all the tested fibres (Figure 7(b)). Therefore, the impact of the studied fibres on the repair of genotoxic damage caused by oxidative stress was checked. Oxidative stress was induced by incubation of cell cultures with H_2O_2 . The amount of DNA in the head after incubation of cell cultures with the tested fibres was higher than in the control (culture incubated with H_2O_2) for all tested compounds (except for the lowest dose of the

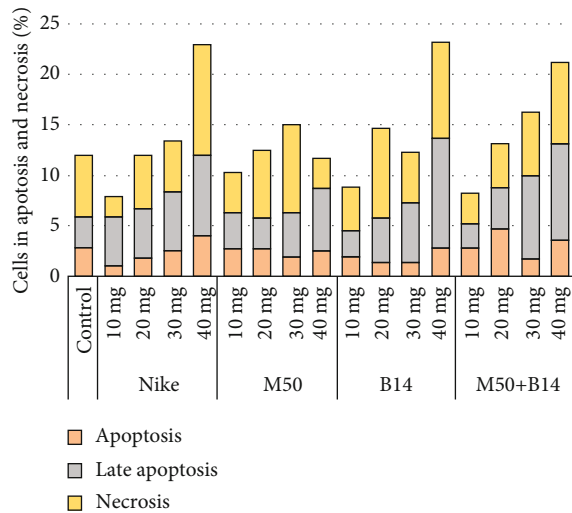


FIGURE 5: Apoptosis and necrosis of the NHDF cells after 48-hour incubation with the tested flax fibres in four different weights (10, 20, 30, and 40mg). The results are presented as the percentage of apoptotic and necrotic cells. The results are the means of 5 independent experiments.

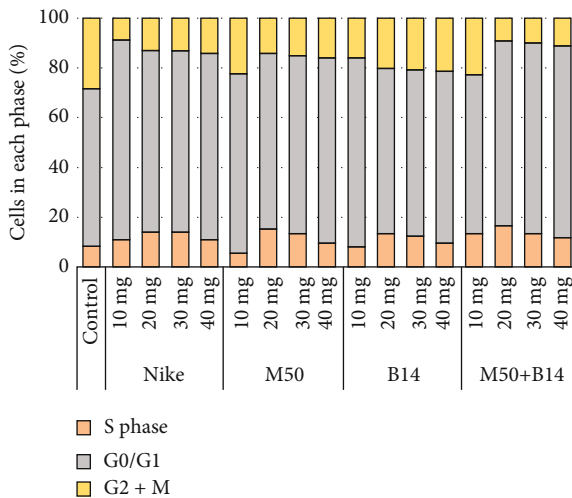


FIGURE 6: Cell cycle in NHDF cells after 48-hour incubation with the tested flax fibres in four different weights (10, 20, 30, and 40mg). The results are presented as the percentage of cells in each phase. The results are the means of 5 independent experiments.

tested Nike fibre). The strongest reparations were observed after the incubation of cell cultures in the presence of combined M50 and B14 fibre at a dose of 30 mg (Figure 7(a)).

4. Discussion

Despite the wide range of various commercially available dressings, new solutions are still being sought in the treatment of particularly difficult to heal wounds. The flax has been used as a dressing for thousands of years. Its positive effect on injuries is well known [12–14]. Currently, it is used in the treatment of severely healing wounds, too [15, 16]. Flax is a plant that grows widely in the Middle East and temperate

and Mediterranean climates. Cultivated for several thousand years, it serves as a source of oil and fibres for humans, not only in medicine but also in the textile, paper, cosmetics, and food industries. Flax fibre differs in composition from cotton fibre, and it contains mainly various polysaccharide polymers, such as cellulose (covers about 70% of fibre weight) and hemicellulose, the bundles of which are supplemented by pectin and phenolic polymer, lignin [17].

Wound healing is a multistage process consisting of three phases: (1) inflammation, cell proliferation, and tissue remodeling to restore tissue integrity after an earlier disruption of its continuity. Due to the rapid development of the transformation of modern molecular biology, research has been carried out for several decades to improve the quality of plant/fibre production [18] to develop the best-modified plants for use in medicine, including wound treatment. It enhances the productivity and quality of flax by influencing its length, thickness, softness, and elasticity. Genetic engineering allows us to identify and modify flax's bioactive components responsible for health-promoting properties. These changes should affect the immune cells that migrate to the lesions in the first phase. The purpose of these cells is to remove damaged tissue and initiate blood clotting processes. In our work, we showed a significant effect of the studied fibres on the increase in the amount of total protein of THP-1 cells (inflammation model) at low doses of M50 fibre, which indicates the possibility of using this fibre in the first phase of healing.

On the other hand, the combined M50+B14 fibre is recommended in subsequent phases because it was toxic to the model cell line in inflammation. In the second phase of wound healing, however, there is an intensive proliferation of cells along with the secretion of substances contained in the extracellular matrix (ECM). In the first stage of this phase, the formed tissue is highly vascularized and hydrated. At this stage, it is important to reduce inflammation, as shown by the use of higher concentrations of M50 and the combination of test fibres (M50+B14). Simultaneously, we showed an intense increase in cell proliferation—skin and endothelial fibroblasts after applying the tested fibres.

The metabolic profile of transgenic flax relates to changes in the level of, e.g., polyunsaturated fatty acids, lignan complexes, carotenoids, flavonoids, and phenylpropanoids [19–22]. In response to stress caused by the attack of pathogens (viruses, bacteria), the synthesis of lignin increases, which affects the cross-linking process and reduces the plasticity of the fibres. In transgenic flax fibres, there was an increase in the level of cellulose to lignin by silencing the CAD protein gene, an enzyme that catalyzes the biosynthesis of lignin monomers [23]. In the process of wound healing, it is very important to maintain a balance in the production of free radicals, both oxygen and nitrate. This disorder may affect the protracted phase of inflammation. Hence, the modifications mentioned above influencing the growth of flavonoids, which have anti-inflammatory and antioxidative activities, positively influenced the level of free oxygen radicals in our study. We have shown that during oxidative stress (caused exogenously by the presence of H_2O_2), a decrease in the level of free oxygen radicals was observed. At the same

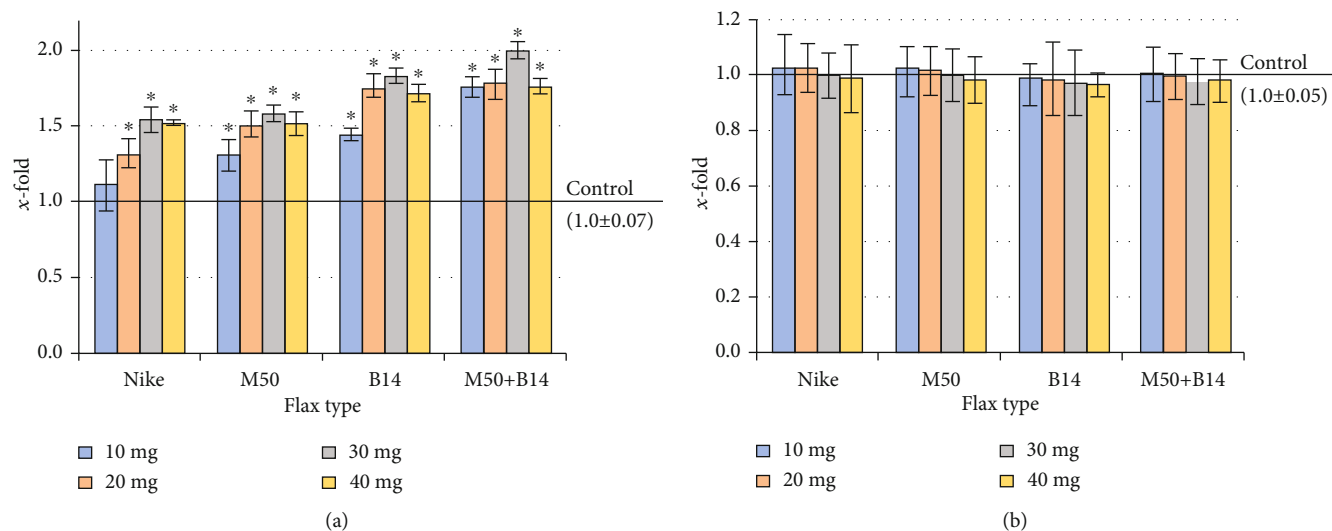


FIGURE 7: The level of DNA damage in NHDF cells cultured for 48 h with the presence of the tested flax fibres in four different weights (10, 20, 30, and 40mg): (a) subsequently exposed to H₂O₂ (100 μM, 30 min, 4°C); (b) not exposed to H₂O₂. The results are presented as *x*-fold-ratio to control culture (cells without fibres; *x*-fold = 1.0). The results are the means of 5 independent experiments ± SEM. The statistical significance of differences between the results for the tested flax fibres compared to the control was calculated using Tukey's post hoc test (**p* < 0.05).

time, along with the reduction in the level of free oxygen radicals, increased repair of DNA damage was observed.

Preclinical studies of dressings from genetically modified flax were carried out in which the presence of a new metabolite of flax, which belongs to the terpenoids pathway, was observed. There are biological endocannabinoids (produced by human cells, e.g., anandamide or plant-derived terpenophenolics) and synthetic cannabinoids (e.g., HU-243, WIN-55,212-2). Reports show the important role of terpenophenol as an agent with analgesic and anti-inflammatory properties [24, 25]. Preclinical studies have demonstrated the antioxidant, anti-inflammatory, antiviral, and vasodilating properties of linseed dressings. The positive effects of treatment of difficult-to-heal wounds with new linen dressings characterized by greater hygroscopic properties and overproduction of polyphenols were manifested by reducing fibrosis, wound exudate, reducing the level of pain, promoting granulation, creating an effective barrier against unwanted tissues, fibrous tissue, and microorganisms [16].

Our previous studies of W92 fibres confirmed their positive effect on ulcer healing. The study applied the dressing for four weeks and then assessed the size of the wound and the exudate. It was shown that W92 fibres reduce exudate and wound size by 55% [26]. Based on these data, an attempt was made to modify flax to obtain better properties genetically. In this study, M flax is characterized by a genetic modification that influences a strong and stable overexpression of the *cDNA*. As a result, it affects the increased synthesis of polyhydroxybutyrate (PHB), β-ketothiolase (*phb A*), acetoacetyl-CoA reductase (*phb B*), and PHB synthase (*phb C*) (16). As a consequence of this modification, an improvement in the biomechanical properties of the new fibre was obtained by binding PHB with cellulose into polymers through hydrogen and ester bonds during plant growth. On contact with body fluid, PHB decomposes, releasing D, L-

β-hydroxybutyrate, and as a normal component of blood and tissues, it promotes cell proliferation, preventing apoptotic cell death [27].

In conclusion, a limitation of this manuscript is the lack of assessment of the level of proinflammatory cytokines important in the wound healing process. Despite this, our study showed *in vitro* that modified flax possesses even better properties than the traditional flax. The investigation has shown clearly the beneficial effects of flax understudy on cell lines. It was shown that the level of necrosis was higher for conventional flax than modified flax. A higher level of total cell protein (fibroblast, keratinocytes, and dermal microvascular endothelial cells) concentration was observed for all flax types tested compared to controls. M50 and B14 showed high levels of reparations in the genotoxicity study turn; the lowest level of apoptotic cells was observed in cultures treated with the M50 fibre. The conducted tests showed that the tested, modified flax varieties have a positive effect on tissue cultures. The flax lines tested appear to be promising for further *in vivo* testing.

Data Availability

The data underlying this article will be shared on a reasonable request to Tomasz Gębarowski (email: tomasz.gebarowski@umed.wro.pl).

Conflicts of Interest

The authors declare no conflicts of interest regarding the publication of this paper.

Authors' Contributions

TG, BW, and KG conceived the overall project objectives. TG, BW, and KG designed the experiments. TG and BW conducted the experiments. TG, MJ, and BW interpreted the data and prepared the original draft of the manuscript with contributions from all authors. KG, PP, and MŻ contributed to the data interpretation review and editing. MŻ was responsible for the plant material. KG was the supervisor.

Acknowledgments

The publication was prepared under the project financed from the funds granted by the Ministry of Science and Higher Education in the "Regional Initiative of Excellence" programme for the years 2019–2022, project number 016/RID/2018/19, the amount of funding 11,998,121.30 PLN.

References

- [1] P. B. Adamson, "Surgery in ancient Mesopotamia," *Medical History*, vol. 35, no. 4, pp. 428–435, 1991.
- [2] E. Teall, "Medicine and doctoring in ancient Mesopotamia," *Grand Valley Journal of History*, vol. 3, no. 1, 2014.
- [3] J. Scurlock, *Sourcebook for Ancient Mesopotamian Medicine*, SBL Press, Atlanta, Georgia, 2014.
- [4] K. J. Wade, "The sword and the knife: a comparison of ancient Egyptian treatment of sword injuries and present day knife trauma," *Resenha Médica*, vol. 24, no. 1, pp. 47–56, 2017.
- [5] A. Saber, "Ancient Egyptian surgical heritage," *Journal of Investigative Surgery*, vol. 23, no. 6, pp. 327–334, 2011.
- [6] E. A. Pikoulis, J. C. B. Petropoulos, C. Tsigris et al., "Trauma management in ancient Greece: value of surgical principles through the years," *World Journal of Surgery*, vol. 28, no. 4, pp. 425–430, 2004.
- [7] S. Brorson, "Management of fractures of the humerus in Ancient Egypt, Greece, and Rome: an historical review," *Clinical Orthopaedics, and Related Research*, vol. 467, no. 7, pp. 1907–1914, 2009.
- [8] V. Belfiglio, "Sanitation in Roman military hospitals," *International Journal of Community Medicine and Public Health*, vol. 2, no. 4, pp. 462–465, 2015.
- [9] C. H. A. Wittens, R. G. J. M. Pierik, and H. van Urk, "The surgical treatment of incompetent perforating veins," *European Journal of Vascular and Endovascular Surgery*, vol. 9, no. 1, pp. 19–23, 1995.
- [10] L. G. Ovington, "The evolution of wound management," *Home Healthcare Nurse*, vol. 20, no. 10, pp. 652–656, 2002.
- [11] M. Wróbel-Kwiatkowska, K. Turnau, K. Góralska, T. Anielska, and J. Szopa, "Effects of genetic modifications to flax (*Linum usitatissimum*) on arbuscular mycorrhiza and plant performance," *Mycorrhiza*, vol. 22, no. 7, pp. 493–499, 2012.
- [12] G. J. McDougall, "Accumulation of wall-associated peroxidases during wound-induced suberization of flax," *Journal of Plant Physiology*, vol. 142, no. 6, pp. 651–656, 1993.
- [13] M. R. Farahpour, H. Taghikhani, M. Habibi, and M. A. Zandieh, "Wound healing activity of flaxseed *Linum usitatissimum* L. in rats," *African Journal of Pharmacy and Pharmacology*, vol. 5, no. 21, pp. 2386–2389, 2011.
- [14] H. L. Bos, M. J. A. Van Den Oever, and O. C. J. J. Peters, "Tensile and compressive properties of flax fibres for natural fibre reinforced composites," *Journal of Materials Science*, vol. 37, no. 8, pp. 1683–1692, 2002.
- [15] L. P. F. Abbade and S. Lastoria, "Venous ulcer: epidemiology, physiopathology, diagnosis, and treatment," *International Journal of Dermatology*, vol. 44, no. 6, pp. 449–456, 2005.
- [16] K. Skórkowska-Telichowska, M. Zuk, A. Kulma et al., "New dressing materials derived from transgenic flax products to treat long-standing venous ulcers - a pilot study," *Wound Repair and Regeneration*, vol. 18, no. 2, pp. 168–179, 2010.
- [17] T. A. Gorshkova, S. E. Wyatt, V. V. Salnikov et al., "Cell-wall polysaccharides of developing flax plants," *Plant Physiology*, vol. 110, no. 3, pp. 721–729, 1996.
- [18] J. N. Cobb, G. Declerck, A. Greenberg, R. Clark, and S. McCouch, "Next-generation phenotyping: requirements and strategies for enhancing our understanding of genotype-phenotype relationships and its relevance to crop improvement," *TAG Theoretical and applied genetics Theoretische und angewandte Genetik*, vol. 126, no. 4, pp. 867–887, 2013.
- [19] M. Zuk, A. Prescha, M. Stryczewska, and J. Szopa, "Engineering flax plants to increase their antioxidant capacity and improve oil composition and stability," *Journal of Agricultural and Food Chemistry*, vol. 60, no. 19, pp. 5003–5012, 2012.
- [20] M. Fujisawa and N. Misawa, "Enrichment of carotenoids in flaxseed by introducing a bacterial Phytoene synthase gene," *Methods in Molecular Biology*, vol. 643, pp. 201–211, 2010.
- [21] K. Prasad, "Hypocholesterolemic and antiatherosclerotic effect of flax lignan complex isolated from flaxseed," *Atherosclerosis*, vol. 179, no. 2, pp. 269–275, 2005.
- [22] M. Żuk, A. Kulma, L. Dymińska et al., "Flavonoid engineering of flax potentiate its biotechnological application," *BMC Biotechnology*, vol. 11, no. 1, p. 10, 2011.
- [23] M. Czemplik, U. Korzun-Chłópicka, M. Szatkowski, M. Działo, J. Szopa, and A. Kulma, "Optimization of phenolic compounds extraction from flax shives and their effect on human fibroblasts," *Evidence-based Complementary and Alternative Medicine*, vol. 2017, Article ID 3526392, 2017.
- [24] N. I. Krinsky and E. J. Johnson, "Carotenoid actions and their relation to health and disease," *Molecular Aspects of Medicine*, vol. 26, no. 6, pp. 459–516, 2005.
- [25] M. Stryczewska, A. Kostyn, A. Kulma et al., "Flax fiber hydrophobic extract inhibits human skin cells inflammation and causes remodeling of extracellular matrix and wound closure activation," *BioMed Research International*, vol. 2015, Article ID 862391, 2015.
- [26] V. Antonov, J. Marek, M. Bjelkova, P. Smirous, and H. Fischer, "Easily available enzymes as natural retting agents," *Biotechnology Journal*, vol. 2, no. 3, pp. 342–346, 2007.
- [27] S. B. Gelvin, "Agrobacterium-mediated plant transformation: the biology behind the "gene-jockeying" tool," *Microbiology and Molecular Biology Reviews*, vol. 67, no. 1, pp. 16–37, 2003.

Research Article

The Regenerative Potential of Donkey and Human Milk on the Redox-Sensitive and Proliferative Signaling Pathways of Skin Fibroblasts

H. Kocic¹, T. Langerholm², M. Kostic³, S. Stojanovic³, S. Najman³, M. Krstic³, I. Nestic³, A. Godic⁴, and U. Wollina⁵

¹Clinic for Dermatology, University Clinical Center Faculty of Medicine, Nis, Serbia

²Faculty of Agriculture, University of Maribor, Maribor, Slovenia

³Medical Faculty, University of Nis, Nis, Serbia

⁴Department of Dermatology, University Hospital Lewisham, London SE13 6LH, UK

⁵Department of Dermatology and Allergology, Städtisches Klinikum Dresden, Dresden, Germany

Correspondence should be addressed to H. Kocic; hristinakyu@yahoo.com

Received 6 July 2020; Revised 11 September 2020; Accepted 14 October 2020; Published 11 November 2020

Academic Editor: Reggiani Vilela Gon alves

Copyright © 2020 H. Kocic et al. This is an open access article distributed under the Creative Commons Attribution License, which permits unrestricted use, distribution, and reproduction in any medium, provided the original work is properly cited.

The influence of milk bioactive peptides on skin regenerative potential and rejuvenation is very often limited because of allergic reactions. The current study is aimed at exploring the influence of donkey colostrum and mature milk, human colostrum and mature milk, and β -casein and β -casomorphine-7, on the growth and inflammatory response of the culture of cultured skin fibroblasts exposed to these conditions for twenty-four hours. Their effects on the growth-regulatory kinases and redox-sensitive, proinflammatory transcriptional factor NF- κ B were detected by using specific primary antibodies against NF- κ B p65, Akt-1, phospho-Akt-1, Erk-1, phospho-Erk-1, JNK, phospho-JNK, phospho-STAT-1, and CD26, while logarithmic integrated fluorescence intensity patterns were recorded by flow cytometry. The downregulation of NF- κ B p65 was observed after the exposure of skin fibroblasts to donkey milk and human colostrum, while β -casein and β -casomorphine-7 exerted the opposite effect, which suggests that noncasein bioactive peptides of donkey and human milk may be responsible for anti-inflammatory properties. The exposure to all milk species examined and β -casein leads to the activation of growth-regulatory kinases (Akt1/2/3 kinase, Erk kinase, JNK kinase, and Stat-1 kinase), especially for the p-Erk pathway, which suggests that essential amino acids of casein may be responsible for Erk-induced cell cycle activation and proliferation. The opposite effect was observed when cells were exposed to β -casomorphine-7, which may affect the skin fibroblast survival and their proliferative and regenerative potential. Donkey milk did not significantly change the CD26 antigen expression. In conclusion, our results suggest that among cell signaling molecules, the most sensitive but nonspecific downstream effector is p-Erk kinase, which may point to donkey milk usefulness in wound healing, regenerative, and aesthetic dermatology. The noncasein bioactive peptides of donkey milk may be responsible for the anti-inflammatory property of donkey milk and colostrum, which may indicate the usefulness in the treatment of inflammatory skin diseases.

1. Introduction

Skin fibroblasts exert a primary biological role in production and degradation of the extracellular matrix (ECM) [1–4]. The ECM consists of collagen, adhesive proteins, and other space-filling substances. Environmental and metabolic factors, immunological stimulators, UV irradiation, and other

epigenetic factors may modulate fibroblast regulatory kinases, oxidant-sensitive transcriptional factors, or apoptotic proteins signaling, having a profound influence on growth, differentiation, apoptosis, and systemic response. Inflammatory cytokines, mainly interleukins (IL-1 β , IL-6, IL-13, IL-33), prostaglandins, transforming factor- β (TGF- β), and leukotrienes, can induce a transition of skin

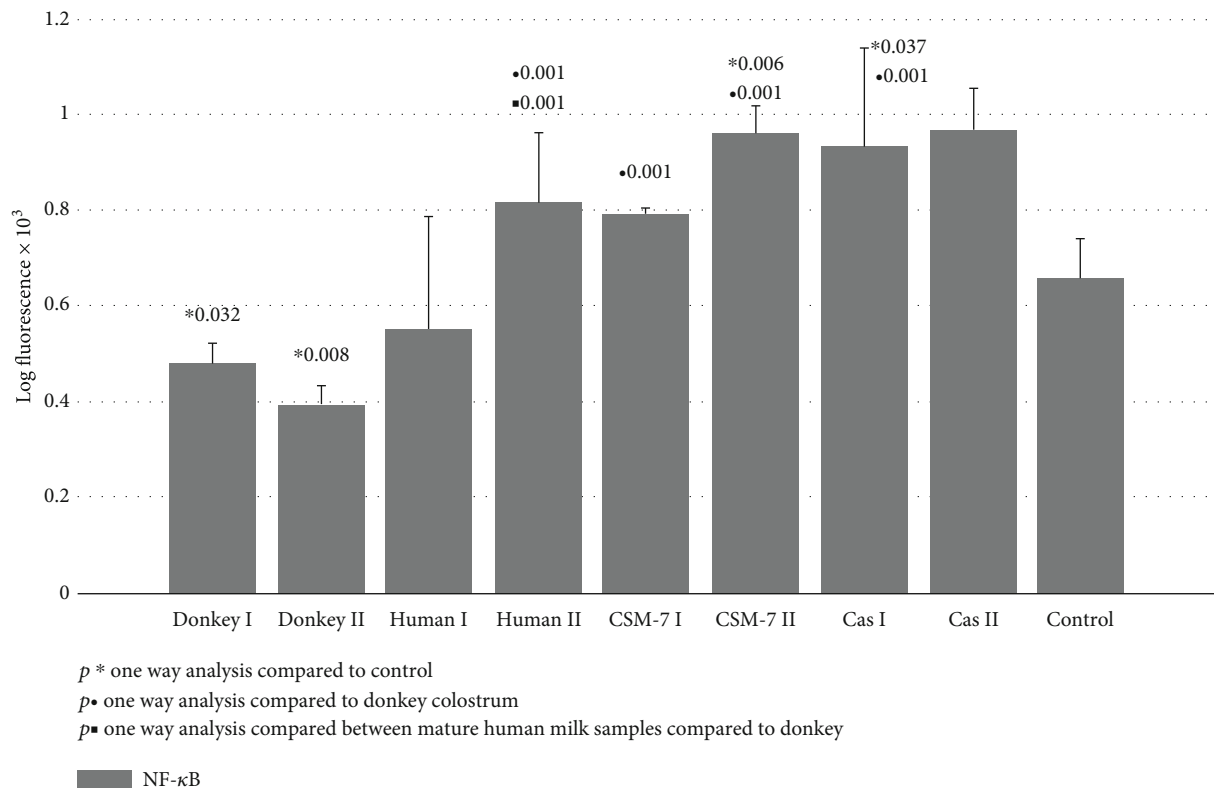


FIGURE 1: NF- κ B p65 signaling of skin fibroblast cultures exposed to different milk samples, β -casein, and β -casomorphine-7. Fibroblasts exposed to the following milk species: donkey colostrum (donkey 1); donkey mature milk (donkey 2); human colostrum (human 1); human mature milk (human 2); casein 1/10 (cas I); casein 1/100, (cas II); beta-casomorphine-7, 1/10, (CSM I); beta-casomorphine-7, 1/100 (CSM II); and control group. Each group comprised of 4-6 culture samples.

fibroblasts to myofibroblasts and may upregulate fibroblasts chemotaxis, collagen production, or secretion of their inflammatory cytokines and reactive oxygen species. Their uncontrolled stimulation may be harmful, resulting in an enormous fibrotic response or chronic systemic inflammation [5–7]. The identification and characterization of the cell-signaling pathways for skin fibroblast may be valuable in developing therapeutic approaches in skin regeneration and wound healing [8–10]. Additionally, the inhibition of some surface proteins with peptidase activity, such as the antigen CD26, may reduce skin scarring [11–14].

Among the growth-regulatory kinases, the key regulators of cellular metabolism, proliferation, regeneration, and differentiation are Akt kinase and the mitogen-activated protein kinases (MAPKs), mainly Erk kinases [15–19]. A family of JNK kinases and transcription factor NF- κ B can respond to different oxidative stress stimuli and to cytokine stimulation. Signal transducers and activators of transcription (Stat) represent a family of proteins, which can serve as transcription factors to a variety of growth factors and cytokines. The process of wound healing proceeds into three phases: inflammation, tissue formation, and tissue remodeling [20]. On the other hand, programmed cell death or apoptosis dysregulation may induce excessive scarring and fibrosis. Different cell signals may be involved in the induction of apoptosis controlling the tissue repair. In a wound healing process, both,

the production of growth factors and myofibroblast apoptosis, orchestrate the phases of tissue repair [21, 22].

Milk proteins provide an important source of bioactive peptides, which can demonstrate specific physiological functions and some of them hormone-like activities. These effects may be local or systemic [23]. So far, opiate, antithrombotic, antihypertensive, immunomodulatory, antioxidative, antimicrobial, anticancer, mineral-carrying, and growth-promoting properties have been reported. A low casein/whey protein ratio may play a role in preventing allergenic sensitization to constituent cows' milk proteins [24–29]. Low casein content may also decrease the presence and harmful effect of partially degraded bioactive casein derivatives, such as beta casomorphin-7 [23, 30, 31].

We hypothesized that the treatment of human fibroblasts with donkey milk and human milk, casein, and beta-casomorphine-7 might modulate their growth-regulatory kinases, redox-sensitive transcriptional nuclear factor kappa B (NF- κ B), and immunocompetent antigen CD26 expression through epigenetic mechanisms, which might have an influence on skin fibroblasts proliferative and inflammatory potential. We report the effect of different milk species on the expression of NF- κ B; Akt-1, 2, 3; phospho-Akt-1, 2, 3; Erk-1/2; phospho-Erk-1/2; JNK; phospho-JNK; phospho-Stat-1; and CD26 in L929 skin fibroblasts culture.

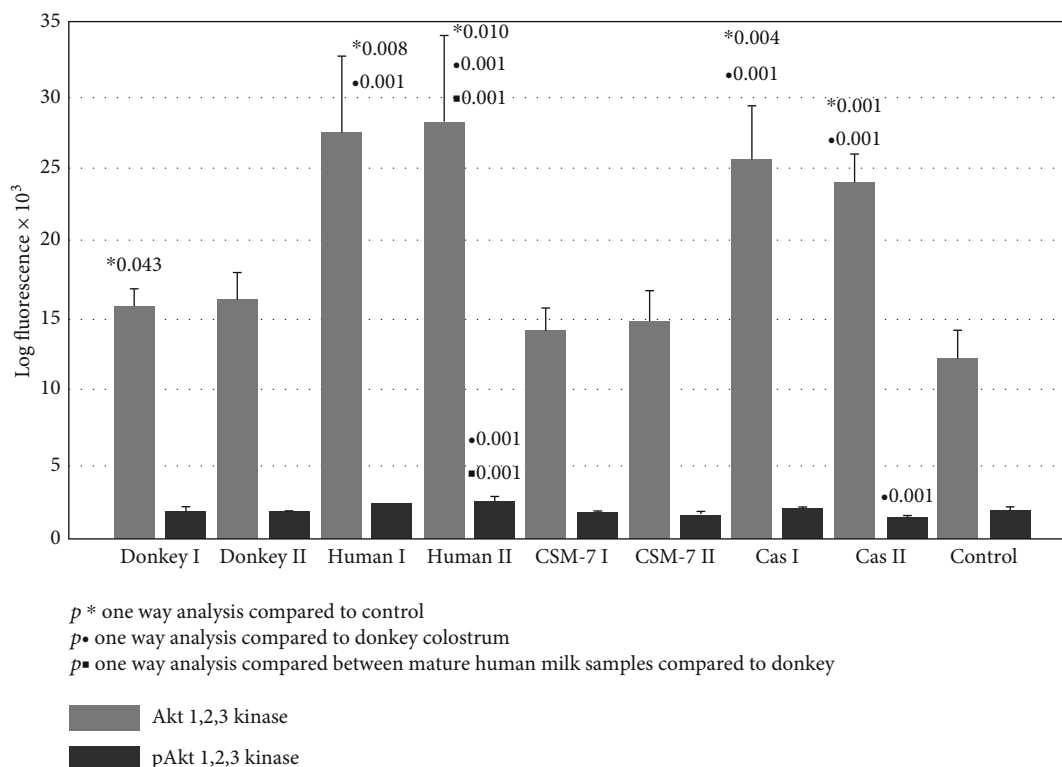


FIGURE 2: Akt1/2/3 kinase and p-Akt1/2/3 kinase signaling of skin fibroblast cultures exposed to different milk samples, β -casein, and β -casomorphine-7. Fibroblasts exposed to the following milk species: donkey colostrum (donkey 1); donkey mature milk (donkey 2); human colostrum (human 1); human mature milk (human 2); casein 1/10 (cas I); casein 1/100, (cas II); beta-casomorphine-7, 1/10, (CSM I); beta-casomorphine-7, 1/100 (CSM II); and control group. Each group comprised of 4-6 culture samples.

2. Materials and Methods

2.1. Milk Sample Collection. All milk samples were collected according to the stage of lactation and equilibrated to protein level. Donkey colostrum samples were collected from five donkeys (*Equus asinus asinus*) one day after the delivery. In addition, samples of mature milk were collected from the same animals three months after the delivery. Human breast milk was collected from five puerperal women who had delivered healthy infants at full-term without medical complications during pregnancies. Informed consents to participate in the study were also obtained. The first milk sample (colostrum) was collected immediately after the first appearance of milk; the second sample was collected one month afterwards. The milk samples collected were prepasteurized at 60°C for 5 min and kept at -17°C.

2.2. Cell Culture. Mouse skin fibroblasts (L929 fibroblast cell line) were purchased from the American Type Culture Collection (ATCC, Manassas, Virginia, USA). The cells were maintained in Dulbecco's Modified Eagle Medium (DMEM GibcoBRL, Rockville, MD, USA), supplemented with 10% fetal calf serum (FCS), 2 mM glutamine, 50 U/mL penicillin, and 50 μ g/mL streptomycin at 37°C in a 5% CO₂ incubator. The cells were plated in 24-well tissue culture dishes (2 × 10⁶ cells/well), using 1 mL of medium in each well. Forty-eight hours later, the milk samples, diluted 1/100 in

medium, were added to the wells and incubated at 37°C for further twenty-four hours. The concentration of β -casein and β -casomorphine-7 was calculated according to their approximate dose in milk and diluted 1/10 (dose I) and 1/100 (dose II) [32]. The groups of fibroblasts examined were treated with the following milk/protein samples: donkey colostrum (donkey 1); donkey mature milk (donkey 2); human colostrum (human 1); human mature milk (human 2); casein 1/10, i.e., 2.4 mg/mL of medium (cas I); casein 1/100, i.e., 0.24 mg/mL of medium (cas II); beta-casomorphine-7, 1/10, i.e., 3 μ g/mL of medium (CSM I); beta-casomorphine-7, 1/100, i.e., 0.3 μ g/mL of medium (CSM II), and control group maintained in above mentioned culture conditions (DMEM supplemented with 10% FCS, 2 mM glutamine, 50 U/mL penicillin, and 50 μ g/mL streptomycin). Each group consisted of 4-6 culture samples.

2.3. Flow Cytometry. Specific primary antibodies against NF- κ B p65 (sc-372), Akt-1 (sc-56878), phospho-Akt-1 (sc-135651), Erk-1 (sc-135900), phospho-Erk-1 (sc-136521), JNK (sc-7345), phospho-JNK (sc-293137), phospho-STAT-1 (sc-51700), and CD26 (sc-9153) were purchased from Santa Cruz Biotechnology (Santa Cruz, CA, USA). As a staining control, a mouse IgG was used in combination with a FITC-goat-anti-mouse secondary antibody. Cells were fixed in 4% formaldehyde and permeabilized with 0.1% Triton X-100 in PBS (pH 7.4). To avoid any nonspecific binding

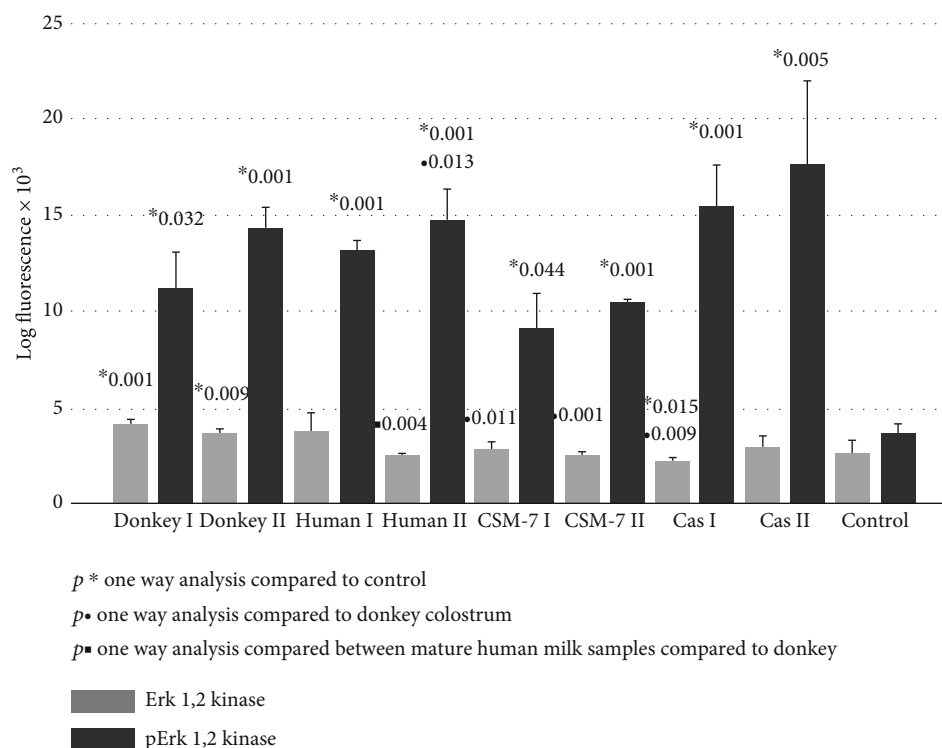


FIGURE 3: Erk1/2 kinase and p-Erk1/2 kinase signaling of skin fibroblast cultures exposed to different milk samples, β -casein, and β -casomorphine-7. Fibroblasts exposed to the following milk species: donkey colostrum (donkey 1); donkey mature milk (donkey 2); human colostrum (human 1); human mature milk (human 2); casein 1/10 (cas I); casein 1/100, (cas II); beta-casomorphine-7, 1/10, (CSM I); beta-casomorphine-7, 1/100 (CSM II); and control group. Each group comprised of 4-6 culture samples.

and background fluorescence during immunostaining, the cells were incubated with specific primary antibodies at 4°C in PBS containing 1% BSA overnight. After that, they were washed and incubated at room temperature for 1 h with corresponding FITC-conjugated secondary antibodies (goat anti-mouse IgG, sc-2010, mouse anti-goat IgG, sc-2354, and goat anti-rabbit IgG, sc-2012), purchased from Santa Cruz Biotechnology (CA, USA). The cells were then analyzed for corresponding cell signaling molecules by flow cytometry on a LSR BD Fortessa Flow cytometer. The obtained logarithmic integrated fluorescence intensity patterns were recorded and analyzed by software BD FACSDiva™, version 8.0.

2.4. Cell Viability Assay. Skin fibroblast cell lines were seeded in 96-well plates (Greiner Bio-One, Frickenhausen Germany) at a density of 2×10^4 cells per well. Twenty-four hours later, diluted sterile milk samples, β -casomorphine-7, and β -casein were added to the cells. Cell viability was tested by using the Trypan Blue Dye Exclusion method. The percentage of viable cells was calculated according to the following obtained absorbance (ABS):

$$\% \text{ cell viability} = (\text{ABS value of treated cells} / \text{ABS value of control cells}) \times 100$$

2.5. Statistical Analysis. All data are presented as mean \pm SD. Statistical analysis was performed using one-way analysis of variance ANOVA, SPSS version 20.0 ($p < 0.05$; statistically significant). *Post hoc* test was carried out to determine the differences: (a) between the means of treated groups and con-

trol group, (b) between the means of donkey colostrum and other groups, and (c) between the means of the groups of mature milk for each of 11 parameters (NF- κ B, Akt1/2/3, p-Akt1/2/3, Erk-1/2, p-Erk-1/2, JNK, p-JNK, p-STAT-1, and CD26).

3. Results

In this study, we investigated whether the exposure of skin fibroblasts to different milk species, β -casein, and β -casomorphine-7 affects cell viability, inflammatory response, and proliferative pathways.

3.1. MTT Assay. The MTT assay explored cellular metabolic activity and cell viability. Based on or experimental MTT assay data, none of the milk species and peptides cultured with skin fibroblasts exerted a significant influence on cell viability, except β -casomorphine-7.

3.2. Flow Cytometric Analyses. Significant downregulation of NF- κ B p65 subunit expression was detected in skin fibroblasts exposed to donkey milk samples (colostrum and mature milk), compared to the intact fibroblasts. On the other hand, its quantitative expression was especially pronounced in fibroblasts, exposed to β -casomorphine-7 and β -casein I (Figure 1).

Significant upregulation of Akt1/2/3 kinase after fibroblasts exposure to the above mentioned milk species and β -casein was documented. The activity of its active

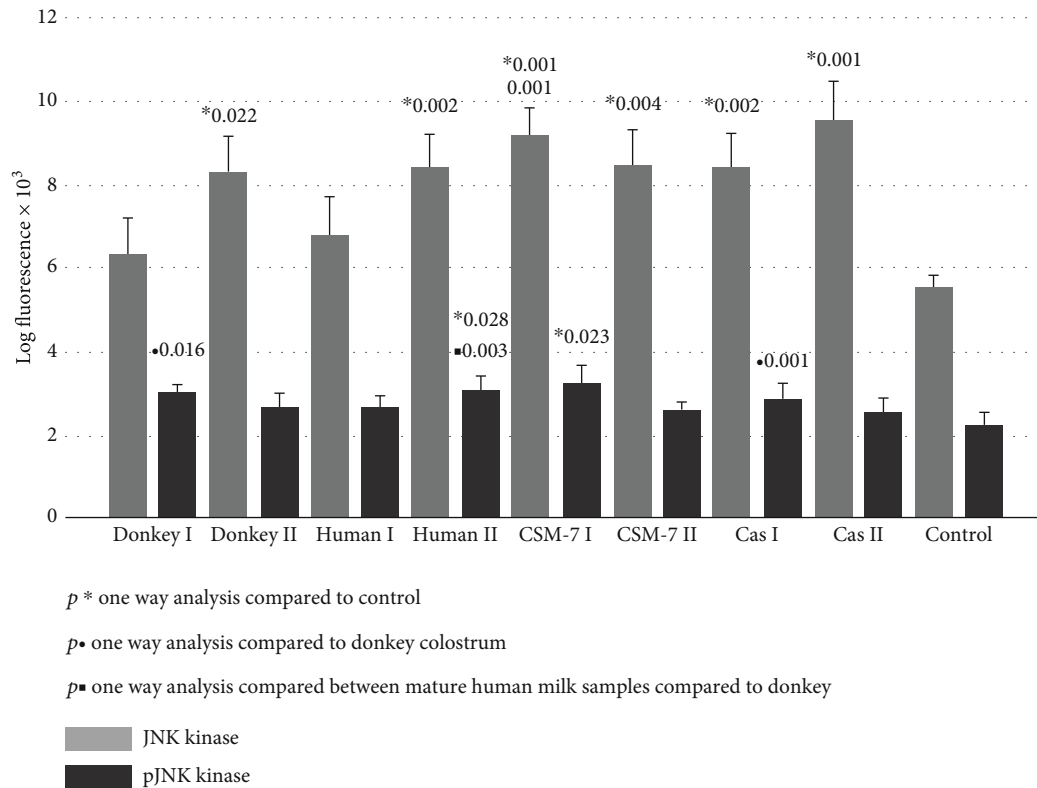


FIGURE 4: JNK kinase and p-JNK kinase signaling of skin fibroblast cultures exposed to different milk samples, β -casein, and β -casomorphine-7. Fibroblasts exposed to the following milk species: donkey colostrum (donkey 1); donkey mature milk (donkey 2); human colostrum (human 1); human mature milk (human 2); casein 1/10 (cas I); casein 1/100, (cas II); beta-casomorphine-7, 1/10, (CSM I); beta-casomorphine-7, 1/100 (CSM II); and control group. Each group comprised of 4-6 culture samples.

phosphorylated form (p-Akt1/2/3) did not increase significantly (Figure 2). Contrary to Akt1/2/3 kinase, the Erk1/2 kinase active-phosphorylated form (p-Erk1/2) was upregulated almost three to four times in all treated groups. The most remarkable effect of about fivefold increase was observed after β -casein treatment (Figure 3).

Figure 4 represents the quantitative expression of proliferative downstream signaling pathway of the JNK kinase. All investigated treatments upregulated JNK kinase and p-JNK kinase up to 45%. A significant decrease in activated Stat-1 kinase (p-Stat-1) expression was documented following a fibroblasts' culture treatment with mature donkey and cow milk (Figure 5). The quantitative expression of surface antigen CD26 was significantly upregulated after treatment with human milk (Figure 5).

4. Discussion

The human skin is the largest organ of the body, continuously exposed to a variety of environmental influences. Such influences may induce skin aging, inflammation, or serious damage to the skin. The main challenges in treatment of chronic wounds are to stimulate skin regeneration, to decrease inflammation, and to preserve the skin smoothness and elasticity [4, 8–12]. Skin fibroblasts play a key role in the production of extracellular matrix, collagen, and elastin [4, 9]. Milk treatment can soothe irritated skin, can hydrate

dry skin, and can replenish lost nutrients. It has been reported that skin wrinkles were treated with implanted autologous fibroblasts, which resulted in a significant improvement in periorbital skin flaccidity [33–35].

Donkey milk has been famous throughout history for its nutritional, therapeutic, and cosmetic properties [23, 24]. Both colostrum and milk from donkeys may be useful in the treatment of human immune-related diseases [26–28]. The low allergenicity of donkey's milk may be due to its low casein content, since the main allergens in cow's milk are caseins (α s1 and β type). The proportion of noncasein (whey) proteins is 35-50% in donkey milk, while in cow's milk these proteins represent about 20% [25, 30, 31]. Since fibroblasts may actively participate in inflammatory and immune responses, we evaluated the expression of the main redox-sensitive transcription factor activation, activator of inflammatory response, and the NF- κ B-p65 subunit. The expression of its active p65 subunit decreased significantly after donkey milk treatment but increased after the treatment with β -casein and β -casomorphine-7 (Figure 1). This suggests that noncasein bioactive peptides of donkey milk may be responsible for anti-inflammatory property of donkey milk and colostrum [36]. It has been reported that free radical activation of NF- κ B may occur under the stimulation of fibroblasts with cytokines (TNF- α and IL-1), bacterial TLR-4 activating product lipopolysaccharide (LPS), reactive oxygen species (ROS), and other DNA-damaging agents.

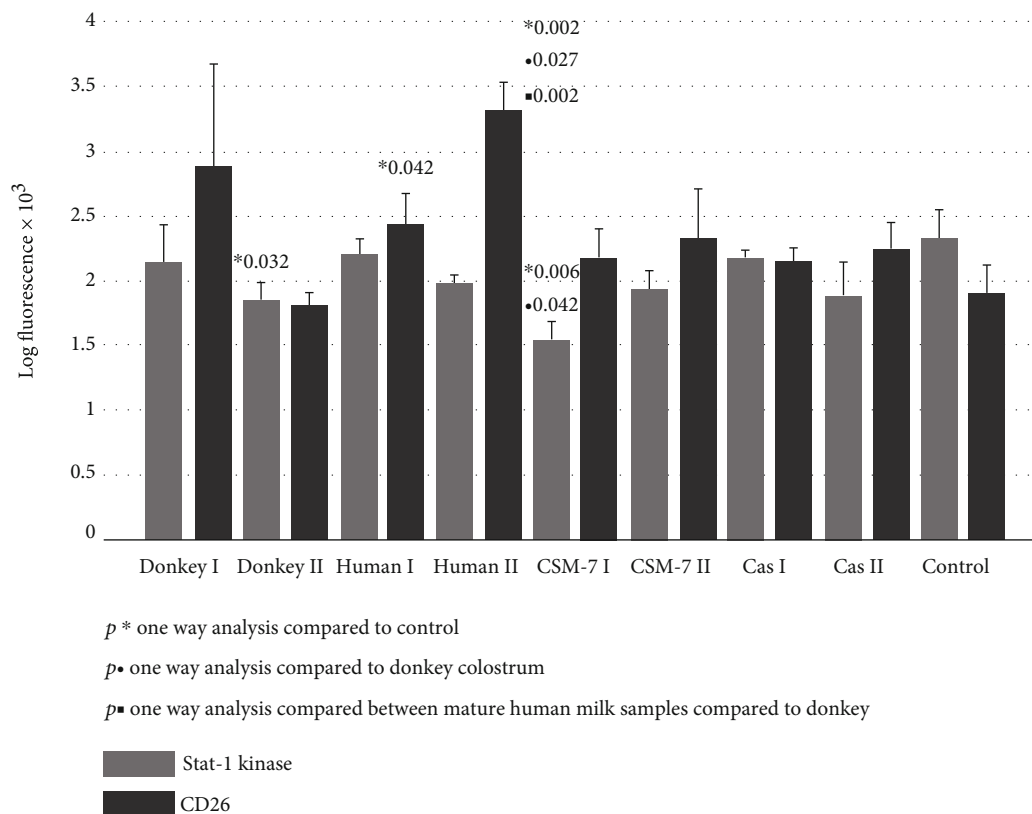


FIGURE 5: p-STAT-1 kinase and CD26 signaling of skin fibroblast cultures exposed to different milk samples, β -casein, and β -casomorphine-7. Fibroblasts exposed to the following milk species: donkey colostrum (donkey 1); donkey mature milk (donkey 2); human colostrum (human 1); human mature milk (human 2); casein 1/10 (cas I); casein 1/100, (cas II); beta-casomorphine-7, 1/10, (CSM I); beta-casomorphine-7, 1/100 (CSM II); and control group. Each group comprised of 4-6 culture samples.

Activated NF- κ B may induce the expression of inflammatory cytokines, matrix-metalloproteinases (MMP), and collagenases, responsible for ECM destruction [32, 33]. The overexpression of NF- κ B is involved in fibroblast apoptosis, together with the increased Bax ratio [33]. Our results suggest that donkey milk may ameliorate free-radicals induced inflammatory skin disorders through the NF- κ B active p65 unit suppression of the skin fibroblasts.

In our study, we further investigated a possible favorable effect of donkey milk, compared to casein and β -casomorphine-7 and to human milk species, on skin fibroblasts' proliferative potential. We demonstrated that among the kinase pathways, the most susceptible was Erk1/2 kinase (Figure 3), which was upregulated in all tested samples at least three times. Intracellular signaling pathways responsible for survival, proliferation, and differentiation consist of a family of different serine/threonine/tyrosine kinases, uniquely activated by dual phosphorylation of corresponding residues upon stimulation by growth factors, cytokines, hormones, or other mitogens. MAP kinases are grouped into three families, which are extracellular-signal-regulated kinases (Erks), Jun amino-terminal kinases (JNKs), and stress-activated protein kinases (p38/SAPKs) [15–17]. The activation of Erk kinase occurs by phosphorylation of Thr202/Tyr204 motifs. Once activated, p-Erk may activate about 150 downstream cell-signaling proteins, responsible

for survival, cell cycle activation, proliferation, differentiation, and cell metabolism [17–19, 37]. The activation of Erk-1/2 is able to inhibit apoptosis induced by oxidative stress, osmotic stress, hypoxia, or by growth factor withdrawal. It occurs by external Fas death receptors and TNF-related apoptosis inducing ligand (TRAIL) [38]. In addition, Erk activity is reduced in the adult skin compared to young individuals [39]. All tested milk species and β -casein were able to potentiate p-Erk pathway, which may suggest that the essential amino acids of casein may be responsible for Erk-induced cell cycle activation, proliferation, differentiation, and cell metabolism. Akt kinase family includes serine/threonine kinases, which play a fundamental role in regulating cell metabolism, proliferation, and survival. Their continual activation may lead to the development of cancer phenotype, while Akt1/2 knockout mice, which have dwarfism and skin, muscular, and bone atrophy, die immediately after birth [38]. Serine/threonine phosphorylation is needed for full Akt kinase activation, but in our study, we detected only pAkt1/2/3 activation after exposure to human milk and β -casein (Figure 2). In addition, we found that increase of JNK and the p-JNK pathways is far less than that of p-Erk (Figure 4), indicating that stimulation is shifted in favor of the Erk activity. The phosphorylation of JNK at Thr183 and 185 positions is required for its full activation. It has been reported that JNK takes part in biosynthesis of ECM,

remodeling of fibroblasts into myofibroblasts, and matrix contraction after stimulation by inflammatory cytokines and growth factors [40–42]. In addition to MAP kinases, several members of the signal transducers and activators (Stat), which belong to a family of transcription factors, especially Stat-1, may be recruited by growth hormone stimulation. The results of our study suggest that the Stat signaling pathway was suppressed after exposure to donkey milk and β -casomorphine-7 (Figure 5). Fibroblasts act as antigen-presenting cells in a number of immune and inflammatory reactions, by expressing various antigens on their surface, by secreting inflammatory cytokines (IL-1, IL-6, TNF- α , and GM-CSF) and chemokines (IL-8, RANTES, eotaxin, and MCP). Surface antigen CD26, which exerts dipeptidyl peptidase-4 (DPP4) activity, is a typical marker for fibroblast lineage. Its importance in fibrosis and scar prevention was documented by using specific inhibitors against DPP-4 [8]. No significant increase in the CD26 expression was observed after the cells were exposed to donkey milk, what consistently correlates with an absence of inflammatory response in skin fibroblasts (Figure 5).

Possible limitations of the study lie in the fact that the metabolic properties of fibroblast cell culture may vary in early and late cell generations, showing *in vitro* senescence, ageing, and differentiation [43].

In conclusion, the downregulation of the redox-sensitive inflammatory transcription factor NF- κ B pathway observed after skin fibroblast exposure to donkey milk may suggest that noncasein bioactive peptides of donkey milk may be responsible for the anti-inflammatory properties. This may suggest usefulness in the treatment of inflammatory skin diseases. Another important finding of our study is that among cell signaling molecules, the most sensitive downstream effector is p-Erk kinase. Stimulated p-Erk pathway may point to donkey milk usefulness in wound healing, regenerative, and aesthetic dermatology.

Data Availability

All data used were included within the article.

Disclosure

Presented results are a part of the thesis: Kocic Hristina: Effects of milk, milk-derived bioactive peptides and L-arginine on cell signaling in skin fibroblasts (<https://dk.um.si/Dokument.php?dn=&id=131016>) (University Maribor-Medical Faculty 2018).

Conflicts of Interest

The authors declare that there is no conflict of interest.


References

- [1] M. Babu, "Dermal-epidermal communication in wound healing," *Wounds*, vol. 13, pp. 183–189, 2001.
- [2] G. Gabbiani, "The myofibroblast in wound healing and fibrocontractive diseases," *The Journal of Pathology*, vol. 200, no. 4, pp. 500–503, 2003.
- [3] T. J. Shaw and P. Martin, "Wound repair: a showcase for cell plasticity and migration," *Current Opinion in Cell Biology*, vol. 42, pp. 29–37, 2016.
- [4] L. E. Tracy, R. A. Minasian, and E. J. Caterson, "Extracellular matrix and dermal fibroblast function in the healing wound," *Adv Wound Care (New Rochelle)*, vol. 5, no. 3, pp. 119–136, 2016.
- [5] Y. Asano, "Recent advances in animal models of systemic sclerosis," *The Journal of Dermatology*, vol. 43, no. 1, pp. 19–28, 2016.
- [6] S. J. Flavell, T. Z. Hou, S. Lax, A. D. Filer, M. Salmon, and C. D. Buckley, "Fibroblasts as novel therapeutic targets in chronic inflammation," *British Journal of Pharmacology*, vol. 153, no. S1, pp. S241–S246, 2008.
- [7] P. Fuschiotti, "Role of IL-13 in systemic sclerosis," *Cytokine*, vol. 56, no. 3, pp. 544–549, 2011.
- [8] Y. Rinkevich, G. G. Walmsley, M. S. Hu et al., "Skin fibrosis. Identification and isolation of a dermal lineage with intrinsic fibrogenic potential," *Science*, vol. 348, no. 6232, p. aaa2151, 2015.
- [9] L. Baumann, "Skin ageing and its treatment," *The Journal of Pathology*, vol. 211, no. 2, pp. 241–251, 2007.
- [10] T. Krieg and M. Heckmann, "Regulatory mechanisms of fibroblast activity," *Recenti Progressi in Medicina*, vol. 80, no. 11, pp. 594–598, 1989.
- [11] T. D. Geppert and P. E. Lipsky, "Antigen presentation by interferon γ -treated endothelial cells and fibroblasts: differential ability to function as antigen presenting despite comparable la expression," *Journal of Immunology*, vol. 135, pp. 3750–3762, 1985.
- [12] R. S. Smith, T. J. Smith, T. M. Blieden, and R. P. Phipps, "Fibroblasts as sentinel cells. Synthesis of chemokines and regulation of inflammation," *Journal of Immunology*, vol. 151, pp. 317–322, 1997.
- [13] H. Takada, J. Mihara, I. Morisaki, and S. Hamada, "Induction of interleukin-1 and -6 in human gingival fibroblast cultures stimulated with *Bacteroides* lipopolysaccharides," *Infection and Immunity*, vol. 59, no. 1, pp. 295–301, 1991.
- [14] R. R. Patil and R. F. Borch, "Granulocyte-macrophage colony-stimulating factor expression by human fibroblasts is both upregulated and subsequently downregulated by interleukin-1," *Blood*, vol. 85, no. 1, pp. 80–86, 1995.
- [15] M. Abdalla, A. Goc, L. Segar, and P. R. Somanath, "Akt1 mediates α -smooth muscle actin expression and myofibroblast differentiation via myocardin and serum response factor," *The Journal of Biological Chemistry*, vol. 288, no. 46, pp. 33483–33493, 2013.
- [16] J. Q. Cheng, C. W. Lindsley, G. Z. Cheng, H. Yang, and S. V. Nicosia, "The Akt/PKB pathway: molecular target for cancer drug discovery," *Oncogene*, vol. 24, no. 50, pp. 7482–7492, 2005.
- [17] Z. Lu and S. Xu, "ERK1/2 MAP kinases in cell survival and apoptosis," *Life*, vol. 58, no. 11, pp. 621–631, 2006.
- [18] R. K. Bhogal and C. A. Bona, "Regulatory Effect of Extracellular Signal-Regulated Kinases (ERK) on Type I Collagen Synthesis in Human Dermal Fibroblasts Stimulated by IL-4 and IL-13," *International Reviews of Immunology*, vol. 27, no. 6, pp. 472–496, 2009.
- [19] Z. Xia, M. Dickens, J. Raingeaud, R. J. Davis, and M. E. Greenberg, "Opposing effects of ERK and JNK-p38 MAP kinases on apoptosis," *Science*, vol. 270, no. 5240, pp. 1326–1331, 1995.

- [20] Y.-S. Wu and S.-N. Chen, "Apoptotic cell: linkage of inflammation and wound healing," *Frontiers in Pharmacology*, vol. 5, 2014.
- [21] D. G. Greenhalgh, "The role of apoptosis in wound healing," *The International Journal of Biochemistry & Cell Biology*, vol. 30, no. 9, pp. 1019–1030, 1998.
- [22] S. E. Wilson, S. S. Chaurasia, and F. W. Medeiros, "Apoptosis in the initiation, modulation and termination of the corneal wound healing response," *Experimental Eye Research*, vol. 85, no. 3, pp. 305–311, 2007.
- [23] F. Tidona, A. Criscione, A. M. Guastella, A. Zuccaro, S. Bordonaro, and D. Marletta, "Bioactive peptides in dairy products," *Italian Journal of Animal Science*, vol. 8, no. 3, pp. 315–340, 2016.
- [24] E. Salimei and F. Fantuz, "Equid milk for human consumption," *International Dairy Journal*, vol. 24, no. 2, pp. 130–142, 2012.
- [25] S. Vincenzetti, P. Polidori, P. Mariani, N. Cammertoni, F. Fantuz, and A. Vita, "Donkey's milk protein fractions characterization," *Food Chemistry*, vol. 106, no. 2, pp. 640–649, 2008.
- [26] A. Carroccio, F. Cavataio, G. Montalto, D. D'Amico, L. Alabrese, and G. Iacono, "Intolerance to hydrolysed cow's milk proteins in infants: clinical characteristics and dietary treatment," *Clinical & Experimental Allergy*, vol. 30, no. 11, pp. 1598–1603, 2000.
- [27] S. Vincenzetti, L. Foghini, S. Pucciarelli et al., "Hypoallergenic properties of donkey's milk: a preliminary study," *Veterinaria Italiana*, vol. 50, no. 2, pp. 99–107, 2014.
- [28] E. Bertino, "Detailed proteomic analysis on DM: insight into its hypoallergenicity," *Frontiers in Bioscience*, vol. E2, no. 2, pp. 526–536, 2010.
- [29] G. Monti, S. Viola, C. Baro et al., "Tolerability of donkey's milk in 92 highly-problematic cow's milk allergic children," *Journal of Biological Regulators and Homeostatic Agents*, vol. 26, Suppl 3, pp. 75–82, 2012.
- [30] A. S. Egitto, L. Miclo, C. Lopez, A. Adam, J. M. Girardet, and J. L. Gaillard, "Separation and characterization of mares' milk α 1-, β -, κ -caseins, γ -casein-like, and proteose peptone component 5-like peptides," *Journal of Dairy Science*, vol. 85, no. 4, pp. 697–706, 2002.
- [31] V. Cunsolo, E. Cairone, R. Saletti, V. Muccilli, and S. Foti, "Sequence and phosphorylation level determination of two donkey β -caseins by mass spectrometry," *Rapid Communications in Mass Spectrometry*, vol. 23, no. 13, pp. 1907–1916, 2009.
- [32] I. De Noni, R. J. FitzGerald, H. J. T. Korhonen et al., "Review of the potential health impact of β -casomorphins and related peptides," *EFSA Sci Report*, vol. 231, pp. 1–107, 2009.
- [33] S. Tavakol, S. Zare, E. Hoveizi, B. Tavakol, and S. M. Rezaayat, "The impact of the particle size of curcumin nanocarriers and the ethanol on beta_1-integrin overexpression in fibroblasts: a regenerative pharmaceutical approach in skin repair and anti-aging formulations," *Daru*, vol. 27, no. 1, pp. 159–168, 2019.
- [34] D. V. Messadi, H. S. Doung, Q. Zhang et al., "Activation of NFkappaB signal pathways in keloid fibroblasts," *Archives of Dermatological Research*, vol. 296, no. 3, pp. 125–133, 2004.
- [35] L. P. Eça, D. G. Pinto, A. M. S. de Pinho, M. P. V. Mazzetti, and M. E. Y. Odo, "Autologous fibroblast culture in the repair of aging skin," *Dermatologic Surgery*, vol. 38, 2 Part 1, pp. 180–184, 2012.
- [36] H. Kocic, *Effets of milk, milk-derived bioactive peptides and L-arginine on cell signaling in skin fibroblasts*, University Maribor Medical Faculty, 2018, UDK 613.287+637.12:577.112:576.311.3(043.3) <https://dk.um.si/Dokument.php?dn=&id=131016>.
- [37] H. K. Koul, M. Pal, and S. Koul, "Role of p38 MAP Kinase Signal Transduction in Solid Tumors," *Genes & Cancer*, vol. 4, no. 9–10, pp. 342–359, 2013.
- [38] X. D. Peng, P. Z. Xu, M. L. Chen et al., "Dwarfism, impaired skin development, skeletal muscle atrophy, delayed bone development, and impeded adipogenesis in mice lacking Akt1 and Akt2," *Genes & Development*, vol. 17, no. >11, pp. 1352–1365, 2003.
- [39] Y. H. Jang, G.-B. Koo, J.-Y. Kim, Y.-S. Kim, and Y. C. Kim, "Prolonged Activation of ERK Contributes to the Photorejuvenation Effect in Photodynamic Therapy in Human Dermal Fibroblasts," *Journal of Investigative Dermatology*, vol. 133, no. 9, pp. 2265–2275, 2013.
- [40] R. J. Davis, "Signal transduction by the JNK group of MAP kinases," *Cell*, vol. 103, no. 2, pp. 239–252, 2000.
- [41] L. Chang and M. Karin, "Mammalian MAP kinase signalling cascades," *Nature*, vol. 410, no. 6824, pp. 37–40, 2001.
- [42] D. Javelaud, J. Laboureau, E. Gabison, F. Verrecchia, and A. Mauviel, "Disruption of basal JNK activity differentially affects key fibroblast functions important for wound healing," *The Journal of Biological Chemistry*, vol. 278, no. 27, pp. 24624–24628, 2003.
- [43] P. Van Gansen and N. Van Lerberghe, "Potential and limitations of cultivated fibroblasts in the study of senescence in animals. A review on the murine skin fibroblasts system," *Archives of Gerontology and Geriatrics*, vol. 7, no. 1, pp. 31–74, 1988.

Research Article

Antioxidant and Antimicrobial Potentials of Seed Oil from *Carthamus tinctorius L.* in the Management of Skin Injuries

Ikram Khémiri ¹, **Badiaa Essghaier**,² **Najla Sadfi-Zouaoui**,² and **Lotfi Bitri**¹

¹Unité de Physiologie des Systèmes de Régulations et des Adaptations, Faculté des Sciences de Tunis, Université de Tunis El Manar, Campus Universitaire, 2092 Tunis, Tunisia

²Laboratoire de Mycologie, Pathologies et Biomarqueurs, Faculté des Sciences de Tunis, Université de Tunis El Manar, Campus Universitaire, 2092 Tunis, Tunisia

Correspondence should be addressed to Ikram Khémiri; ikram.khemiri@fst.utm.tn

Received 16 July 2020; Accepted 20 October 2020; Published 5 November 2020

Academic Editor: Reggiani Vilela Gon alves

Copyright © 2020 Ikram Khémiri et al. This is an open access article distributed under the Creative Commons Attribution License, which permits unrestricted use, distribution, and reproduction in any medium, provided the original work is properly cited.

Infection of skin injuries by pathogenic microbial strains is generally associated if not treated with a lasting wound bed oxidative stress status, a delay in healing process, and even wound chronicity with several human health complications. The aim of the current study was to explore the antioxidant and antimicrobial potentialities of safflower (*Carthamus tinctorius L.*) extracted oil from seeds by cold pressing which would be beneficial in the management of skin wounds. Antioxidant capacity of the oil was evaluated (scavenging ability against 1,1-diphenyl-2-picrylhydrazyl radical (DPPH) and 2,2'-azino-bis 3-ethylbenzothiazoline-6-sulfonic acid (ABTS), and ferric reducing antioxidant power (FRAP)). Total phenolic, total flavonoid, total carotenoid, and total chlorophyll contents were determined. Antimicrobial activities of safflower oil were tested against 10 skin pathogenic microorganisms: 4 bacterial strains (*Escherichia coli*, *Enterobacter cloacae*, *Staphylococcus aureus*, and *Streptococcus agalactiae*), 3 yeast species strains (*Candida albicans*, *Candida parapsilosis*, and *Candida sake*), and 3 fungi species (*Aspergillus niger*, *Penicillium digitatum*, and *Fusarium oxysporum*). A notable antioxidant capacity was demonstrated for the tested oil that exhibited moreover high antibacterial effects by both bacteriostatic and bactericidal pathways including lysozyme activity. An antifungal effect was further observed on the spore's germination. Safflower oil could be considered as a good natural alternative remedy in the management of skin wounds and their possible microbial infections.

1. Introduction

The skin is one of the most important organs in the human body in weight, surface, and function. Mainly, it ensures a physical protection from mechanical and chemical trauma added to an immunological defence against environmental microbiota. The loss of parts or all of the skin layers (epidermis and dermis) causes a breakdown of the protective function of this organ. The most common skin injuries are erosions, lacerations, punctures, surgical wounds, ulcers, and burns. Wound healing process main target is to restore the integrity of the skin barrier and thus preserve the body's health [1]. Despite the fact that acute skin injuries can heal spontaneously within a few days, it is mandatory in several

cases to take care of the wounds in order to help the process along and avoid infections and complications which can range from minor self-limited infections [2] to life-threatening invasive clinical diseases [3–5].

Untreated skin wound infections have been reported to be detrimental to the healing process, inducing wound chronicity, morbidity, and even mortality [6–8]. This is of wide concern in public health, especially in geriatrics [9, 10]. Diabetic, pressure, and vascular ulcers are the major forms of chronic wounds [11, 12]. Due to peripheral vascular disease, reduced blood flow and thus reduced tissue nutrition and oxygenation can lead to increased vulnerability of the skin to pathogens from the surrounding microbiota [9, 12]. Poorly treated decubitus ulcers in bedridden or elderly

patients can even cause sepsis, especially in nosocomial infections. This is due to the fact that older adults are more likely to develop infectious complications [13, 14].

Several studies have reported that the colonization of the wound bed with opportunistic skin pathogenic strains (bacteria, yeast, and fungi) is commonly associated with infections and a delay of wound closure [15–17]. Bacteria belonging to the genera *Staphylococcus*, *Enterococcus*, *Enterobacter*, *Escherichia*, and *Streptococcus* have been reported to be associated with skin infections in the case of postsurgical complications, certain burns (especially second- and third-degree burns), and diabetic foot ulcers and bedsores [18–22]. They have been related to produce biofilms which are sometimes persistent and hard to treat and eradicate [23–25]. Other studies have also shown the involvement of other microorganisms such as yeasts of the genus *Candida* and fungi of the genera *Aspergillus*, *Fusarium*, and *Penicillium* in the infection of skin wounds and the impairment of the wound healing process [16, 22, 26, 27].

Over the recent past decades, the widespread use and overconsumption of systemic and topical medicines have led to the emergence of drug-resistant microbial strains [28, 29] such as methicillin-resistant *Staphylococcus aureus* [14, 30–32] and multiresistant *Candida* species [33] which caused serious public health problems.

The cutaneous wound healing is a dynamic and definite organized process which can be divided into four major overlapping steps: hemostasis to stop local hemorrhage after blood capillary rupture, inflammation to fight contaminating microorganisms, angiogenesis and reepithelialization to close the wound, and finally maturation and remodeling of the scar. Since the early phases of the inflammatory process, the wound bed is invaded by inflammatory cells such as neutrophils followed by lymphocytes and monocytes. They release prooxidant mediators such as reactive oxygen species (ROS) like hydroxyl radical ($\text{OH}^{\cdot-}$), hydroxyl peroxide (H_2O_2), and superoxide radical anion ($\text{O}_2^{\cdot-}$) and reactive nitrogen species (RNS) such as nitric oxide (NO) in sufficient amounts in order to create a molecular microenvironment beneficial to microbial cell lysis [3, 34–36]. After that, several antioxidants are released in the wound bed to counteract the prooxidant factors thanks to their free-radical scavenging properties and thus quench damage caused by oxidative stress which leads to disturbances in cell physiology (lipids, proteins, carbohydrates, and DNA) and even to necrosis. Insufficient amounts of endogenous antioxidants especially in elderly and/or immune-depressed patients with underlying pathologies could compromise the healing process and lead to wound chronicity and complications.

Various beneficial health effects of herbal extracts have been proven and used since antiquity and continue to be so nowadays. There is a worldwide growing interest of researchers to prospect new pharmaceutical approaches, mainly based on ethnopharmacological relevance bioactive compounds, that can be extracted from all parts of plants (flowers, fruits, leaves, stems, roots, and seeds) [37–39]. Several studies have reported the effectiveness of nontoxic plant extracts in wound healing [40–45].

Fixed vegetable oils extracted from seeds are natural extracts rich in several active biocompounds such as fatty acids, vitamins, and sterols [46]. The investigation of potential effects of fixed vegetable oils and their different components in the healing of skin wounds has attracted the interest of several researchers around the world [47–52].

Safflower (*Carthamus tinctorius L.*), a member of the *Asteraceae* family, is a thistle-like herbaceous annual plant. It can withstand arid or semiarid climates with seasonal rainfall. Its orange-colored flowers are rich in carthamin, an orange or red pigment used as a dye [53]. The seeds of apical capitulas harvested at the latest vegetative stage are rich in a slightly yellow colored edible oil. *Carthamus tinctorius L.* is one of the mostly used aromatic herbals for medicinal purposes, especially in traditional pharmacopeias. Various studies have been carried out on some parts of this plant such as leaf and flower extracts [54–56] and their biological effects.

The present work was designed to study the antioxidant and antimicrobial potentials, beneficial in the treatment of skin wounds, of the natural vegetable oil extracted by cold pressing of safflower (*Carthamus tinctorius L.*) seeds.

2. Materials and Methods

2.1. Safflower Crude Edible Seed Oil Extraction. Safflower (*Carthamus tinctorius L.*) seeds were harvested in June 2017 from flower heads of plants grown in the northwest of Tunisia. The seeds were then sieved manually in order to clean them from impurities and dust. The edible seed oil was extracted by first cold pressing, using a machine (SMIR, MUV2 65). This method does not use any chemical products during the extraction process and ensures the preservation of oil components. The extracted seed oil was then stored until use in anti-UV hermetic clean bottles as previously described [57].

2.2. Physicochemical Properties of Extracted Safflower Seed Oil. The tests were carried out according to the official methods of AOCS (American Oil Chemists' Society, International). Moisture ratio of the dried seeds was estimated according to ISO 665:2000. Saponification index was assessed according to the Norm ISO 3657:2013. Refractive index was determined with an Abbe refractometer with temperature adjustment at 20°C. Peroxide value was determined in meq O_2/kg of oil according to NF T60-220:1998. Iodine value ($\text{g I}_2/100 \text{ g oil}$) and acid index (mg KOH/g oil) were calculated according to the AOAC official method 940.28, 2013, and NF ISO 660-1996, respectively. Density was estimated at 20° as mass/volume (g/cm^3).

2.3. Determination of Safflower Oil Antioxidant Capacity

2.3.1. Scavenging Ability against Free Radicals DPPH (1,1-Diphenyl-2-Picrylhydrazyl Radical) and ABTS (2,2'-Azinobis-3-Ethylbenzothiazoline-6-Sulfonate). Scavenging activity of Safflower seed oil against DPPH and ABTS free radicals was evaluated as described [58]. 180 μL of 0.1 mM DPPH solution was mixed with 20 μL of safflower oil. The mixture was shaken vigorously then left to incubate at room temperature in the dark for 30 min. The absorbance was

measured at 520 nm using a spectrophotometer (Thermo Fisher Scientific Multiskan Go).

In order to produce ABTS radical cation, 2.5 mM potassium persulphate was mixed with 7 mM ABTS solution (at pH 7.4) and left in the dark for 16 h. A dilution of the mixture was carried out until absorbance of 0.70 ± 0.02 at 734 nm was reached. 180 μ L of fresh ABTS diluted solution was added to 20 μ L of the dissolved oil sample. Absorbance (A) was measured 6 min after the mixing. The maximum absorbance of DPPH and ABTS of the sample was recorded as A_{sample} and of the blank control as A_{blank} . The measurements were performed in triplicate. The results were expressed as Vit. C eq/g oil. Ascorbic acid was used as a standard. The percentage inhibition (%) of the free radical DPPH and ABTS was calculated as follows:

$$I\% = \left[\frac{A_{\text{blank}} - A_{\text{sample}}}{A_{\text{blank}}} \right] \times 100. \quad (1)$$

2.3.2. Ferric Reducing Antioxidant Power (FRAP). The FRAP of the safflower seed oil was evaluated using the method of Benzie and Strain [59] with slight modifications [60]. The fresh FRAP reagent was prepared daily as required, by mixing 2.5 mL of 20 mM ferric chloride hexahydrate ($\text{FeCl}_3 \cdot 6\text{H}_2\text{O}$) solution with 25 mL of acetate buffer 0.1 M (pH 3.6) ($\text{CH}_3\text{COONa} \cdot 3\text{H}_2\text{O}$; CH_3COOH) and 2.5 mL of 10 mM TPTZ (2,4,6-tri(2-pyridyl)-s-triazine) solution in 40 mM hydrochloric acid (HCl). The mixture was incubated at 37°C in a water bath for 10 min. The oil sample was diluted with n-hexane (V/4 V) in order to enhance contact between it and the working FRAP reagent. An aliquot of 300 μ L of this diluted oil sample was added to 2 mL of FRAP reagent then made up to volume 10 mL with redistilled water. The reaction mixture was left to incubate for 30 min at 37°C, then centrifuged at 15000 rpm for 10 min to remove solids. A blue-colored compound (Fe (II)-tripyrindyltriazine) was formed from the colorless oxidized form Fe (III) by the action of electron-donating antioxidants in the oil sample. The absorbance was measured at 593 nm with a spectrophotometer (Thermo Fisher Scientific Multiskan Go) against a blank reading sample of 2 mL of FRAP reagent made up to 10 mL with redistilled water. A standard curve was prepared using various increasing concentrations (0.005–0.050 mM) of fresh $\text{FeSO}_4 \cdot 7\text{H}_2\text{O}$ and used on the same day of the preparation. All the measurements were done in triplicate. The FRAP value was expressed as $\mu\text{mol Fe}^{2+}/\text{kg oil}$.

2.4. Total Phenolic Content. Safflower oil total phenolic content was assessed using the Folin-Ciocalteu method as described [61]. Absorbance was determined at 765 nm against a blank. Measurements were performed in triplicate. Gallic acid was used as a standard. Total phenolics were expressed as gallic acid equivalents per g of oil (GA eq/g oil).

2.5. Total Flavonoid Content. Total flavonoid content in safflower seed oil was assayed as described [62] and slightly modified [57]. 1.5 mL of 2% aluminium trichloride solution (AlCl_3) was added to 1.5 mL DMSO dissolved oil. The mixture was left to incubate in the dark for 30 min at room temperature. The absorbance was determined at 430 nm against a blank. The measurements were performed in triplicate.

Quercetin was used as a standard. Total flavonoids in the tested oil were expressed as mg of quercetin equivalents per g of oil (mg Q eq/g oil).

2.6. Total Carotenoid and Chlorophyll Contents. Total carotenoid and chlorophyll contents were determined by the colorimetric method as described [63]. Safflower seed oil (1.5 g) was dissolved in 5 mL cyclohexane. The maximum absorption was measured at the wavelength of 470 nm that corresponds to the carotenoid fraction and at 670 nm which corresponds to the chlorophyll fraction. The amounts of the two fractions were calculated using the following formulae:

$$\begin{aligned} \text{Carotenoid (mg/kg)} &= \frac{A_{470} \times 10^6}{2.000} \times 100 \times d, \\ \text{Chlorophyll (mg/kg)} &= \frac{A_{670} \times 10^6}{613} \times 100 \times d, \end{aligned} \quad (2)$$

where A is the absorbance, d is the spectrophotometer cell thickness = 1 cm, “2.000” is the specific extinction coefficient of lutein (xanthophyll, major carotenoid fraction component), and “613” is the specific extinction of chlorophyll a (pheophytin, major chlorophyll fraction component).

2.7. In Vitro Antimicrobial Assays

2.7.1. Test Microbial Strains. Safflower extracted oil was tested against 10 human pathogenic microorganisms obtained from our collection at the Laboratory of Mycology, Pathologies and Biomarkers (Faculty of Sciences of Tunis, University of Tunis El Manar, Tunisia). This collection was obtained after carrying out isolation and rigorous identification from Tunisian patients’ clinical samples: 2 gram-negative bacterial strains (*Escherichia coli* and *Enterobacter cloacae*), 2 gram-positive bacterial strains (*Staphylococcus aureus* and *Streptococcus agalactiae*), 3 yeast species strains (*Candida albicans*, *Candida parapsilosis*, and *Candida sake*), and 3 fungi species (*Aspergillus niger*, *Penicillium digitatum*, and *Fusarium oxysporum*). Antibiotic Ceftazidime (CAZ30) and antifungals Voriconazole (VCZ) and Amphotericin B served as reference drugs.

2.7.2. Detection of Antimicrobial Activity. Antibacterial and antifungal assays were performed by the agar well diffusion method [64] and broth microdilution method using sterile Mueller–Hinton media (Bio-Rad, France) for bacterial strains and potato dextrose agar (Bio-Rad, France) for antifungal tests. A fresh cell suspension (0.1 mL) adjusted to 10^7 CFU/mL for bacteria and 10^6 spores/mL for fungus was inoculated onto the surface of agar plates. Thereafter, wells with 6 mm in diameter were punched in the inoculated agar medium with sterile Pasteur pipette, and 50 μ L of the dissolved oil was added to each well. Negative controls consisted of 50 μ L DMSO, used to dissolve the oil (1 V/2 V). The plate was allowed to stand for 2 h to permit the diffusion of the oil followed by incubation at 37°C for 24 h for bacterial strains and 72 h for fungi at 28°C. The antimicrobial activity was evaluated by measuring the inhibition zones (clear areas

around the wells) against the test microorganisms. All tests were carried out in triplicate.

2.7.3. Determination of Minimum Inhibitory Concentration (MIC) and Minimal Bactericidal Concentration (MBC). The minimum inhibitory concentration (MIC) of the tested oil against six bacterial strains was determined accordingly to the microdilution broth method as described [64]. MIC was estimated visually (absence of turbidity) with 3 independent measurements. Minimal bactericidal concentration (MBC) was determined from the microdilution plates used in the MIC assay, according to [65] with modifications [66]. Aliquots (10 μ L) of each well without visible growth were transferred to TSA plates, incubated at 36°C for 24 h, and colony growth was verified as previously reported [67].

2.7.4. Lysozyme Activity. The lysozyme activity of the oil was assayed at 1/4 (v/v) by incubation at 37°C with pathogenic gram-positive bacteria: *Staphylococcus aureus* and *Streptococcus agalactiae*.

The mixed reaction was containing 0.1 mL of diluted oil (1/4) and 0.1 mL of suspension bacterial cell prepared in phosphate buffer after incubation for 60 min at 37°C. The activity was tested turbidimetrically by measuring the decrease in absorbance at 660 nm of the bacterial strain suspensions [66, 67]. Data were the average of three replications and were expressed in arbitrary units per mL (AU/mL).

2.7.5. Determination of Bactericidal Activity. The antimicrobial activity of the tested oil was expressed in arbitrary units per mL (AU/mL), and it was determined by an agar diffusion assay [68]. Briefly, a serial twofold dilution of oil in DMSO and 50 μ L of each dilution were spotted onto a TSB agar soft plate seeded with 10^7 CFU/mL of *Staphylococcus aureus*. The AU/mL was calculated as

$$\text{AU/mL} = 1000 \times \frac{D}{A}, \quad (3)$$

where A is the volume of the tested oil spotted on an agar plate (50 μ L in this case) and D is the reciprocal of the highest dilution showing a clear inhibition of the indicator strain.

2.7.6. Oil Effects on Viability and Morphology of Fungal Spores. All tested fungi were grown at 28°C on PDA for 10 to 15 days. Sterile water (20 mL) was added to each plate, and the surface was softly scraped with a sterile loop to release the spores. The resulting fungal spore suspension was filtered through a sterile 30 μ m filter to remove the mycelial fragments. The conidial suspension of each fungus was adjusted to a concentration of 10^5 spores/mL by counting with a haemocytometer. To investigate the effects of the described oil on spore germination, 50 μ L of conidial suspensions (10^5 spores/mL) and 50 μ L of the oil (1:2, v/v) were pipetted into an Eppendorf tube containing 1 mL with 5% glucose in sterile distilled water; the mix was then incubated at 25°C for 24 h. Control tubes were inoculated only with fungal spores of each tested fungus. Spore's germination inhibition percentage ($I\%$) was determined by microscopic examination of spores in the presence of the oil (E), com-

pared to the control tube containing only the spore suspensions (C) [69]. The used formula was

$$I (\%) = \frac{C - E}{C} \times 100. \quad (4)$$

To determine the effect of the tested oil on the morphological spore's germination, 100 μ L from each tube was directly observed with optical microscopy (CETI) at 40x.

2.8. Statistical Analysis. The statistical data analysis was performed using SPSS statistics 20.0 (SPSS Inc., Chicago, Illinois, USA) followed by t -test to assess the effect of treatments. The results were expressed as mean values \pm SEM. A difference was considered significant if $p < 0.05$.

3. Results

3.1. Physicochemical Properties of Safflower Seed Oil. The physicochemical properties of the tested oil are reported in Table 1. The moisture ratio of the dried seeds was of $4.71 \pm 0.03\%$. Safflower seed oil extracted by first cold pressing is a bright yellowish-amber fluid oil with characteristic vegetal smell. It is a natural, free of solvents, dry, and noncomedogenic oil. It has a density of 0.921 ± 0.002 at 20°C (g/cm³), a refractive index at 20°C of 1.477 ± 0.001 , a saponification value of 191.2 ± 0.350 mg KOH/g oil, an iodine index of 137.5 ± 0.450 g $I_2/100$ g oil, a peroxide value of 1.985 ± 0.043 meq O_2/kg oil, and an acidity index of 1.523 ± 0.041 mg KOH/g oil.

3.2. Antioxidant Activities of Safflower Seed Oil. The results have shown that safflower seed oil exhibited high scavenging effects against DPPH and ABTS free radicals. We registered a percentage of inhibition compared to Vit. C 89.41 ± 0.38 Vit. C eq/g oil and 88.52 ± 0.45 Vit. C eq/g oil, respectively. The FRAP value of safflower seed oil was estimated at 247.5 ± 0.034 μ mol Fe^{2+}/kg oil (Table 2).

3.3. Total Phenolic, Total Flavonoid, Total Carotenoid, and Total Chlorophyll Contents. Table 3 presents the data of the total phenolic, total flavonoid, total carotenoid, and total chlorophyll amounts measured in the safflower oil sample. They were, respectively, of 98.52 ± 0.80 GA eq/g oil, 35.79 ± 0.34 Q eq/g oil, 18.43 ± 0.020 mg/kg oil, and 3.9 ± 0.10 mg/kg oil.

3.4. Antimicrobial Activity of Safflower Seed Extracted Oil

3.4.1. Antibacterial Activity. The tested oil dissolved in DMSO at 1/3 (v/v) proved high antibacterial activity since it was active against three bacterial species *Escherichia coli*, *Streptococcus agalactiae*, and *Enterobacter cloacae* from a total of four bacterial species. The diameter inhibition values vary with the bacterial species from 13.0 mm to 15.0 mm (Table 4).

In order to determine the bacteriostatic and/or bactericidal effects of the described oil, a volume from each well without visible growth was transferred to TSA plates, incubated at 37°C for 24 h, and colony growth was examined.

TABLE 1: Physicochemical properties of first cold pressed safflower seed oil.

Parameters	
Physical state at room temperature	Liquid
Colour	Bright yellowish-amber
Odour	Characteristic vegetal smell
Texture	Dry oil
Property	Fluid, noncomedogenic
Density at 20°C	0.921 ± 0.002
Refractive index at 20°C	1.477 ± 0.001
Saponification value (mg KOH/g oil)	191.2 ± 0.350
Iodine index (g I ₂ /100 g oil)	137.5 ± 0.450
Peroxide value (meq O ₂ /kg oil)	1.985 ± 0.043
Acidity index (mg KOH/g oil)	1.523 ± 0.041

*Values given are the means of three measurements ± standard error.

The obtained results showed that our oil has a bacteriostatic effect against all tested bacterial species since we observed a bacterial colony after incubation. MIC and MBC obtained values were, respectively, 1/16 and 1/32 for *Escherichia coli* and *Streptococcus agalactiae*.

The highest antibacterial activity was observed against *Enterobacter cloacae* by giving the maximum diameter of inhibition of 15 mm and the high MIC and MIB values, respectively, of 1/32 and 1/64. This data was also confirmed by its most activity than the antibiotic used here Ceftazidime (CAZ30) compared to other antibacterial activity against other species which were less than those exhibited by Ceftazidime (CAZ30) (Figure 1).

The bactericidal activity expressed in AU/mL was of 320 AU mL⁻¹ against *Escherichia coli* and *Streptococcus agalactiae* and 640 against *Enterobacter cloacae* (Table 4).

A low value of lysozyme activity was also detected against two tested gram-positive pathogenic strains *Streptococcus agalactiae* and *Staphylococcus aureus*. We found 11.5 and 6.5 AU, respectively (Figure 2).

3.4.2. Antifungal Activity. The obtained results have shown that safflower oil exhibited a significant antifungal activity against two *Candida* species, with a diameter zone inhibition of 15.5 mm for *Candida parapsilosis* and 15.0 mm for *Candida sake*. No growth-inhibitory action on *Candida albicans* was observed. Fungicidal activity was obtained on the three fungal species (*Aspergillus niger*, *Penicillium digitatum*, and *Fusarium oxysporum*) with an inhibition zone diameter of ranging from 11 to 12.5 mm (Table 5).

Comparing the antifungal activity of safflower oil with that of two antifungal drugs, we could note that it has antifungal effects on all the tested fungal strains. Its effectiveness was quite similar to that of Amphotericin B against *Aspergillus niger*. Nonetheless, its antifungal efficiency was weaker than that of Voriconazole (VCZ) except for *Fusarium oxysporum* where safflower exhibited antifungal effect as well as Amphotericin B where VCZ had no effect on this strain (Figure 3).

From our data, it appeared that safflower oil was able to reduce spores' germination of the three tested fungi with a high percentage of inhibition of 84.8% for *Aspergillus niger* and more than 88% for the other tested fungi, compared to untreated controls.

Microscopic observation of spore germination morphology of conidial suspensions treated with safflower oil at 1/4 (v/v) compared to conidial suspension in the absence of the oil has shown a marked reduction of the length of the germinative tube and the ramification rate of the spores. For instance, Figure 4 shows the observation of *Aspergillus niger*'s spore germination in the absence of any treatment (Figure 4(a)) and after treatment with safflower oil (Figure 4(b)). Similar effects were observed for *Penicillium digitatum* and *Fusarium oxysporum* spores.

4. Discussion

Our results have shown that the oil extracted from safflower seeds under cold pressing exhibited high antioxidant activities through its scavenging activities on free radicals DPPH and ABTS and its strong ferric reducing antioxidant power (FRAP). Moreover, we registered notable antimicrobial effects of safflower oil against human skin opportunistic pathogenic bacteria, yeast, and fungi, which commonly alter the healing of skin wounds. These properties would allow the tested oil to promote the healing process of cutaneous injuries by topical application.

Skin injury can be considered as an oxidative stress-inducing factor. The wound repair process requires an increase in the consumption of oxygen O₂ which is a paramount factor in the mitochondrial production of adenosine triphosphate (ATP), the energetic molecule used by all actors in the healing process, especially during the early phases, hemostasis and inflammation. Although the rupture of the blood vessels caused by the skin injury induces a state of hypoxia, it seems that the lack of O₂ starts to jump the healing process via the release of HIF-1 [70] and huge amounts of oxygen reactive species (ROS) in the wound site [34, 71]. Oxygen- (O₂-) derived molecules are known as reactive oxygen species (ROS) such as H₂O₂.

When the platelets and neutrophils are exposed to the cutaneous ECM and collagen after the capillary rupture, they get activated and release chemical mediators in the wound bed and a large amount of ROS. At homeostatic low doses, these compounds are beneficial and intervene since the first minutes after skin trauma in several ROS-signaling pathways [35, 36]. First of all, ROS stimulate the constriction of the vessels surrounding the wound to reduce blood loss, in parallel with the activation of the hemostatic cascade, the formation of thrombin, and as a result a thrombus that can stop local hemorrhage.

They also provide further signals within the intercellular network that supports the wound healing process and activate the recruitment of immunocytes to migrate to the wound site to fight invading pathogens [72, 73]. It has been reported that during the inflammatory phase, neutrophils intervene first, because of their abundance in the blood, followed by some innate immune cells like mast cells and dendritic epidermal T cells (DETCs) and by monocytes

TABLE 2: Antioxidant activities of safflower seed oil.

Scavenging activity against DPPH radical % inhibition (Vit. C eq/g oil)	Scavenging activity against ABTS radical % inhibition (Vit. C eq/g oil)	FRAP value ($\mu\text{mol Fe}^{2+}/\text{kg oil}$)
89.41 \pm 0.38	88.52 \pm 0.45	247.5 \pm 0.034

*Values given are the means of three measurements \pm standard error.

TABLE 3: Total phenolic, total flavonoid, total carotenoid, and total chlorophyll contents of safflower seed oil.

Total phenolics (GA eq/g oil)	Flavonoids (mg Q eq /g oil)	Carotenoids (mg/kg oil)	Total chlorophylls (mg/kg oil)
98.52 \pm 0.80	35.79 \pm 0.34	18.43 \pm 0.020	3.9 \pm 0.010

*Values given are the means of three measurements \pm standard error.

TABLE 4: Antibacterial activity of safflower seed oil on the tested bacterial strains.

Microorganisms	MIC	MBC	Diameter zone inhibition (mm)	Bactericidal activity (AU/mL)
Bacteria				
<i>Escherichia coli</i>	1/16	1/32	13.0 \pm 1.4	320
<i>Streptococcus agalactiae</i>	1/16	1/32	13.5 \pm 0.7	320
<i>Enterobacter cloacae</i>	1/32	1/64	15.0 \pm 0.0	640
<i>Staphylococcus aureus</i>	-	-	-	-

Values given are the means of three measurements \pm standard error. -: absence of activity.

which then differentiate into mature macrophages which are strongly activated in the wound bed during the acute inflammatory process. These cells then release a plethora of interacting molecules, active mediators such as chemotactic, and growth factors, cytokines, and chemokines (IL-1, IL-6, VEGF, TNF- α ,...) with proinflammatory and proteolytic enzymatic properties [71–73]. PDGF and TGF- β are released by the recruited platelets to attract more platelets, fibroblasts, and inflammatory cells. TNF- α has been reported to be an essential factor in promoting centripetal migration of keratinocytes from the edges to the center of the wound site and allowing reepithelialization and closure of the epidermis [74].

Furthermore, other amounts of ROS are released during phagocytosis to stunt bacterial and fungus proliferation via bacteriostatic and fungistatic actions. Skin wounds get sometimes worse if not well managed, especially under bad care conditions that lead to infections and the extension of the inflammatory phase, with an enhancement of ROS and free radical production which are detrimental to wound healing [36, 70]. In addition, it should be noted that under normal healing conditions, endogenous antioxidants such as SOD, GPx, and Trx-1 and Trx-2 are secreted and released in the wound bed to counteract the oxidative stress damages induced by the free radicals produced during the inflammatory phase [36]. It is therefore the physiologic balance between prooxidant factors and antioxidant agents that would be one of the keys to efficient tissue repair. But in case of reduction of secretion of endogenous antioxidants in certain patients especially the elderly with underlying pathologies such as immunological depressed status, diabetes mellitus, hemiplegia, and tetraplegia that impair autonomic mobility, the damages caused by oxidative stress are amplified, leading to wound infections, delayed healing, and chronicity of wounds. This is of a great concern in nursing and wound care.

Supplementation by topical application on the wound bed with exogenous compounds which have antioxidant potential, such as safflower oil, would be an effective strategy in wound management. The antioxidant properties of safflower oil could be attributed to its richness in several bioactive compounds such as polyphenols, flavonoids, carotenoids, and chlorophylls which were detected in our oil extract. In fact, various studies have proven the very potent antioxidant potential of these compounds [69, 71–73] and their protective effects in human health against oxidative-stress-induced diseases and physiological disruptions [75–77]. Moreover, it has been shown that safflower seeds' oil is particularly rich in α tocopherol-vitamin E [78] and in phytosterols such as campesterol, stigmasterol, and β -sitosterol which have strong potential antioxidant effects [79]. Topical management of skin wounds by this oil could promote the healing process as it is mainly composed at a high percentage by unsaturated fatty acids [80] especially linoleic acid (C18:2n-6) and oleic acid (C18:1 n-9) which are important components of the cell membranes [81].

Additionally, it is known that linoleic acid is a precursor in the synthesis pathways of several bioactive mediators (thromboxanes, prostaglandins, and leukotrienes) which are very active in the neoangiogenesis and dermal regeneration [82]. In addition, the tested oil was described to be very rich in phospholipids such as phosphatidylethanolamine, phosphatidylcholine, and phosphatidylinositol which are major components of the cell membranes. So, safflower oil may provide crucial lipid elements for the genesis of the cells which are newly formed during the healing process [83, 84, 85].

Another criterion seems to be necessary during the early stages of the healing process, namely, a good level of hydration in the wound. In some cases like deep wounds, burns, bedsores, and skin ulcers, wound management requires the

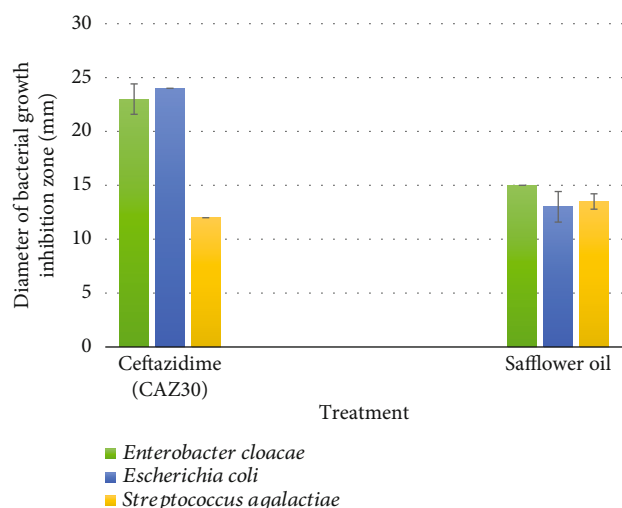


FIGURE 1: The antibacterial effect of safflower oil on used bacterial species compared to the antibiotic used standard Ceftazidime (CAZ30). Values measured represent the diameters of bacterial growth inhibition zone expressed in mm. Safflower oil showed lower bactericidal activity against *Escherichia coli* and *Enterobacter cloacae* than Ceftazidime (CAZ30). However, its effect against *Streptococcus agalactiae* was greater than that of CAZ30.

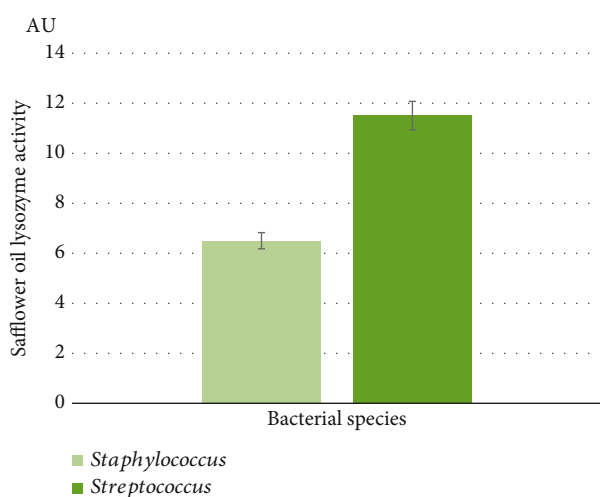


FIGURE 2: Lysozyme activity of safflower oil tested at 1/4 (v/v) by incubation at 37°C with pathogenic gram-positive bacteria: *Streptococcus agalactiae* and *Staphylococcus aureus*. Data are the average of three replications, and bars present the standard error of the means. A lysozyme activity was greater on *Streptococcus agalactiae* rather than on *Staphylococcus aureus*.

use of a variety of products such as hydrogel dressings that provide both hydration and the removal of debris and waste from the wound bed. Safflower extracted oil could ensure a good level of wound hydration by providing an insulating barrier between the external environment and the exudate in the wound bed, thus preserving it from dryness and promoting the effectiveness of the healing actors.

Our study showed that the oil extracted by cold pressing from safflower seeds had high antibacterial activities by both bacteriostatic and bactericidal ways of action against the

TABLE 5: Antifungal activity of safflower seed oil on the tested fungal species.

Microorganisms	Diameter zone inhibition (mm)
Yeasts	
<i>Candida albicans</i>	-
<i>Candida parapsilosis</i>	15.5 ± 0.7
<i>Candida sake</i>	15.0 ± 1.4
Fungi	
<i>Aspergillus niger</i>	11.0 ± 1.4
<i>Penicillium digitatum</i>	11.0 ± 0.0
<i>Fusarium oxysporum</i>	12.5 ± 0.7

Values given are the means of three measurements ± standard error. -: absence of activity.

tested pathogenic bacterial strains (*Enterobacter cloacae*, *Escherichia coli*, and *Streptococcus agalactiae*). Under the same conditions of extraction and experimentation, *Opuntia ficus indica* oil was less efficient than safflower oil as we noted antibacterial activity only against *Enterobacter cloacae* [66]. An antifungal potential against the fungal-tested strains (*Candida parapsilosis*, *Candida sake*, *Aspergillus niger*, *Penicillium digitatum*, and *Fusarium oxysporum*) was noted. However, no activity has been detected against *Candida albicans* and *Staphylococcus aureus* based on diameter inhibition zone measurement. On another hand, we registered a lysozyme activity. Due to its muramidase activity, lysozyme has long been known to exert its antimicrobial action by specially hydrolyzing the 1,4-D-linkage between N-acetylmuramic acid and N-acetyl-D-glucosamine of cell wall peptidoglycan which is the major component of the gram-positive bacterial cell wall [86], hence inducing bacterial lysis and providing some protection against bacterial infection. It is likely oil lysozyme activity against the tested *Staphylococcus aureus* strain was not sufficient to inhibit its growth on the agar plates. This lysozyme activity of safflower oil may enhance its potency to inactivate some bacterial strains and allows the understanding of one of its ways of action.

Our results corroborate other findings on the antimicrobial effects of *Carthamus tinctorius*. A recent study showed that methanolic and aqueous extracts from the seeds of this species had antibacterial activities against *Escherichia coli* and *Acinetobacter baumannii* with inhibition diameters of 3 mm and 5 mm, respectively, while based on MICs, the same extracts exhibited antibacterial effects against *Escherichia coli*, *Staphylococcus aureus*, *Acinetobacter baumannii*, *Klebsiella pneumoniae*, and *Pseudomonas aeruginosa* [87]. In addition, it has been proven that flower extracts from *Carthamus tinctorius L.* harvested at the latter stage of flowering have significant antimicrobial effects against a fungal strain (*Candida albicans*) and some bacterial strains (*Escherichia coli* (ATCC 25218), methicillin-resistant *Staphylococcus aureus* (ATCC 25923), *Pseudomonas aeruginosa* (ATCC 27853), *Bacillus cereus* (ATCC 14759)). The most potent activity has been against *Escherichia coli* with an inhibition zone of 26 mm [87].

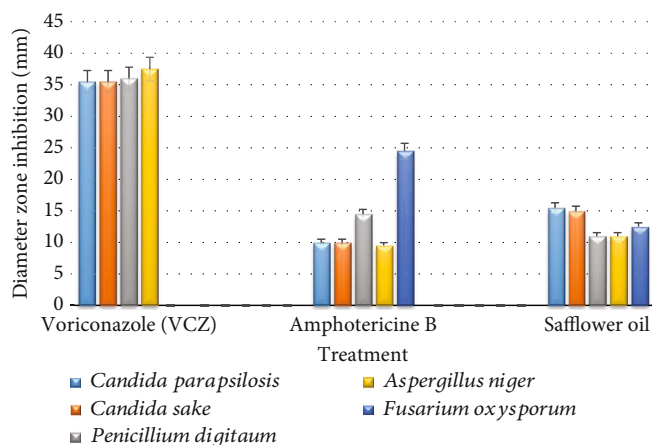


FIGURE 3: Comparison of the antifungal activities between antifungal drugs and safflower oil on the tested fungal species. Values measured represent diameters of fungal growth inhibition zone (mm). Voriconazole (VCZ) and Amphotericin B were used as positive controls. Safflower oil treatment significantly reduced the percentage of spores' germination and branching of the germ tubes of the tested fungal strains.

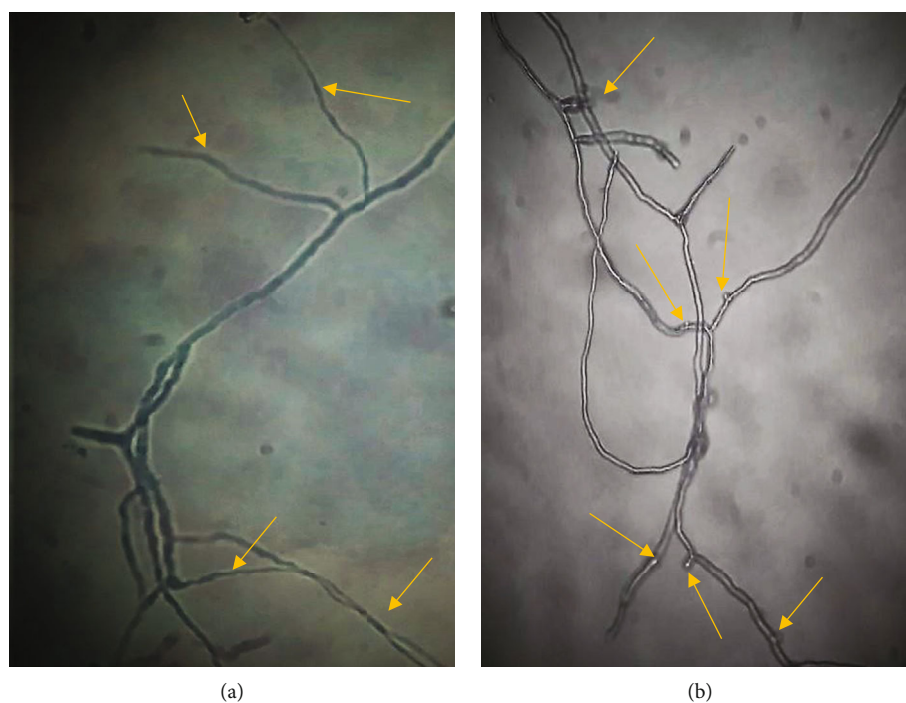


FIGURE 4: Microscopic morphology ($\times 400$) of *Aspergillus niger* spores' germination under normal conditions (a) and after treatment with safflower oil (b). The arrows indicate the spores' germinative tubes. Safflower oil reduced markedly the length of *Aspergillus niger* spores' germination tube compared to the controls.

Several studies outlined that antimicrobial activities of plant extracts are due to their phenolic contents which cause cell membrane disruption, thus inducing cytoplasmic element spillage and cell necrosis [88–90]. Safflower oil phenolics may contribute by this way to inactivate bacterial growth. Moreover, as it is rich with polyunsaturated fatty acids (oleic and linoleic acids), safflower oil could act against both bacteria and fungi. Fatty acids were reported to inhibit some membrane enzymes like glucosyltransferase and to activate autolytic cell wall enzymes, leading to cell death (bactericidal or fungicidal effects). Moreover, they were cited to reduce energy pathway production in the mitochondria, hence inhibiting

bacterial (bacteriostatic effect) or fungal growth (fungistatic action) [87]. This is in line with our results since we found a slowdown in fungal spore germination. In addition, these fatty acid-related antimicrobial effects could be combined with those of the phytosterols present in safflower seed extracted oil to enhance its effectiveness against microbial infections.

5. Conclusion

The present study revealed that the oil extracted by cold pressing from the seeds of safflower (*Carthamus tinctorius L.*) exhibited high antioxidant effects and antimicrobial

potentialities against several opportunistic skin pathogens. It seemed to act by bacteriostatic and bactericidal pathways as well as a strong antifungal growth inhibition.

A judicious strategy for the management of acute and especially chronic skin injuries would be to administer topically a multitherapy composed of antioxidants, one or more antimicrobials (antibiotics and antifungals depending on the patient's condition), and skin regenerating and restructuring compounds, safe from health side effects. The bioactive components of *Carthamus tinctorius* L. seed oil extracted by cold pressing may allow it to be considered as a good alternative natural therapeutic for the management of skin injuries, and the prevention of skin infections.

Abbreviations

CFU:	Colony-forming unit
DMSO:	Dimethylsulfoxide
MIC:	Minimum inhibitory concentration
MBC:	Minimal bactericidal concentration
PDA:	Potato dextrose agar
TSA:	Trypticase soy agar
TSB:	Trypticase soy broth
AU/mL:	Arbitrary unit per mL
FRAP:	Ferric reducing antioxidant power
PDGF:	Platelet-derived growth factor
TNF- α :	Tumor necrosis factor alpha
IL-1:	Interleukin 1
IL-6:	Interleukin 6
VEGF:	Vascular endothelial growth factor
EGF:	Epidermal growth factor
FGF:	Fibroblast growth factor
TGF:	Transforming growth factor
KGF:	Keratinocyte growth factor
SOD:	Superoxide dismutase
GPx:	Glutathione peroxidase
Trx-1:	Thioredoxin-1
Trx-2:	Thioredoxin-2.

Data Availability

The data used to support the findings of this study are available from the corresponding author upon request.

Conflicts of Interest

The authors declare they have no conflicts of interests.

References

- [1] P.-H. Wang, B.-S. Huang, H.-C. Horng, C. C. Yeh, and Y. J. Chen, "Wound healing," *Journal of the Chinese Medical Association*, vol. 81, no. 2, pp. 94–101, 2018.
- [2] F. A. Lopez and S. Lartchenko, "Skin and soft tissue infections," *Infectious Disease Clinics of North America*, vol. 24, no. 4, pp. 759–772, 2006.
- [3] V. Lobo, A. Patil, A. Phatak, and N. Chandra, "Free radicals, antioxidants and functional foods: impact on human health," *Pharmacognosy Reviews*, vol. 4, no. 8, pp. 118–126, 2010.
- [4] M. Asadi, D. H. Alamdari, H. R. Rahimi et al., "Treatment of life-threatening wounds with a combination of allogenic platelet-rich plasma, fibrin glue and collagen matrix, and a literature review," *Experimental and Therapeutic Medicine*, vol. 8, no. 2, pp. 423–429, 2014.
- [5] C. Oshikata, N. Tsurikisawa, A. Saito et al., "Fatal pneumonia caused by *Penicillium digitatum*; a case report," *BMC Pulmonary Medicine*, vol. 13, no. 1, pp. 1–4, 2013.
- [6] L. Ovington, "Bacterial toxins and wound healing," *Ostomy/wound management*, vol. 49, 7A Suppl, 8, 2003.
- [7] R. Edwards and K. G. Harding, "Bacteria and wound healing," *Current Opinion in Infectious Diseases*, vol. 17, no. 2, pp. 91–96, 2004.
- [8] L. P. Da Silva, R. L. Reis, V. M. Corrello, and A. P. Marques, "Hydrogel-based strategies to advance therapies for chronic skin wounds," *Annual Review of Biomedical Engineering*, vol. 21, 2019.
- [9] R.-M. Allman, P.-S. Goode, N.-B.-S. Burst, A.-A. Bartolucci, and D.-R. Thomas, "Pressure ulcers, hospital complications and disease severity: impact on hospital costs and length of stay," *Advances in skin & wound care*, vol. 12, pp. 22–30, 1999.
- [10] S. Gist, I. Tio-Matos, S. Falzgraf, S. Cameron, and M. Beebe, "Wound care in the geriatric client," *Clinical Interventions in Aging*, vol. 4, p. 269, 2009.
- [11] J. Webster, P. Scuffham, M. Stankiewicz, and W.-P. Chaboyer, "Negative pressure wound therapy for skin grafts and surgical wounds healing by primary intention," *Cochrane Database of Systematic Reviews*, vol. 10, 2014.
- [12] A.-E. Pino, S. Taghya, C. Chapman, and J.-H. Bowker, "Lower-limb amputations in patients with diabetes mellitus," *Orthopedics*, vol. 34, pp. 885–892, 2011.
- [13] C. Ruppen, J. Notter, C. Strahm, B. Sonderegger, and P. Sendi, "Osteoarticular and skin and soft-tissue infections caused by *Streptococcus agalactiae* in elderly patients are frequently associated with bacteremia," *Diagnostic Microbiology and Infectious Disease*, vol. 90, no. 1, pp. 55–57, 2018.
- [14] C. A. Muto, J. A. Jernigan, B. E. Ostrowsky et al., "SHEA guideline for preventing nosocomial transmission of multidrug-resistant strains of *Staphylococcus aureus* and *Enterococcus*," *Infectious Control & Hospital Epidemiology*, vol. 24, no. 5, pp. 362–386, 2003.
- [15] K. Chiller, B. A. Selkin, and G. J. Murakawa, "Skin microflora and bacterial infections of the skin," *Journal of Investigative Dermatology Symposium Proceedings*, vol. 6, no. 3, pp. 170–174, 2001.
- [16] M. N. Babic, P. Zalar, B. Zenko, H. J. Schroers, S. Dzeroski, and N. Gunde-Cimerman, "Candida and Fusarium species known as opportunistic human pathogens from customer-accessible parts of residential washing machines," *Fungal Biology*, vol. 119, no. 2-3, pp. 95–113, 2015.
- [17] M. L. Mangoni, A. M. Mc Dermott, and M. Zasloff, "Antimicrobial peptides and wound healing: biological and therapeutic considerations," *Experimental Dermatology*, vol. 25, no. 3, pp. 167–173, 2016.
- [18] K. M. Amsler, T. A. Davies, W. Shang, M. R. Jacobs, and K. Bush, "In vitro activity of ceftobiprole against pathogens from two phase 3 clinical trials of complicated skin and skin structure infections," *Antimicrobial Agents and Chemotherapy*, vol. 52, no. 9, pp. 3418–3423, 2008.
- [19] N. Van der Mee-Marquet, L. Fourny, L. Arnault et al., "Molecular characterization of human-colonizing *Streptococcus*


- agalactiae strains isolated from throat, skin, anal margin, and genital body sites," *Journal of Clinical Microbiology*, vol. 46, no. 9, pp. 2906–2911, 2008.
- [20] M. A. Ekpo and P. C. Etim, "Antimicrobial activity of ethanolic and aqueous extracts of *Sida acuta* on microorganisms from skin infections," *Journal of Medicinal Plants Research*, vol. 3, no. 9, pp. 621–624, 2009.
- [21] Z. Petkovsek, K. Elersic, M. Gubina, D. Zgur-Bertok, and M. S. Erjavec, "Virulence potential of *Escherichia coli* isolates from skin and soft tissue infections," *Journal of Clinical Microbiology*, vol. 48, no. 9, pp. 3462–3463, 2010.
- [22] I. Zanardi, S. Burgassi, E. Paccagnini, M. Gentile, V. Bocci, and V. Travagli, "What is the best strategy for enhancing the effects of topically applied ozonated oils in cutaneous infections?," *BioMed Research International*, vol. 2013, 6 pages, 2013.
- [23] G. A. James, E. Swogger, R. Wolcott et al., "Biofilms in chronic wounds," *Wound Repair and Regeneration*, vol. 16, no. 1, pp. 37–44, 2008.
- [24] A. Omar, J. B. Wright, G. Schultz, R. Burrell, and P. Nadworny, "Microbial biofilms and chronic wounds," *Microorganisms*, vol. 5, no. 1, p. 9, 2017.
- [25] M. Malone, T. Bjarnsholt, A. J. McBain et al., "The prevalence of biofilms in chronic wounds: a systematic review and meta-analysis of published data," *Journal of Wound Care*, vol. 26, no. 1, pp. 20–25, 2017.
- [26] R. Weller, R. J. Price, A. D. Ormerod, N. Benjamin, and C. Leifert, "Antimicrobial effect of acidified nitrite on dermatophyte fungi, *Candida* and bacterial skin pathogens," *Journal of Applied Microbiology*, vol. 90, no. 4, pp. 648–652, 2001.
- [27] R. K. Angaman, B. M. A. B. Orsot, D. Camara, K. Abo, and N. G. Zirihi, "Etude ethnobotanique de plantes de la flore du Département d'Abengourou, en Côte d'Ivoire et évaluation in vitro de l'activité antifongique d'extraits de *Terminalia superba* Engl. Diels sur deux espèces de champignons, *Aspergillus niger* Van Tieghem et *Fusa*," *International Journal of Biological and Chemical Sciences*, vol. 12, no. 3, pp. 1208–1224, 2018.
- [28] A. J. Brink and G. A. Richards, "The role of multidrug and extensive-drug resistant Gam-negative bacteria in skin and soft tissue infections," *Current Opinion in Infectious Diseases*, vol. 33, no. 2, pp. 93–100, 2020.
- [29] A. Muller, I. Patry, D. Talon et al., "Mise en place d'un outil informatisé de surveillance de la résistance bactérienne et de la consommation antibiotique dans un centre hospitalier universitaire," *Pathologie-Biologie*, vol. 54, no. 2, pp. 112–117, 2006.
- [30] R. M. Klevens, M. A. Morrison, J. Nadle et al., "Invasive methicillin-resistant *Staphylococcus aureus* infections in the United States," *Journal of the American Medical Association*, vol. 298, no. 15, pp. 1763–1771, 2007.
- [31] R. J. White, K. Cutting, and A. Kingsley, "Topical antimicrobials in the control of wound bioburden," *Ostomy/Wound Management*, vol. 52, no. 8, pp. 26–58, 2006.
- [32] F. Guérin, "Infections à *Enterobacter cloacae* complex: résistance aux antibiotiques et traitement," *Journal des Anti-infectieux*, vol. 17, no. 3, pp. 79–89, 2015.
- [33] C. Carbone, M. D. C. Teixeira, M. D. C. Sousa et al., "Clotrimazole-loaded Mediterranean essential oils NLC: a synergic treatment of *Candida* skin infections," *Pharmaceutics*, vol. 11, no. 5, p. 231, 2019.
- [34] S. Werner and R. Grose, "Regulation of wound healing by growth factors and cytokines," *Physiological Reviews*, vol. 83, no. 3, pp. 835–870, 2003.
- [35] J. Kanta, "The role of hydrogen peroxide and other reactive oxygen species in wound healing," *Acta Medica (Hradec Králove)*, vol. 54, no. 3, pp. 97–101, 2011.
- [36] C. Dunnill, T. Patton, J. Brennan et al., "Reactive oxygen species (ROS) and wound healing: the functional role of ROS and emerging ROS-modulating technologies for augmentation of the healing process," *International Wound Journal*, vol. 14, no. 1, pp. 89–96, 2017.
- [37] P. Wikaningtyas and E. Y. Sukandar, "The antibacterial activity of selected plants towards resistant bacteria isolated from clinical specimens," *Asian Pacific Journal of Tropical Biomedicine*, vol. 6, no. 1, pp. 16–19, 2016.
- [38] R. S. Pawar, S. Kumar, F. A. Toppo, P. K. Lakshmi, and P. Suryavanshi, "*Sida cordifolia* Linn. accelerates wound healing process in type 2 diabetic rats," *Journal of Acute Medicine*, vol. 6, no. 4, pp. 82–89, 2016.
- [39] R. K. Bijauliya, S. Alok, M. Kumar, D. K. Chanchal, and S. Yadav, "A comprehensive review on herbal cosmetics," *International Journal of Pharmaceutical Sciences and Research*, vol. 8, no. 12, pp. 4930–4949, 2017.
- [40] A. Henriques, S. Jackson, R. Cooper, and N. Burton, "Free radical production and quenching in honeys with wound healing potential," *Journal of Antimicrobial Chemotherapy*, vol. 58, no. 4, pp. 773–777, 2006.
- [41] M. Panchatcharam, S. Miriyala, V. S. Gayathri, and L. Suguna, "Curcumin improves wound healing by modulating collagen and decreasing reactive oxygen species," *Molecular and Cellular Biochemistry*, vol. 290, no. 1–2, pp. 87–96, 2006.
- [42] N. Farahpour and J. Mirzakhani, "Hydroethanolic *Pistacia atlantica* hulls extract improved wound healing process; evidence for mast cells infiltration, angiogenesis and RNA stability," *International Journal of Suregey*, vol. 17, pp. 88–98, 2015.
- [43] R. L. Thangapazham, S. Sharad, and R. K. Maheshwari, "Phytochemicals in wound healing," *Advances in Wound Care*, vol. 5, no. 5, pp. 230–241, 2016.
- [44] S. Karimzadeh and M. R. Farahpour, "Topical application of *Salvia officinalis* hydroethanolic leaf extract improves wound healing process," *Indian Journal of Experimental Biology*, vol. 55, no. 2, pp. 98–106, 2017.
- [45] R. Manzuoerh, M. R. Farahpour, A. Oryan, and A. Sonboli, "Effectiveness of topical administration of *Anethum graveolens* essential oil on MRSA-infected wounds," *Biomedicine & Pharmacotherapy*, vol. 109, pp. 1650–1658, 2019.
- [46] C. Li, Y. Yao, G. Zhao et al., "Comparison and analysis of fatty acids, sterols, and tocopherols in eight vegetable oils," *Journal of Agricultural and Food Chemistry*, vol. 59, no. 23, pp. 12493–12498, 2011.
- [47] J. Djerrou, Z. Maameri, Y. Hamdo-Pacha et al., "Effect of virgin fatty oil of *Pistacia lentiscus* on experimental burn wound's healing in rabbits," *African Journal of Traditional, Complementary and Alternative Medicines*, vol. 7, no. 3, pp. 258–263, 2010.
- [48] M. R. Farahpour and S. Fathollahpour, "Topical co-administration of flaxseed and pistachio ointment promoted wound healing; evidence for histopathological features," *Comparative Clinical Pathology*, vol. 24, no. 6, pp. 1455–1461, 2015.
- [49] S. B. Khedir, S. Bardaa, N. Chabchoub, D. Moalla, Z. Sahnoun, and T. Rebai, "The healing effect of *Pistacia lentiscus* fruit oil on laser burn," *Pharmaceutical Biology*, vol. 55, no. 1, pp. 1407–1414, 2017.

- [50] S. Bardaa, N. Chabchoub, M. Jridi et al., "The effect of natural extracts on laser burn wound healing," *Journal of Surgical Research*, vol. 201, no. 2, pp. 464–472, 2016.
- [51] S. Bardaa, N. B. Halima, F. Aloui et al., "Oil from pumpkin (*Cucurbita pepo* L.) seeds: evaluation of its functional properties on wound healing in rats," *Lipids in Health and Disease*, vol. 15, no. 1, p. 73, 2016.
- [52] I. Khémiri, B. Essghaier Hédi, N. Sadfi Zouaoui, N. Ben Gdara, and L. Bitri, "The antimicrobial and wound healing potential of *Opuntia ficus indica* L. inermis Extracted oil from Tunisia," *Evidence-Based Complementary and Alternative Medicine*, vol. 2019, 10 pages, 2019.
- [53] R. Laursen and C. Mouri, "Decomposition and analysis of carthamin in safflower-dyed textiles," *E-Preservation Science*, vol. 10, pp. 35–37, 2013.
- [54] H. L. Zhang, A. Nagatsu, T. Watanabe, and H. Okuyama, "Antioxidative compounds isolated from safflower (*Carthamus tinctorius* L.) oil cake," *Chemical and Pharmaceutical Bulletin*, vol. 45, no. 12, pp. 1910–1914, 1997.
- [55] J. Y. Lee, E. J. Chang, H. J. Kim, J. H. Park, and S. W. Choi, "Antioxidative flavonoids from leaves of *Carthamus tinctorius*," *Archives of Pharmacal Research*, vol. 25, no. 3, pp. 313–319, 2002.
- [56] N. Salem, K. Msaada, G. Hamdaoui, F. Limam, and B. Marzouk, "Variation in phenolic composition and antioxidant activity during flower development of safflower (*Carthamus tinctorius* L.)," *Journal of Agricultural and Food Chemistry*, vol. 59, no. 9, pp. 4455–4463, 2011.
- [57] I. Khémiri and L. Bitri, "Effectiveness of *Opuntia ficus indica* L. inermis Seed oil in the protection and the healing of experimentally induced gastric mucosa ulcer," *Oxidative Medicine and cellular Longevity*, vol. 2019, 17 pages, 2019.
- [58] H. Bendaoud, M. Romdhane, J. P. Souchard, S. Cazaux, and J. Bouajila, "Chemical composition and anticancer and antioxidant activities of *Schinus molle* L. and *Schinus terebenthifolius* Raddi berries essential oils," *Journal of Food Science*, vol. 75, pp. 466–472, 2010.
- [59] I. F. Benzie and J. J. Strain, "[2] Ferric reducing/antioxidant power assay: direct measure of total antioxidant activity of biological fluids and modified version for simultaneous measurement of total antioxidant power and ascorbic acid concentration," *Methods in enzymology*, vol. 299, pp. 15–27, 1999.
- [60] A. Szydłowska-Czerniak, C. Dianoczki, K. Recseg, G. Karlovits, and E. Szlyka, "Determination of antioxidant capacities of vegetable oils by ferric-ion spectrophotometric methods," *Talanta*, vol. 76, no. 4, pp. 899–905, 2008.
- [61] C. El Kar, A. Ferchichi, F. Attia, and J. Bouajila, "Pomegranate (*Punica granatum*) juices: chemical composition, micronutrient cations and antioxidant capacity," *Journal of Food Science*, vol. 76, pp. 795–800, 2011.
- [62] T. Bahorun, B. Gressier, F. Trotin et al., "Oxygen species scavenging activity of phenolic extracts from hawthorn fresh plant organs and pharmaceutical preparations," *Arzneimittel-forschung*, vol. 46, no. 11, pp. 1086–1089, 1996.
- [63] M. I. Minguéz-Mosquera, B. Gandul-Rojas, A. Montano-Asqueino, and J. Garrido-Fernandez, "Determination of chlorophylls and carotenoids by high-performance liquid chromatography during olive lactic fermentation," *Journal of Chromatography A*, vol. 585, no. 2, pp. 259–266, 1991.
- [64] J. R. Tagg and A. R. McGiven, "Assay system for bacteriocins," *Applied Microbiology*, vol. 21, no. 5, p. 943, 1971.
- [65] O. Y. Celiktas, E. E. Hameskocabas, E. Bedir, F. VardarSukan, T. Ozek, and K. H. C. Baser, "Antimicrobial activities of methanol extracts and essential oils of *Rosmarinus officinalis*, depending on location and seasonal variations," *Food Chemistry*, vol. 100, no. 2, pp. 553–559, 2007.
- [66] I. Khémiri, B. Essghaier-Hédi, N. Sadfi-Zouaoui, N. Ben Gdara, and L. Bitri, "The antimicrobial and wound healing potential of *Opuntia ficus indica* L. inermis extracted oil from Tunisia," *Evidence-Based Complementary and Alternative Medicine*, vol. 2019, 10 pages, 2019.
- [67] H. Sehim, B. Essghaier, E. Barea, N. Sadfi-Zouaoui, and M. F. Zid, "Synthesis, structural study, magnetic susceptibility and antimicrobial activity of the first (μ -oxo)-bis(oxalato)-vanadium(IV) 1D coordination polymer," *Journal of Molecular Structure*, vol. 1175, pp. 865–873, 2019.
- [68] M. Graciela, M. Vignolo, N. De Kairuz, A. P. Aida, H. De Ruiz, and G. Oliver, "Influence of growth conditions on the production of lactocin 705, a bacteriocin produced by *Lactobacillus casei* CRL 705," *Journal of Applied Bacteriology*, vol. 78, pp. 5–10, 1995.
- [69] N. Sarangi, P. Athukorala, W. G. Dilantha Fernando, K. Y. Rashid, and T. D. Kievit, "The role of volatile and non-volatile antibiotics produced by *Pseudomonas chlororaphis* strain PA23 in its root colonization and control of *Sclerotinia sclerotiorum*," *Biocontrol Science and Technology*, vol. 20, no. 8, pp. 875–890, 2010.
- [70] P. G. Rodriguez, F. N. Felix, D. T. Woodley, and E. K. Shim, "The role of oxygen in wound healing: a review of the literature," *Dermatologic Surgery*, vol. 34, no. 9, pp. 1159–1169, 2008.
- [71] G. C. Gurtner, S. Werner, Y. Barrandon, and M. T. Longaker, "Wound repair and regeneration," *Nature*, vol. 453, no. 7193, pp. 314–321, 2008.
- [72] S. Zaja-Milatovic and A. Richmond, "CXC chemokines and their receptors: a case for a significant biological role in cutaneous wound healing," *Histology and histopathology*, vol. 23, no. 11, pp. 1399–1407, 2008.
- [73] T. A. Wilgus, "Immune cells in the healing skin wound; influential players at each stage of repair," *Pharmacological Research*, vol. 58, no. 2, pp. 112–116, 2008.
- [74] Y. Li, J. Fan, M. Chen, W. Li, and D. T. Woodley, "Transforming growth factor- α : a major human serum factor that promotes human keratinocyte migration," *The Journal of Investigative Dermatology*, vol. 126, no. 9, pp. 2096–2105, 2006.
- [75] C. Rice-Evans, N. Miller, and G. Paganga, "Antioxidant properties of phenolic compounds," *Trends in Plant Science*, vol. 2, no. 4, pp. 152–159, 1997.
- [76] H. Zielinski and H. Kozłowska, "Antioxidant activity and total phenolics in selected cereal grains and their different morphological fractions," *Journal of Agricultural and Food Chemistry*, vol. 48, no. 6, pp. 2008–2016, 2000.
- [77] Z. Huan-Xia, Z. Hai-Sheng, and Y. Shu-Fang, "Phenolic compounds and its antioxidant activities in ethanolic extracts from seven cultivars of Chinese jujube," *Food Science and Human Wellness*, vol. 3, pp. 183–190, 2014.
- [78] C. Rice-Evans, N. J. Miller, and G. Paganga, "Structure-antioxidant activity relationships of flavonoids and phenolic acids," *Free Radical Biology and Medicine*, vol. 20, no. 7, pp. 933–956, 1996.
- [79] Ö. Erol-Dayi, N. Arda, and G. Erdem, "Protective effects of olive oil phenolics and gallic acid on hydrogen peroxide-

- induced apoptosis," *European Journal of Nutrition*, vol. 51, no. 8, pp. 955–960, 2012.
- [80] M. B. Katkade, H. M. Syed, R. R. Andhale, and M. D. Sontakke, "Fatty acid profile and quality assessment of safflower (*Carthamus tinctorius*) oil," *Journal of Pharmacognosy and Phytochemistry*, vol. 7, pp. 3581–3585, 2018.
- [81] L. Xican, W. Xiaoting, and H. Ling, "Correlation between antioxidant activities and phenolic contents of *Radix Angelicae Sinensis* (Dangugui)," *Molecules*, vol. 14, pp. 5349–5361, 2009.
- [82] B. Samanci and E. Ozkaynak, "Effect of planting date on seed yield, oil content and fatty acid composition of safflower (*Carthamus tinctorius*) cultivars grown in the Mediterranean region of Turkey," *Journal of Agronomy and Crop Science*, vol. 189, no. 5, pp. 359–360, 2003.
- [83] K. Nauman, K. Rao Sanallah, M. I. Hussain, F. Muhammad, A. Asif, and A. Iftikhar, "A comprehensive characterization of safflower oil for its potential applications as a bioactive food ingredient. A review," *Trends in Food Science & Technology*, vol. 66, pp. 176–186, 2017.
- [84] M. Vosoghkia, L. H. Ghareaghagh, M. Ghavami, M. Gharachorloo, and B. Delkosh, "Evaluation of oil content and fatty acid composition in seeds of different genotypes of safflower (*Carthamus tinctorius* L.)," *International Journal of Agricultural Science and Research*, vol. 2, pp. 59–66, 2011.
- [85] A. M. Rotunda and M. S. Kolodney, "Mesotherapy and phosphatidylcholine injections: historical clarification and review," *Dermatologic Surgery*, vol. 32, no. 4, pp. 465–480, 2006.
- [86] V. A. Proctor and F. E. Cunningham, "The chemistry of lysozyme and its use as a food preservative and a pharmaceutical," *Critical Reviews in Food Science & Nutrition*, vol. 26, no. 4, pp. 359–395, 1988.
- [87] E. S. Abdel Moneim, M. S. Sherif, A. E. Ahmed, A. Mohanad, and N. V. Vajid, "Evaluation of antimicrobial activity of safflower (*Carthamus tinctorius*) and its synergistic effect with antibiotic," *EC Microbiology*, vol. 14, no. 3, pp. 160–166, 2018.
- [88] H. Jaberian, K. Piri, and J. Nazari, "Phytochemical composition and in vitro antimicrobial and antioxidant activities of some medicinal plants," *Food Chemistry*, vol. 136, no. 1, pp. 237–244, 2013.
- [89] W. Kchaou, F. Abbès, R. B. Mansour, C. Blecker, H. Attia, and S. Besbes, "Phenolic profile, antibacterial and cytotoxic properties of second grade date extract from Tunisian cultivars (*Phoenix dactylifera* L.)," *Food Chemistry*, vol. 194, pp. 1048–1055, 2016.
- [90] Ö. G. Üstündağ, S. Erşan, E. Özcan, G. Özcan, N. Kayra, and F. Y. Ekinci, "Black tea processing waste as a source of antioxidant and antimicrobial phenolic compounds," *European Food Research and Technology*, vol. 242, no. 9, pp. 1523–1532, 2016.

Review Article

Peptides from Animal Origin: A Systematic Review on Biological Sources and Effects on Skin Wounds

Raul Santos Alves,¹ Levy Bueno Alves,² Luciana Schulthais Altoé,¹
Mariáurea Matias Sarandy,¹ Mariella Bontempo Freitas,³ Nelson José Freitas Silveira,²
Rômulo Dias Novaes,⁴ and Reggiani Vilela Gonçalves ³

¹Department of General Biology, Federal University of Viçosa, Viçosa, 36570-900 Minas Gerais, Brazil

²Laboratory of Molecular Modeling and Computer Simulation-MolMod-CS, Institute of Chemistry, Federal University of Alfenas, Alfenas, 37130-001 Minas Gerais, Brazil

³Department of Animal Biology, Federal University of Viçosa, Viçosa, 36570-900 Minas Gerais, Brazil

⁴Institute of Biomedical Sciences, Department of Structural Biology, Federal University of Alfenas, Alfenas, 37130-001 Minas Gerais, Brazil

Correspondence should be addressed to Reggiani Vilela Gonçalves; reggysvilela@yahoo.com.br

Received 9 July 2020; Revised 2 September 2020; Accepted 5 October 2020; Published 23 October 2020

Academic Editor: Víctor M. Mendoza-Núñez

Copyright © 2020 Raul Santos Alves et al. This is an open access article distributed under the Creative Commons Attribution License, which permits unrestricted use, distribution, and reproduction in any medium, provided the original work is properly cited.

Background. Skin wounds are closely correlated with opportunistic infections and sepsis risk. Due to the need of more efficient healing drugs, animal peptides are emerging as new molecular platforms to accelerate skin wound closure and to prevent and control bacterial infection. **Aim.** The aim of this study was to evaluate the preclinical evidence on the impact of animal peptides on skin wound healing. In addition, we carried out a critical analysis of the studies' methodological quality. **Main Methods.** This systematic review was performed according to the PRISMA guidelines, using a structured search on the PubMed-Medline, Scopus, and Web of Science platforms to retrieve studies published until August 25, 2020 at 3:00 pm. The studies included were limited to those that used animal models, investigated the effect of animal peptides with no association with other compounds on wound healing, and that were published in English. Bias analysis and methodological quality assessments were examined through the SYRCLE's RoB tool. **Results.** Thirty studies were identified using the PRISMA workflow. In general, animal peptides were effective in accelerating skin wound healing, especially by increasing cellular proliferation, neoangiogenesis, collagenogenesis, and reepithelialization. Considering standardized methodological quality indicators, we identified a marked heterogeneity in research protocols and a high risk of bias associated with limited characterization of the experimental designs. **Conclusion.** Animal peptides show a remarkable healing potential with biotechnological relevance for regenerative medicine. However, rigorous experimental approaches are still required to clearly delimit the mechanisms underlying the healing effects and the risk-benefit ratio attributed to peptide-based treatments.

1. Introduction

Due to the disruption of innate defense mechanisms, skin wounds are a serious risk factor for opportunistic infections, bacteremia, and sepsis [1–3]. In the United States, recent estimates indicate that at least US\$25 billion are spent annually in the treatment of 6.5 million patients with chronic wounds [4]. The treatment of skin wounds is a challenging task, espe-

cially considering that the available treatments have limited spectrum of action on cellular and molecular mechanisms involved in tissue repair [5–9]. Skin wound healing requires a series of cellular and molecular interdependent events in order to restore tissue integrity after trauma [5]. This process is mediated by growth factors, cytokines, and resident and transitory cells and is organized in phases involving inflammation, cell proliferation, and tissue remodeling/maturation

[6]. In the inflammatory phase, immune cells such as neutrophils and macrophages migrate to the lesion area to remove tissue debris, promote antimicrobial defenses, and trigger cell proliferation [7]. The proliferative phase is marked by intense cellular activity and different cell migration to the wound bed. At this stage, fibroblasts form the granulation tissue, composed of cells and a network of blood vessels, reestablishing regional circulation [8]. The remodeling phase corresponds mainly to changes in the extracellular matrix of the scar tissue, where most type III collagen fibers are progressively replaced by type I fibers, which are more resistant and abundant in intact skins [9]. Two subsets of macrophages (M1 or M2) are commonly identified in this process, exerting complementary effects in early and late stages of tissue repair [10]. M1 macrophages are activated by interferon-gamma (IFN- γ), exerting potent nitric oxide-mediated antimicrobial effects and proinflammatory responses in the initial stages of tissue repair [11]. As an overlapping event between proliferative and remodeling phases, M2 macrophages are activated by cytokines such as IL-4, IL-10, or IL-13 [11]. These cells play an essential role on the effective resolution of the inflammation, mainly through angiogenesis and extracellular matrix resorption and remodeling [10, 11].

Wound healing is a complex and time-sensitive process often impaired by several factors such as infections, metabolic comorbidities (i.e., diabetes, dyslipidemia, malnutrition, and circulation disorders such as thrombosis, atherosclerosis, and hemorrhage), as well as the presence of foreign bodies that may delay wound healing by stimulating a chronic inflammatory response [1]. In a continuous effort to improve the pharmacological management of skin wounds, the screening of natural molecules capable of modulating the biological processes involved in tissue repair is proposed as a rational and promising strategy for the biotechnological development of more efficient healing drugs [12]. In order to achieve greater therapeutic efficacy, the search for new molecules also is aimed at overcoming current limitations of healing drugs, especially the technical difficulty in obtaining the active metabolites, the high cost of drug production, the formation of hypertrophic scars, and the risk of selecting treatment-resistant microorganisms, an aspect that represents a global concern [13, 14].

Due to its antimicrobial, immunomodulatory, promitotic, collagenogenic, and neoangiogenic potential, animal peptides are suggested as promising agents for new therapeutic approaches in skin wound treatment [1, 12, 15, 16]. Besides, their molecular abundance, low cost of isolation techniques, high molecular stability, and their broad spectrum of biological properties are also encouraging characteristics. However, the main animal peptides, physicochemical characteristics of the bioactive molecules, effective doses, and routes of administration are not completely understood. Considering that current evidence is based on fragmented data, it is unclear whether and to what extent animal peptides are effective in the skin wound treatment. In addition, it is currently difficult to understand the metabolic pathways and mechanisms of actions activated by these peptides during skin repair. Thus, we used the systematic review framework to evaluate preclinical evidence on the impact of animal peptides on skin wound

healing. In addition to characterize the biological sources of these peptides and its chemical sequences, the methodological quality of all studies reviewed was critically evaluated.

2. Methodology

2.1. Retrieval of Research Records. This systematic review followed the Preferred Reporting Items for Systematic Reviews and Meta-Analyses (PRISMA) workflow [17], which is used as a guide for study selection, screening, and eligibility. Studies were selected through an advanced search on the platforms PubMed-Medline (<https://www.ncbi.nlm.nih.gov/pubmed>), Scopus (<https://www.scopus.com/home.uri>) and Web of Science (<https://www.webofknowledge.com>), on August 25, 2020, at 3:00 pm. We used a comprehensive search strategy for retrieving all relevant studies, with a primary search in electronic databases and a secondary search in the reference lists from all relevant studies identified in the primary search. For all databases, the search filters were based on three complementary levels: (i) intervention: animal peptides; (ii) biological process: wound healing; and (iii) target organ: skin. The PubMed-Medline platform filters were built using the hierarchical distribution of MeSH (Medical Subject Headings) terms to retrieve the indexed studies. Non-MeSH descriptors were characterized by the TIAB algorithm (Title and Abstract). To identify preclinical studies, a standardized experimental animal filter was applied [18]. The search filters used for the PubMed-Medline search platform were adapted to Scopus and Web of Science databases, except for the experimental animal filter used in Scopus, which was provided by the site. The complete search strategy is shown in the supplementary file (S1 Table).

2.2. Selection of Relevant Studies. Only studies that met all the inclusion criteria as described below were selected: (i) *in vivo* studies using animal models; (ii) studies that investigated the effect of animal peptides with no association with other compounds on wound healing; and (iii) original studies published in English. The following studies were excluded: (i) nonanimal peptides; (ii) unreported origin of peptides; (iii) investigations of other organs, pathologies, or therapies; (iv) sutured wounds; (v) *in vitro* and *ex vivo* studies; (vi) unreachable studies; (vii) secondary research (i.e., literature reviews, comments, letters, and editorials); and (viii) gray literature (i.e., video-audio media). When it was difficult to obtain the full-text papers, the authors were requested to provide it by email.

2.3. Data Extraction and Management. Two independent reviewers (RSA and LSA) conducted the literature search, removed duplicated articles, and screened titles and abstracts with respect to eligibility criteria. After initial screening, full-text articles of potentially relevant studies were independently assessed for eligibility by two reviewers (RSA and LSA). The kappa test was done for the selection and data extraction ($\kappa = 0.922$). Selections were then compared, and inconsistencies were resolved in consultation with three other reviewers (MMS, RDN, and RVG). Data from each study were extracted using well-defined data as follows: (i)

publications characteristics (author, year of publication, and country of origin); (ii) animal models (animal, strain, sex, age, weight, and associated pathology); (iii) cutaneous wounds (type of lesion, site, initial area, number, and presence of infection); (iv) peptide characteristics (name, origin, and amino acid sequence); (v) intervention characteristics (route of administration, concentration, vehicle, frequency, and duration); (vi) primary outcome (wound closure); and (vii) secondary outcomes (cell proliferation and differentiation, synthesis of extracellular matrix components, recruitment of inflammatory cells, neoangiogenesis, inflammatory mediators, and oxidative markers). Quantitative data related to the wound area were directly collected from the tables or the main text provided in each study. When these data were graphically represented, the values of the wound area were obtained using the Image-Pro Plus 4.5 image analysis software (Media Cybernetics, MD, USA). The wound area was compared amongst experimental groups, and the results were expressed in percentage of wound closure.

2.4. Bias Analysis. The risk of bias was analyzed using the SYStematic Review Centre for Laboratory animal Experimentation (SYRCLE) Risk of Bias (RoB) tool [19]. This instrument is based on the Cochrane Collaboration RoB Tool, which is adjusted for aspects of bias that play a specific role in animal intervention studies. The goal was to avoid discrepancies in the assessment of methodological quality in the field of animal experimentation. To increase transparency and applicability, signaling questions were answered to facilitate judgment based on the following domains: (i) sequence generation; (ii) baseline characteristics; (iii) allocation concealment; (iv) random housing; (v) blinding; (vi) random outcome assessment; (vii) incomplete outcome data; (viii) selective outcome; and (ix) other sources of bias. Two reviewers (RSA and RVG) independently assessed the risk of bias for each study; any disagreements were resolved by discussion and consensus with two other reviewers among the authors (MMS and RDN). The SYRCLE chart was built using the Review Manager 5.3 program (Copenhagen: The Nordic Cochrane Centre, The Cochrane Collaboration).

3. Results

3.1. Included Studies. We found 1734 articles, of which 376 were duplicated and 1220 studies were excluded due to inadequate research theme. Among the excluded studies, 502 did not use peptides; 458 were related to other tissues, pathologies, or therapies; 108 were reviews; 68 did not evaluate the wound healing process; 57 used peptides of nonanimal origin; 10 were unreachable; 9 were not written in English; 3 were studies *in vitro*; 2 were comments; 1 was an *ex vivo* study; 1 was a letter; 1 was a video-audio media. The remaining 138 articles were carefully analyzed, of which 108 were excluded for not meeting the eligibility criteria (S2 Table). Thus, 30 relevant articles were selected. After reading the reference list of all selected articles, no relevant article was found. PRISMA diagram indicates the study selection process (Figure 1). The selected studies were conducted in 7 different countries, mainly China ($n = 18$, 60%), followed by

Taiwan and United States of America ($n = 4$, 13% each), Portugal, Korea, India, and Saudi Arabia ($n = 1$, 3% each).

3.2. Characteristics of Preclinical Models. The most used animal model was mice ($n = 20$, 67%), followed by rat ($n = 8$, 27%), pig, and rabbit ($n = 1$, 3% each). The most used strain was Balb/C for mice ($n = 6$, 30%) and Sprague-Dawley for rat ($n = 6$, 75%), but 30% of the studies did not report this information ($n = 9$). Most studies included only males ($n = 19$, 63%), 17% used only females ($n = 5$), 3% used both ($n = 1$), and 17% did not report this data ($n = 5$). The age of the animals ranged from 6 to 12 weeks for mice, 6 to 43 weeks for rats, and 6 weeks for pigs. This information was not reported in 57% of the studies ($n = 17$). Animal weight ranged from 20 to 26 g for mice, 150 to 600 g for rats, and 10 to 13 kg for pigs. This information was underreported in most studies ($n = 14$, 47%). Most studies were performed on health animals ($n = 26$, 87%), 10% used diabetic models ($n = 3$), and 3% used ischemic model ($n = 1$). The main characteristics related to animal models are described in detail in S3 Table.

3.3. Characteristics of Skin Wounds. Most studies investigated excisional wounds ($n = 27$, 90%), followed by burns ($n = 2$, 7%) and incisional wounds ($n = 1$, 3%). The most used site for wounds was the back of the animal ($n = 29$, 97%) and 3% performed the injury on the abdomen ($n = 1$). The initial wound area was reported in all studies ($n = 30$, 100%). The number of wounds ranged from 1 to 6 per animal ($n = 27$, 90%), and 10% did not report this information ($n = 3$). *Staphylococcus aureus* and *Escherichia coli* were the microorganisms used in experiments with infected wounds ($n = 5$, 17%), and bacterial load concentration ranged from 2×10^5 to 10^{10} Colony Forming Unit (CFU). The main characteristics related to skin wounds are detailed in S4 Table.

3.4. Characteristics of Animal Peptides and Treatments. The name and origin of the peptides used were reported in all studies ($n = 30$, 100%). Most of the peptides originated from amphibians ($n = 11$, 37%), followed by mammals and fishes ($n = 8$, 27% each), jellyfish, mollusk, and insect ($n = 1$, 3% each). The amino acid sequences in these peptides were described in 63% of the studies ($n = 19$). The most commonly used route of peptide administration was topical ($n = 20$, 67%), followed by oral ($n = 6$, 20%), subcutaneous ($n = 2$, 7%), intravenously ($n = 1$, 3%), and 3% evaluated two routes (topical and intraperitoneal) ($n = 1$). The most used vehicle was saline solution ($n = 13$, 43%), followed by phosphate-buffered saline ($n = 10$, 33%), Dulbecco's phosphate-buffered ($n = 2$, 7%), water ($n = 2$, 7%), and 10% did not report this information ($n = 3$). Most studies applied the intervention twice a day ($n = 10$, 33%), followed by once a day ($n = 8$, 27%), single application ($n = 2$, 7%), three times per day, continuous intervention, every three days, and twice or every two days ($n = 1$, 3% each). In 20% of the studies, this information was underreported ($n = 6$). Duration of intervention ranged from 5 to 11 days in 27% of studies ($n = 8$), 12 to 16 days in 10% of studies ($n = 3$), 22 to 26 days in 3% of the studies ($n = 1$), 27 to 31 days in 3% of the studies

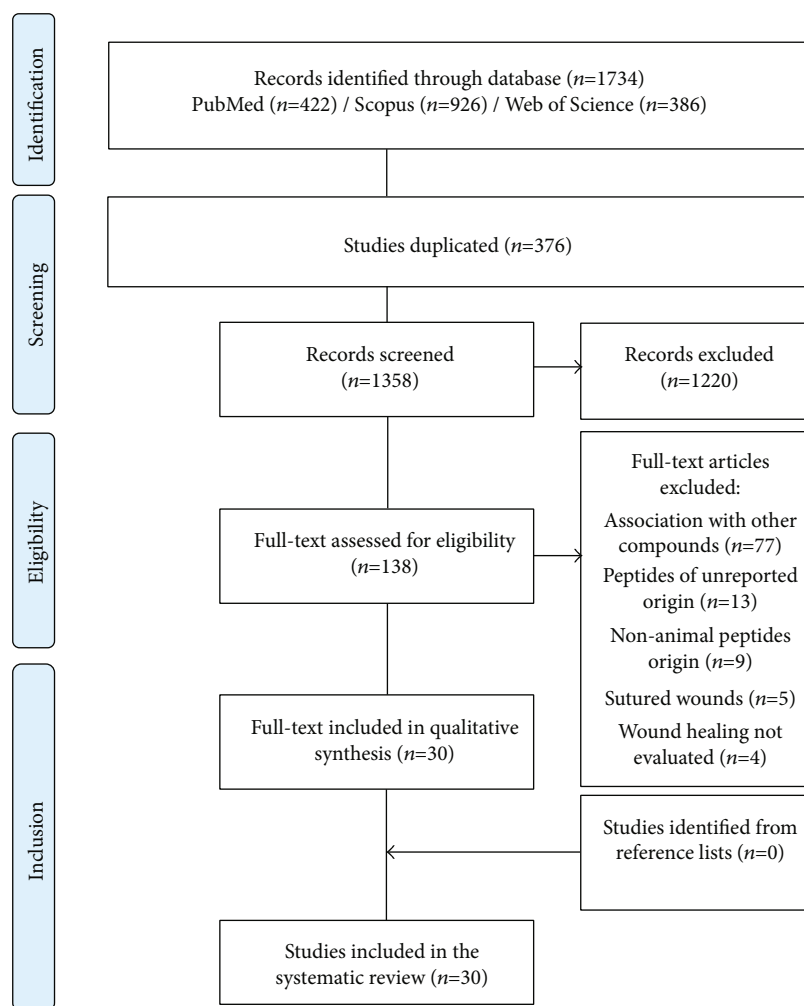


FIGURE 1: PRISMA (Preferred Reporting Items for Systematic Reviews and Meta-Analyses) flow diagram. The flowchart indicates the research records obtained at all standardized stages of the search process required for the development of systematic reviews and meta-analyses. Based on the PRISMA statement (<http://www.prisma-statement.org>).

($n = 1$), and 57% did not report this data ($n = 17$). The peptide-related characteristics and treatment protocols are described in S5-S6 Tables, respectively. Main outcome (reduction in wound size) in the treatment of skin wounds using peptides of animal origin is described in Table 1.

3.5. Main Biological Outcomes. In general, studies identified in this review support the evidence that animal peptides exert healing properties on skin wound. Although the reports are heterogeneous, all studies ($n = 30$, 100%) show that animal peptides are effective in accelerating wound closure. Most studies that performed histological analysis ($n = 23$; 77%) reported improvement in the processes of reepithelialization and dermal regeneration, inflammatory cell recruitment, and blood vessel and collagen fiber formation. Immunohistochemical analyses were performed in 50% of the studies ($n = 15$), which showed the effects of peptides in the quantitative increase of myofibroblasts, inflammatory cells, blood vessel density, and growth factors such as factors β -fibroblast growth factor (β -FGF), vascular endothelial growth factor (VEGF), and transforming growth factor- β 1 (TGF- β 1), as

well as the reduction of proinflammatory cytokines such as interleukin-1 β (IL-1 β), interleukin-6 (IL-6), and tumor necrosis factor- α (TNF- α). Enzyme-linked immunosorbent assay (ELISA) was performed in 33% of the studies ($n = 10$), which reported a reduction in proinflammatory cytokines such as IL-6 and TNF- α , as well as an increase in growth factor VEGF and TGF- β 1. Reverse transcription-polymerase chain reaction (RT-PCR) was performed in 10% of the studies ($n = 3$), which highlighted the influence of peptides on the upregulation of growth factor-related genes such as epidermal growth factor (EGF), transforming growth factor- β (TGF- β), and VEGF, and also on the gene related to macrophage migration inhibition factor (MIF), and downregulation of genes related to proinflammatory cytokines such as IL-6 and TNF- α , as well as the expression of the CXCL5 gene. The Western blot technique was performed in 7% of the studies ($n = 2$), which highlighted the increased expression of angiogenic proteins such as hypoxia-inducible factor-1 α , endothelial nitric oxide synthase, and inducible nitric oxide synthase, as well as VEGF and TGF- β 1. Oxidative stress analysis was performed in 7% of the studies ($n = 2$), in which

TABLE 1: Continued.

RF	P	R	Intervention		Main outcome*									
					Normal wound		Infected wound		Diabetic wound		Ischemic wound		Radiation + wound	
			A	C	RWS (%)	DA (PI)	RWS (%)	DA (PI)	RWS (%)	DA (PI)	RWS (%)	DA (PI)	RWS (%)	DA (PI)
[16]	OA-GL21	Topic	Twice daily	1 μ g/ml 10 μ g/ml 100 μ g/ml	-3% 44% 53%	9	?	?	?	?	?	?	?	?
[36]	Cathelicidin-NV	Topic	Twice daily	200 μ g/ml	91%	10	?	?	?	?	?	?	?	?
[37]	Pollock Collagen Peptide (PCP)	Oral	?	0.5 g/kg 2 g/kg	27% 48%	12	?	?	?	?	?	?	?	?
[38]	OA-FF10	Topic	Twice daily	1 μ M 10 μ M 100 μ M	52% 52% 68%	8	?	?	?	?	?	?	?	?
[39]	Collagen peptides (CP1/CP2)	Oral	Once daily	0.3 g/kg 0.6 g/kg 0.9 g/kg 0.1 nM	-27%/-92% -20%/-71% 47%/-17% 13%	7	?	?	?	?	?	?	?	?
[40]	OA-GL12	Topic	Twice daily	1 nM 10 nM	44% 63%	10	?	?	?	?	?	?	?	?
[41]	Ot-WHP	Topic	Once daily	200 μ g/ml	63%	8	?	?	?	?	?	?	?	?
[42]	Active peptides (APs)	Oral	?	0.5 g/kg 2 g/kg	60% 80%	14	?	?	?	?	?	?	?	?
[43]	Skin collagen peptide (Ss-SCP/Tn-SCP)	Oral	?	2 g/kg	59%/45%	12	?	?	?	?	?	?	?	?
[44]	Cathelicidin-DM	I.v.	Once daily	10 mg/kg	?	?	?	?	?	?	?	?	?	?

*Results shown as a percentage of reduction in the average wound area of the groups treated with peptide compared to the control group on a given postinjury day. RF: reference; P: peptides; R: route; A: application; C: concentration; RWS: reduction in wound size; DA: day analyzed; PI: postinjury; ?: not reported or unclear; I.p.: intraperitoneal; S.c.: subcutaneous; I.v.: intravenously; CP1: collagen peptides bands at 10-15 kDa; CP2: collagen peptides <25 kDa; Ss-SCP: *Salmo salar* skin collagen peptides; Tn-SCP: *Tilapia nilotica* skin collagen peptides.

peptides increased glutathione (GSH) level and the activity of antioxidant enzymes such as superoxide dismutase (SOD) and catalase (CAT); as well as reduced the level of malondialdehyde (MDA), a lipid peroxidation marker. All relevant results involving the use of animal peptides in the treatment of skin wounds are described in Table 2.

3.6. Reporting Bias. Regarding the analysis of bias obtained with SYRCLÉ's RoB tool, the highest risks of bias found in the studies were related to the methods used in the generation and application of the animal allocation sequence, housing procedures, and animal selection for outcome assessment. Regarding baseline similarities, 10% of the studies reported sufficient information to conclude that the distribution was balanced among the intervention and control groups at the beginning of the experiment ($n = 3$), and 90% did not report sufficient information on the homogeneity of the experimental models ($n = 27$). Regarding the measures used to blind caregivers and/or investigators, only 3% reported this information ($n = 1$). Considering the evalua-

tors, two studies (7%) reported that the outcomes were collected in a blind manner, 10% reported that the evaluation was performed by independent researchers, but does not provide information on blinding ($n = 3$), and 83% did not report this information at all ($n = 25$). Regarding incomplete results adequately addressed, 77% did not report or showed unclear information ($n = 23$). Considering the item that evaluates whether the study is free of selective outcome reports, 50% did not make clear the expected results ($n = 15$). Other potential risks of bias that could compromise the evidence (i.e., additional treatment or drugs and interventions applied to different parts of the body within one participant) were found in 50% of the studies ($n = 15$). Results from bias analysis are shown in Figure 2.

4. Discussion

In order to meet a comprehensive interpretation of the evidence reported in this systematic review, in addition to the research outcomes, we conducted an analysis of the

TABLE 2: All relevant results reported in all studies included in the systematic review on peptides of animal origin applied in the treatment of skin wounds.

Peptide source	Outcomes	
	Increased	Reduced
Human [21, 22, 24, 31]	Wound closure [21, 22, 24, 31] Reepithelialization [24] Inflammatory cells [21, 22] Blood vessels [21, 22, 24, 31] Tensile strength [21]	Wound area [21, 22, 24, 31] Inflammatory cells [31] IL-1 β , IL-6, and TNF- α [31]
Other mammals [20, 29, 32, 33]	Wound closure [20, 29, 32, 33] Reepithelialization [20, 29] Dermal regeneration [20, 32] Inflammatory cells [32] Blood vessels [20, 32, 33] Collagen [20, 29, 32, 33] SOD, CAT, GSH, and MIF [32] Hexosamine [29, 33] Ascorbate and Proteins [29] Tensile strength [29] Collagen contraction temperature [29] DNA, NO, VEGF, and TGF- β 1 [33]	Wound area [20, 29, 32, 33] MDA, TNF- α , and NF- κ B [32] Lipid peroxidation [29]
Amphibian [1, 13, 16, 25, 27, 28, 36, 38, 40, 41, 44]	Wound closure [1, 13, 16, 25, 27, 28, 36, 38, 40, 41, 44] Reepithelialization [13, 16, 25, 27, 28, 36, 40, 41] Dermal regeneration [13, 16, 25, 27, 28, 36, 40, 41] Inflammatory cells [13, 27, 41] Blood vessels [28] Collagen [36, 41] Myofibroblasts [25, 27, 36, 41] MCP-1 and VEGF [36] TNF- α [36, 41] TGF- β [41] TGF- β 1 [13, 27, 36] CXCL1 and CCL2 [41] HIF-1 α , eNOS, and iNOS in diabetic wounds [28]	Wound area [1, 13, 16, 25, 27, 28, 36, 38, 40, 41, 44] Inflammatory cells [28] IL-6 and TNF- α in diabetic wounds [28]
Fish [12, 15, 26, 30, 34, 35, 37, 43]	Wound closure [12, 15, 26, 30, 34, 35, 37, 43] Reepithelialization [12, 26, 34, 35, 37, 43] Dermal regeneration [12, 26, 34, 35, 37, 43] Inflammatory cells [26, 34] Collagen [34, 37, 43] VEGF [26, 30, 43] EGF and TGF- β [30, 37] FGF [43] bFGF [37] T β R2 [37] IL-1 [30] IL-10 [43] NOD2 and BD14 [43] Hydroxyproline [37]	Wound area [12, 15, 26, 30, 34, 35, 37, 43] Inflammatory cells [12] IL-6 [12, 26, 30, 34] TNF [30] MCP-1 [26] TNF- α [12, 26] CRP [34] CXCL5 [12] Bacterial loads [12, 26, 34]
Jellyfish [39]	Wound closure, Reepithelialization, Dermal regeneration, Collagen, β -FGF, and TGF- β 1	Wound area
Mollusk [42]	Wound closure, Reepithelialization, Dermal regeneration, CD31, EGF, FGF, TGF- β , T β R2, IL-1, and IL-10	Wound area, Inflammatory cells, and Smad7
Insect [23]	Wound closure, Reepithelialization, and Inflammatory cells	Wound area

IL: interleukin; TNF: tumor necrosis factor; SOD: superoxide dismutase; CAT: catalase; GSH: glutathione; MIF: macrophage migration inhibitory factor; DNA: deoxyribonucleic acid; NO: nitric oxide; VEGF: vascular endothelial growth factor; TGF: transforming growth factor; MDA: malondialdehyde; NF- κ B: transcription factor kappa-B; MCP: monocyte chemoattractant protein; HIF: hypoxia-inducible factor; eNOS: endothelial nitric oxide synthase; iNOS: inducible nitric oxide synthase; EGF: epidermal growth factor; CRP: C-reactive protein; FGF: fibroblast growth factor; T β R: transforming growth factor- β receptor.

experimental models used in the selected studies to investigate the impact of animal peptides on skin wound healing. In our view, mapping these peptides and selecting well-designed animal models are critical for assessing the effectiveness of new molecules with healing potential. These aspects can contribute to clarify the potential biotechnological applicability of peptide-based strategies in regenerative medicine, an essential assumption to support clinical trials [45].

4.1. Relevance of Animal Models in Studies on Skin Wound Healing. Although pigs were used in only one study identified in the systematic review, this is the animal model whose skin is more similar to humans, which makes them an interesting model for preclinical studies on wound healing [46]. However, as these animals demand high husbandry costs and more restrictive ethical issues, their use has been increasingly limited. In contrast, mice and rats were the most used animal models, an aspect potentially associated with its greater availability, low cost, and easy handling. In addition, mice, rats, and humans exhibit the same stages of wound healing, with immunoinflammatory and microstructural convergences mainly based on similar profiles of regulatory molecules (i.e., cytokines and growth factors) and composition of extracellular matrix (i.e., glycosaminoglycan's, collagen and non-collagen proteins) [47].

Rodents, especially mice and rats, are also often useful to investigate the effect of healing agents in pathological conditions such as diabetes [28, 31, 32], which was the associated disease most investigated in the studies reviewed. While streptozotocin was used to induce type I diabetes [31, 32], type II diabetes was studied using *db/db* mice model [28]. Although diabetes develops from different physiopathological mechanisms in streptozotocin-induced and *db/db* animals, both models are valid to investigate the human disease. In this sense, induced-animals and diabetic humans share similar metabolic abnormalities, especially hyperglycemia, vasculopathy, and neuropathy [48]. As these are disturbances associated with delayed wound healing in diabetes [49], chemically-induced and genetic models represent robust and realistic experimental constructs, which exhibits marked relevance and applicability in studies on healing products [28, 31, 32].

4.2. Relevance of Wound Models. The frequent use of rodents, excision wounds were consistently investigated in the studies reviewed. However, the number and size of the wounds were highly variable. Due to the complete skin removal, all phases of tissue repair are more pronounced in excisional than in incisional wounds [50]. Thus, excisional injuries are widely used in second intention healing models [22, 26, 31, 40]. In these cases, the intense inflammatory process and the marked tissue remodeling favor the analysis of the effectiveness of healing products [26]. In addition to the type (first vs. second intention), the number of wounds exerts a relevant impact on the therapeutic outcome. Although most studies evaluated the healing potential of animal peptides on 1 or 2 wounds produced in each animal, 4 and 6 wounds were also reported. The main limitations of models based on multiple wounds

are related to repeated biopsies on nearby wounds [22, 51]. As wound tissue collection creates additional damage to the skin, the acute inflammatory process is reactivated [51]. In this case, the upregulation of cytokine and growth factors might influence the adjacent wound repair [52]. Thus, it would be ideal to investigate changes in only 1 wound per animal, to reduce the construct bias and its impact on the evidence. However, as models with 2 or more wounds are often required in time-dependent analysis of the healing process, the selection of these models should be carefully considered.

Regarding investigations on infected wounds, *S. aureus* was consistently used to induce wound infection. As *S. aureus* is an important human pathogen often associated to bacterial skin infections [53], preclinical models based on this bacteria are relevant and realistic. The emergence of multidrug-resistant microorganisms stimulates an important challenge in regenerative medicine: the development of more efficient products to treat infected wounds [14]. Efficient antimicrobial products are also relevant since the colonization of wounds by microorganisms amplifies inflammation and oxidative tissue damage, slowing or inhibiting the progression of the healing process [12, 26, 34]. Thus, studies on the treatment of infected wounds are urgent, especially considering that controlling infection is essential to reduce the risk of developing chronic wounds [54].

4.3. Relevance of Therapeutic Protocols. Although most studies used a diluted aqueous solution and applied the peptides topically, the number of applications and the treatment period was highly variable. The use of water, saline, or sodium phosphate buffer as a vehicle indicated that animal peptides exhibit an interesting hydrophilic characteristic. These vehicles are relevant to avoid the development of cytotoxicity, which can occur with the use of organic solvents such as ethanol and dimethyl sulfoxide [55]. Unlike recommendations for different types of vehicles, there is no consensus on the dose and duration of treatment. Essentially, these aspects of dosimetry depend on the biological effect and the organic tolerability of each molecule. Thus, although the therapeutic effects are influenced by the dose and time of treatment, generalizations cannot be established for molecules with potentially different chemical and biological properties.

4.4. Effect of Animal Peptides on Wound Healing. Currently, identifying animal peptides with healing properties opens a new perspective for the treatment of skin wounds [16, 32, 34]. In general, reviewed studies indicate that peptides originating from mammals, amphibians, fishes, jellyfish, mollusk, and insect exert beneficial effects in stimulating wound closure. However, peptides obtained from the fish species *Parachanna marmoratus* [26] and *Oreochromis niloticus* [12, 30] demonstrated positive effects only in infected wounds, suggesting that some peptides facilitate wound recovery by exerting antimicrobial effects and controlling opportunistic infections. This feature might be associated with the peptides' biochemical characteristics, since the peptides tilapia piscidin 3 (TP3) and tilapia piscidin 4 (TP4), both originating from *Oreochromis niloticus*, have similar amino acids sequence

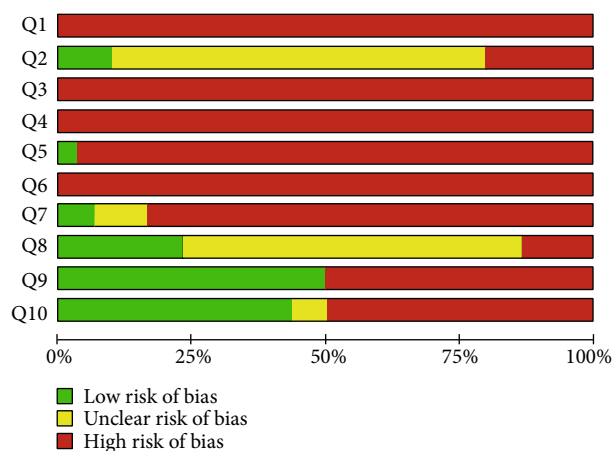


FIGURE 2: Results of the risk of bias for all studies included in the systematic review. The items in the SYSystematic Review Centre for Laboratory animal Experimentation (SYRCLE) Risk of Bias assessment (Q1–Q10) were scored with “yes” indicating low risk of bias, “no” indicating high risk of bias, or “unclear” indicating an unclear risk of bias. Q1–Q3 consider selection bias, Q4–Q5 consider performance bias, Q6–Q7 consider detection bias, Q8 considers attrition bias, Q9 considers reporting bias, and Q10 considers other biases. Q: Question. Q1: Was the allocation sequence adequately generated and applied?; Q2: Were the groups similar at baseline or were they adjusted for confounders in the analysis?; Q3: Was the allocation adequately concealed?; Q4: Were the animals randomly housed during the experiment?; Q5: Were the caregivers and/or investigators blinded from knowledge which intervention each animal received during the experiment?; Q6: Were animals selected at random for outcome assessment?; Q7: Was the outcome assessor blinded?; Q8: Were incomplete outcome data adequately addressed?; Q9: Are reports of the study free of selective outcome reporting?; and Q10: Was the study apparently free of other problems that could result in high risk of bias?

and share the same antibacterial action. Studies that evaluated mainly the antibacterial characteristics of the animal peptides showed a reduction of bacterial load on the wound area after treatment [12, 26].

Animal peptides have been shown to act on the activation and proliferation of different cells involved in the wound healing process. The increase in fibroblasts, myofibroblasts, and endothelial cells potentiate the processes of dermal regeneration and wound closure, acting on the formation, contraction, and nutrition of granulation tissue, respectively [25, 27, 36, 41]. Several peptides were found to increase blood vessel density, in order to adequate nutrient and oxygen delivery to newly formed tissue [20, 21, 24, 33]. There is evidence that animal peptides may increase VEGF biosynthesis and stimulate neoangiogenesis, which is essential for a more efficient healing due to the influx of molecules required for the proper morphofunctional organization of the scar tissue [26, 30, 33, 36]. TGF- β 1 was additionally increased in response to animal peptides, which is a growth factor effective in stimulating cell proliferation, differentiation, and migration; as well as collagenogenesis in the granulation tissue [13, 27, 36, 39]. In addition, peptides obtained from

mammals, amphibians, fishes, and insect increased the recruitment of inflammatory cells, which contributes to the removal of damaged cells and matrix debris in the injured tissue and protects against local infections during the inflammatory phase, accelerating wound closure [13, 21, 23, 26, 27, 34]. Several cells of the immune system are involved in wound healing, such as neutrophils, monocytes/macrophages, mast cells, and lymphocytes [21]. Most studies have evaluated the effect of peptides on the recruitment of macrophages due to their critical roles in the healing process, coordinating complex processes of cell proliferation and extracellular matrix biosynthesis [12, 13, 21, 26, 27]. However, the peptide TP3, originating from the fish *Oreochromis niloticus*, was effective in reducing the number of inflammatory cells in infected wounds, an effect related to the peptide’s antimicrobial action in directly attenuating tissue bacterial load, reducing the antigenic load and immunological activation [12]. Although it remains poorly understood, these results help to clarify potential mechanisms of action of the peptides and their modulating action in skin wound healing.

Some studies included in this review have evaluated the skin healing effect of animal peptides when comorbidities also occur, such as ischemia and diabetes. In the ischemic animal model, TP508 peptide from human thrombin significantly accelerated wound closure by stimulating anti-inflammatory processes and increasing tissue vascularization [22]. Diabetes was a condition widely studied, since the skin wound healing is often interrupted or delayed by abnormal glycation products and microvascular disturbances, contributing to the development of chronic wounds [56–59]. In addition, diabetic wounds often remain in the inflammatory stage for a long time, impairing the healing process due to the release of proinflammatory cytokines such as IL-6 and TNF- α [60]. Thus, studies evaluating the relevance of animal peptides on skin wound healing in diabetic animals are required, especially considering essential parameters such as immunological effectors, neoangiogenesis, and wound closure to characterize the effect of the treatments. In diabetic models, most peptides identified significantly stimulated wound closure compared to untreated animals, increasing vascularization [31, 32], collagenogenesis, and dermal regeneration [32]. In addition, the human proinsulin C peptide reversed the increase of inflammatory cells in diabetic wounds, preventing an excessive inflammatory response and extensive secondary tissue damage, and consequently stimulating the rapid progression from the inflammatory to the proliferative phase [31]. These effects were associated with decreased proinflammatory cytokine production. Camel milk peptide increased the activity of antioxidant enzymes such as SOD, CAT, and GST, reducing the negative effects of excessive reactive oxygen species formation and lipid peroxidation [32]. However, a study testing CW49 peptide originating from the amphibian *Odorrana grahami* indicated a moderate effect on the healing process in a diabetic model [28]. In this study, wound closure was improved only in the early stages in the healing progression, when increased reepithelialization and dermal regeneration rates, blood vessel density, proangiogenic proteins, and reduced recruitment of inflammatory cells and proinflammatory cytokines were reported.

4.5. Limitations. Systematic reviews are essential tools for summarizing evidence accurately and reliably, assisting risk assessment, and providing evidence of the benefits of health-related interventions [61]. However, the methodological quality of the studies included in this review was predominantly classified as high risk or unclear risk of bias, indicating that most features needed for a bias study evaluation were not sufficiently reported. Incomplete characterization of animal models, peptide acquisition and characterization, treatment protocols, outcome measures, and mechanisms involved in the healing process all contributed to the increased risk of bias. Along with these limitations, results were presented only as graphics in most studies, which made it difficult to assess the absolute values related to the wound area. We hope that our critical analysis helps accelerating preclinical research and reducing methodological bias by improving experimental control and accuracy of research reports.

5. Conclusion

In general, we identified that the evidence on the healing potential of animal peptides is mainly based on valid and realistic preclinical models that share similar tissue repair phases with those observed in humans. From studies using these models, we identified that animal peptides are potentially effective in accelerating the skin wound healing. For most of the identified peptides, the beneficial effect is mainly associated with cell proliferation stimulation, neoangiogenesis, collagenogenesis, reepithelization, and wound contraction. However, the healing property of a small group of tilapia-derived peptides (TP3 and TP4) is potentially related to the antibacterial effects of these molecules. Despite the beneficial healing effects, the risk of bias and methodological divergences observed in some studies make the current evidence limited to the experimental contexts applied to the animal models analyzed. Considering that research papers on animal peptides promoting wound healing are relatively recent, there is a growing need to increase the number of investigations and improve the experimental protocols and research reports. We hope that our critical analysis helps accelerating preclinical research and reducing methodological bias by improving experimental control and accuracy of the research reports in this area.

Conflicts of Interest

No competing financial interests exist.

Acknowledgments

The authors are grateful to the support provided by Fundação do Amparo à Pesquisa do Estado de Minas Gerais (FAPEMIG, processes APQ-01895-16, PPM-00687-17, and PPM-00077-18), Conselho Nacional de Desenvolvimento Científico e Tecnológico (CNPq, processes 303972/2017-3, 423594/2018-4, 305093/2017-7, and MCTIC 408503/2018-1), and Coordenação de Aperfeiçoamento de Pessoal de Nível Superior - Brazil (CAPES, finance code 001).

Supplementary Materials

S1 Table: complete search strategy with search filters and number of research records recovered in the PubMed-Medline, Scopus, and Web of Science databases. *: In the PubMed-Medline database, standardized animal filters were obtained in “Hooijmans CR, Tillema A, Leenaars M, Ritskes-Hoitinga M. Enhancing search efficiency by means of a search filter for finding all studies on animal experimentation in PubMed. *Laboratory Animals* 2010;44:170-175.”. S2 Table: studies excluded during the process of eligibility. S3 Table: general characteristics of the preclinical models used in all studies investigating the relevance of animal peptides in the treatment of skin wounds. ♂: male; ♀: female; ?: not reported or unclear; wk: weeks. S4 Table: general characteristics of skin wounds used in preclinical models investigating the relevance of animal peptides as healing agents. ?: not reported or unclear; *S. aureus*: *Staphylococcus aureus*; *E. coli*: *Escherichia coli*; D: diameter; CFU: colony-forming unit. S5 Table: description of the main characteristics related to peptides included in the systematic review on peptides of animal origin applied in the treatment of skin wounds. S6 Table: treatment protocols used in all studies investigating the relevance of animal peptides in the treatment of skin wounds. ?: not reported or unclear; SAL: saline solution; PBS: phosphate-buffered saline solution; DPBS: Dulbecco's phosphate-buffered saline; I.p.: intraperitoneal; S.c.: subcutaneous; I.v.: intravenously. S7 Table: PRISMA 2009 Checklist. *From*: Moher D, Liberati A, Tetzlaff J, Altman DG, The PRISMA Group (2009). Preferred Reporting Items for Systematic Reviews and Meta-Analyses: The PRISMA Statement. *PLoS Med* 6(7): e1000097. doi:10.1371/journal.pmed1000097. (*Supplementary Materials*)

References

- [1] X. Li, Y. Wang, Z. Zou et al., “OM-LV20, a novel peptide from odorous frog skin, accelerates wound healing in vitro and in vivo,” *Chemical Biology & Drug Design*, vol. 91, no. 1, pp. 126–136, 2018.
- [2] C. Morin, A. Roumegous, G. Carpentier et al., “Modulation of inflammation by Cicaderma ointment accelerates skin wound healing,” *The Journal of Pharmacology and Experimental Therapeutics*, vol. 343, no. 1, pp. 115–124, 2012.
- [3] B. F. Mittag, T. C. C. Krause, H. Roehrs, M. J. Meier, and M. T. R. Danski, “Cuidados com Lesão de Pele: Ações da Enfermagem,” *Estima*, vol. 15, no. 1, pp. 19–25, 2017.
- [4] O. Golubnitschaja, L. S. Veaser, E. Avishai, and V. Costigliola, “Wound healing: proof-of-principle model for the modern hospital: patient stratification, prediction, prevention and personalisation of treatment,” in *The Modern Hospital*, pp. 357–366, Springer, Cham, Switzerland, 2019.
- [5] M. G. Roubelakis, et al. O. Trohatou, A. Roubelakis et al., “Platelet-rich plasma (PRP) promotes fetal mesenchymal stem/stromal cell migration and wound healing process,” *Stem Cell Reviews and Reports*, vol. 10, no. 3, pp. 417–428, 2014.
- [6] R. J. de Mendonça and J. Coutinho-Netto, “Aspectos celulares da cicatrização,” *Anais Brasileiros de Dermatologia*, vol. 84, no. 3, pp. 257–262, 2009.

- [7] I. M. Balsa and W. T. N. Culp, "Wound care," *The Veterinary Clinics of North America. Small Animal Practice*, vol. 45, no. 5, pp. 1049–1065, 2015.
- [8] C. A. Balbino, L. M. Pereira, and R. Curi, "Mecanismos envolvidos na cicatrização: uma revisão," *Revista Brasileira de Ciências Farmacêuticas*, vol. 41, no. 1, pp. 27–51, 2005.
- [9] J. A. Phillips and L. J. Bonassar, "Matrix metalloproteinase activity synergizes with $\alpha 2\beta 1$ integrins to enhance collagen remodeling," *Experimental Cell Research*, vol. 310, no. 1, pp. 79–87, 2005.
- [10] C. Mills, "M1 and M2 macrophages: oracles of health and disease," *Critical Reviews in Immunology*, vol. 32, no. 6, pp. 463–488, 2012.
- [11] J. Lichtnekert, T. Kawakami, W. C. Parks, and J. S. Duffield, "Changes in macrophage phenotype as the immune response evolves," *Current Opinion in Pharmacology*, vol. 13, no. 4, pp. 555–564, 2013.
- [12] H.-N. Huang, Y.-L. Chan, C.-F. Hui, J.-L. Wu, C.-J. Wu, and J.-Y. Chen, "Use of tilapia piscidin 3 (TP3) to protect against MRSA infection in mice with skin injuries," *Oncotarget*, vol. 6, no. 15, pp. 12955–12969, 2015.
- [13] X. Cao, Y. Wang, C. Wu et al., "Cathelicidin-OA1, a novel antioxidant peptide identified from an amphibian, accelerates skin wound healing," *Scientific Reports*, vol. 8, no. 1, p. 943, 2018.
- [14] H. Xu, Y. Zhang, X. Feng, K. Tie, Y. Cao, and W. Han, "Catesbeianin-1, a novel antimicrobial peptide isolated from the skin of *Lithobates catesbeianus* (American bullfrog)," *Biotechnology Letters*, vol. 39, no. 6, pp. 897–903, 2017.
- [15] Z. Zhang, J. Wang, Y. Ding, X. Dai, and Y. Li, "Oral administration of marine collagen peptides from Chum Salmon skin enhances cutaneous wound healing and angiogenesis in rats," *Journal of the Science of Food and Agriculture*, vol. 91, pp. 2173–2179, 2011.
- [16] W. Bian, B. Meng, X. Li et al., "OA-GL21, a novel bioactive peptide from *Odorrana andersonii*, accelerated the healing of skin wounds," *Bioscience Reports*, vol. 38, no. 3, article BSR20180215, 2018.
- [17] D. Moher, A. Liberati, J. Tetzlaff, D. G. Altman, and The PRISMA Group, "Preferred reporting items for systematic reviews and meta-analyses: the PRISMA statement," *PLoS Medicine*, vol. 6, no. 7, article e1000097, 2009.
- [18] C. R. Hooijmans, A. Tillema, M. Leenaars, and M. Ritskes-Hoitinga, "Enhancing search efficiency by means of a search filter for finding all studies on animal experimentation in PubMed," *Laboratory Animals*, vol. 44, no. 3, pp. 170–175, 2010.
- [19] C. R. Hooijmans, M. M. Rovers, R. B. M. de Vries, M. Leenaars, M. Ritskes-Hoitinga, and M. W. Langendam, "SYRCLE's risk of bias tool for animal studies," *BMC Medical Research Methodology*, vol. 14, no. 1, p. 43, 2014.
- [20] K. M. Malinda, H. K. Kleinman, G. S. Sidhu et al., "Thymosin $\beta 4$ accelerates wound healing," *The Journal of Investigative Dermatology*, vol. 113, no. 3, pp. 364–368, 1999.
- [21] J. Stiernberg, A. M. Norfleet, W. R. Redin, W. S. Warner, R. R. Fritz, and D. H. Carney, "Acceleration of full-thickness wound healing in normal rats by the synthetic thrombin peptide, TP508," *Wound Repair and Regeneration*, vol. 8, no. 3, pp. 204–215, 2000.
- [22] A. M. Norfleet, Y. Huang, L. E. Sower, W. R. Redin, R. R. Fritz, and D. H. Carney, "Thrombin peptide TP508 accelerates closure of dermal excisions in animal tissue with surgically induced ischemia," *Wound Repair and Regeneration*, vol. 8, no. 6, pp. 517–529, 2000.
- [23] P. H. A. Lee, J. A. Rudisill, K. H. Lin et al., "HB-107, a nonbacteriostatic fragment of the antimicrobial peptide cecropin B, accelerates murine wound repair," *Wound Repair and Regeneration*, vol. 12, no. 3, pp. 351–358, 2004.
- [24] R. Ramos, J. P. Silva, A. C. Rodrigues et al., "Wound healing activity of the human antimicrobial peptide LL37," *Peptides*, vol. 32, no. 7, pp. 1469–1476, 2011.
- [25] H. Liu, L. Mu, J. Tang et al., "A potential wound healing-promoting peptide from frog skin," *The International Journal of Biochemistry & Cell Biology*, vol. 49, pp. 32–41, 2014.
- [26] H.-N. Huang, C.-Y. Pan, Y.-L. Chan, J.-Y. Chen, and C.-J. Wu, "Use of the antimicrobial peptide pardaxin (GE33) to protect against methicillin-resistant *Staphylococcus aureus* infection in mice with skin injuries," *Antimicrobial Agents and Chemotherapy*, vol. 58, no. 3, pp. 1538–1545, 2014.
- [27] L. Mu, J. Tang, H. Liu et al., "A potential wound-healing-promoting peptide from salamander skin," *The FASEB Journal*, vol. 28, no. 9, pp. 3919–3929, 2014.
- [28] H. Liu, Z. Duan, J. Tang, Q. Lv, M. Rong, and R. Lai, "A short peptide from frog skin accelerates diabetic wound healing," *The FEBS Journal*, vol. 281, no. 20, pp. 4633–4643, 2014.
- [29] P. Banerjee, L. Suguna, and C. Shanthi, "Wound healing activity of a collagen-derived cryptic peptide," *Amino Acids*, vol. 47, no. 2, pp. 317–328, 2015.
- [30] H.-N. Huang, Y.-L. Chan, C.-J. Wu, and J.-Y. Chen, "Tilapia piscidin 4 (TP4) stimulates cell proliferation and wound closure in MRSA-infected wounds in mice," *Marine Drugs*, vol. 13, no. 5, pp. 2813–2833, 2015.
- [31] Y.-C. Lim, M. P. Bhatt, M.-H. Kwon et al., "Proinsulin C-peptide prevents impaired wound healing by activating angiogenesis in diabetes," *The Journal of Investigative Dermatology*, vol. 135, no. 1, pp. 269–278, 2015.
- [32] H. Ebaid, B. Abdel-salam, I. Hassan, J. Al-Tamimi, A. Metwalli, and I. Alhazza, "Camel milk peptide improves wound healing in diabetic rats by orchestrating the redox status and immune response," *Lipids in Health and Disease*, vol. 14, no. 1, p. 132, 2015.
- [33] C. Liu, Y. Hao, J. Huang et al., "Ghrelin accelerates wound healing in combined radiation and wound injury in mice," *Experimental Dermatology*, vol. 26, no. 2, pp. 186–193, 2017.
- [34] H.-N. Huang, C.-Y. Pan, H.-Y. Wu, and J.-Y. Chen, "Antimicrobial peptide epinecidin-1 promotes complete skin regeneration of methicillin-resistant *Staphylococcus aureus*-infected burn wounds in a swine model," *Oncotarget*, vol. 8, no. 13, pp. 21067–21080, 2017.
- [35] Z. Hu, P. Yang, C. Zhou, S. Li, and P. Hong, "Marine collagen peptides from the skin of Nile Tilapia (*Oreochromis niloticus*): characterization and wound healing evaluation," *Marine Drugs*, vol. 15, no. 4, p. 102, 2017.
- [36] J. Wu, J. Yang, X. Wang et al., "A frog cathelicidin peptide effectively promotes cutaneous wound healing in mice," *The Biochemical Journal*, vol. 475, no. 17, pp. 2785–2799, 2018.
- [37] T. Yang, K. Zhang, B. Li, and H. Hou, "Effects of oral administration of peptides with low molecular weight from Alaska Pollock (*Theragra chalcogramma*) on cutaneous wound healing," *Journal of Functional Foods*, vol. 48, pp. 682–691, 2018.

- [38] N. Liu, Z. Li, B. Meng et al., "Accelerated wound healing induced by a novel amphibian peptide (OA-FF10)," *Protein and Peptide Letters*, vol. 26, no. 4, pp. 261–270, 2019.
- [39] F. F. Felician, R. H. Yu, M. Z. Li et al., "The wound healing potential of collagen peptides derived from the jellyfish *Rhopilema esculentum*," *Chinese Journal of Traumatology*, vol. 22, no. 1, pp. 12–20, 2019.
- [40] Y. Song, C. Wu, X. Zhang et al., "A short peptide potentially promotes the healing of skin wound," *Bioscience Reports*, vol. 39, no. 3, article BSR20181734, 2019.
- [41] X. He, Y. Yang, L. Mu et al., "A frog-derived immunomodulatory peptide promotes cutaneous wound healing by regulating cellular response," *Frontiers in Immunology*, vol. 10, 2019.
- [42] F. Yang, X. Qin, T. Zhang, C. Zhang, and H. Lin, "Effect of oral administration of active peptides of *Pinctada martensii* on the repair of skin wounds," *Marine Drugs*, vol. 17, no. 12, p. 697, 2019.
- [43] F. Mei, J. Liu, J. Wu et al., "Collagen peptides isolated from *Salmo salar* and *Tilapia nilotica* skin accelerate wound healing by altering cutaneous microbiome colonization via upregulated NOD2 and BD14," *Journal of Agricultural and Food Chemistry*, vol. 68, no. 6, pp. 1621–1633, 2020.
- [44] Y. Shi, C. Li, M. Wang et al., "Cathelicidin-DM is an antimicrobial peptide from *Duttaphrynus melanostictus* and has wound-healing therapeutic potential," *ACS Omega*, vol. 5, no. 16, pp. 9301–9310, 2020.
- [45] V. Mielgo, A. Valls i Soler, and C. Rey-Santano, "Dobutamine in paediatric population: a systematic review in juvenile animal models," *PLoS One*, vol. 9, no. 4, article e95644, 2014.
- [46] T. P. Sullivan, W. H. Eaglstein, S. C. Davis, and P. Mertz, "The pig as a model for human wound healing," *Wound Repair and Regeneration*, vol. 9, no. 2, pp. 66–76, 2001.
- [47] R. E. Mirza, M. M. Fang, E. M. Weinheimer-Haus, W. J. Ennis, and T. J. Koh, "Sustained inflammasome activity in macrophages impairs wound healing in type 2 diabetic humans and mice," *Diabetes*, vol. 63, no. 3, pp. 1103–1114, 2014.
- [48] K. Srinivasan and P. Ramarao, "Animal models in type 2 diabetes research: an overview K," *The Indian Journal of Medical Research*, vol. 136, pp. 451–472, 2012.
- [49] D. G. Greenhalgh, "Wound healing and diabetes mellitus," *Clinics in Plastic Surgery*, vol. 30, no. 1, pp. 37–45, 2003.
- [50] Y. Ozay, S. Guzel, E. G. Ozkorkmaz et al., "Effects of methanolic extract of *Verbascum inulifolium* Hub.-Mor. on incisional and excisional skin wounds in diabetic and non-diabetic rats," *Indian Journal of Experimental Biology*, vol. 57, pp. 157–167, 2019.
- [51] H. E. Koschwanez and E. Broadbent, "The use of wound healing assessment methods in psychological studies: a review and recommendations," *British Journal of Health Psychology*, vol. 16, no. 1, pp. 1–32, 2011.
- [52] C. Qing, "The molecular biology in wound healing & non-healing wound," *Chinese Journal of Traumatology*, vol. 20, no. 4, pp. 189–193, 2017.
- [53] S. Krishna and L. S. Miller, "Innate and adaptive immune responses against *Staphylococcus aureus* skin infections," *Seminars in Immunopathology*, vol. 34, no. 2, pp. 261–280, 2012.
- [54] E. J. Mudge, "Recent accomplishments in wound healing," *International Wound Journal*, vol. 12, no. 1, pp. 4–9, 2015.
- [55] L. Jamalzadeh, H. Ghafoori, R. Sariri et al., "Cytotoxic effects of some common organic solvents on MCF-7, RAW-264.7 and human umbilical vein endothelial cells," *Avicenna Journal of Medical Biochemistry*, vol. 4, no. 1, p. 10, 2016.
- [56] T. Mustoe, "Understanding chronic wounds: a unifying hypothesis on their pathogenesis and implications for therapy," *American Journal of Surgery*, vol. 187, no. 5, pp. S65–S70, 2004.
- [57] R. A. Norman and M. Bock, "Wound care in geriatrics," *Dermatologic Therapy*, vol. 16, no. 3, pp. 224–230, 2003.
- [58] L. Blanes, I. S. Duarte, J. A. Calil, and L. M. Ferreira, "Avaliação clínica e epidemiológica das úlceras por pressão em pacientes internados no Hospital São Paulo," *Revista da Associação Médica Brasileira*, vol. 50, no. 2, pp. 182–187, 2004.
- [59] A. Martin, M. R. Komada, and D. C. Sane, "Abnormal angiogenesis in diabetes mellitus," *Medicinal Research Reviews*, vol. 23, no. 2, pp. 117–145, 2003.
- [60] R. J. Snyder, "Treatment of nonhealing ulcers with allografts," *Clinics in Dermatology*, vol. 23, no. 4, pp. 388–395, 2005.
- [61] A. Liberati, D. G. Altman, J. Tetzlaff et al., "The PRISMA statement for reporting systematic reviews and meta-analyses of studies that evaluate health care interventions: explanation and elaboration," *PLoS Medicine*, vol. 6, no. 7, article e1000100, 2009.